

IAEA HUMAN HEALTH SERIES

No. 38

Atlas of Non-FDG PET-CT in Diagnostic Oncology



IAEA

International Atomic Energy Agency

IAEA HUMAN HEALTH SERIES PUBLICATIONS

The mandate of the IAEA human health programme originates from Article II of its Statute, which states that the “Agency shall seek to accelerate and enlarge the contribution of atomic energy to peace, health and prosperity throughout the world”. The main objective of the human health programme is to enhance the capabilities of IAEA Member States in addressing issues related to the prevention, diagnosis and treatment of health problems through the development and application of nuclear techniques, within a framework of quality assurance.

Publications in the IAEA Human Health Series provide information in the areas of: radiation medicine, including diagnostic radiology, diagnostic and therapeutic nuclear medicine, and radiation therapy; dosimetry and medical radiation physics; and stable isotope techniques and other nuclear applications in nutrition. The publications have a broad readership and are aimed at medical practitioners, researchers and other professionals. International experts assist the IAEA Secretariat in drafting and reviewing these publications. Some of the publications in this series may also be endorsed or co-sponsored by international organizations and professional societies active in the relevant fields.

There are two categories of publications in this series:

IAEA HUMAN HEALTH SERIES

Publications in this category present analyses or provide information of an advisory nature, for example guidelines, codes and standards of practice, and quality assurance manuals. Monographs and high level educational material, such as graduate texts, are also published in this series.

IAEA HUMAN HEALTH REPORTS

Human Health Reports complement information published in the IAEA Human Health Series in areas of radiation medicine, dosimetry and medical radiation physics, and nutrition. These publications include reports of technical meetings, the results of IAEA coordinated research projects, interim reports on IAEA projects, and educational material compiled for IAEA training courses dealing with human health related subjects. In some cases, these reports may provide supporting material relating to publications issued in the IAEA Human Health Series.

All of these publications can be downloaded cost free from the IAEA web site:

<http://www.iaea.org/Publications/index.html>

Further information is available from:

Marketing and Sales Unit
International Atomic Energy Agency
Vienna International Centre
PO Box 100
1400 Vienna, Austria

Readers are invited to provide their impressions on these publications. Information may be provided via the IAEA web site, by mail at the address given above, or by email to:

Official.Mail@iaea.org.

ATLAS OF NON-FDG PET-CT
IN DIAGNOSTIC ONCOLOGY

The following States are Members of the International Atomic Energy Agency:

AFGHANISTAN	GEORGIA	OMAN
ALBANIA	GERMANY	PAKISTAN
ALGERIA	GHANA	PALAU
ANGOLA	GREECE	PANAMA
ANTIGUA AND BARBUDA	GRENADA	PAPUA NEW GUINEA
ARGENTINA	GUATEMALA	PARAGUAY
ARMENIA	GUYANA	PERU
AUSTRALIA	HAITI	PHILIPPINES
AUSTRIA	HOLY SEE	POLAND
AZERBAIJAN	HONDURAS	PORTUGAL
BAHAMAS	HUNGARY	QATAR
BAHRAIN	ICELAND	REPUBLIC OF MOLDOVA
BANGLADESH	INDIA	ROMANIA
BARBADOS	INDONESIA	RUSSIAN FEDERATION
BELARUS	IRAN, ISLAMIC REPUBLIC OF	RWANDA
BELGIUM	IRAQ	SAINT LUCIA
BELIZE	IRELAND	SAINT VINCENT AND THE GRENADINES
BENIN	ISRAEL	SAMOA
BOLIVIA, PLURINATIONAL STATE OF	ITALY	SAN MARINO
BOSNIA AND HERZEGOVINA	JAMAICA	SAUDI ARABIA
BOTSWANA	JAPAN	SENEGAL
BRAZIL	JORDAN	SERBIA
BRUNEI DARUSSALAM	KAZAKHSTAN	SEYCHELLES
BULGARIA	KENYA	SIERRA LEONE
BURKINA FASO	KOREA, REPUBLIC OF	SINGAPORE
BURUNDI	KUWAIT	SLOVAKIA
CAMBODIA	KYRGYZSTAN	SLOVENIA
CAMEROON	LAO PEOPLE'S DEMOCRATIC REPUBLIC	SOUTH AFRICA
CANADA	LATVIA	SPAIN
CENTRAL AFRICAN REPUBLIC	LEBANON	SRI LANKA
CHAD	LESOTHO	SUDAN
CHILE	LIBERIA	SWEDEN
CHINA	LIBYA	SWITZERLAND
COLOMBIA	LIECHTENSTEIN	SYRIAN ARAB REPUBLIC
COMOROS	LITHUANIA	TAJIKISTAN
CONGO	LUXEMBOURG	THAILAND
COSTA RICA	MADAGASCAR	TOGO
CÔTE D'IVOIRE	MALAWI	TRINIDAD AND TOBAGO
CROATIA	MALAYSIA	TUNISIA
CUBA	MALI	TURKEY
CYPRUS	MALTA	TURKMENISTAN
CZECH REPUBLIC	MARSHALL ISLANDS	UGANDA
DEMOCRATIC REPUBLIC OF THE CONGO	MAURITANIA	UKRAINE
DENMARK	MAURITIUS	UNITED ARAB EMIRATES
DJIBOUTI	MEXICO	UNITED KINGDOM OF GREAT BRITAIN AND NORTHERN IRELAND
DOMINICA	MONACO	UNITED REPUBLIC OF TANZANIA
DOMINICAN REPUBLIC	MONGOLIA	UNITED STATES OF AMERICA
ECUADOR	MONTENEGRO	URUGUAY
EGYPT	MOROCCO	UZBEKISTAN
EL SALVADOR	MOZAMBIQUE	VANUATU
ERITREA	MYANMAR	VENEZUELA, BOLIVARIAN REPUBLIC OF
ESTONIA	NAMIBIA	VIET NAM
ESWATINI	NEPAL	YEMEN
ETHIOPIA	NETHERLANDS	ZAMBIA
FIJI	NEW ZEALAND	ZIMBABWE
FINLAND	NICARAGUA	
FRANCE	NIGER	
GABON	NIGERIA	
	NORTH MACEDONIA	
	NORWAY	

The Agency's Statute was approved on 23 October 1956 by the Conference on the Statute of the IAEA held at United Nations Headquarters, New York; it entered into force on 29 July 1957. The Headquarters of the Agency are situated in Vienna. Its principal objective is "to accelerate and enlarge the contribution of atomic energy to peace, health and prosperity throughout the world".

IAEA HUMAN HEALTH SERIES No. 38

ATLAS OF NON-FDG PET–CT IN DIAGNOSTIC ONCOLOGY

INTERNATIONAL ATOMIC ENERGY AGENCY
VIENNA, 2021

COPYRIGHT NOTICE

All IAEA scientific and technical publications are protected by the terms of the Universal Copyright Convention as adopted in 1952 (Berne) and as revised in 1972 (Paris). The copyright has since been extended by the World Intellectual Property Organization (Geneva) to include electronic and virtual intellectual property. Permission to use whole or parts of texts contained in IAEA publications in printed or electronic form must be obtained and is usually subject to royalty agreements. Proposals for non-commercial reproductions and translations are welcomed and considered on a case-by-case basis. Enquiries should be addressed to the IAEA Publishing Section at:

Marketing and Sales Unit, Publishing Section
International Atomic Energy Agency
Vienna International Centre
PO Box 100
1400 Vienna, Austria
fax: +43 1 26007 22529
tel.: +43 1 2600 22417
email: sales.publications@iaea.org
www.iaea.org/publications

© IAEA, 2021

Printed by the IAEA in Austria

October 2021

STI/PUB/1924

IAEA Library Cataloguing in Publication Data

Names: International Atomic Energy Agency.

Title: Atlas of non-FDG PET-CT in diagnostic oncology / International Atomic Energy Agency.

Description: Vienna : International Atomic Energy Agency, 2021. | Series: IAEA human health series, ISSN 2075-3772 ; no. 38 | Includes bibliographical references.

Identifiers: IAEAL 21-01410 | ISBN 978-92-0-128920-9 (paperback : alk. paper) | ISBN 978-92-0-129020-5 (pdf) | ISBN 978-92-0-129120-2 (epub)

Subjects: LCSH: Tomography, Emission. | Tomography. | Cancer — Radionuclide imaging. | Oncology.

Classification: UDC 616-073 | STI/PUB/1924

FOREWORD

Positron emission tomography–computed tomography (PET–CT) plays a central role in the management of cancer patients and is an increasingly important part of the overall health care landscape owing to the rising prevalence of non-communicable diseases, the need for early and accurate diagnostic methods, technological developments both in hardware and in software, the availability of new tracers and the acceptance of this technology in emerging markets.

Fluorodeoxyglucose (FDG) PET–CT has earned global recognition as a significant tool in the modern management of cancer patients and is rapidly becoming an important imaging modality for patients with cardiac, neurological and infectious/inflammatory conditions. Despite its proven benefits as a PET radiopharmaceutical in oncology, FDG has limitations in the assessment of several relevant tumours such as prostate cancer. In addition, new therapeutic options available today in the management of cancer have underscored the need for assessing tumour characteristics other than metabolism. Therefore, there has been a pressing need for the development and clinical assessment of additional PET radiopharmaceuticals that can enable imaging and precise characterization of various aspects of a wide range of malignant tumours.

It is hoped that this publication will be beneficial to medical professionals from IAEA Member States for learning and teaching. The IAEA wishes to thank the contributors to the drafting and review of the publication for contributing their knowledge, time and effort. The IAEA officers responsible for this publication were R. Nuñez Miller, F. Giammarile and D. Paez of the Division of Human Health.

EDITORIAL NOTE

Although great care has been taken to maintain the accuracy of information contained in this publication, neither the IAEA nor its Member States assume any responsibility for consequences which may arise from its use.

This publication does not address questions of responsibility, legal or otherwise, for acts or omissions on the part of any person.

Guidance provided here, describing good practices, represents expert opinion but does not constitute recommendations made on the basis of a consensus of Member States.

The use of particular designations of countries or territories does not imply any judgement by the publisher, the IAEA, as to the legal status of such countries or territories, of their authorities and institutions or of the delimitation of their boundaries.

The mention of names of specific companies or products (whether or not indicated as registered) does not imply any intention to infringe proprietary rights, nor should it be construed as an endorsement or recommendation on the part of the IAEA.

The IAEA has no responsibility for the persistence or accuracy of URLs for external or third party Internet web sites referred to in this book and does not guarantee that any content on such web sites is, or will remain, accurate or appropriate.

CONTENTS

1.	INTRODUCTION	1
1.1.	Background	1
1.2.	Objective	1
1.3.	Scope	1
1.4.	Structure	2
2.	ACETATE (¹¹ C)	2
2.1.	General characteristics	2
2.2.	Pharmacokinetics	3
2.3.	Methodology	4
2.4.	Clinical aspects	4
3.	BEVACIZUMAB (⁸⁹ Zr)	7
3.1.	General characteristics	7
3.2.	Pharmacokinetics	7
3.3.	Methodology	8
3.4.	Clinical aspects	8
4.	CHOLINE (¹¹ C)	12
4.1.	General characteristics	12
4.2.	Pharmacokinetics	12
4.3.	Methodology	14
4.4.	Clinical aspects	14
5.	CHOLINE (¹⁸ F)	29
5.1.	General characteristics	29
5.2.	Pharmacokinetics	29
5.3.	Methodology	31
5.4.	Clinical aspects	31
6.	FLUORO-DIHYDROTESTOSTERONE — FDHT (¹⁸ F)	46
6.1.	General characteristics	46
6.2.	Pharmacokinetics	46
6.3.	Methodology	47
6.4.	Clinical aspects	47
7.	F-DOPA (¹⁸ F)	52
7.1.	General characteristics	52
7.2.	Pharmacokinetics	52
7.3.	Methodology	53

7.4.	Clinical aspects	54
8.	FLUROESTRADIOL, FES (¹⁸ F).....	73
8.1.	General characteristics	73
8.2.	Pharmacokinetics.....	73
8.3.	Methodology	74
8.4.	Clinical aspects	74
9.	FLUROETHYL-TYROSINE, FET (¹⁸ F)	79
9.1.	General characteristics	79
9.2.	Pharmacokinetics.....	79
9.3.	Methodology	81
9.4.	Clinical aspects	81
10.	FLUROTHYMIDINE, FLT (¹⁸ F).....	98
10.1.	General characteristics	98
10.2.	Pharmacokinetics.....	99
10.3.	Methodology	100
10.4.	Clinical aspects	100
11.	FLUCICLOVINE, FACBC (¹⁸ F)	103
11.1.	General characteristics	103
11.2.	Pharmacokinetics.....	103
11.3.	Methodology	104
11.4.	Clinical aspects	105
12.	FMISO (¹⁸ F)	113
12.1.	General characteristics	113
12.2.	Pharmacokinetics.....	113
12.3.	Methodology	115
12.4.	Clinical aspects	115
13.	FAZA (¹⁸ F)	117
13.1.	General characteristics	117
13.2.	Pharmacokinetics.....	117
13.3.	Methodology	118
13.4.	Clinical aspects	118
14.	EXENDIN (⁶⁸ Ga)	120
14.1.	General characteristics	120
14.2.	Pharmacokinetics.....	120
14.3.	Methodology	122
14.4.	Clinical aspects	122

15.	5-HYDROXYTRYPTOPHAN, HTP (¹¹ C).....	124
15.1.	General characteristics	124
15.2.	Pharmacokinetics.....	124
15.3.	Methodology	125
15.4.	Clinical aspects	125
16.	METHIONINE (¹¹ C)	128
16.1.	General characteristics	128
16.2.	Pharmacokinetics.....	128
16.3.	Methodology	129
16.4.	Clinical aspects	130
17.	SODIUM FLUORIDE, NaF (¹⁸ F).....	141
17.1.	General characteristics	141
17.2.	Pharmacokinetics.....	141
17.3.	Methodology	142
17.4.	Clinical aspects	142
18.	SODIUM IODIDE, NaI (¹²⁴ I)	151
18.1.	General characteristics	151
18.2.	Pharmacokinetics.....	151
18.3.	Methodology	152
18.4.	Clinical aspects	152
19.	PSMA LIGAND (⁶⁸ Ga)	156
19.1.	General characteristics	156
19.2.	Pharmacokinetics.....	156
19.3.	Methodology	158
19.4.	Clinical aspects	158
20.	SOMATOSTATIN ANALOGUES (⁶⁸ Ga)	179
20.1.	General characteristics	179
20.2.	Pharmacokinetics.....	179
20.3.	Methodology	182
20.4.	Clinical aspects	182
21.	TRASTUZUMAB (⁸⁹ Zr)	219
21.1.	General characteristics	219
21.2.	Pharmacokinetics.....	219
21.3.	Methodology	220
21.4.	Clinical aspects	220
22.	YTTRIUM MICROSPHERES AFTER SELECTIVE INTERNAL RADIATION THERAPY (⁹⁰ Y).....	224

22.1. General characteristics	224
22.2. Pharmacokinetics.....	224
22.3. Methodology	225
22.4. Clinical aspects	225
ABBREVIATIONS.....	229
REFERENCES	231
LIST OF CONTRIBUTORS TO DRAFTING AND REVIEW	239

1. INTRODUCTION

1.1. BACKGROUND

Several non-fluorine-18 fluorodeoxyglucose (non-¹⁸F-FDG) positron emission tomography (PET) radiopharmaceuticals have been introduced into the clinical arena over the last few years, in some countries more rapidly than others. It is expected that the use of these radiopharmaceuticals will continue to spread internationally, since the use of positron emission tomography–computed tomography (PET–CT) with different radiopharmaceuticals, catering to the type of tumour and the biological process that needs to be assessed, enables greater personalization (precision) in medicine.

The constant growth of PET–CT, as well as the increasing use of novel non-¹⁸F-FDG PET–CT radiopharmaceuticals, creates a need for training in the proper acquisition and interpretation of complex imaging studies with compounds that have very different biodistribution, normal variants and pitfalls. In addition, the use of several of these non-¹⁸F-FDG PET radiopharmaceuticals, such as ⁶⁸Ga labelled prostate specific membrane antigen (⁶⁸Ga-PSMA) and ⁶⁸Ga labelled octreotide, constitutes an integral part of the evaluation of patients who are potential candidates for ‘theranostic’ medicine combining therapeutics and diagnostics in individualized treatment. This further increases their clinical relevance and the need for accurate imaging methodology.

1.2. OBJECTIVE

The objective of this publication is to provide a case based presentation of the normal biodistribution, variants and pitfalls, and different imaging patterns for the main indications for each of the new non-¹⁸F-FDG PET radiopharmaceuticals. This should facilitate the interpretation of non-¹⁸F-FDG PET–CT procedures in order to ensure that, in clinical practice, the study report is accurate and helpful.

1.3. SCOPE

This publication contains sections for each of the most commonly used non-¹⁸F-FDG PET radiopharmaceuticals. Some of these radiopharmaceuticals are already commercially available in many countries (e.g. ⁶⁸Ga-DOTATATE and ⁶⁸Ga-DOTATOC, and ⁶⁸Ga-PSMA), and some are still under investigation (e.g. ⁸⁹Zr-trastuzumab). Furthermore, this list will have to be updated, as the use of some radiopharmaceuticals is increasing, while others will gradually see less use. Nevertheless, this atlas provides a good overview as it presents 160 clinical cases representing the current state of non-FDG PET–CT imaging in oncology. While the imaging protocol of the PET component of the study is presented in detail for the PET–CT studies performed with each radiopharmaceutical, this approach has not been used for describing the CT component. Since all sections discuss oncological clinical applications, CT can be performed using either low dose or diagnostic techniques, with or without contrast enhanced parameters, depending on the specific clinical question and the institutional expertise and requirements.

The length of the sections varies according to the number of cases included. The sections dedicated to the most commonly used non-¹⁸F-FDG PET radiopharmaceuticals contain more cases and more extensive overviews compared to the sections dedicated to the radiopharmaceuticals solely used for research. Guidance provided here, describing good practices, represents expert opinion but does not constitute recommendations made on the basis of a consensus of Member States.

1.4. STRUCTURE

This publication contains 22 sections, including 160 cases of patients with various malignancies. The radiopharmaceuticals are classified in alphabetical order, with each in its own section. Longer sections reflect the more extensive use of particular radiopharmaceuticals.

The sections are structured in a simple way in order to facilitate interpretation of the studies. Each section begins with a brief overview of the physical and chemical characteristics of the non- ^{18}F -FDG PET radiopharmaceutical and of the physiological biodistribution, and continues with a simple list of the main parameters for the PET–CT imaging protocol, based mainly on the protocol used by the corresponding authors in their home centres. A list of the most common current indications is then presented. The sections conclude with a review of several cases, which cover different variants and pitfalls, and the main indications for each type of study. Each case has a simple structure containing the following information: (1) clinical indication for the PET–CT study; (2) brief clinical history; (3) main relevant PET–CT findings; (4) teaching point(s); (5) keywords.

2. ACETATE (^{11}C)

2.1. GENERAL CHARACTERISTICS

Name: ^{11}C -acetate

Synonyms: $\text{CH}_3[^{11}\text{C}]\text{O}_2$

Radioisotope

^{11}C is a short half-life PET radioisotope (20.4 min) emitting positrons of maximum β energy (E_{max}) 0.970 MeV. Owing to the abundance of carbon in the chemistry of life and biomolecules, all ^{11}C labelled radiopharmaceuticals demonstrate identical behaviour to natural compounds, allowing tracing of biological processes [1].

Radiosynthesis

Owing to the short half-life of the radionuclide, the tracer production is usually performed on-site (Fig. 2.1). ^{11}C -acetate can be produced by reaction of a Grignard reagent with the ^{11}C - CO_2 produced from a gas target in a cyclotron (radiochemical yield $72\% \pm 12\%$ in 20 min, specific activity >18.5 GBq/ μmol , radiochemical purity $>95\%$). Automated systems provide radiochemical yields of 60–80% and radiochemical purity of 99% in 15–23 min [1].

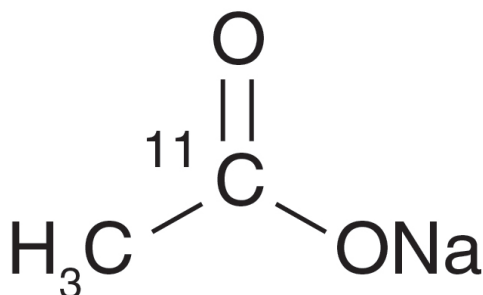


FIG. 2.1. Molecular structure of ^{11}C -acetate.

2.2. PHARMACOKINETICS

2.2.1. Physiological biodistribution and metabolism

After injection, the tracer is dispersed in many human tissues, including the pancreas, bowels, liver, kidneys and spleen, which get the highest doses. The tracer is not excreted in urine under normal circumstances (Fig. 2.2). ^{11}C -acetate is typically incorporated into the cellular membrane in proportion to the cellular proliferation rate or, alternatively, oxidized to carbon dioxide and water. ^{11}C -acetate may also be converted into amino acids.



FIG. 2.2. Normal biodistribution of ^{11}C -acetate.

2.2.2. Mechanism of retention

Like the natural acetate molecule, ^{11}C -acetate is converted by acetyl-CoA synthetase in the cytosol or mitochondria to acetyl-CoA and further incorporated by the action of fatty acid synthetase enzyme into fatty acids. These are then integrated into the intracellular phosphatidylcholine membrane microdomains (dominant pathway in cancer cells) or alternatively oxidized through the tricarboxylic acid cycle in mitochondria to carbon dioxide and water (dominant pathway in normal myocardium).

2.2.3. Pharmacology and toxicology

Uptake of ^{11}C -acetate is proportional to fatty acid synthesis as well as to myocardial blood flow, and therefore myocardial oxygen consumption. In rodents, ^{11}C -acetate is cleared from all organs except the pancreas within 1 hour. In humans, more than 80% of the tracer is cleared from normal tissues within 20 min. While it is taken up in primary prostate cancer and its metastases, increased activity has been also reported in hyperplastic and benign prostate tissue. No urinary excretion is seen. No toxic effects have been demonstrated.

2.3. METHODOLOGY

2.3.1. Activity, administration, dosimetry

The intravenous (IV) administered activity ranges from 500 to 1480 MBq. The organs receiving the highest absorbed dose are the pancreas (0.017 mGy/MBq or 62.9 mrad/mCi), bowel (0.011 mGy/MBq or 40.7 mrad/mCi), kidneys (0.0092 mGy/MBq or 34.0 mrad/mCi) and spleen (0.0092 mGy/MBq or 34.0 mrad/mCi). The effective dose equivalent is 0.0062 mSv/MBq (22.9 mrem/mCi) [2–7].

2.3.2. Imaging protocol

A fasting period of at least 4 hours prior to administration of the radiotracer is suggested. Imaging is performed following the IV injection of a dose of 4–5 MBq/kg and an uptake period of 10–20 min. Acquisition of the PET component starts from the pelvis with an acquisition time of 3 min/bed position. For the CT component, see general comments in Section 1.3.

2.4. CLINICAL ASPECTS

2.4.1. Indications

The first clinical application of ^{11}C -acetate was in prostate cancer, mainly for disease restaging in the case of biochemical recurrence (BCR) [3]. ^{11}C -acetate has also been applied to other urological malignancies, such as renal cell and bladder cancer [4].

An important application at present is well differentiated hepatocellular carcinoma (HCC) [5], a tumour with known false negative results using ^{18}F -FDG PET–CT. The use of ^{11}C -acetate in addition to ^{18}F -FDG in evaluating patients with HCC can increase the diagnostic accuracy, as demonstrated by a small number of well designed studies [6].

Other clinical applications of ^{11}C -acetate imaging include brain tumours [7] and lung carcinoma.

The main limitation for the clinical use of ^{11}C -acetate is its limited availability and the need for an on-site cyclotron for its production. Despite this limitation, the tracer can be considered as accurate and useful, particularly for the detection of non- ^{18}F -FDG-avid neoplasm, such as differentiated HCC and renal cell carcinoma.

2.4.2. Cases

2.4.2.1. Case No. 2.1

Clinical indication for PET–CT: HCC, restaging

Clinical history

A 78 year old man with metastatic HCC after liver transplantation underwent ^{11}C -acetate and ^{18}F -FDG PET–CT in a single day.

PET–CT findings

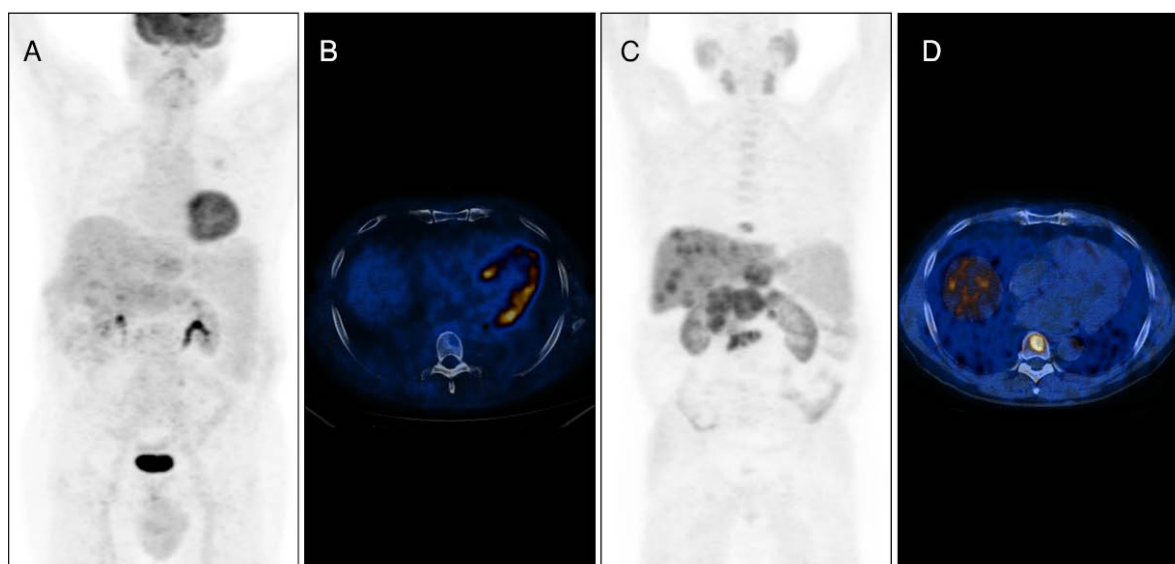
(A): ^{18}F -FDG, maximum intensity projection (MIP); (B): ^{18}F -FDG, fused transaxial slice of upper abdomen; (C): ^{11}C -acetate, MIP; (D): ^{11}C -acetate, same cut as in (B).

There are multiple areas of increased ^{11}C -acetate uptake in the liver, and in lymph node (LN) and lytic bone metastases, with only faint or no corresponding uptake of ^{18}F -FDG.

Teaching point

In well differentiated HCC, ^{11}C -acetate PET–CT can provide clinically significant information.

Keywords: HCC, restaging, ^{11}C -acetate, ^{18}F -FDG



Clinical indication for PET–CT: Poorly differentiated HCC, staging

Clinical history

A 69 year old patient with newly diagnosed HCC underwent a single day acquisition of ^{11}C -acetate and ^{18}F -FDG PET–CT.

PET–CT findings

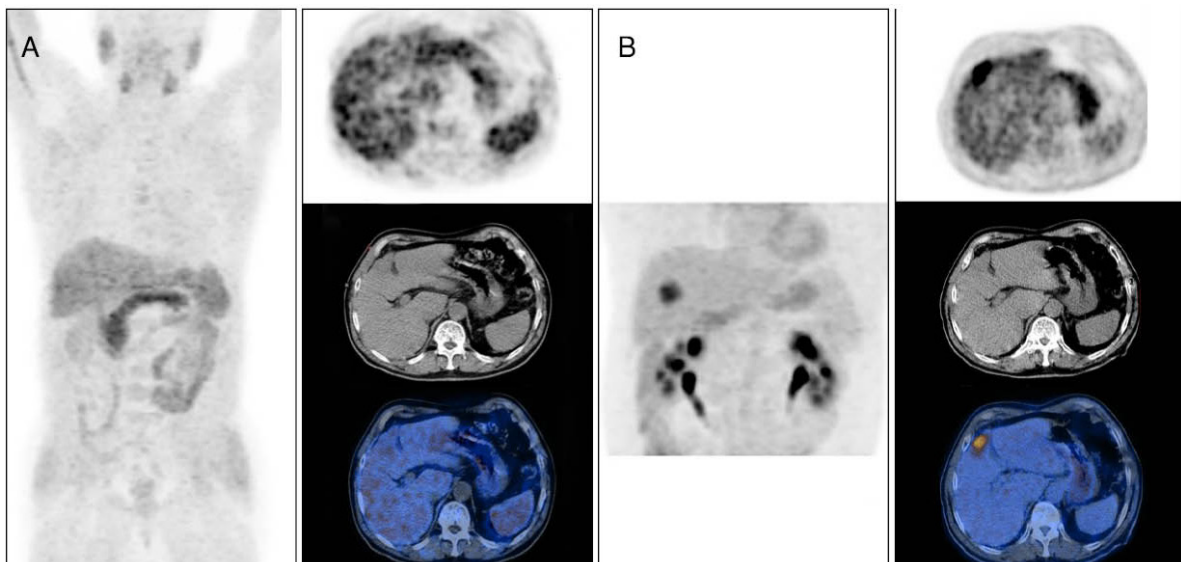
(A): ^{11}C -acetate, PET, CT and fused transaxial slices of upper abdomen and MIP; (B): ^{18}F -FDG, partial MIP and same slices as in (A).

There are no abnormal findings on the ^{11}C -acetate study (A), while increased focal ^{18}F -FDG uptake is demonstrated in a hypodense lesion in liver segment 4 seen on the CT component (B), consistent with the primary HCC.

Teaching point

In poorly differentiated HCC, the complementary information provided by ^{18}F -FDG imaging may significantly increase the accuracy of ^{11}C -acetate PET–CT.

Keywords: HCC, staging, ^{11}C -acetate, ^{18}F -FDG



3. BEVACIZUMAB (^{89}Zr)

3.1. GENERAL CHARACTERISTICS

Name: ^{89}Zr -bevacizumab

Synonyms: ^{89}Zr -N-succinyl-desferrioxamine-bevacizumab; ^{89}Zr -desferrioxamine-bevacizumab

Radioisotope

^{89}Zr is a long half-life PET radioisotope (78.4 hours) emitting positrons of E_{max} 0.395 5 keV, usually obtained from biomedical cyclotrons at a proton energy of 14 MeV using natural ^{89}Y targets [8, 9].

Radiosynthesis

The routine production of radiometal labelled antibodies is a process consisting of two steps: (1) development of conjugated antibody and (2) radiolabelling [8, 9]. In this case, reconstituted bevacizumab is conjugated with tetrafluorphenol-N-succinyl-desferal-Fe, purified and stored at 28°C. ^{89}Zr -oxalate produced according to good manufacturing practice guidelines is used for radiolabelling the conjugate (Fig. 3.1). Quality control is performed to ensure radiochemical purity (>95%), antigen binding (>60%) and stability [8, 9].

3.2. PHARMACOKINETICS

3.2.1. Metabolism

Bevacizumab's biological half-life is about 20 days. Its metabolism routes are not clear.

3.2.2. Mechanism of retention

Vascular endothelial growth factor A (VEGF-A) is overexpressed in most malignant and premalignant breast lesions. Bevacizumab is a recombinant humanized immunoglobulin G monoclonal antibody developed against the VEGF-A antigen. When it is labelled by ^{89}Zr it can be used in imaging of malignancies.

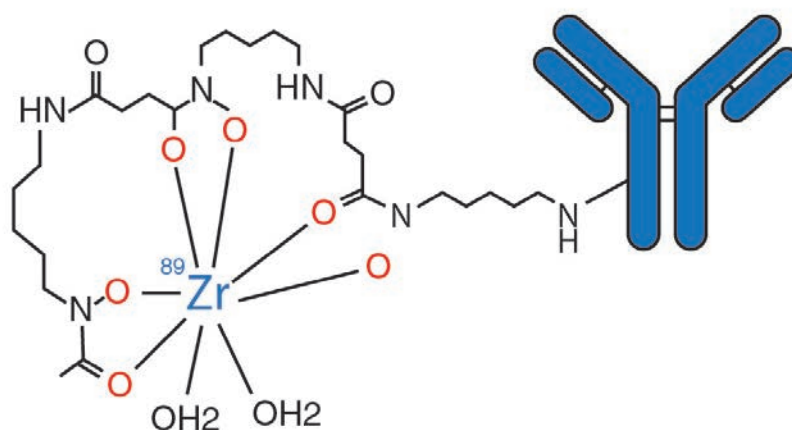


FIG. 3.1. Molecular structure of ^{89}Zr -bevacizumab.

3.2.3. Pharmacology and toxicology

While no data for radiolabelled ^{89}Zr -bevacizumab are available, the doses of the cold antibody (Avastin) used for cancer chemotherapy are in the range of 5–15 mg/kg. The total amount of antibody used in a single ^{89}Zr PET scan is 5 mg, far below the clinically administered levels.

3.3. METHODOLOGY

3.3.1. Activity, administration, dosimetry

The administered activity of ^{89}Zr -bevacizumab is 0.1 mg and 0.9 MBq/kg. The mean effective dose per patient is 0.9 mSv/MBq (with a standard deviation of 0.3 mSv/MBq) [8, 10–16].

3.3.2. Imaging protocol

No special patient preparation is required prior to administration of the radiotracer. Imaging is performed following the IV injection of a dose of 37 MBq. The uptake period is 4 days. Acquisition of the PET component starts from the pelvis and the acquisition time is 5 min/bed position. For the CT imaging protocol, see general comments in Section 1.3.

3.4. CLINICAL ASPECTS

3.4.1. Indications

PET–CT using this tracer has been investigated at the University Medical Centre Groningen, the Netherlands. Several studies have been published using this experimental tracer to assess the VEGF-A receptor status in the microenvironment of both benign and malignant lesions, especially for therapy stratification [8, 10–16]. Because it is still investigational, scans using this tracer are not routinely performed in clinical practice.

3.4.2. Cases

Cases courtesy of A. Brouwers, University Medical Centre Groningen, the Netherlands.

3.4.2.1. Case No. 3.1

Clinical indication for PET–CT: Metastatic paraganglioma; to assess the VEGF-A receptor status in known metastatic lesions

Clinical history

A 31 year old man with metastatic paraganglioma, SDHB mutation positive, diagnosed 3 years earlier with a large inoperable presacral mass. After ^{131}I -metaiodobenzylguanidine (miBG) treatment (2×7400 MBq), he developed tumour progression with new bone metastases. Embolization followed by debulking of the presacral tumour mass was performed. Because the disease was ongoing and progressive,

several treatment lines were applied, including selective embolization in a large bone lesion in the skull and palliative radiation therapy (RT) in other osseous metastases, and a systemic mechanistic target of rapamycin inhibitor (everolimus), followed by three cycles of ^{177}Lu -DOTATATE. Finally, experimental systemic therapy with the receptor tyrosine kinase inhibitor sunitinib was considered.

PET–CT findings

(Left): MIP; (centre): PET, fused and CT sagittal slices; (right): transaxial slices of pelvis.

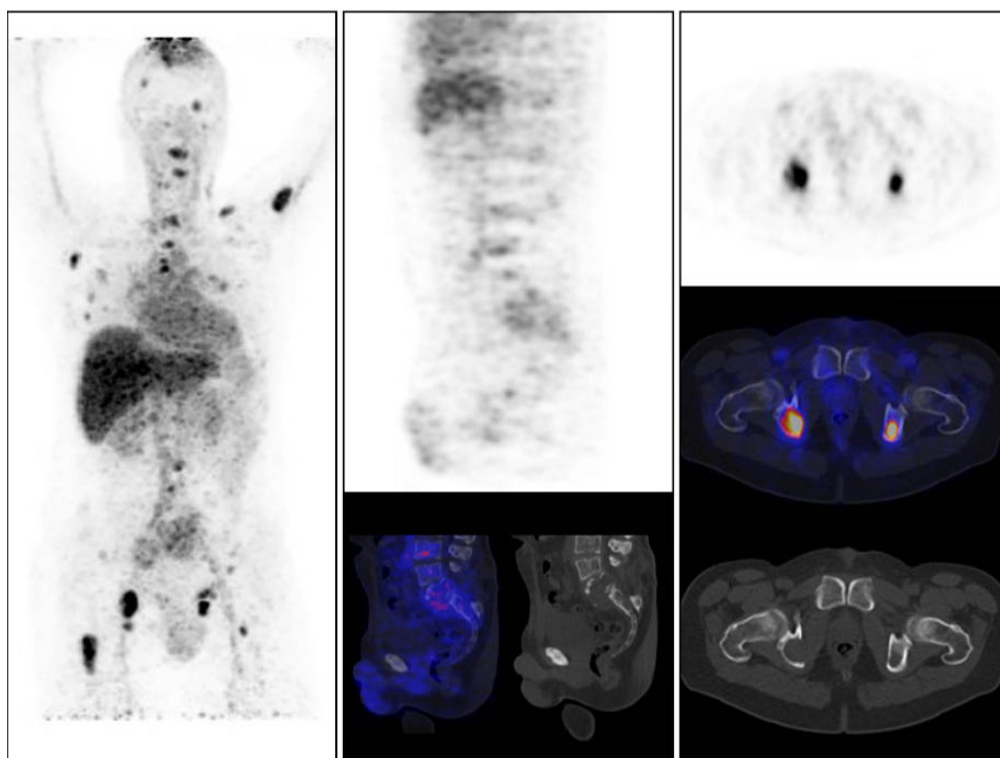
There is ^{89}Zr -bevacizumab uptake in the known bone metastases, of lower intensity in the previously extensively treated presacral and skull lesions.

Follow-up: Anti-VEGF-A treatment with the receptor tyrosine kinase inhibitor sunitinib was started in an experimental treatment setting.

Teaching point

^{89}Zr -bevacizumab PET–CT contributed to therapy stratification. Based on the study findings, experimental treatment with sunitinib, which also interferes with VEGF-A was initiated.

Keywords: Metastatic paraganglioma, VEGF-A status, therapy stratification, ^{89}Zr -bevacizumab



3.4.2.2. Case No. 3.2

Clinical indication for PET–CT: Multiple hemangioblastomas in the central nervous system (CNS); ^{89}Zr -bevacizumab PET–CT was requested prior to therapy stratification for assessing the VEGF-A receptor status in known lesions

Clinical history

A 37 year old man presented with multiple CNS hemangioblastomas, with negative mutation analysis for Von Hippel–Lindau. The first hemangioblastoma, in the cerebellum, had been surgically removed. Partial paraplegia occurred after removal of an additional hemangioblastoma in the T-12 vertebra. The patient had disease progression and developed high intracranial pressure, so a ventriculo-peritoneal drain was inserted. Because of life threatening hemangioblastomas located in the brain stem, experimental systemic therapy with a VEGF-A blocking monoclonal antibody (bevacizumab) was considered.

PET–CT findings

(Left): MIP; (right): PET, CT and fused sagittal slices of head.

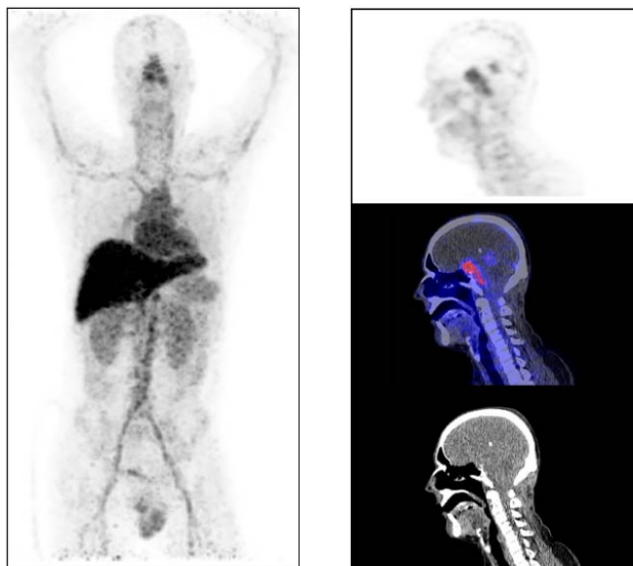
There is ^{89}Zr -bevacizumab uptake in two brain stem lesions.

Follow-up: Anti-VEGF-A treatment (monoclonal antibody bevacizumab) was started in an experimental treatment setting.

Teaching point

Treatment with the monoclonal antibody bevacizumab was instituted based on ^{89}Zr -bevacizumab PET–CT findings.

Keywords: CNS hemangioblastomas, VEGF-A status, therapy stratification, ^{89}Zr -bevacizumab



3.4.2.3. Case No. 3.3

Clinical indication for PET–CT: Metastatic renal cell carcinoma, prior to therapy stratification

Clinical history

A 62 year old woman with a history of right renal cell carcinoma had undergone nephrectomy 17 years earlier. Ten years after that, she presented with a right upper lobe lung metastasis that was excised. She was subsequently treated with various lines of systemic treatment but showed disease progression with development of bone metastases and local recurrence. ^{89}Zr -bevacizumab PET–CT was requested to assess VEGF-A receptor status prior to experimental treatment.

PET–CT findings

(Left): MIP; (top right:) transaxial fused slices of lower chest; (bottom right): transaxial fused slices of mid-abdomen.

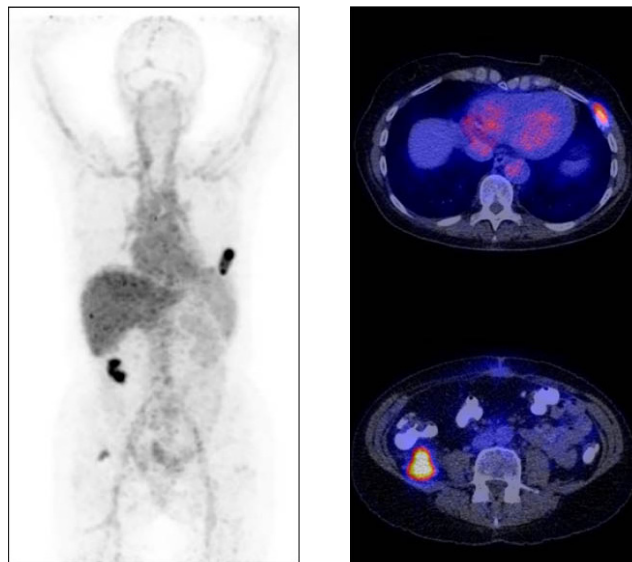
There is increased tracer uptake in the right lumbar region consistent with local recurrence, and in lesions in the left lower ribs and right femoral head, consistent with known bone metastases.

Follow-up: A mechanistic target of rapamycin inhibitor (everolimus) was started in a setting of a clinical trial.

Teaching point

Therapy stratification in this patient was based on the ^{89}Zr -bevacizumab PET–CT study, and treatment with a mechanistic target of rapamycin inhibitor was initiated.

Keywords: Metastatic renal cell carcinoma, VEGF-A receptor status, ^{89}Zr -bevacizumab



4. CHOLINE (^{11}C)

4.1. GENERAL CHARACTERISTICS

Name: ^{11}C -choline

Synonyms: [^{11}C]CH, ^{11}C -choline chloride

Radioisotope

^{11}C is a short half-life PET radioisotope (20.4 min) emitting positrons of E_{max} 0.970 MeV. Owing to the abundance of carbon in the chemistry of life and biomolecules, ^{11}C radiopharmaceuticals demonstrate identical behaviour to natural compounds, allowing tracing of biological processes.

Radiosynthesis

^{11}C -choline is synthesized by ^{11}C -methylation of dimethyl-ethanolamine in acetone, followed by solid phase extraction isolation of the product from dimethyl-ethanolamine on a cation exchange cartridge (Fig. 4.1). The cartridge is rinsed with ethanol to remove residual dimethyl-ethanolamine before elution of the product with sterile saline through a sterilization filter [17–21].

4.2. PHARMACOKINETICS

4.2.1. Physiological biodistribution and metabolism

Choline is an important component of phospholipids in cell membranes. Tissues with increased metabolism will also show increased uptake of choline. Because tumour cells have a high metabolic rate, their choline uptake is high in order to keep up with the demand for synthesis of phospholipids in their cellular membranes. Owing to its similarity to natural choline, ^{11}C -choline is absorbed and trapped in malignant cells in its phosphorylated form and thus used for cancer imaging.

After IV injection, ^{11}C -choline rapidly clears from the circulation (in less than 3 min). The highest normal tissue uptake is seen in the renal cortex, liver, pancreas, salivary glands, prostate and pituitary gland. Uptake in the thyroid is variable and of mild intensity. There is almost no uptake in the brain. Based on the relatively low urinary excretion, renal uptake is predominantly limited to the organ itself, rather than via the formation of urine. In most cases, no radioactive urine is seen in the ureters or bladder (Fig. 4.2 (top)). Intense tracer uptake can often be seen in the vein in which the tracer has been injected. Variable tracer uptake of moderate intensity can be seen in the bowel. Diffuse, faint uptake in the bone marrow can be found, especially due to rebound after treatment (Fig. 4.2 (bottom)) [17–21].

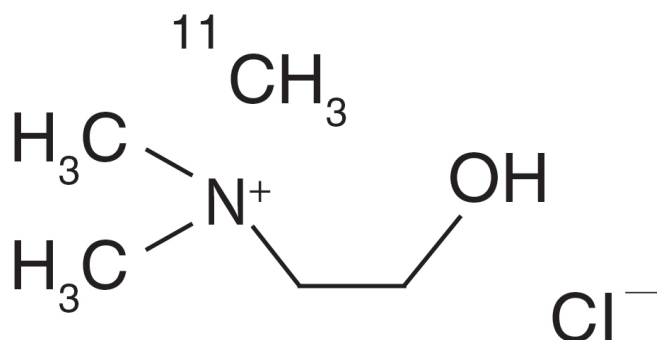


FIG. 4.1. Molecular structure of ^{11}C -choline.

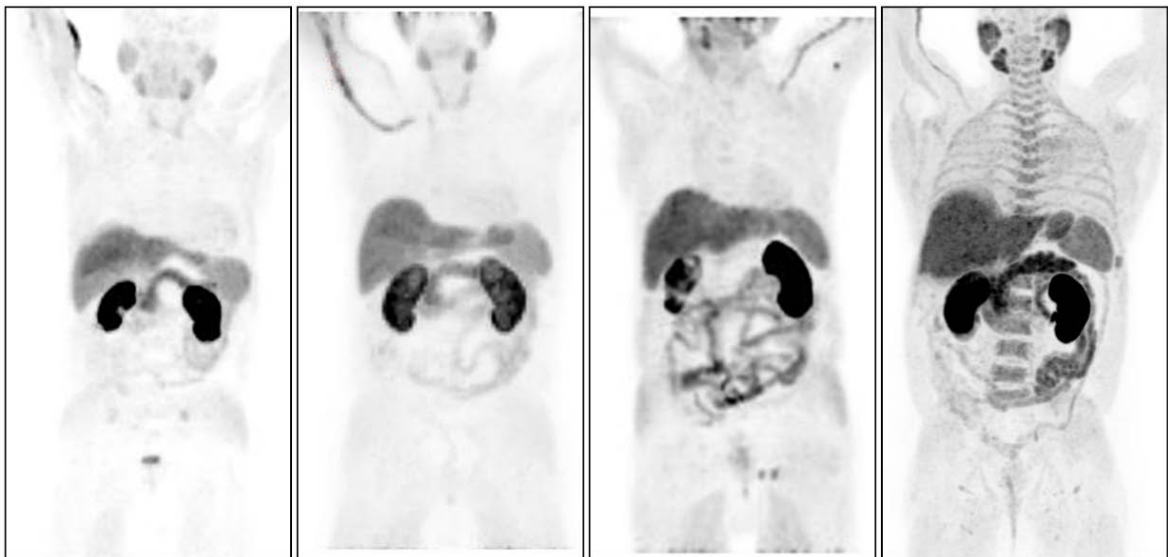
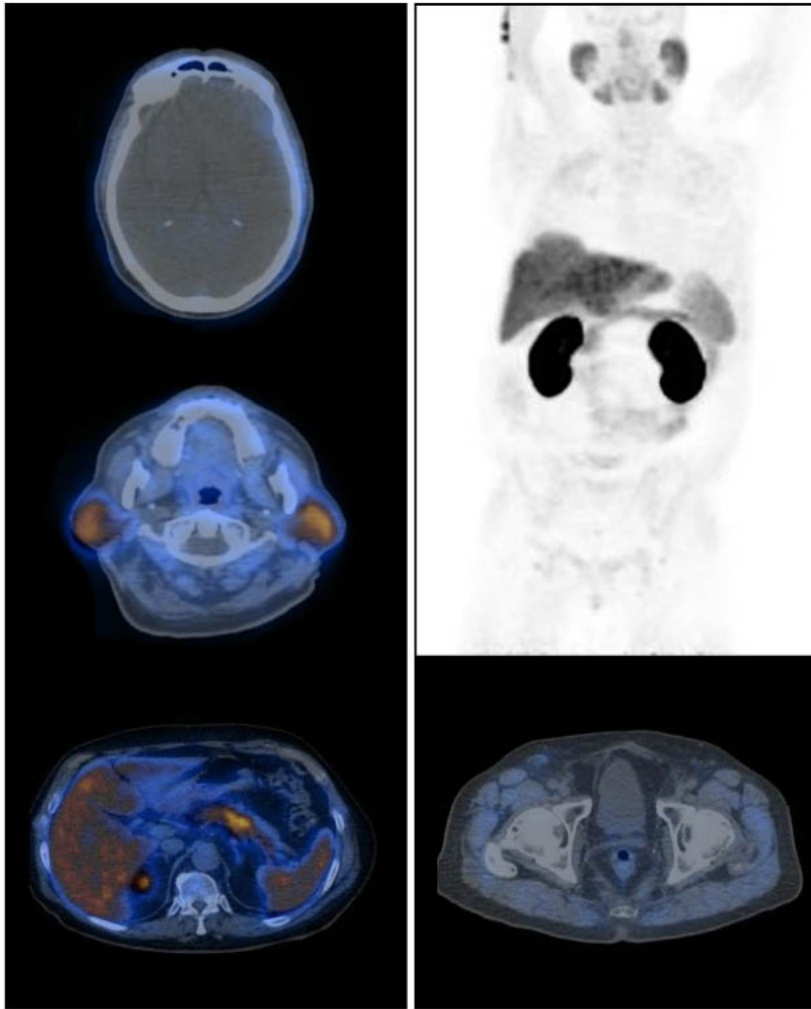


FIG. 4.2. Four examples of normal biodistribution of ^{11}C -choline.

4.2.2. Mechanism of retention

Choline is phosphorylated by choline kinase and incorporated into various phospholipids in the body. In certain tissues, including the kidney and liver, choline oxidation is prominent. The oxidative metabolite of choline, betaine, is excreted into the urine.

4.2.3. Pharmacology and toxicology

Choline is a natural compound with no known toxic effects at levels present in the radiolabelled dose. Long term studies have not been performed to evaluate the carcinogenic potential of ^{11}C -choline [17–21].

4.3. METHODOLOGY

4.3.1. Activity, administration, dosimetry

The usual administered IV dose is 4–5 MBq of ^{11}C -choline. It is suggested to inject the ^{11}C -choline with the patient already positioned on the tomograph's bed, to avoid the presence of radioactive urine in the bladder. Delayed images could be useful in selected cases. Keeping in mind the short half-life of the tracer, even delayed images must be acquired as soon as possible. The effective dose is estimated at 0.0040 ± 0.0003 mSv/MBq (0.0148 rem/mCi) for adults. The dose critical organ in adults is the liver, which receives 0.0131 ± 0.0015 mGy/MBq (0.0485 rad/mCi) [22–25].

4.3.2. Imaging protocol

A fasting period of at least 4 hours prior to administration of the radiotracer is suggested. Imaging is performed following the IV injection of a dose of 4–5 MBq/kg and an uptake period of 2–5 min. Acquisition of the PET component starts from the pelvis, with an acquisition time of 2–3 min/bed position. For the CT imaging protocol, see general comments in Section 1.3.

4.4. CLINICAL ASPECTS

4.4.1. Indications

^{11}C -choline PET–CT is used in prostate cancer for staging and restaging in cases of BCR after primary treatment.

^{11}C -choline PET–CT has a role in nodal staging, where it has shown a low sensitivity but a relatively high specificity [24, 25]. It can help direct patients to the most appropriate treatment strategy, such as extended lymph node dissection (LND) or less aggressive primary treatment, including RT or androgen deprivation therapy (ADT).

Restaging of the disease is performed in the case of BCR with prostate specific antigen (PSA) levels up to 0.2 ng/mL following radical prostatectomy or 2.0 ng/mL after RT [24]. The role of choline PET–CT is to differentiate between local and distant relapse. ^{11}C -choline PET–CT should be able to distinguish patients potentially treatable with salvage treatments (oligometastatic) from those affected by multimetastatic spread of the disease, who are ideal candidates for ADT. Appropriate use of this technique has shown a change in the decision making process in approximately half of cases [23].

4.4.2. Cases

4.4.2.1. Case No. 4.1

Clinical indication for PET–CT: High risk prostate cancer, staging

Clinical history

A 54 year old man with prostate cancer, Gleason score 4+4, PSA 23 ng/mL, was a candidate for radical prostatectomy. Magnetic resonance imaging (MRI) showed a primary T3a tumour and bilateral iliac nodal N1 involvement.

PET–CT findings

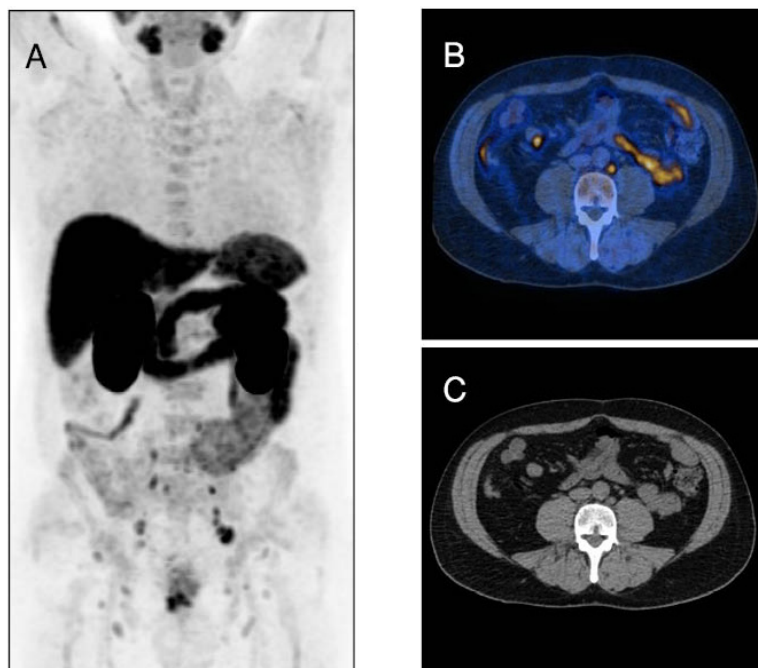
(A): MIP; (B): fused transaxial slices of lower abdomen; (C): CT transaxial slices of lower abdomen.

There are multiple foci of increased tracer uptake in pelvic and abdominal LN metastases as well as pathological uptake in the prostate.

Teaching point

¹¹C-choline PET–CT is of value for staging of high risk prostate cancer with impact on patient management. In this case the patient underwent extended LND.

Keywords: Prostate cancer, staging, change in management, ¹¹C-choline



4.4.2.2. Case No. 4.2

Clinical indication for PET–CT: High risk prostate cancer, staging

Clinical history

A 74 year old man with prostate cancer, Gleason score 4+5, PSA 126 ng/mL, stage T3a according to transrectal ultrasound (US), was considered for radical prostatectomy.

PET–CT findings

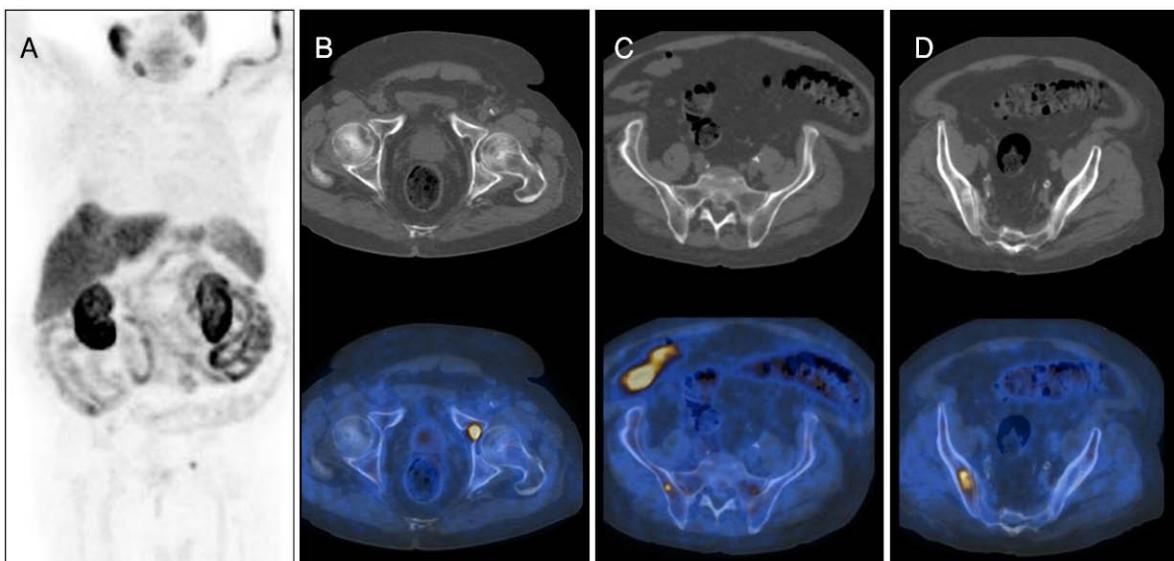
(A): MIP; (B–D): CT and fused transaxial slices of pelvis.

There are multiple foci of increased tracer uptake in the prostate and in bone metastases, in the right upper ilium and left ischium, without corresponding findings on CT (B and C), and in an osteoblastic lesion in the right lower ilium (D).

Teaching point

¹¹C-choline PET–CT is a sensitive method for early detection of bone metastases. Following the PET–CT study the patient was referred for systemic ADT instead of the scheduled surgery.

Keywords: Prostate cancer, staging, change in management, ¹¹C-choline



4.4.2.3. Case No. 4.3

Clinical indication for PET–CT: High risk prostate cancer, staging

Clinical history

A 64 year old man with prostate cancer, Gleason score 4+4, PSA 23 ng/mL, stage T3a according to transrectal US, was a candidate for radical prostatectomy.

PET–CT findings

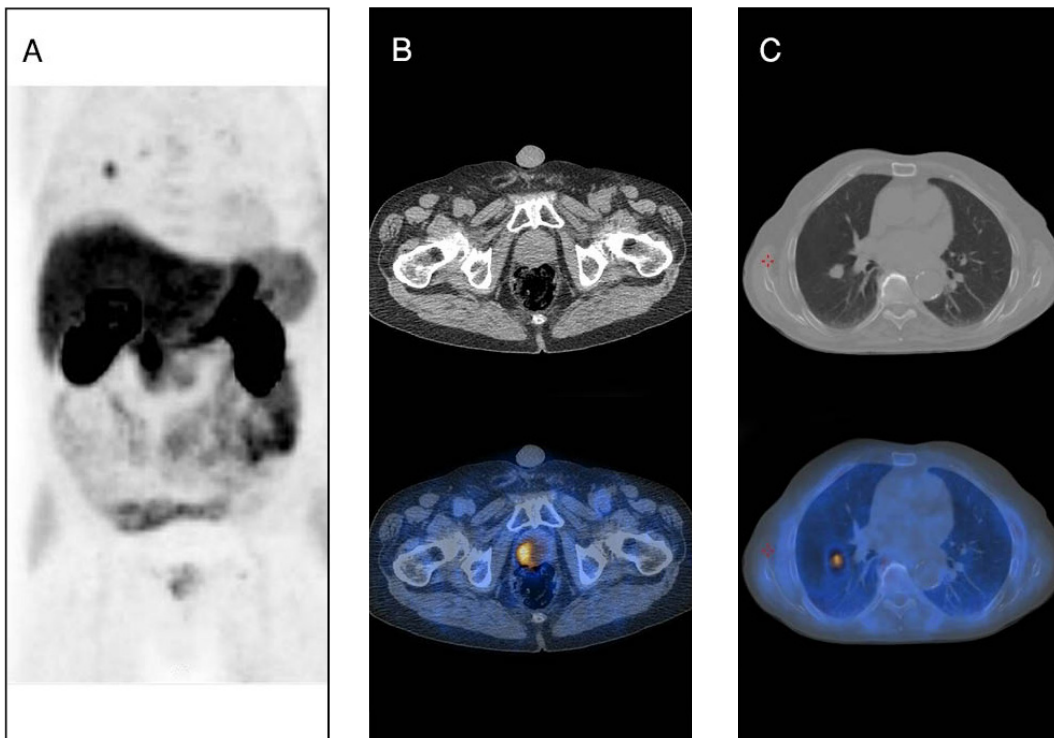
(A): MIP; (B): CT and fused transaxial slices of lower pelvis; (C): CT and fused transaxial slices of mid-chest.

There is focal increased tracer uptake in the right lobe of the prostate (B) and in a 15 mm round solid lesion in the right lung (C).

Teaching point

¹¹C-choline PET–CT, a whole body imaging modality, allows detection of metastases or synchronous, previously unknown, second primary cancers. The patient underwent biopsy of the lung lesion, which allowed diagnosis of a broncho-alveolar lung cancer with moderate tracer uptake.

Keywords: Prostate cancer, synchronous second primary malignancy, ¹¹C-choline



4.4.2.4. Case No. 4.4

Clinical indication for PET–CT: Prostate cancer, BCR

Clinical history

A 58 year old man with prostate cancer, Gleason score 4+4, post-radical prostatectomy, presented with PSA 0.7 ng/mL and PSA doubling time (dt) 10 months. He was a candidate for RT to the prostatic fossa.

PET–CT findings

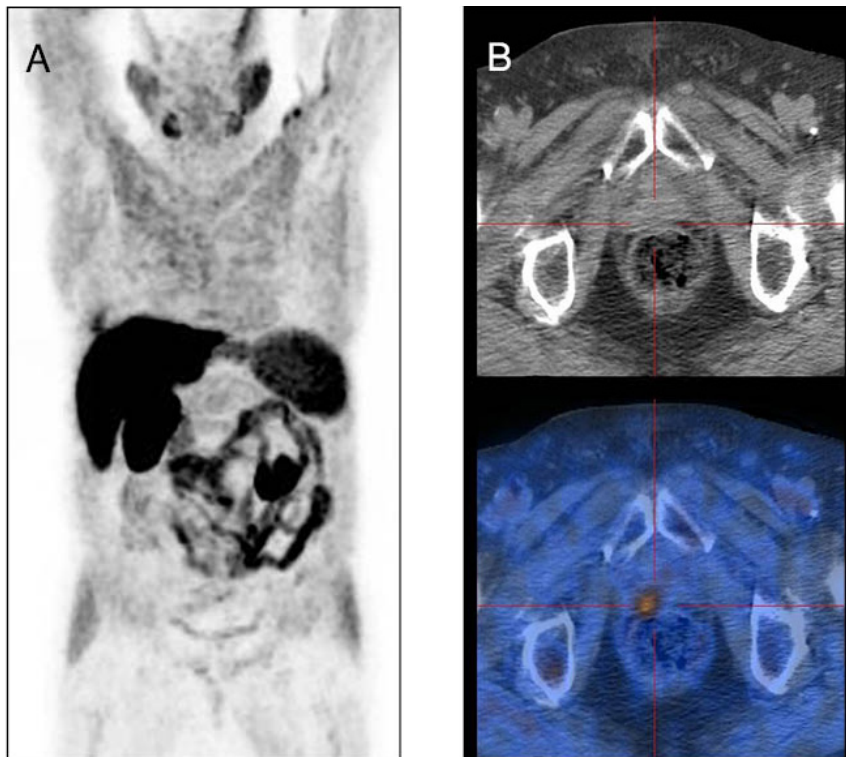
(A): MIP; (B): CT and fused slices of lower pelvis.

There is focal increased tracer uptake in the right side of the prostatic fossa, consistent with local relapse, further confirmed by transrectal US guided biopsy.

Teaching point

Although the sensitivity of ^{11}C -choline PET–CT for detection of local relapse is suboptimal, in this case the study allowed diagnosis of local recurrence and excluded distant metastases, making the patient eligible for salvage RT.

Keywords: Prostate cancer, BCR, local relapse, ^{11}C -choline



4.4.2.5. Case No. 4.5

Clinical indication for PET–CT: Prostate cancer, BCR

Clinical history

A 62 year old man with prostate cancer, Gleason score 4+3, post-radical prostatectomy, presented with PSA 0.4 ng/mL and PSA dt 6 months.

PET–CT findings

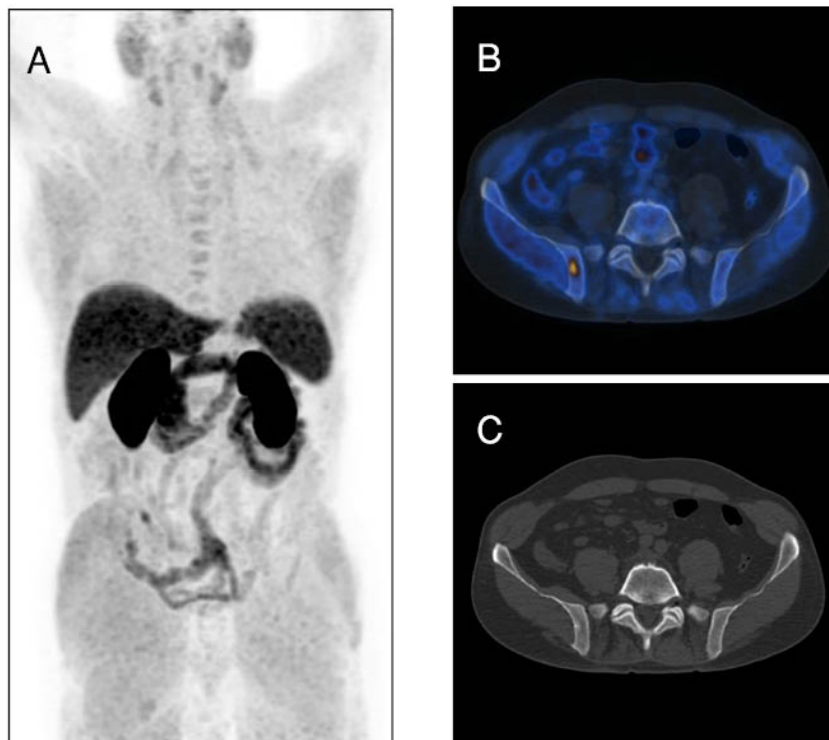
(A): MIP; (B): fused transaxial slices of pelvis; (C): CT transaxial slices of pelvis.

There is focal increased tracer uptake in a small osteoblastic lesion in the right iliac bone.

Teaching point

¹¹C-choline PET–CT has a high sensitivity for detection of small bone metastases in patients with BCR. Identifying patients with oligometastatic disease has a major clinical impact. In this case the patient underwent salvage RT to the bone lesion. Follow-up after 6 months showed a decrease in PSA levels to 0.02 ng/mL.

Keywords: Prostate cancer, BCR, bone metastasis, ¹¹C-choline



4.4.2.6. Case No. 4.6

Clinical indication for PET–CT: Prostate cancer, BCR

Clinical history

A 70 year old man with prostate cancer, Gleason score 4+3, post-radical prostatectomy, presented with PSA 0.6 ng/mL and PSA dt 5 months.

PET–CT findings

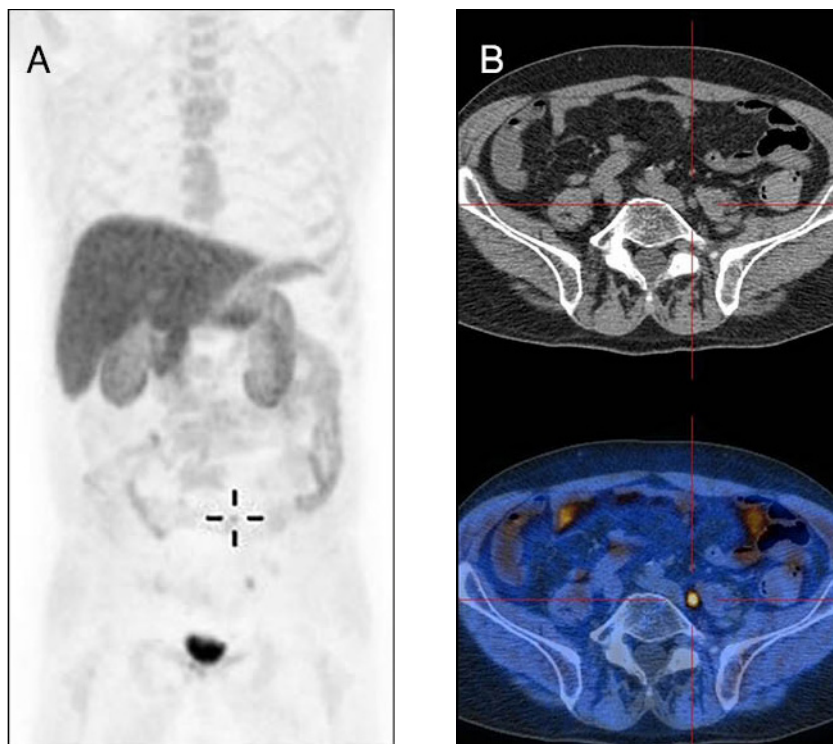
(A): MIP; (B): CT and fused transaxial slices of upper pelvis.

There is focal increased tracer uptake in small round LNs in the left common iliac chain.

Teaching point

¹¹C-choline PET–CT has a high sensitivity for detection of small LN metastases in patients with prostate cancer BCR. In this case with oligometastatic disease, the patient underwent salvage RT to the left iliac chain LNs, with delivery of a boost (60 Gy) to the PET-positive metastases. Follow-up after 6 months showed a decrease in serum PSA levels to 0.01 ng/mL.

Keywords: Prostate cancer, BCR, LN metastases, ¹¹C-choline



4.4.2.7. Case No. 4.7

Clinical indication for PET–CT: Prostate cancer, BCR

Clinical history

A 74 year old man with prostate cancer, Gleason score 4+3, after RT as primary treatment, presented with PSA 0.8 ng/mL that slowly increased to 2.5 ng/mL (PSA dt 16 months).

PET–CT findings

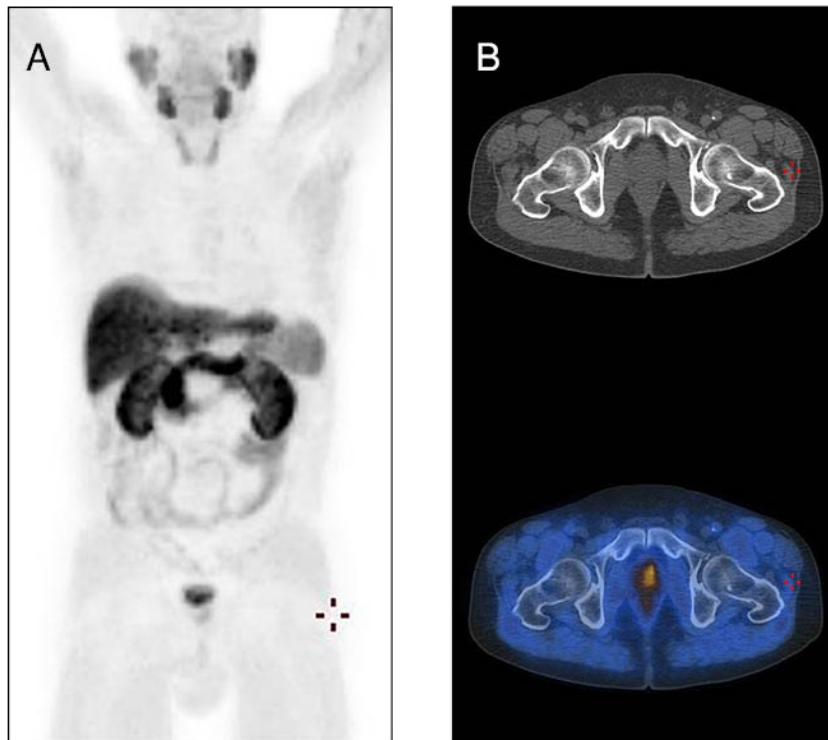
(A): MIP; (B): CT and fused transaxial slices of pelvis.

There is diffuse, faint tracer uptake in the prostate.

Teaching point

The presence of faint or moderate ^{11}C -choline uptake in the prostate, after RT, is difficult to interpret. This may be due to the presence of normal prostatic PSA producing tissue, or to relapse of cancer. Further investigation is needed to assess the presence of residual tumour and guide biopsy if indicated.

Keywords: Prostate cancer, BCR, prostate uptake, ^{11}C -choline



Clinical indication for PET–CT: Prostate cancer, BCR

Clinical history

A 71 year old man with prostate cancer, Gleason score 4+4, post-radical prostatectomy, presented with PSA 1.0 ng/mL and PSA dt 12 months.

PET–CT findings

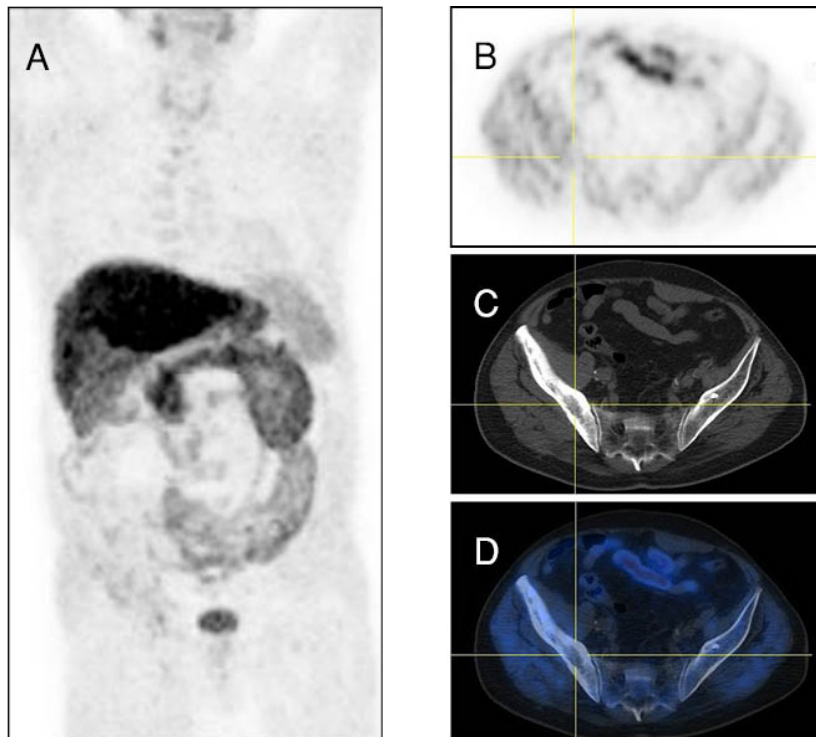
(A): MIP; (B): PET; (C): CT; (D): fused transaxial slices of pelvis.

There is an inhomogeneous, mixed lytic/blastic bone lesion mainly in the cortical aspect of the right iliac bone (C), with no abnormal tracer uptake (A, B, D).

Teaching point

The findings are consistent with Paget’s disease of the right iliac bone, a benign skeletal lesion that in most cases does not show any significant ¹¹C-choline uptake.

Keywords: Prostate cancer, BCR, Paget’s, ¹¹C-choline



Clinical indication for PET–CT: Prostate cancer, staging

Clinical history

A 69 year old man with prostate cancer, Gleason score 4+4, PSA 12.0 ng/mL, was scheduled for radical prostatectomy.

PET–CT findings

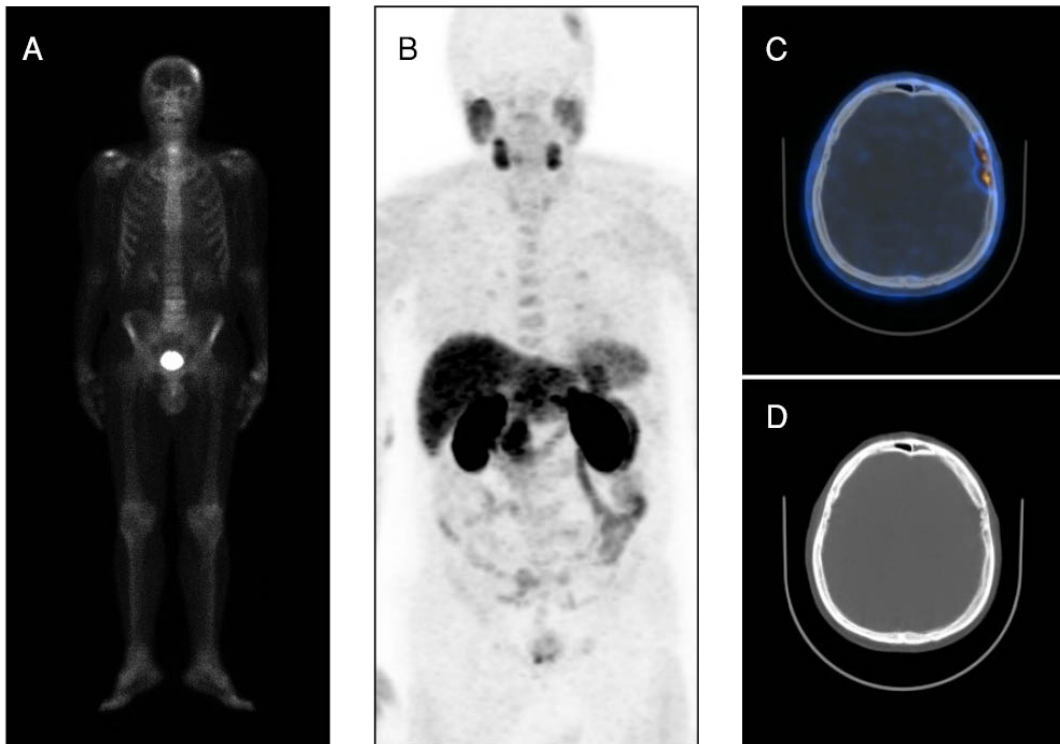
(A): Planar ^{99m}Tc labelled methylene diphosphonate (^{99m}Tc -MDP) bone scan, anterior view; (B): MIP; (C): fused transaxial slice of skull; (D): CT transaxial slice of skull.

There is increased ^{11}C -choline and ^{99m}Tc -MDP uptake in a mixed (mostly lytic) bone lesion in the right parietal bone. This bone lesion was further diagnosed as an osteoid osteoma in an unusual location.

Teaching point

Benign bone lesions can show intense uptake on both the ^{99m}Tc bone scan and the ^{11}C -choline PET–CT study.

Keywords: Prostate cancer, BCR, osteoid osteoma, ^{11}C -choline



4.4.2.10. Case No. 4.10

Clinical indication for PET–CT: Prostate cancer, BCR

Clinical history

A 58 year old man with prostate cancer, Gleason score 4+4, post-radical prostatectomy, presented with PSA 0.9 ng/mL and PSA dt 9 months.

PET–CT findings

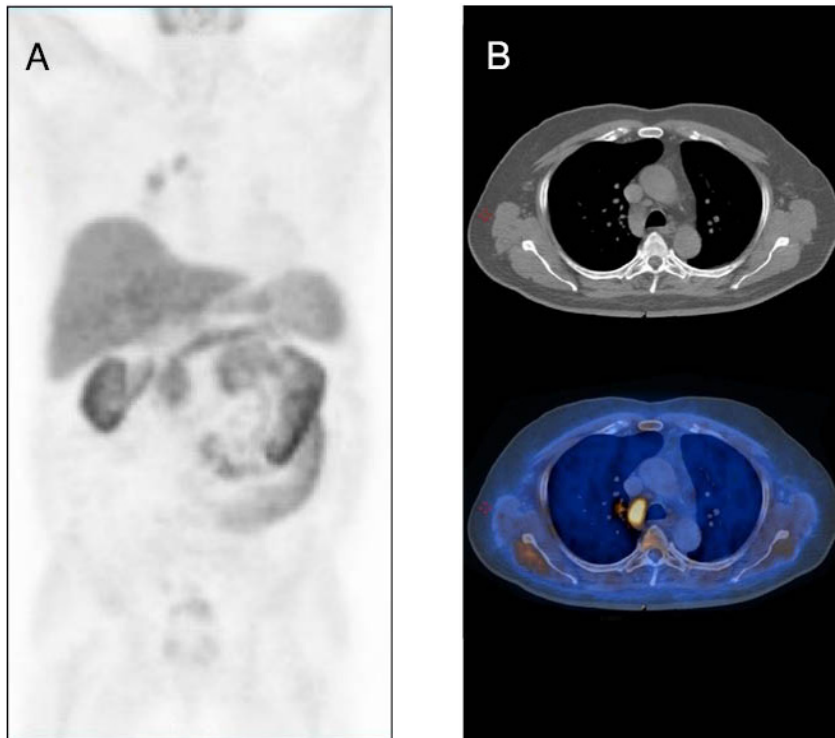
(A): MIP; (B): CT and fused transaxial slices of mid-thorax.

There is increased tracer uptake in enlarged right hilar and paratracheal LNs.

Teaching point

Transbronchial biopsy diagnosed sarcoidosis, a chronic granulomatous disease. Intense uptake of ^{11}C -choline in chronic inflammation has to be considered in cases of tracer-avid findings in unusual locations, such as mediastinal LNs.

Keywords: Prostate cancer, BCR, sarcoidosis, ^{11}C -choline



4.4.2.11. Case No. 4.11

Clinical indication for PET–CT: Prostate cancer, BCR

Clinical history

A 61 year old man with prostate cancer, Gleason score 4+3, post-radical prostatectomy, presented with PSA 0.6 ng/mL and PSA dt 12 months.

PET–CT findings

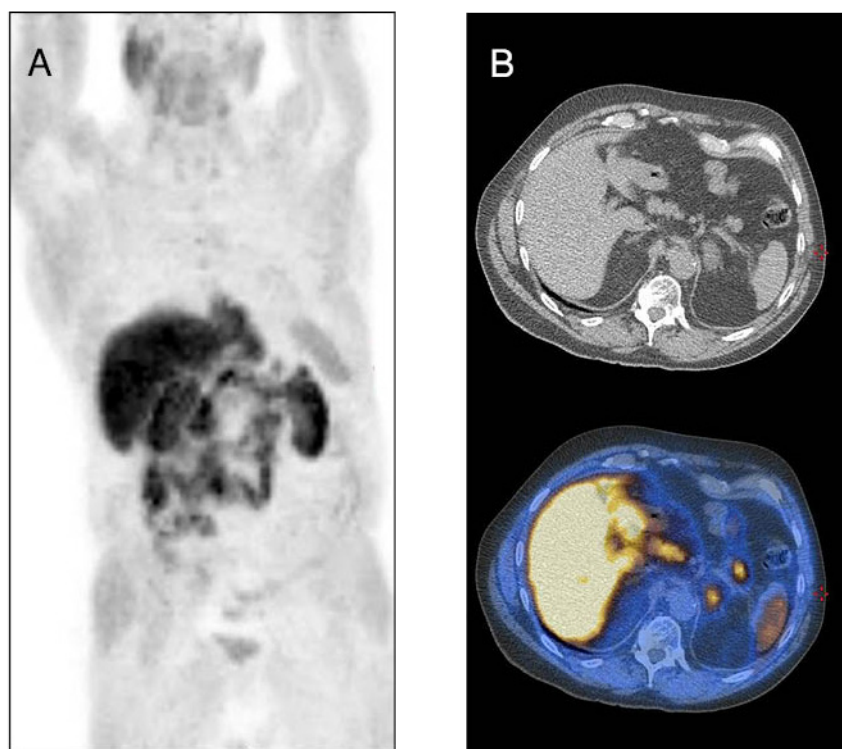
(A): MIP; (B): CT and fused transaxial slices of upper abdomen.

There is increased tracer uptake in an enlarged, 27 mm, hypodense (12 Hounsfield unit) left adrenal gland.

Teaching point

The findings are consistent with a left adrenal adenoma, which usually shows uptake of ^{11}C -choline.

Keywords: Prostate cancer, BCR, adrenal adenoma, ^{11}C -choline



Clinical indication for PET–CT: Prostate cancer, BCR

Clinical history

A 64 year old man with prostate cancer, Gleason score 4+3, post-radical prostatectomy, presented with PSA 0.5 ng/mL and PSA dt 10 months.

PET–CT findings

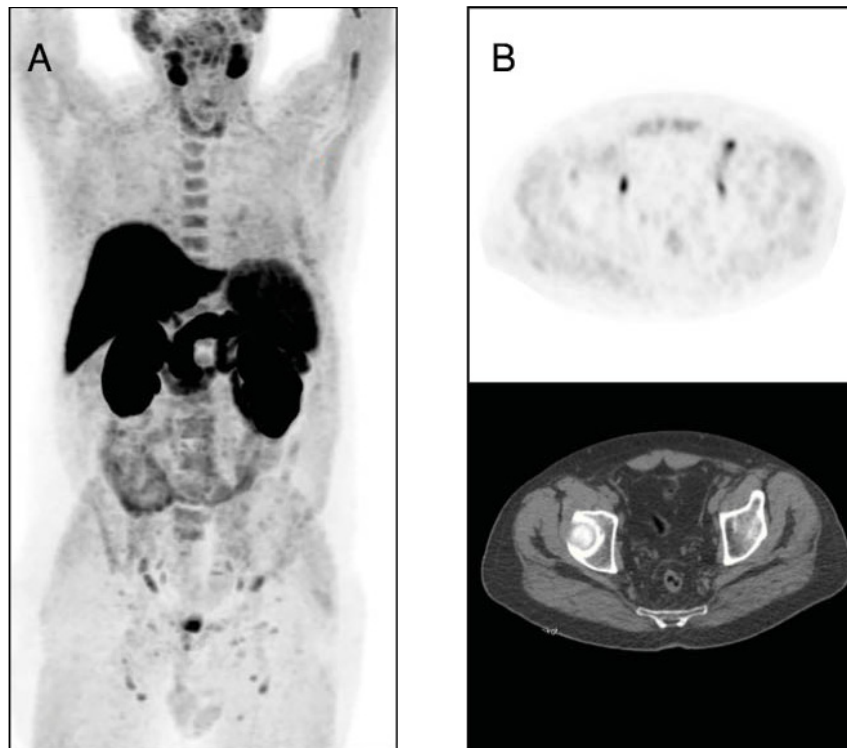
(A): MIP; (B): PET and CT transaxial slices of lower pelvis.

There is bilateral symmetrical increased tracer uptake in inguinal and external iliac, and reactive LNs.

Teaching point

Metastatic spread of prostate cancer to inguinal LNs is uncommon. Important considerations include the symmetrical distribution of the tracer, the shape of these LNs (fatty hilum) on CT, as well as the low risk of relapse according to PSA values and kinetics.

Keywords: Prostate cancer, BCR, reactive LNs, ¹¹C-choline



4.4.2.13. Case No. 4.13

Clinical indication for PET–CT: Prostate cancer, BCR

Clinical history

A 58 year old man with prostate cancer, Gleason score 4+5, post-radical prostatectomy, presented with PSA 12 ng/mL, PSA dt 6 months and testosterone rebound (TTR) 13 months during ADT.

PET–CT findings

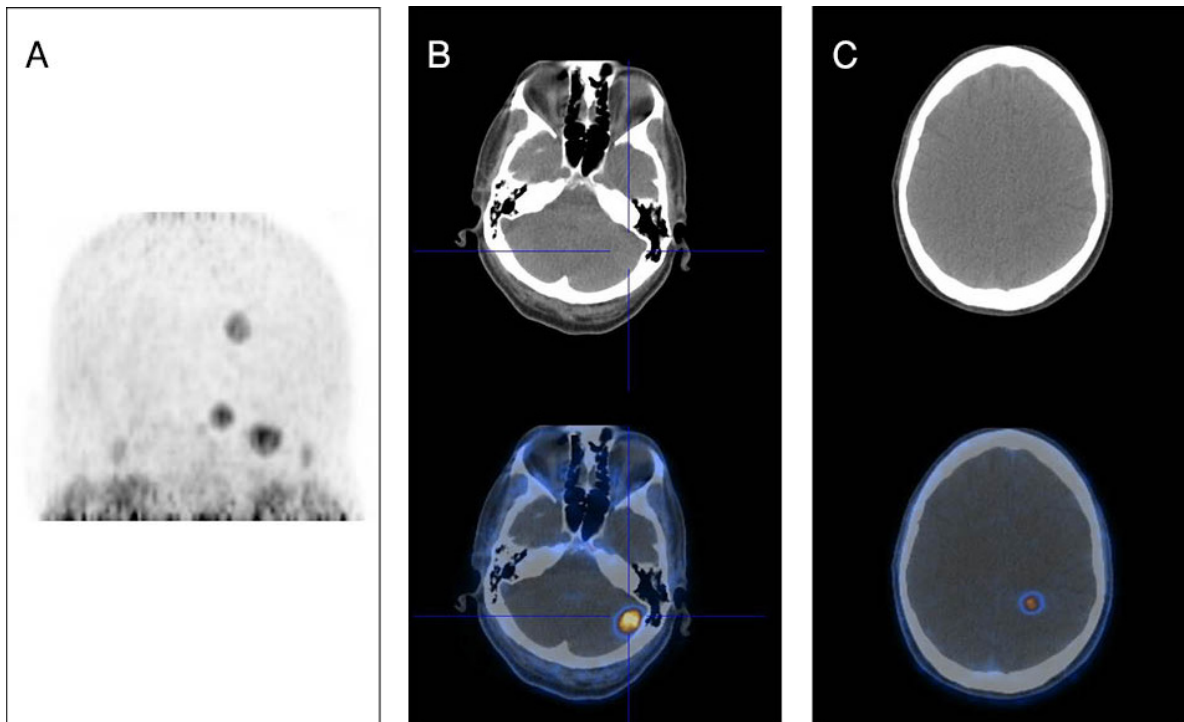
(A): MIP of head; (B, C): CT and fused transaxial slices of head.

There are multiple foci of increased tracer uptake in the brain, most prominent in the left parietal region and the left cerebellum.

Teaching point

Brain metastases from prostate cancer, although uncommon, may occur. The brain needs to be included in the scan in patients with suspected CNS involvement. The low physiological uptake of ^{11}C -choline in the brain facilitates the detection of brain metastases.

Keywords: Prostate cancer, BCR, brain metastases, ^{11}C -choline



Clinical indication for PET–CT: Prostate cancer, BCR

Clinical history

A 59 year old man with prostate cancer, Gleason score 4+4, post-radical prostatectomy, presented with PSA 1423 ng/mL at 3 months after treatment with ^{223}Ra .

PET–CT findings

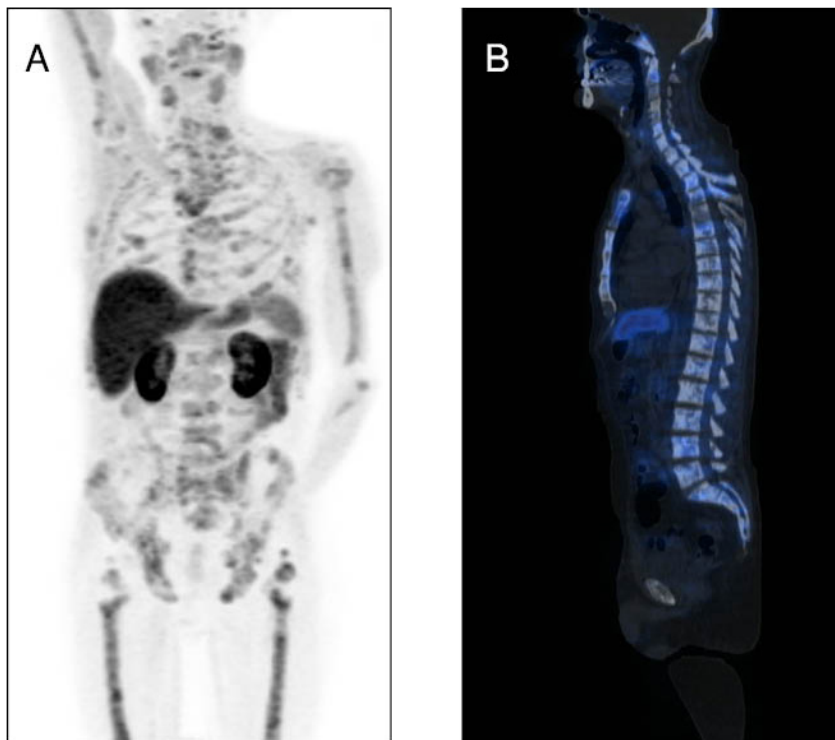
(A): MIP; (B): fused sagittal slices.

There is inhomogeneous increased tracer uptake in the entire axial and appendicular skeleton, consistent with diffuse metastatic bone involvement.

Teaching point

^{11}C -choline PET–CT can assess response to ^{223}Ra treatment with high accuracy.

Keywords: Prostate cancer, BCR, ^{223}Ra treatment, ^{11}C -choline



5. CHOLINE (¹⁸F)

5.1. GENERAL CHARACTERISTICS

Name: ¹⁸F-fluorocholine

Synonyms: ¹⁸F-CH, ¹⁸F-CHO, ¹⁸F-CHOL

Radioisotope

¹⁸F is a short half-life PET radioisotope (109.7 min) emitting positrons of E_{\max} 1.656 MeV. Owing to the high chemical stability of C–F bonds in organic compounds as well as the high water solubility of F compounds, ¹⁸F tracers usually show suitable stability and biodistribution in humans. Although the F chemistry is complicated, the vast application of ¹⁸F labelled compounds in nuclear medicine has led to development of efficient automated radiopharmaceutical production methods allowing large scale production of ¹⁸F tracers for clinical use.

Radiosynthesis

¹⁸F is routinely produced by proton irradiation of enriched ¹⁸O water in biomedical cyclotrons, followed by ¹⁸F-KF formation and activation using Kryptofix 222. The reaction of active ¹⁸F-fluoride with dibromomethane leads to ¹⁸F-fluorobromomethane, which in reaction with N, N-dimethylaminoethanol provides ¹⁸F-choline (Fig. 5.1). This process has been automated using commercially available synthesizers (15–25% radiochemical yield, >99% radiochemical purity, specific activity >37 GBq/μmol in 35 min) [26–28].

5.2. PHARMACOKINETICS

5.2.1. Physiological biodistribution and metabolism

The tracer is phosphorylated by choline kinase and incorporated into various phospholipids. In certain tissues, including the kidney and liver, choline oxidation is prominent. The oxidative metabolite of choline, betaine, is excreted into the urine. At 60 min after administration, there is intense physiological ¹⁸F-choline uptake in the lacrimal and salivary glands, as well as in the liver, spleen, pancreas and kidneys. Uptake in the thyroid is variable and of mild intensity. There is almost no uptake in the brain. In most cases, there is radioactive urine in the ureters and bladder (Fig. 5.2) [26–28].

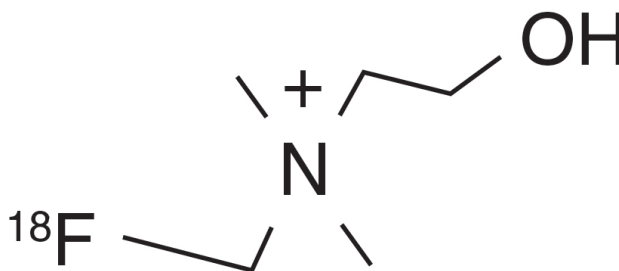


FIG. 5.1. Molecular structure of ¹⁸F-choline.

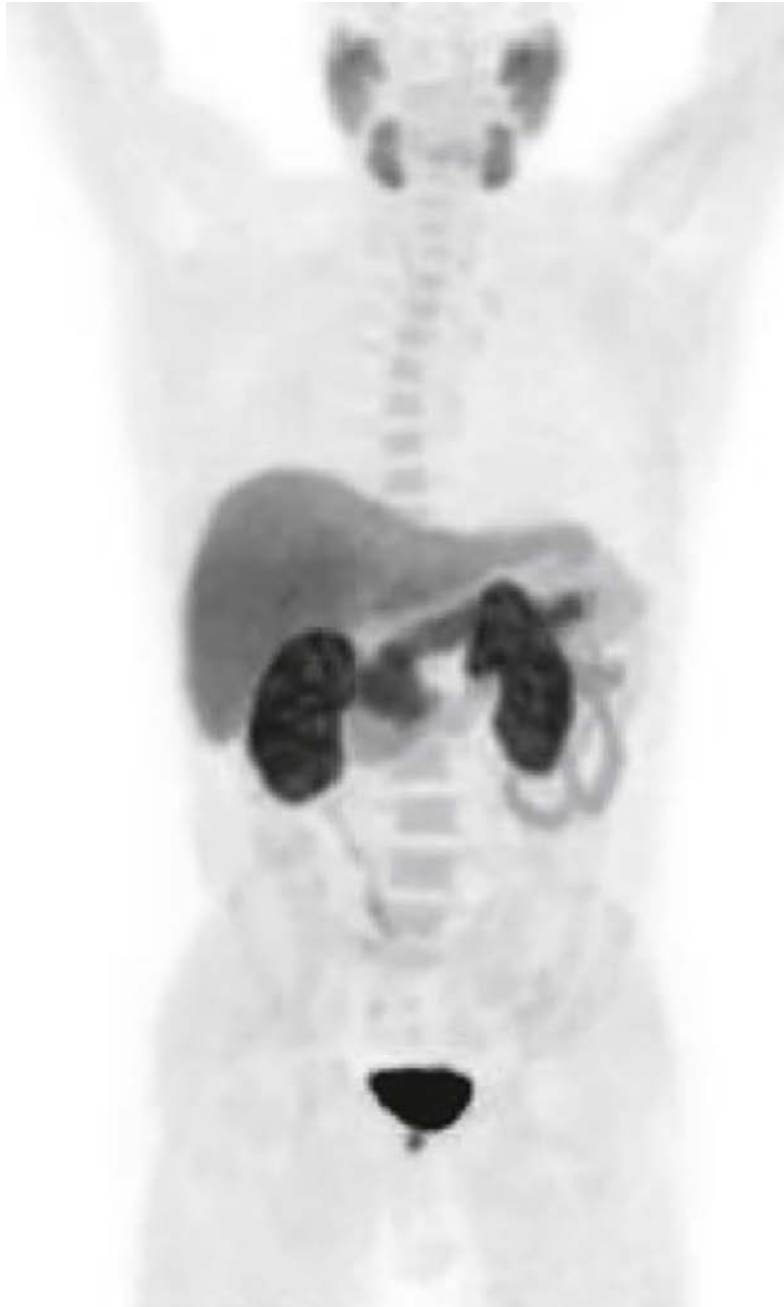


FIG. 5.2. Normal biodistribution of ^{18}F -choline.

5.2.2. Mechanism of retention

^{18}F -choline enters cells mediated by choline transporters. Malignant cells are characterized by overexpression of choline kinase, which catalyses phosphorylation of choline to form phosphorylcholine followed by the generation of phosphatidylcholine in the cell membrane [26–28].

5.2.3. Pharmacology and toxicology

Urinary excretion of ^{18}F -choline reaches $4.9\% \pm 4.8\%$ of the administered activity in female patients and $1.9\% \pm 1.6\%$ in males within 60 min after injection. In acute toxicity studies in mice receiving 1 mg/kg

of body weight of non-radioactive ^{19}F -choline, neither death nor behavioural or movement abnormalities were noted for up to 48 hours after administration. Based on these findings, it has been estimated that the normal amount of ^{18}F -choline in the radiotracer preparation should be approximately 3 ng/kg of body weight (i.e. 300 000 times lower than the amount administered in this toxicity study [26–28]).

5.3. METHODOLOGY

5.3.1. Activity, administration, dosimetry

As ^{18}F -choline is an investigational tracer, there is no current standard for the activity to be administered. The kidney is the critical organ and limits administration levels of ^{18}F -choline to 4.07 MBq/kg (0.110 mCi/kg) in human research studies. The dose critical organ is the kidney, which receives 0.17 and 0.16 mSv/MBq (0.64 and 0.55 rem/mCi) for females and males, respectively. The effective dose equivalent for humans following the administration of 4.07 MBq/kg (0.110 mCi/kg) is approximately 0.01 Sv for females and males, which is below the single-study United States Food and Drug Administration limit of 0.03 Sv for research subjects [29–34].

5.3.2. Imaging protocol

No special patient preparation is required prior to administration of the radiotracer. Imaging is performed following the IV injection of a dose of 300 MBq and an uptake period of 30 min. In patients with prostate cancer, acquisition of the whole body PET component starts from the pelvis. Acquisition time is 2–3 min/bed position. In patients with hyperparathyroidism (HPT), the PET component is acquired from head to thorax, with an acquisition time of 3 min/bed position. For the CT imaging protocol, see general comments in Section 1.3.

5.4. CLINICAL ASPECTS

5.4.1. Indications

In patients with prostate cancer, the indications for ^{18}F -choline are the same as for ^{11}C -choline. In patients with HPT, several studies have provided evidence for the use of ^{18}F -choline in the localization of parathyroid adenoma (PTA) and parathyroid hyperplasia. ^{18}F -choline PET–CT has a high sensitivity and specificity as compared to conventional nuclear medicine scintigraphy with $^{99\text{m}}\text{Tc}$ -sestaMIBI, and may be advocated in sestaMIBI-negative cases, if referral to a PET centre is possible and the tracer is available [29–34].

5.4.2. Cases — prostate cancer

5.4.2.1. Case No. 5.1

Clinical indication for PET–CT: Prostate cancer, BCR

Clinical history

A 72 year old man with prostate cancer, Gleason score 3+3, post-transurethral resection of prostate and RT, presented with PSA 0.8 ng/mL, PSA dt 13 months and TTR 14 months.

PET–CT findings

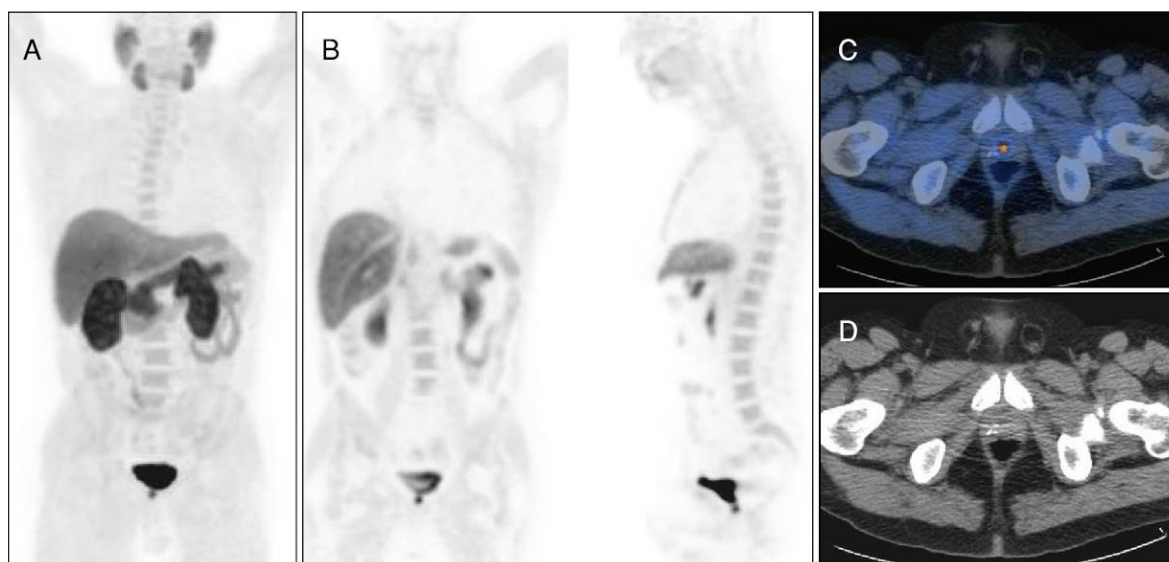
(A): MIP; (B): PET coronal and sagittal transaxial slices; (C): fused transaxial slice of pelvis; (D): CT transaxial slice of pelvis.

There is focal ^{18}F -choline uptake in the centre of the prostate, below the area of high urinary activity in the urinary bladder, which is suspicious, but not diagnostic, for local relapse.

Teaching point

Central, focal areas of increased ^{18}F -choline accumulation below and close to the urinary bladder should be interpreted with caution in patients who have undergone transurethral resection of the prostate.

Keywords: Prostate cancer, BCR, transurethral resection of prostate, ^{18}F -choline



5.4.2.2. Case No. 5.2

Clinical indication for PET–CT: Prostate cancer, BCR

Clinical history

A 78 year old man with prostate cancer, Gleason score 3+4, after brachytherapy as primary treatment, presented with PSA 1.2 ng/mL, PSA dt 12 months and TTR 16 months.

PET–CT findings

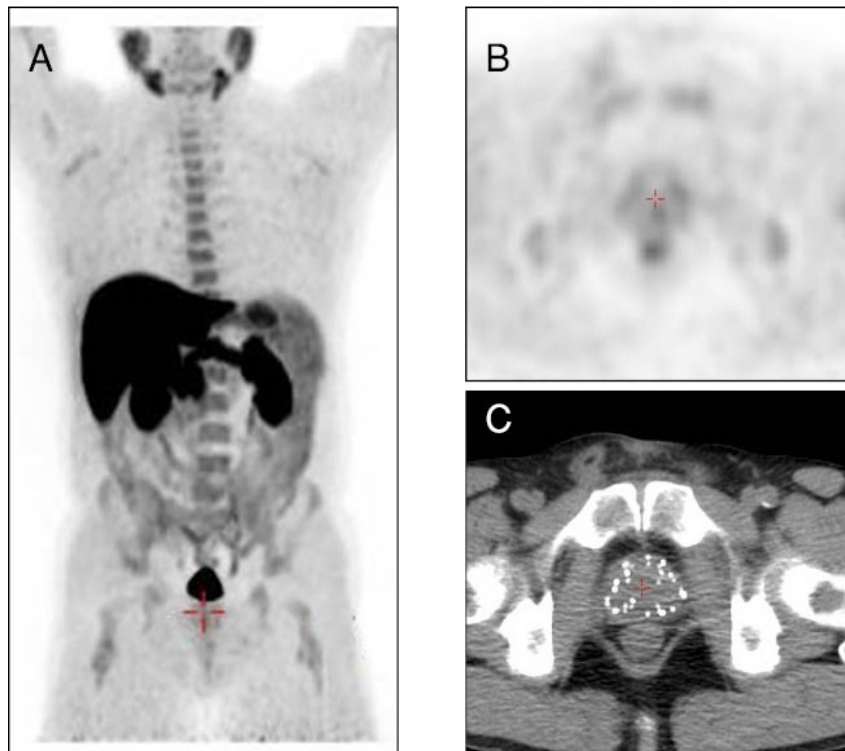
(A): MIP; (B): PET transaxial slice of pelvis; (C): CT transaxial slice of pelvis.

There is mild, homogenous increased tracer uptake in the prostate (red marker), without any further evidence of disease recurrence.

Teaching point

After brachytherapy, mild and homogenous ¹⁸F-choline uptake in the prostate can occur and should not be interpreted as local relapse.

Keywords: Prostate cancer, BCR, local relapse, ¹⁸F-choline



Clinical indication for PET–CT: Prostate cancer, BCR

Clinical history

A 76 year old man with prostate cancer, Gleason score 3+4, treated with RT, presented with PSA 0.4 ng/mL and PSA dt 9 months.

PET–CT findings

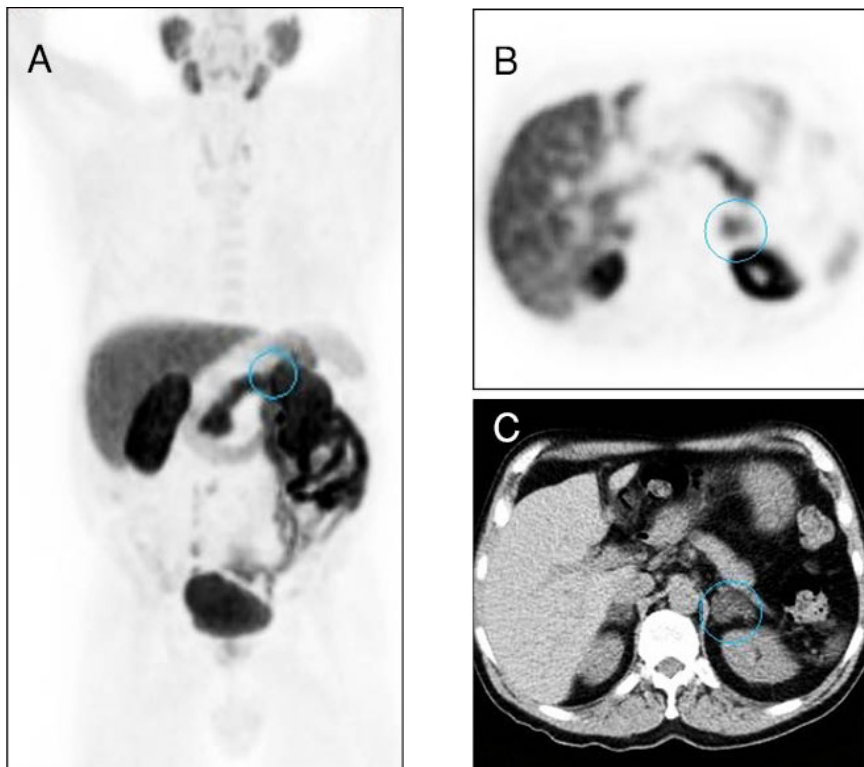
(A): MIP; (B): PET transaxial slice of upper abdomen; (C): CT transaxial slice of upper abdomen.

There is mild tracer uptake in a homogeneous, low density (6 Hounsfield unit) lesion in the left adrenal (blue marker), consistent with a known, nonfunctioning adenoma.

Teaching point

^{18}F -choline is not specific for prostate cancer. Benign lesions such as adrenal adenoma may show ^{18}F -choline uptake.

Keywords: Prostate cancer, adrenal adenoma, ^{18}F -choline



5.4.2.4. Case No. 5.4

Clinical indication for PET–CT: Prostate cancer, BCR

Clinical history

A 59 year old man with prostate cancer, Gleason score 4+5, post-radical prostatectomy, during ADT, presented with PSA 12 ng/mL, PSA dt 4 months and TTR 13 months.

PET–CT findings

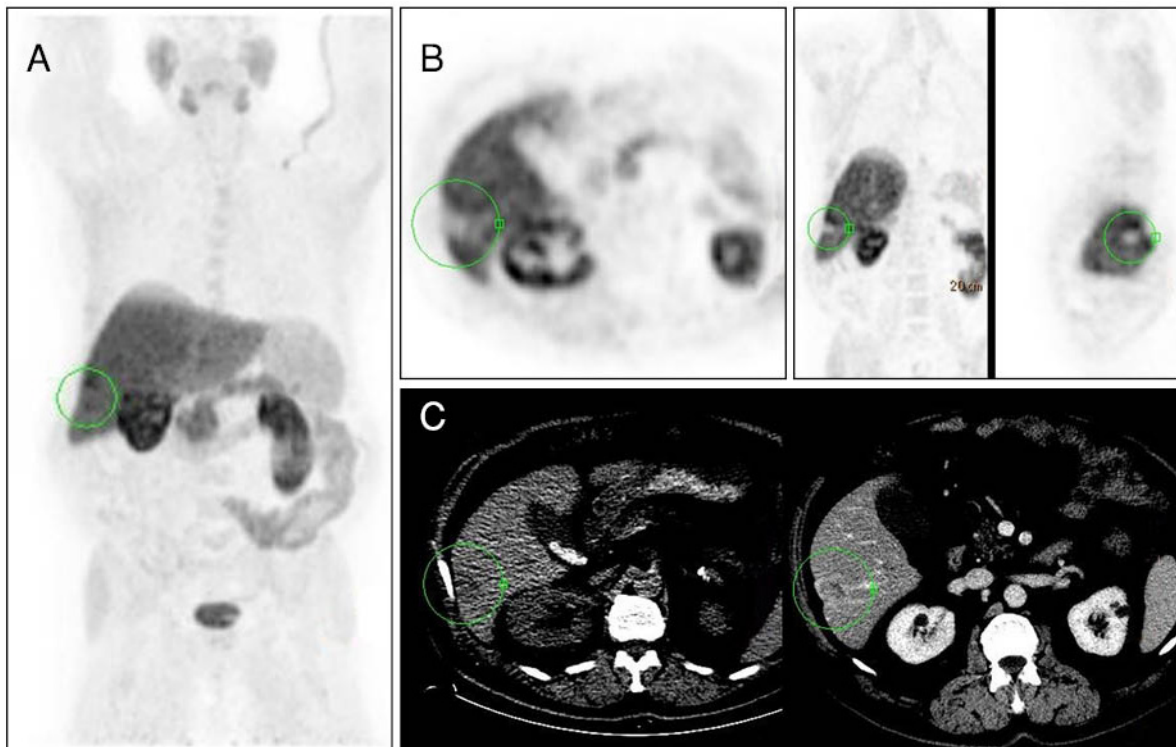
(A): MIP; (B): PET transaxial, coronal and sagittal slices; (C): CT transaxial slices without (left) and with (right) contrast enhancement of the liver.

There is increased tracer uptake and enhancement on CT at the margins of a hypodense lesion in the right lobe of the liver. A hepatic metastasis was confirmed at biopsy.

Teaching point

The accuracy of ^{18}F -choline PET–CT for characterization of liver lesions is very low. The CT component of the study needs to be carefully examined to avoid missing liver lesions.

Keywords: Prostate cancer, BCR, liver metastasis, ^{18}F -choline



Clinical indication for PET–CT: Prostate cancer, BCR

Clinical history

A 67 year old man with prostate cancer, Gleason score 3+4, post-radical prostatectomy, presented with PSA 0.5 ng/mL and PSA dt 14 months.

PET–CT findings

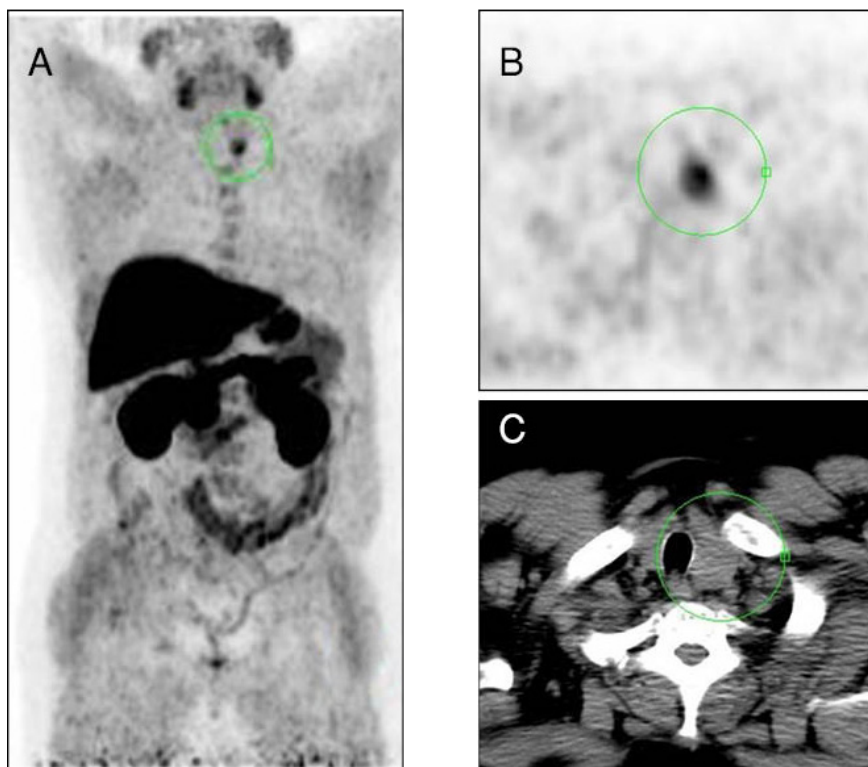
(A): MIP; (B): PET transaxial slice of lower neck; (C): CT transaxial slice of lower neck.

There is focal increased tracer uptake in an enlarged left thyroid lobe (green marker). US guided biopsy diagnosed a benign thyroid nodule.

Teaching point

^{18}F -choline is not specific for prostate cancer. Benign lesions may show high ^{18}F -choline uptake.

Keywords: Prostate cancer, benign thyroid nodule, ^{18}F -choline



Clinical indication for PET–CT: Prostate cancer, BCR

Clinical history

A 71 year old man with prostate cancer, Gleason score 3+4, post-radical prostatectomy, presented with PSA 1.9 ng/mL and PSA dt 13 months.

PET–CT findings

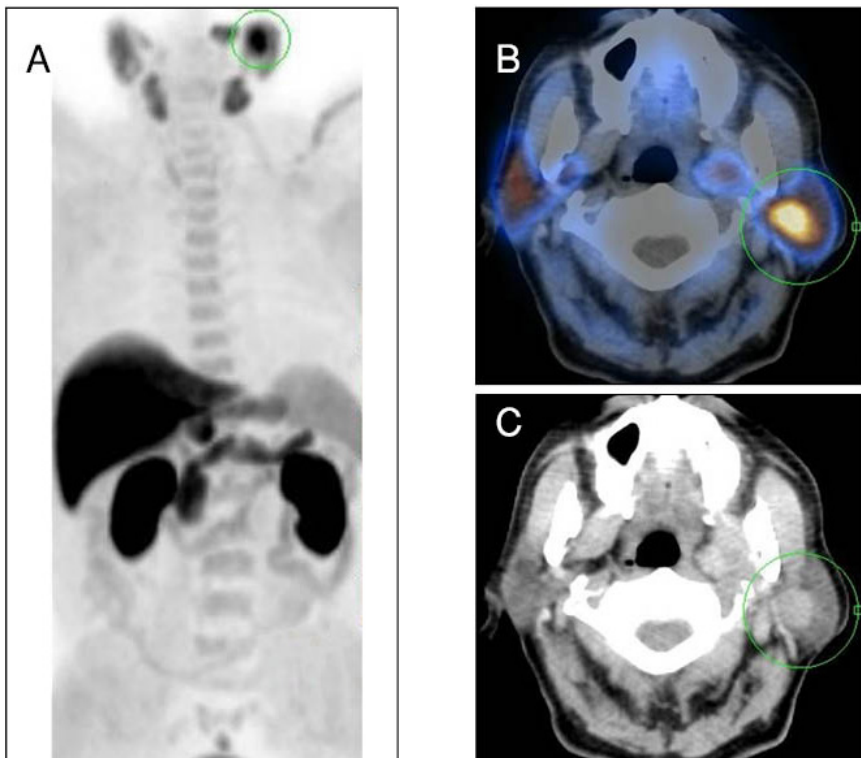
(A): MIP; (B): fused transaxial slice of head; (C): CT transaxial slice of head.

There is focal intense tracer uptake in a well defined solid nodule in the left parotid (green marker), without any additional abnormal findings. US confirmed a Warthin’s tumour.

Teaching point

Benign lesions such as Warthin’s tumour may show intense ¹⁸F-choline uptake. US may be necessary to confirm diagnosis.

Keywords: Prostate cancer, Warthin’s tumour, ¹⁸F-choline



Clinical indication for PET–CT: Prostate cancer, BCR

Clinical history

A 75 year old man with prostate cancer, Gleason score 4+4, post-radical prostatectomy, presented with PSA 3.5 ng/mL and PSA dt 7 months.

PET–CT findings

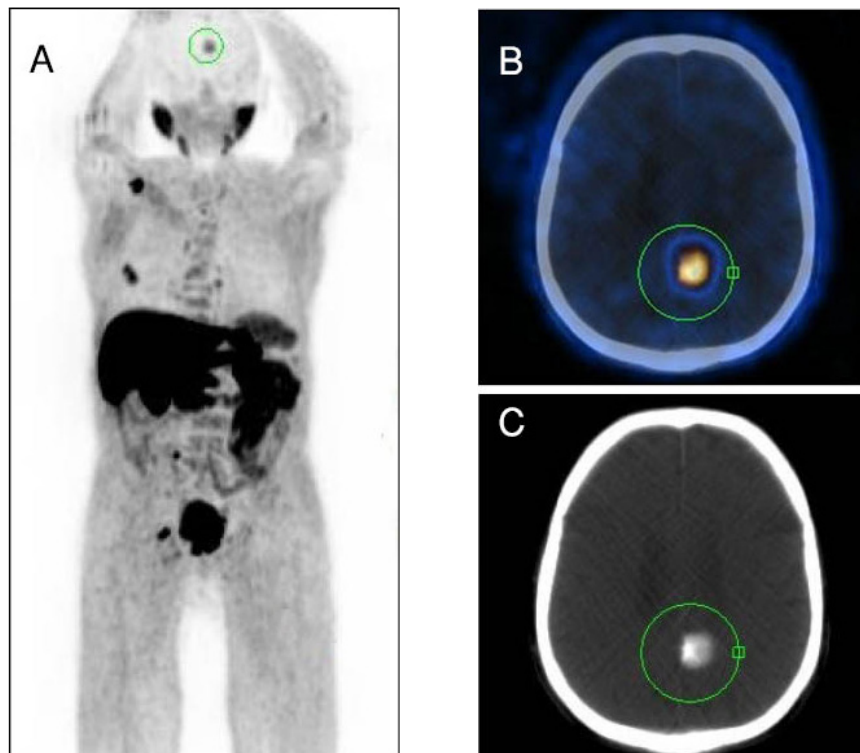
(A): MIP; (B) fused transaxial slice of head; (C): CT transaxial slice of head.

There is intense ^{18}F -choline uptake in multiple bone metastases. In addition, there is intense tracer uptake in a known left parasagittal meningioma also visible on the low dose CT.

Teaching point

Low physiological uptake of ^{18}F -choline in the brain facilitates detection of brain lesions that can be further characterized by conventional imaging modalities.

Keywords: Prostate cancer, meningioma, ^{18}F -choline



Clinical indication for PET–CT: Prostate cancer, BCR

Clinical history

A 70 year old man with prostate cancer, Gleason score 3+4, post-radical prostatectomy, presented with PSA 0.9 ng/mL and PSA dt 15 months.

PET–CT findings

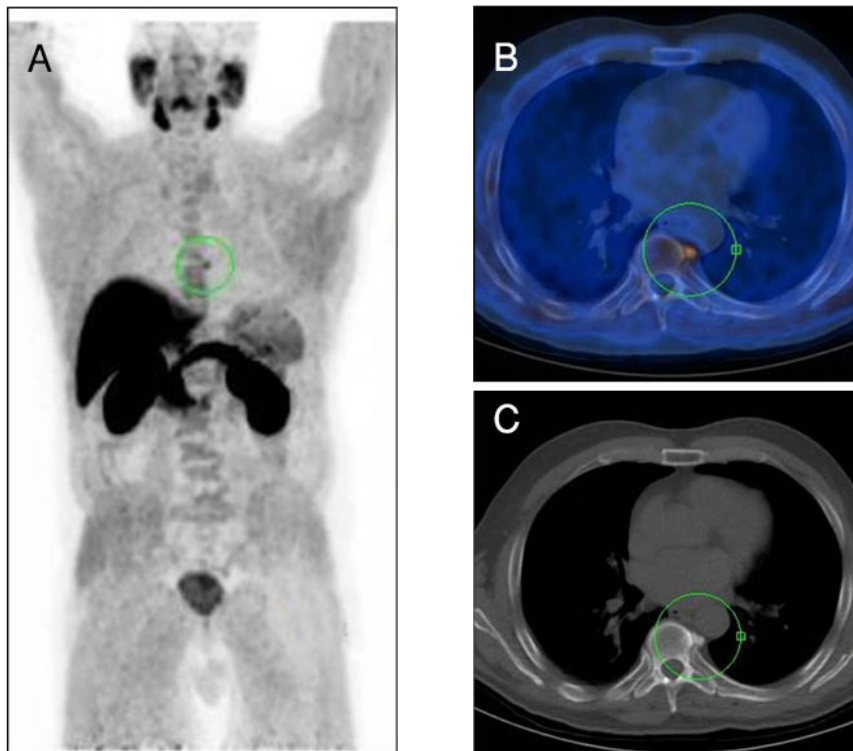
(A): MIP; (B): fused transaxial slice of mid-chest; (C): CT transaxial slice of mid-chest.

There is a single focus of increased ^{18}F -choline uptake in an osteophyte in a mid-thoracic vertebra (green marker).

Teaching point

Benign degenerative bone changes may occasionally show increased ^{18}F -choline uptake, less intense than with ^{18}F -FDG.

Keywords: Prostate cancer, degenerative bone changes, ^{18}F -choline



Clinical indication for PET–CT: Prostate cancer, response evaluation

Clinical history

A 73 year old man with prostate cancer, Gleason score 4+3, post-radical prostatectomy, presented with BCR. He was evaluated before (PSA 2.3 ng/mL, PSA dt 6 months) and after 2 months of hormonal treatment (PSA 0.5 ng/mL).

PET–CT findings

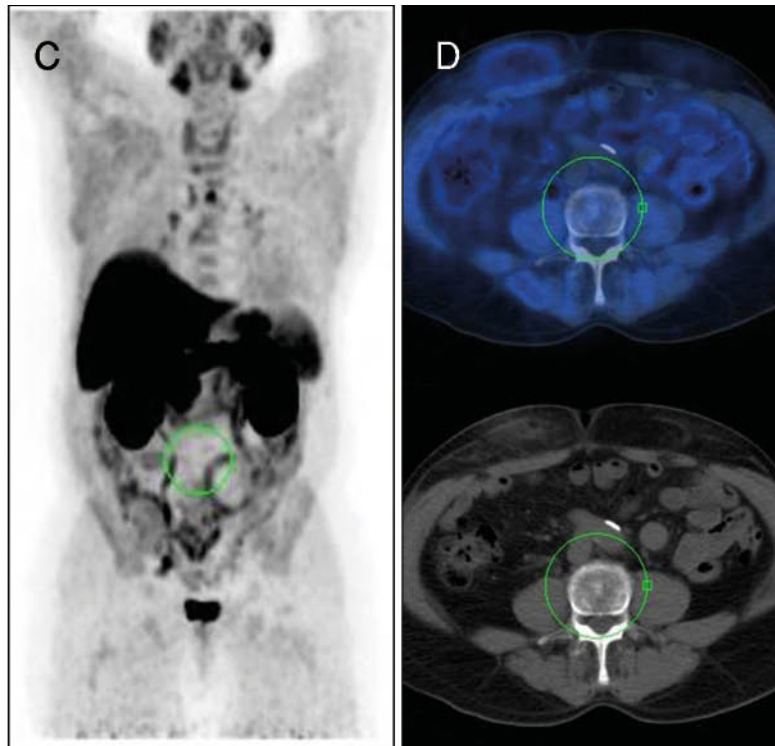
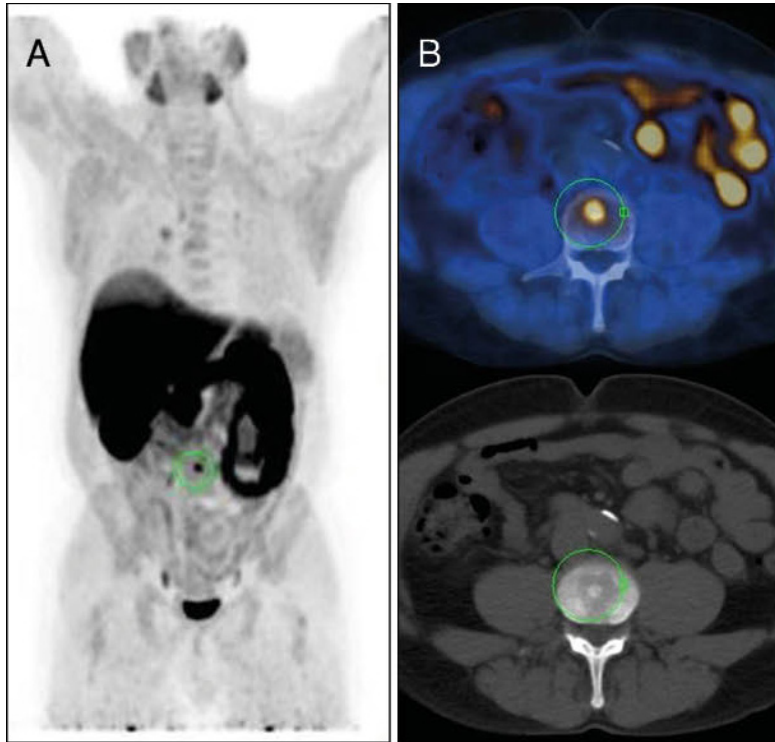
(A): MIP before treatment; (B): CT and fused transaxial slices at mid-thorax level before treatment; (C): MIP after treatment; (D): CT and fused transaxial slices at same (mid-thorax) level after treatment.

Intense tracer uptake in a thoracic vertebra seen before therapy (green marker) is not visible after 2 months of hormonal treatment.

Teaching point

¹⁸F-choline PET–CT allows evaluation of treatment response in patients with prostate cancer. Patients with decreasing, but still elevated, PSA levels after treatment may not show any residual abnormal ¹⁸F-choline uptake, indicating good response.

Keywords: Prostate cancer, therapy evaluation, ¹⁸F-choline



Clinical indication for PET–CT: Prostate cancer, response evaluation

Clinical history

A 68 year old man with prostate cancer, Gleason score 4+4, post-radical prostatectomy, with BCR (PSA 4.6 ng/mL, PSA dt 6 months) was evaluated before and after 6 months of abiraterone treatment (PSA decreased slightly to 3.6 ng/mL).

PET–CT findings

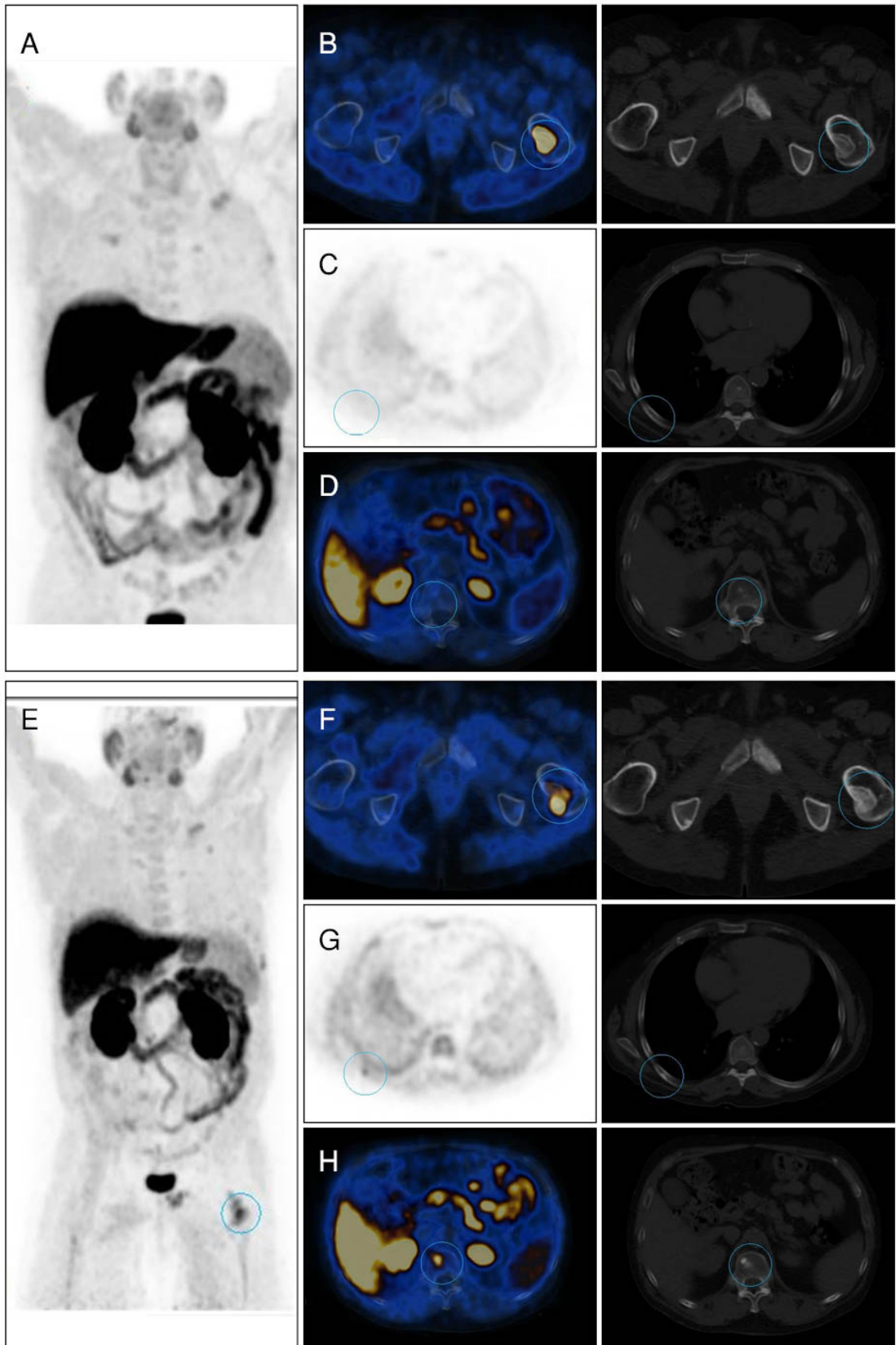
(A–D): images before treatment. (A): MIP; (B): fused and CT transaxial slices of lower pelvis; (C): PET and CT transaxial slices of mid-thorax; (D): fused and CT transaxial slices of upper abdomen. (E–H): similar images at same levels, after treatment.

Intense ¹⁸F-choline uptake seen in the left femur before therapy is decreasing in intensity after 2 months of hormonal treatment. However, in the follow-up study there are two new bone lesions: one in a left lower rib and one in a thoracic dorsal vertebra.

Teaching point

Even in the presence of a decreasing trend in the PSA level, ¹⁸F-choline may detect new hormone resistant lesions, indicating treatment failure.

Keywords: Prostate cancer, therapy evaluation, ¹⁸F-choline



5.4.3. Cases — hyperparathyroidism

Case courtesy of B. Brans, Nuclear Medicine Department, Ghent University Hospital, Belgium.

5.4.3.1. Case No. 5.11

Clinical indication for PET–CT: HPT, suspected PTA

Clinical history

A 46 year old woman presented with thyroid dysfunction and loss of weight. Laboratory investigations indicated hyperthyroidism. ^{99m}Tc -pertechnetate thyroid scintigraphy showed a multinodular hyperfunctioning gland. Treatment was instituted. At follow-up, the patient was asymptomatic and serum Ca levels were normal, but urinary Ca excretion was slightly elevated, as were serum parathyroid hormone (PTH) levels (102 ng/L; normal is 15–65 ng/L). A PTA was suspected. US showed several nodules in the thyroid gland. US of the kidneys was negative for lithiasis. Bone densitometry indicated mild osteopaenia.

Scintigraphy and PET–CT findings

(A): ^{99m}Tc -pertechnetate; (B): ^{99m}Tc -sestaMIBI; (C): ^{18}F -choline PET slice of lower neck; (D): CT transaxial slice of lower neck.

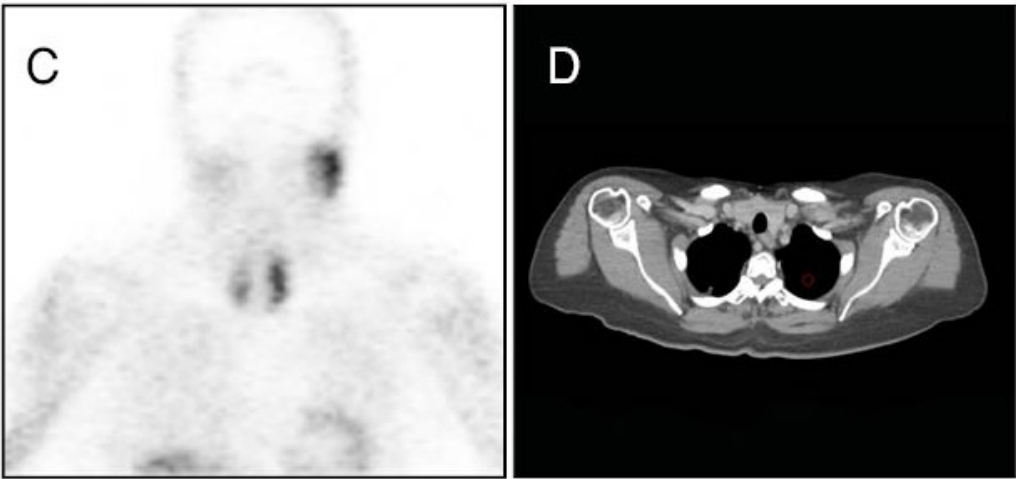
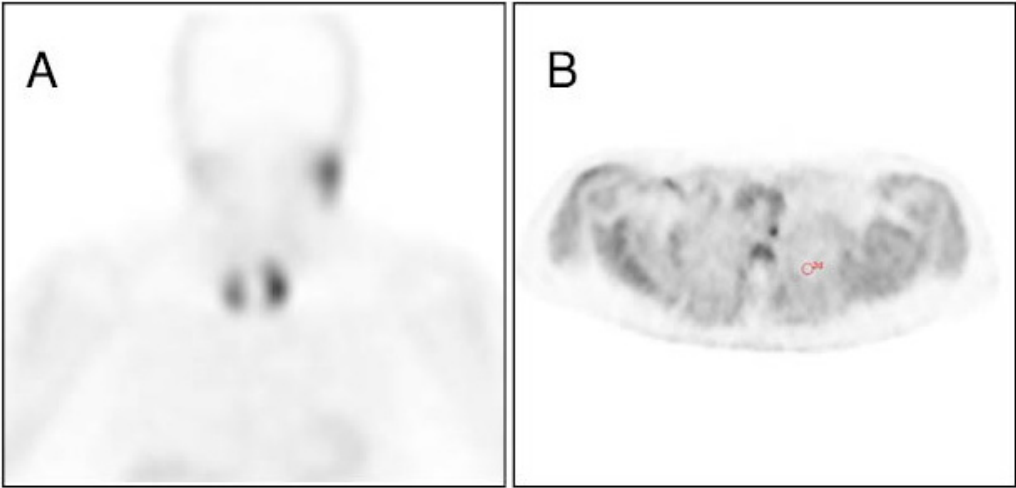
(A) and (B) suggest an area of increased preferential ^{99m}Tc -sestaMIBI activity at the left upper pole of the thyroid. Subtraction images were negative. (C) and (D) show a small, but distinct, focus of abnormal uptake in the left lower neck, between the oesophagus and a posterior extension of the thyroid lobe (‘Zuckermandl lobe’), indicative of a small PTA.

Follow-up: Surgical exploration was suggested but postponed in view of the minimal metabolic consequences of the PTA at this stage.

Teaching points

^{18}F -choline imaging may have equal specificity to conventional ^{99m}Tc -sestaMIBI/pertechnetate scintigraphy performed with washout, subtraction and/or single photon emission computed tomography (SPECT) or SPECT–CT protocols, but PET–CT has a higher sensitivity. In this case, PET–CT detected a small, moderately metabolically active lesion. The diagnostic sensitivity of ^{18}F -choline PET–CT for PTA was found to be 96%, with a positive predictive value of 100%. In sestaMIBI-negative cases, ^{18}F -choline PET–CT may be considered prior to surgery, if available. If positive, no confirmatory investigations such as US or MRI are necessary, and it can be recommended to proceed directly to targeted, minimally invasive surgery.

Keywords: PTA, ^{18}F -choline, ^{99m}Tc -sestaMIBI



6. FLUORO-DIHYDROTESTOSTERONE — FDHT (¹⁸F)

6.1. GENERAL CHARACTERISTICS

Name: ¹⁸F-fluoro-dihydrotestosterone (¹⁸F-FDHT)

Synonyms: 16β-[¹⁸F]fluoro-5α-dihydrotestosterone

Radioisotope

¹⁸F is a short half-life PET radioisotope (109.7 min) emitting positrons of E_{\max} 1.656 MeV. Owing to the high chemical stability of C–F bonds in organic compounds as well as the high water solubility of F compounds, ¹⁸F tracers usually exhibit suitable stability and biodistribution in humans. Although the F chemistry is complicated, the vast application of ¹⁸F labelled compounds in nuclear medicine has led to the development of efficient automated radiopharmaceutical production methods allowing large scale production of ¹⁸F tracers for clinical use.

Radiosynthesis

Although many centres produce the tracer using small scale non-automated methods, fully automated synthesis of ¹⁸F-FDHT using only commercially available components has been reported with radiochemical yields of 25–33%, radiochemical purity of >99% and specific activity >18.5 GBq/μmol in 90 min. The procedure uses low amounts of precursor and appears cost effective (Fig. 6.1) [35–37].

6.2. PHARMACOKINETICS

6.2.1. Physiological biodistribution and metabolism

The free fraction of activity in the plasma was found to be less than 2% at all time points during the investigation, indicating that ¹⁸F-FDHT, as well as its metabolic products, are highly bound to plasma proteins. The more lipophilic metabolites accounted for 75% in a 5 min plasma sample and dropped to 5% in a 30 min plasma sample. It must be assumed that the in vivo metabolism of ¹⁸F-FDHT can vary somewhat between subjects. The normal radiotracer biodistribution exhibits uptake in blood vessels and the liver. The tracer is excreted via the gallbladder and bile ducts to the intestines, and also via the urogenital tract [35–37].

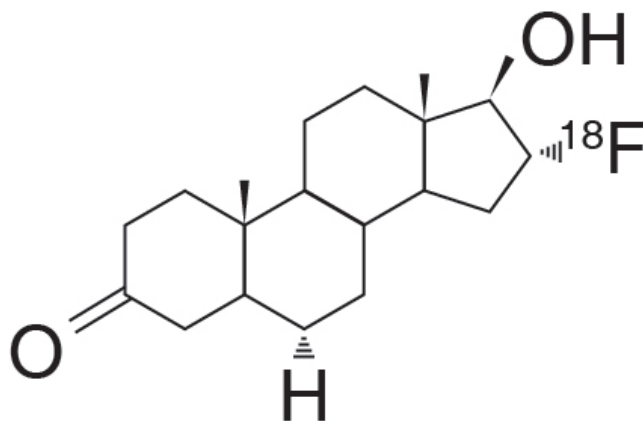


FIG. 6.1. Molecular structure of ¹⁸F-fluoro-dihydrotestosterone.

6.2.2. Mechanism of retention

Upon administration, ^{18}F -FDHT binds to the androgen receptor (AR) and is potentially integrated into AR expressing prostate tumour cells, leading to their successful imaging.

6.2.3. Pharmacology and toxicology

No data are available.

6.3. METHODOLOGY

6.3.1. Activity, administration, dosimetry

Patients are administered an IV bolus of 111–407 MBq of ^{18}F -FDHT. Except for the liver (0.003 33 cGy/MBq) and the urinary bladder wall (0.008 68 cGy/MBq), the mean absorbed dose to each tissue was found to be less than 0.003 cGy/MBq. The effective dose equivalents range between 0.001 52 and 0.002 01 cSv/MBq. These absorbed doses provide the basis for the level of administered activity of ^{18}F -FDHT specified above [38–42].

6.3.2. Imaging protocol

No specific patient preparation is required. Treatment with AR antagonists needs to be stopped for at least 5 weeks prior to the study. Imaging is performed following the IV injection of a dose of 200 MBq and an uptake period of 60 min. Acquisition of the PET component moves from the proximal femur to the skull. Acquisition time is 1–3 min/bed position, depending on body weight (1 min for less than 60 kg, 2 min for 60–90 kg, 3 min for over 90 kg). For the CT imaging protocol, see general comments in Section 1.3.

6.4. CLINICAL ASPECTS

6.4.1. Indications

6.4.1.1. Prostate cancer

^{18}F -FDHT PET–CT is performed when conventional imaging techniques do not suffice for diagnosis or when biopsy is not possible. Furthermore the study can be performed to provide a rationale for AR targeted therapy. The study can also assist to determine the AR binding status (receptor saturation) during AR targeted therapy, providing data that may be used to adjust the treatment dose in the individual patient.

6.4.1.2. Breast cancer

^{18}F -FDHT PET–CT may be performed to provide a rationale for AR targeted therapy.

6.4.1.3. All other diseases with a high probability of androgen receptor expression

^{18}F -FDHT PET–CT may be performed in cases challenging to diagnose.

6.4.2. Cases

Cases courtesy of A. Glaudemans, University Medical Centre Groningen, the Netherlands.

6.4.2.1. Case No. 6.1

Clinical indication for PET–CT: Prostate cancer, staging

Clinical history

A 72 year old man with prostate cancer a known left inguinal LN metastasis.

PET–CT findings

^{18}F -FDHT PET–CT MIP shows abnormal tracer uptake in the known left inguinal nodal metastasis (arrow), with no other AR expressing lesions.

Teaching point

^{18}F -FDHT PET–CT may be used for staging of prostate cancer.

Keywords: Prostate cancer, staging, ^{18}F -FDHT



Clinical indication for PET–CT: Prostate cancer, staging

Clinical history

A 76 year old man with newly diagnosed prostate cancer and known bilateral inguinal LN metastases.

PET–CT findings

¹⁸F-FDHT PET–CT MIP shows multiple areas of abnormal tracer uptake in LNs above and below the diaphragm, including bilateral inguinal, para-iliac, para-aortic and retroperitoneal regions, as well as the pulmonary hilar and bilateral cervical nodes. Furthermore, there is abnormal uptake in several bone metastases in the spine, ribs and pelvis. The findings are consistent with disseminated nodal and skeletal metastatic disease with increased AR expression.

Teaching points:

¹⁸F- FDHT PET–CT allows upstaging of disease.

Keywords: Prostate cancer, upstaging, ¹⁸F- FDHT



6.4.2.3. Case No. 6.3

Clinical indication for PET–CT: Prostate cancer, staging in the presence of equivocal findings on CT.

Clinical history

A 69 year old man with prostate cancer presented with equivocal findings on diagnostic CT, including normal size pelvic LNs and an unclear lesion in the right iliac bone.

PET–CT findings

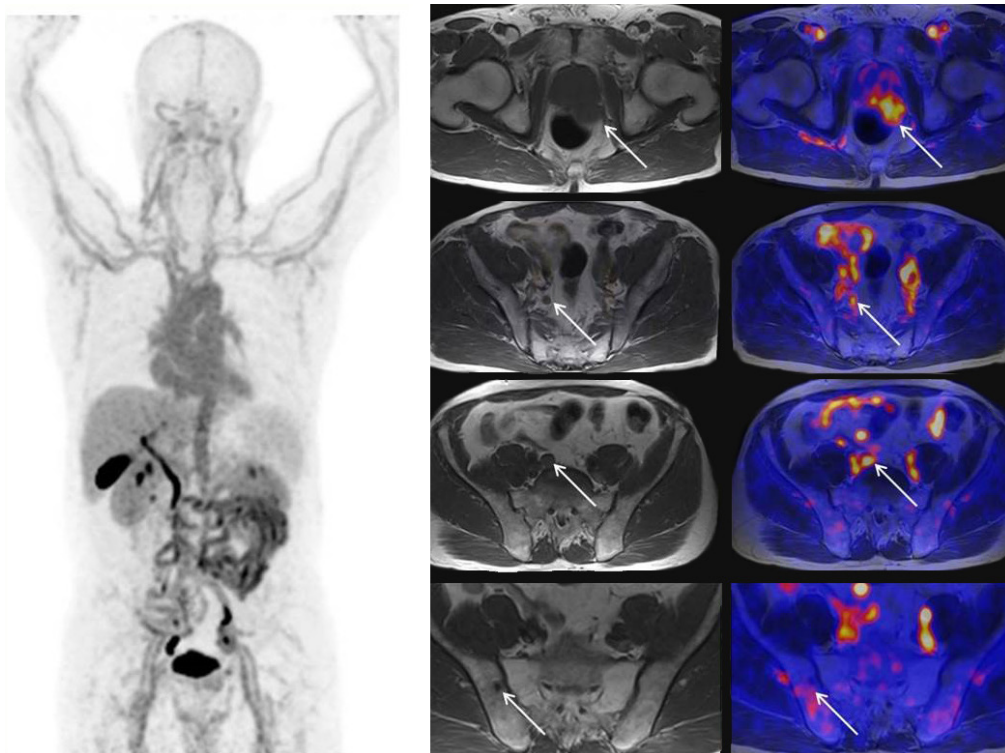
(Left): MIP; (centre): MRI transaxial slices of pelvis; (right): fused transaxial slices of pelvis.

There are foci of abnormal tracer uptake in the prostatic tumour, located dorsally in the left lobe (first row, arrows) and in small pelvic LNs (second and third rows, arrows) consistent with nodal metastases with increased AR expression. There is no tracer uptake in the right iliac bone lesion (fourth row, arrow).

Teaching point

¹⁸F- FDHT may play a role in staging of prostate cancer.

Keywords: Prostate cancer, staging, ¹⁸F-FDHT



6.4.2.4. Case No. 6.4

Clinical indication for PET–CT: Prostate cancer, restaging

Clinical history

An 88 year old man with prostate cancer (cT4N0M0), Gleason score 10, PSA 120 ng/mL, treated with luteinizing hormone releasing hormone agonist, had a normal bone scintigraphy.

PET–CT findings

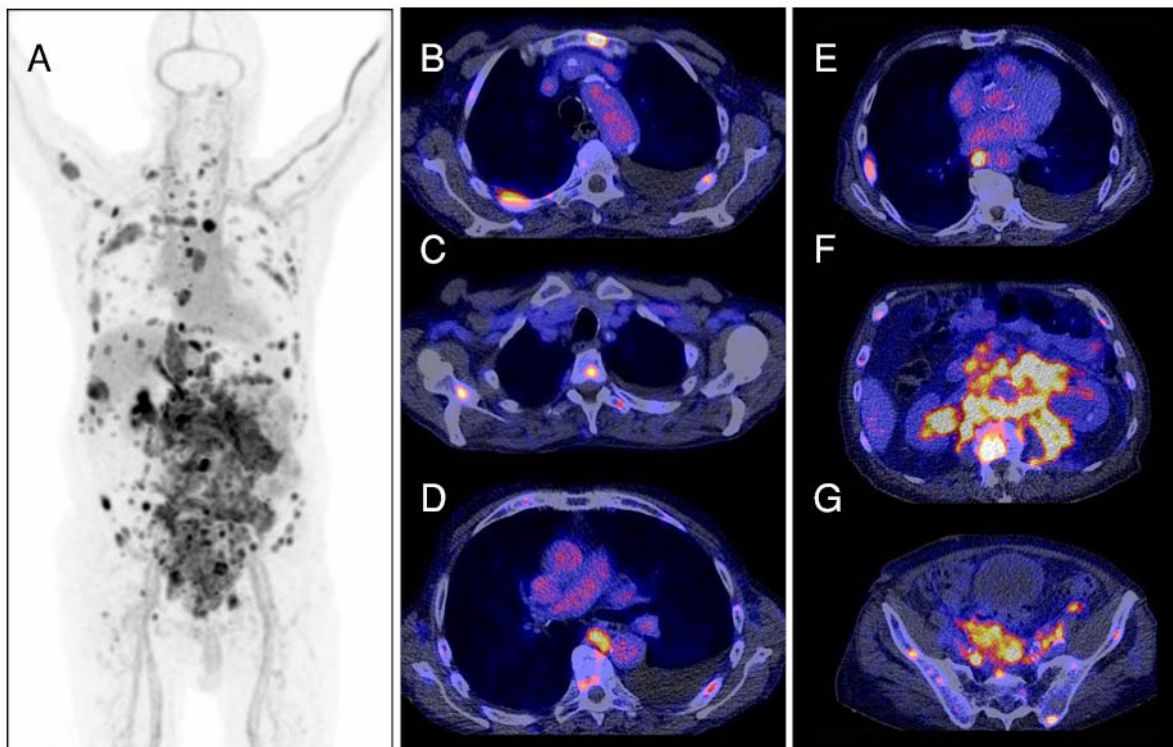
(A): MIP; (B–G): fused transaxial slices at various levels of the chest, abdomen and pelvis.

There is abnormal tracer uptake in disseminated LN metastases above and below the diaphragm (D, E, F), and multiple bone metastases in the sternum, ribs, scapulae, spine, and pelvis (B, C, G), all with high AR expression. The patient was referred for treatment with an AR antagonist.

Teaching points

¹⁸F-FDHT PET–CT plays a role in restaging patients with advanced tumours, with further therapeutic implications.

Keywords: Prostate cancer, restaging, ¹⁸F- FDHT



7. F-DOPA (¹⁸F)

7.1. GENERAL CHARACTERISTICS

Name: ¹⁸F-DOPA

Synonyms: L-3,4-Dihydroxy-6-[¹⁸F]fluorophenylalanine; 6-[¹⁸F]fluoro-L-DOPA; [¹⁸F]FDOPA

Radioisotope

¹⁸F is a short half-life PET radioisotope (109.7 min) emitting positrons of E_{\max} 1.656 MeV. Owing to the high chemical stability of C–F bonds in organic compounds as well as the high water solubility of F compounds, ¹⁸F tracers usually exhibit suitable stability and biodistribution in humans. Although the F chemistry is complicated, the vast application of ¹⁸F labelled compounds in nuclear medicine has led to development of efficient automated radiopharmaceutical production methods allowing large scale production of ¹⁸F tracers for clinical use.

Radiosynthesis

¹⁸F-DOPA can be synthesized by either an electrophilic or nucleophilic process (Fig. 7.1). Electrophilic fluorination of a precursor with ¹⁸F acetyl hypofluorite afforded low radiochemical yield (8%, with 95% chemical purity and specific activity of 7.4 GBq/mmol in 100 min). A recently developed multistep synthesis based on the nucleophilic displacement of a nitro group using the standard ¹⁸F-KF Kryptofix complex had a reported chemical purity of >96%, specific activity of 1 Ci/μmol and radiochemical yield of 23% in 90 min [43].

7.2. PHARMACOKINETICS

7.2.1. Physiological biodistribution and metabolism

¹⁸F-DOPA is converted to 6-[¹⁸F]fluorodopamine (FDA) by alpha amino acid dehydrogenase (AAAD) and retained in the striatum. FDA can be O-methylated by catechol-O-methyltransferase (COMT) to 3-O-methyl-6-[¹⁸F]fluoro-L-dopa, which is uniformly distributed throughout the brain. FDA is also metabolized via monoamine oxidase to yield [¹⁸F]6-fluoro-3,4-dihydroxyphenylacetic acid (FDOPAC) and subsequently by COMT to yield [¹⁸F]6-fluorochomovanillic acid. AAAD and COMT

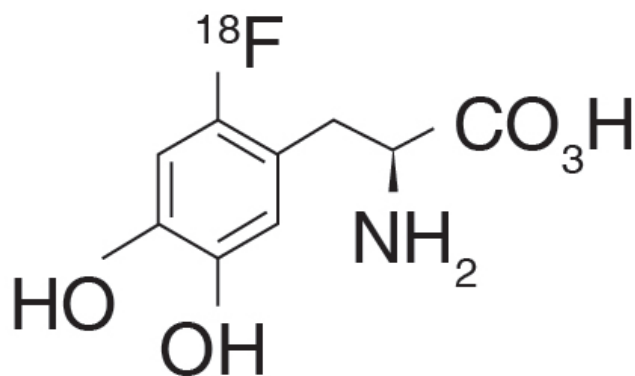


FIG. 7.1. Molecular structure of ¹⁸F-DOPA.

are also present in peripheral tissues such as the liver, kidneys and lung. At 1 hour after administration of ^{18}F -DOPA, there is physiological tracer uptake in the basal ganglia of the brain, as well as high intensity uptake in the gallbladder and pancreas, and moderate to low activity in the liver. Tracer activity can also be seen in the kidneys and/or proximal ureters and the urinary bladder (Fig. 7.2) [43].

7.2.2. Mechanism of retention

^{18}F -DOPA reflects all stages of DOPA transport, storage and metabolism into the neurons, providing important information for understanding dopamine related diseases.

7.3. METHODOLOGY

7.3.1. Activity, administration, dosimetry

The administered activity varies largely in the literature. In a recent study, a fixed amount of 185 MBq ^{18}F -DOPA was injected, and all acquisitions were performed after 1 hour.

Based on murine and human biodistribution data, the bladder wall receives the highest dose (0.215 mGy/MBq or 0.797 rad/mCi). Other organs receiving high doses are the kidneys (0.089 mGy/MBq or 0.329 rad/mCi) and pancreas (0.030 mGy/MBq or 0.110 rad/mCi). The brain, liver and lungs receive <0.008 mGy/MBq (0.029 rad/mCi). Effective dose equivalent following the tracer administration was estimated at 0.026 mSv/MBq (96 mrem/mCi) [43].

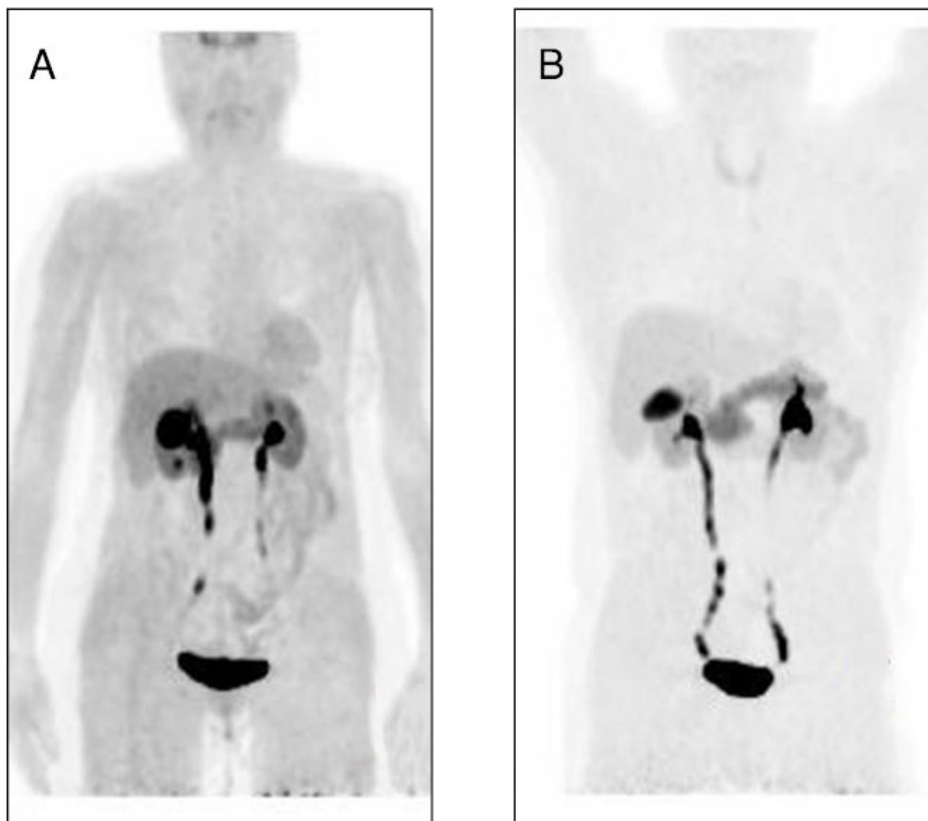


FIG. 7.2. Normal biodistribution of ^{18}F -DOPA in two patients.

7.3.2. Imaging protocol

7.3.2.1. Whole body PET–CT

A fasting period of more than 4 hours prior to administration of the radiotracer is suggested. Imaging is performed following the IV injection of a dose of 2–3 MBq/kg and an uptake period of 60 min. Acquisition time is 2–3 min/bed position. An additional early acquisition, at 10 min after injection, is suggested in cases of medullary thyroid cancer (MTC). For the CT imaging protocol, see general comments in Section 1.3.

7.3.2.2. Brain PET–CT

Imaging is performed following the IV injection of 2–3 MBq/kg and an uptake period of 10 min. Dynamic, one bed position brain acquisition for 40 min, or static, one bed brain acquisitions at 10 and 40–50 min after injection, are performed.

7.4. CLINICAL ASPECTS

7.4.1. Indications

^{18}F -DOPA is the PET tracer of choice for detection of recurrent MTC. Acquiring early (10 min) and late (60 min) images improves the accuracy of ^{18}F -DOPA PET–CT for detection of MTC recurrence [44].

^{18}F -DOPA is also used for characterization of adrenal masses suspected to be pheochromocytomas. ^{18}F -DOPA is very useful to detect multifocal disease and/or potential metastases of malignant pheochromocytomas [45].

In patients with neuroblastoma, ^{18}F -DOPA can clarify doubtful radiolabelled miBG scan results. ^{18}F -DOPA can be an alternative to miBG scintigraphy in neuroblastoma, for initial staging, in suspected relapse and for evaluation of response to therapy [46].

^{18}F -DOPA PET–CT may also have a role in the management of neuroendocrine tumours (NETs). It has a high accuracy for staging, restaging and monitoring response to therapy. It should be emphasized that for this indication, ^{68}Ga -DOTA-peptide tracers are the first choice. However, in patients with absent somatostatin receptor (SSTR) expression, and in centres that do not have availability of ^{68}Ga -DOTA-peptide tracers, ^{18}F -DOPA can play a role [47].

^{18}F -DOPA PET–CT can be also used to differentiate recurrent glioma from post-radiation necrosis and post-operative changes. It is also applied for therapy evaluation and detection of pseudo-response.

7.4.2. Cases

7.4.2.1. Case No. 7.1

Clinical indication for PET–CT: Suspected pheochromocytoma

Clinical history

A 45 year old patient with resistant hypertension raised the clinical suspicion of pheochromocytoma.

PET–CT findings

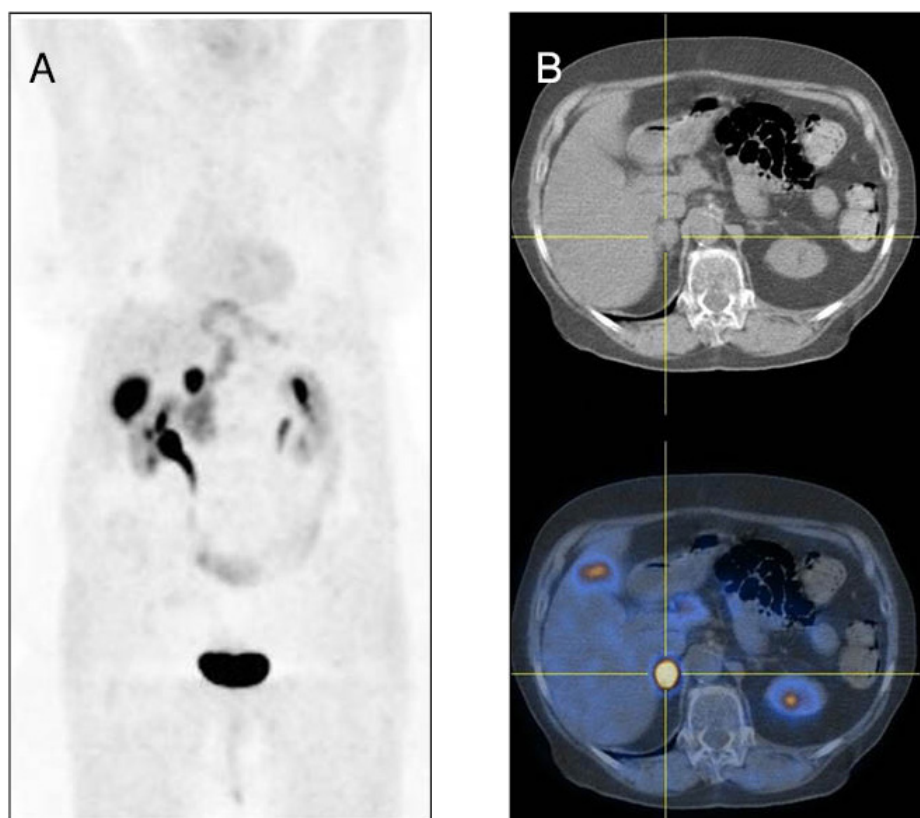
(A): MIP; (B): CT and fused transaxial images of upper abdomen.

There is intense tracer uptake in an enlarged right adrenal gland, consistent with a pheochromocytoma.

Teaching point

^{18}F -DOPA is the imaging method of choice for diagnosis of pheochromocytoma.

Keywords: Pheochromocytoma, ^{18}F -DOPA



Clinical indication for PET–CT: Suspected pheochromocytoma

Clinical history

A 55 year old woman with paroxysmal hypertension and elevated urinary catecholamines and metanephrines had a negative ^{18}F -FDG PET–CT study.

PET–CT findings

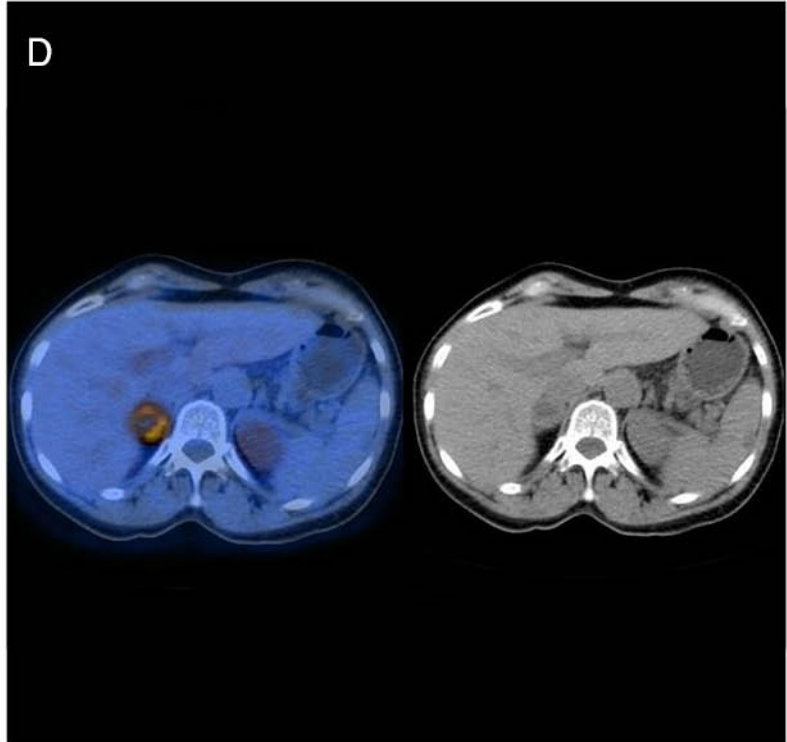
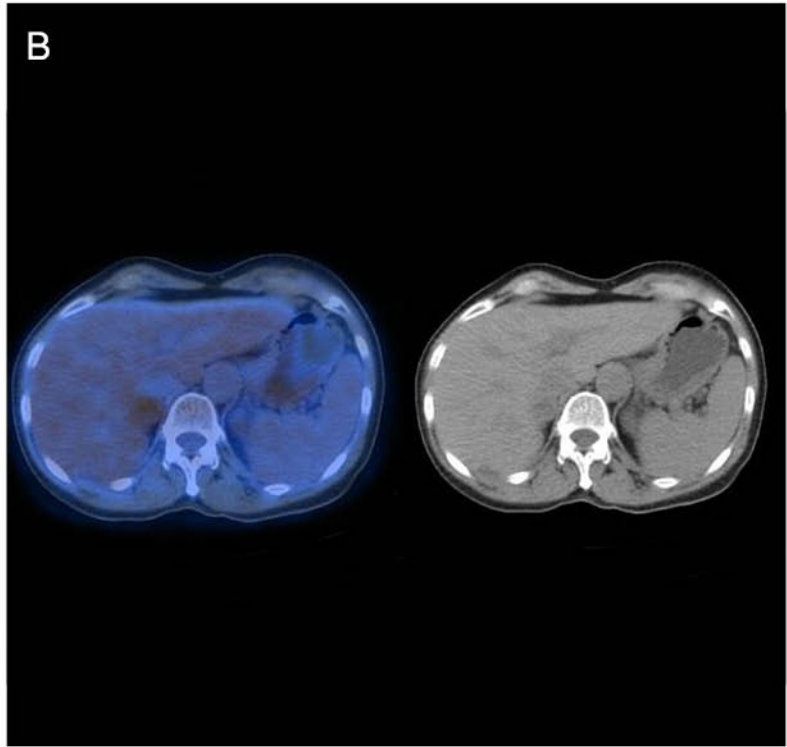
(A): ^{18}F -FDG MIP; (B): ^{18}F -FDG fused and CT transaxial slices of upper abdomen; (C): ^{18}F -DOPA MIP; (D): ^{18}F -DOPA fused and CT transaxial slices at same level as in (B).

There is intense ^{18}F -DOPA uptake in an enlarged right adrenal gland, with no corresponding ^{18}F -FDG uptake, consistent with pheochromocytoma, further confirmed at surgery.

Teaching point

^{18}F -DOPA PET–CT has a high accuracy for detection of pheochromocytoma. It is considered the first choice PET tracer for identification and staging of this disease.

Keywords: Pheochromocytoma, ^{18}F -DOPA, ^{18}F -FDG



Clinical indication for PET–CT: Suspected pheochromocytoma

Clinical history

A 51 year old woman had episodic abdominal pain and hypertension; pheochromocytoma was suspected.

PET–CT findings

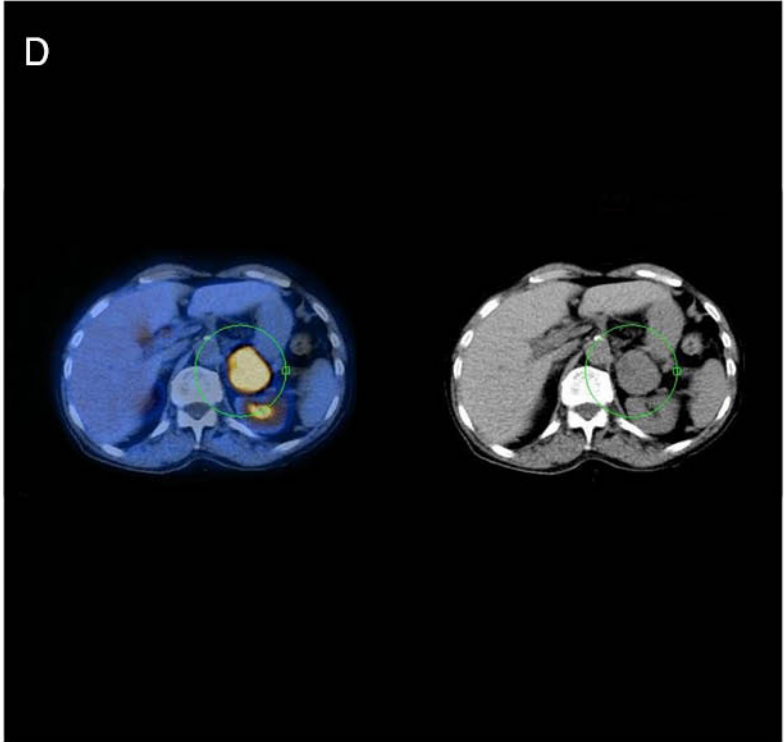
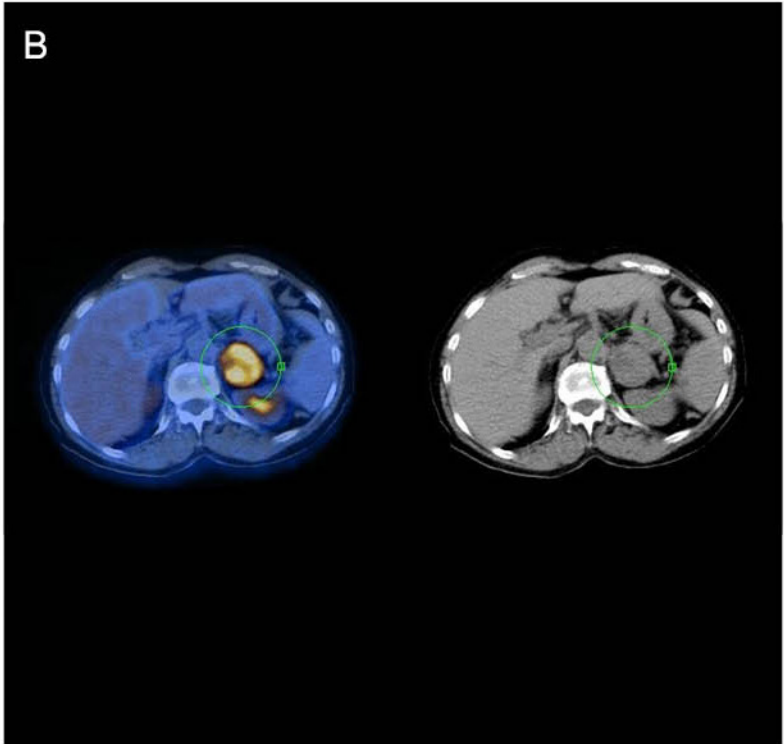
(A): ^{18}F -FDG MIP; (B): ^{18}F -FDG fused and CT transaxial slices of upper abdomen; (C): ^{18}F -DOPA MIP; (D): ^{18}F -DOPA fused and CT transaxial slices at the same level as in (B).

There is intense ^{18}F -FDG and ^{18}F -DOPA uptake in a left adrenal mass (green marker). Surgery diagnosed malignant pheochromocytoma.

Teaching point

Approximately 10% of pheochromocytomas are malignant. They show aggressive behaviour and can metastasize. Both ^{18}F -FDG and ^{18}F -DOPA PET–CT have a high accuracy for staging of this disease.

Keywords: Malignant pheochromocytoma, ^{18}F -DOPA, ^{18}F -FDG



Clinical indication for PET–CT: Suspected abdominal paraganglioma

Clinical history

A 48 year old patient had an abdominal mass; abdominal paraganglioma was suspected.

PET–CT findings

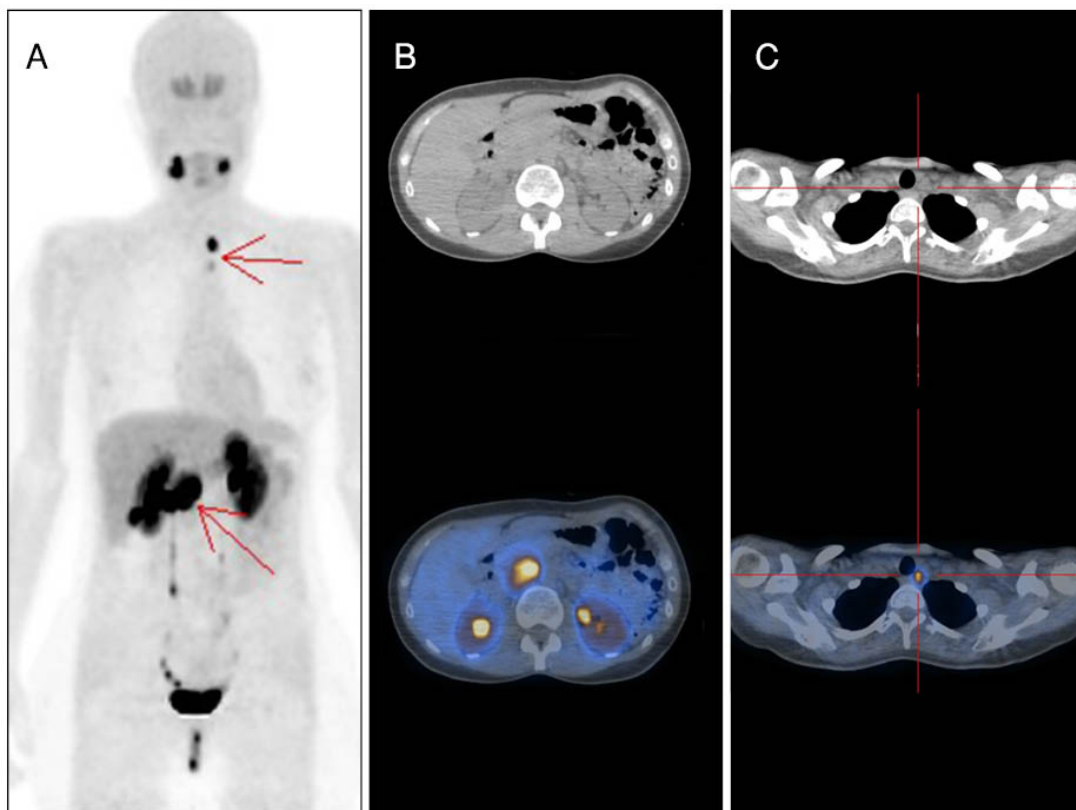
(A): MIP; (B): CT and fused transaxial slices of mid-abdomen; (C): CT and fused transaxial slices of lower neck.

There is intense tracer uptake in the known abdominal mass, and an additional focus in a left paratracheal lesion (arrows) diagnosed at surgery as paraganglioma.

Teaching point

^{18}F -DOPA is the tracer of choice for detection of paraganglioma. The high diagnostic accuracy is due to the whole body imaging capabilities and the high tumour to background ratio.

Keywords: Paraganglioma, ^{18}F -DOPA



Clinical indication for PET–CT: Evaluation of brain lesion

Clinical history

A 61 year old woman presented with an indeterminate left thalamic lesion on MRI, suspected to represent a low grade glioma.

PET–CT findings

(A): MRI transaxial slice of brain; (B): PET transaxial slice; (C): fused PET and MRI transaxial slice.

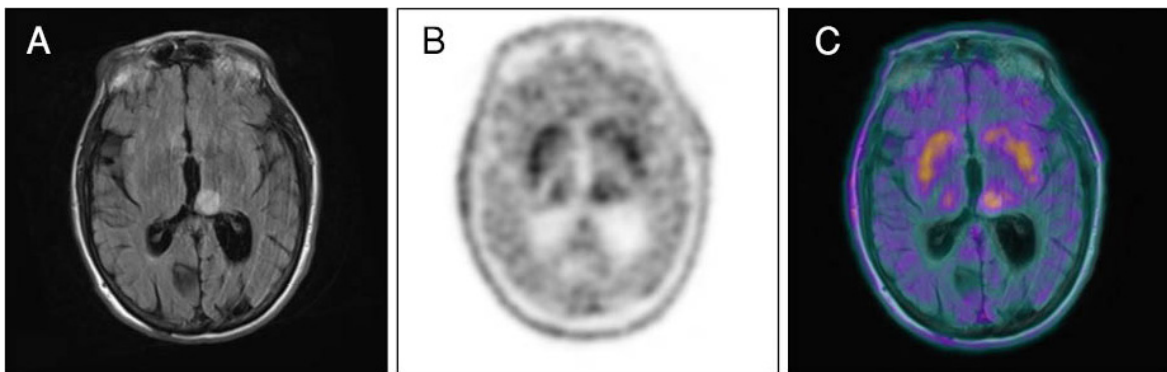
There is mild ^{18}F -DOPA uptake in the thalamic lesion, also suggestive of low grade glioma.

Follow-up: The lack of change observed in a follow-up after two years confirmed the diagnosis.

Teaching point

^{18}F -DOPA can be used as an amino acid tracer in neuro-oncology. This tracer has a higher striatal uptake as compared with ^{18}F -FET.

Keywords: Glioma, ^{18}F -DOPA



Clinical indication for PET–CT: Metastatic NET of unknown primary origin

Clinical history

A 61 year old woman diagnosed with metastatic NET following resection of a hepatic lesion was referred in search of the primary tumour.

PET–CT findings

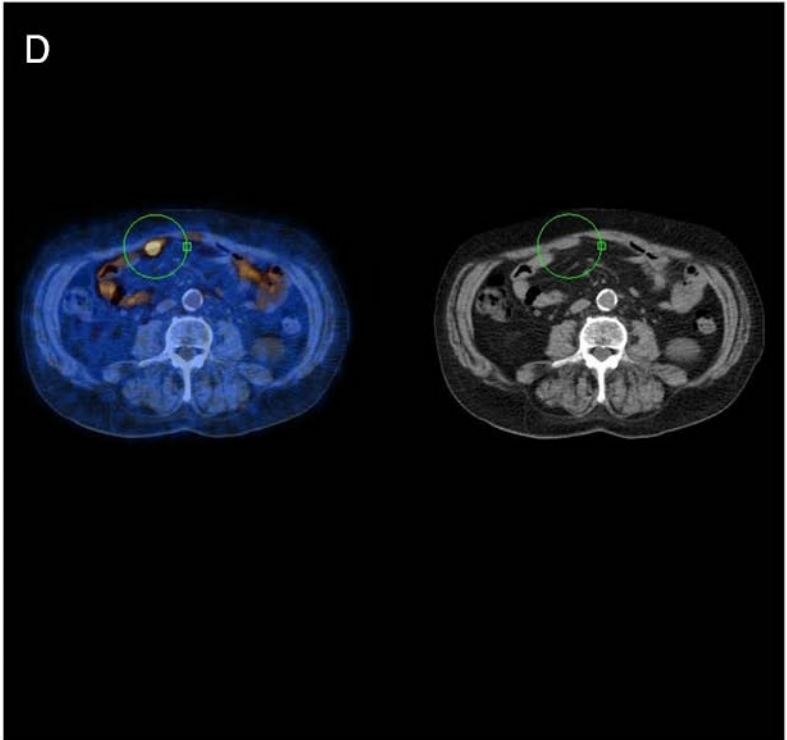
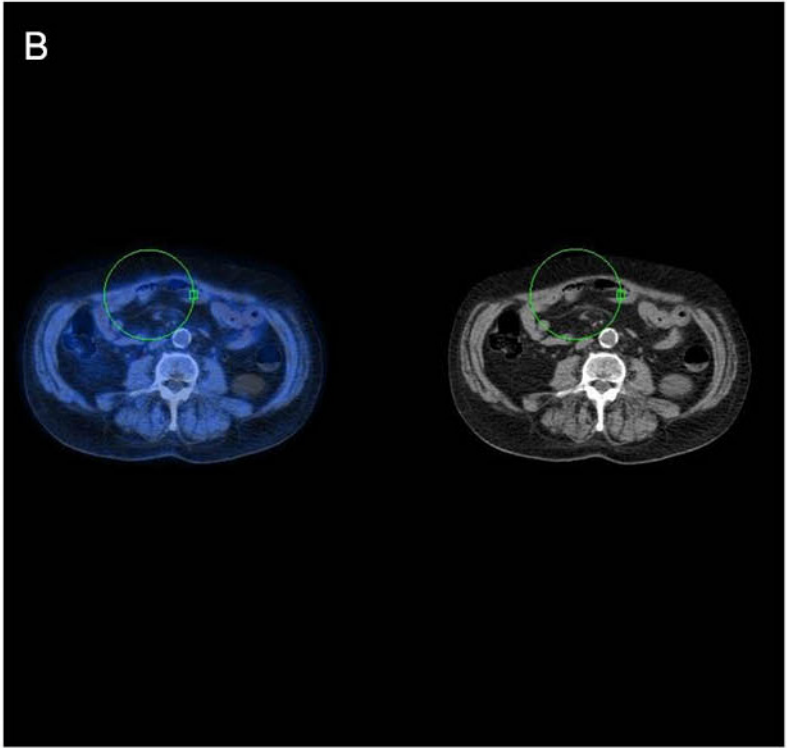
(A): ^{68}Ga -DOTANOC MIP; (B): ^{68}Ga -DOTANOC fused and CT transaxial slices of mid-abdomen; (C): ^{18}F -DOPA MIP; (D): ^{18}F -DOPA fused and CT transaxial slices at the same level as in (B).

No abnormal findings are seen in the ^{18}F -DOPA study. There is focal increased ^{68}Ga -DOTANOC uptake in the small bowel, probably the ileum (green marker).

Teaching point

^{68}Ga -DOTA-peptides are more accurate than ^{18}F -DOPA for evaluation of NETs and should be the first choice PET tracer for detection of tumours of unknown primary origin. In patients with absent SSTR expression, ^{18}F -DOPA imaging may be a useful second method of investigation.

Keywords: Cancer of unknown primary origin, ^{18}F -DOPA, ^{68}Ga -DOTANOC



Clinical indication for PET–CT: Extra-adrenal paraganglioma, pre-operative staging

Clinical history

A 59 year old man with a known paraganglioma was referred following detection of two additional suspicious extra-adrenal cervical lesions on MRI.

PET–CT findings

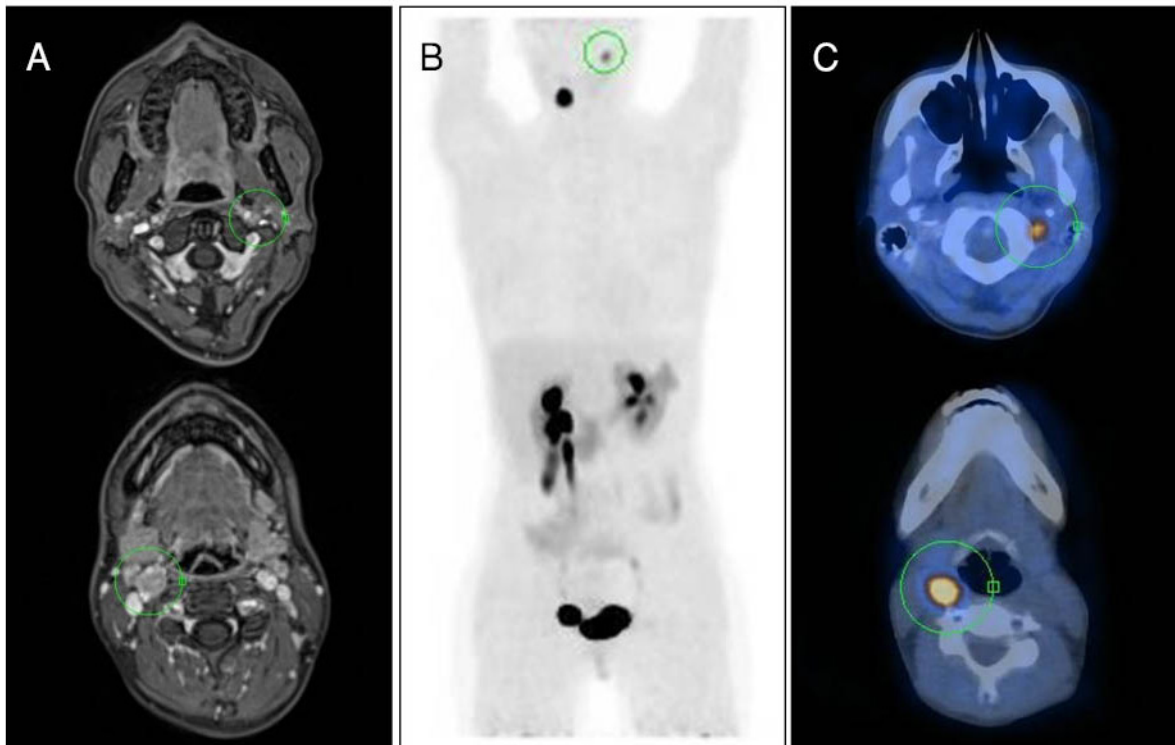
(A): MRI transaxial slices at upper and mid-cervical levels; (B): MIP; (C): fused PET–MRI transaxial slices at the same levels as in (A).

There is intense tracer uptake in two lesions on both sides of the neck (green markers), consistent with extra-adrenal sites of paraganglioma.

Teaching point

¹⁸F-DOPA PET–CT is useful, in addition to anatomical imaging, in the pre-operative localization and molecular assessment of extra-adrenal paragangliomas. However, ⁶⁸Ga-DOTA-peptides are superior to ¹⁸F-DOPA and are considered the PET tracers of choice in this setting.

Keywords: Paraganglioma, ¹⁸F-DOPA



Clinical indication for PET–CT: Staging of lung carcinoid

Clinical history

A 45 year old patient with suspected right lung carcinoid.

PET–CT findings

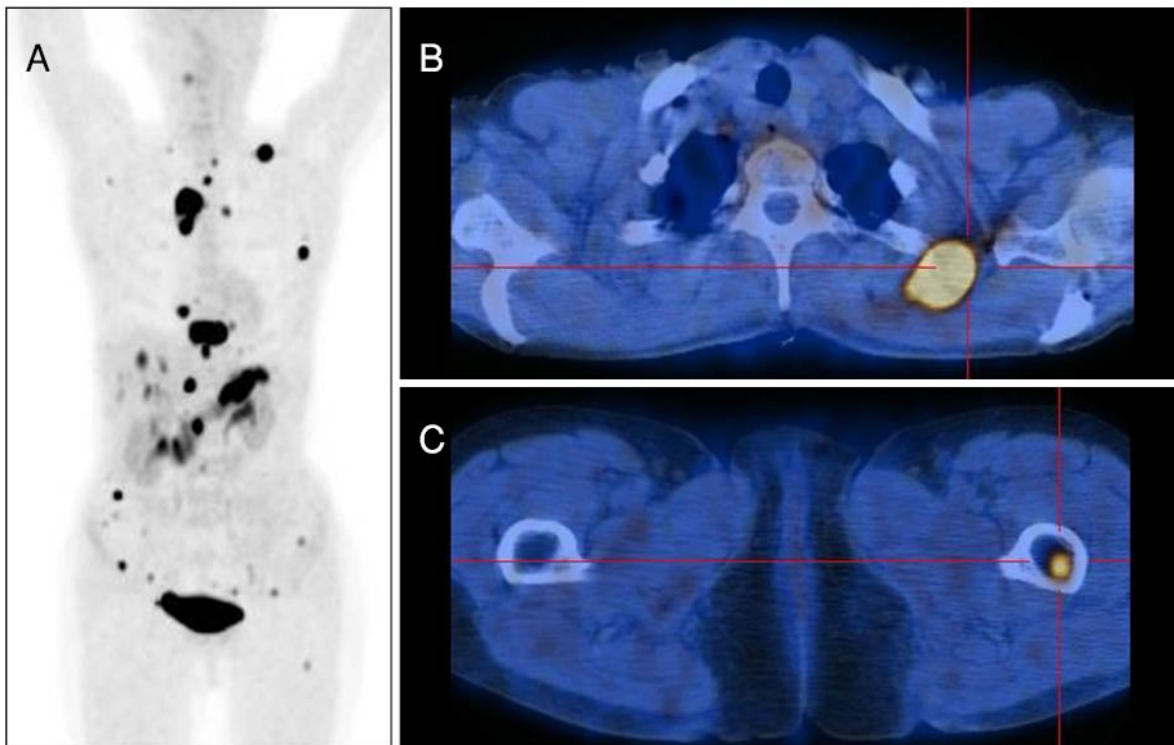
(A): MIP; (B): fused PET–CT images of the upper thorax; (C): fused PET–CT images of the proximal femurs.

There is intense tracer uptake in the right lung as well as in multiple bone and soft tissue lesions, consistent with metastatic carcinoid.

Teaching point

^{18}F -DOPA may help in the staging of lung carcinoid but should only be used when ^{68}Ga -DOTA-peptides are not available.

Keywords: Carcinoid, ^{18}F -DOPA



Clinical indication for PET–CT: Neuroblastoma, staging

Clinical history

A 6 month old girl with newly diagnosed neuroblastoma was referred for staging.

PET–CT findings

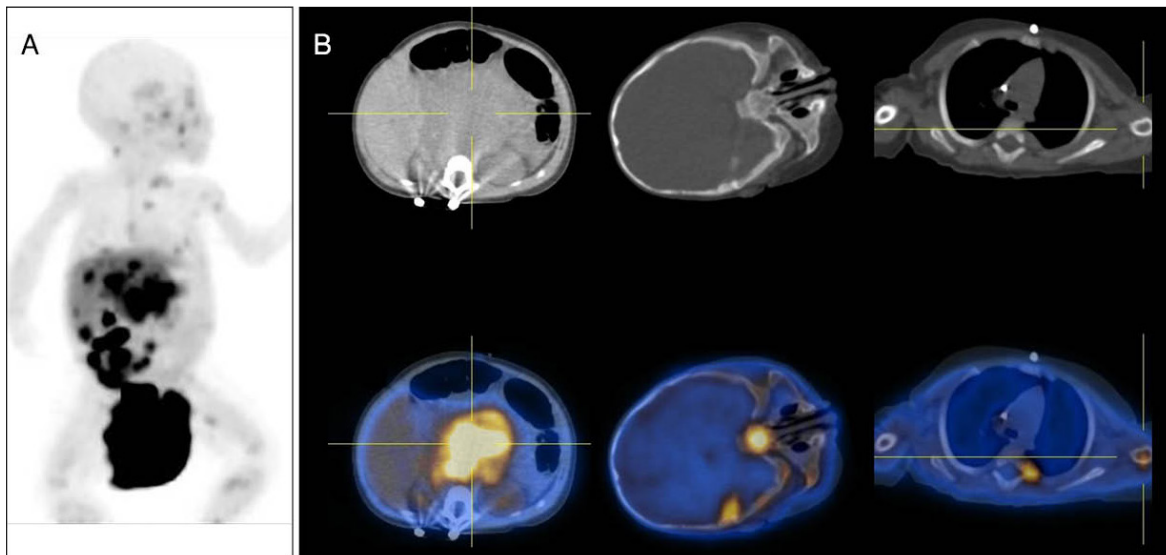
(A): MIP; (B): CT and fused transaxial slices of abdomen, head and chest.

There are foci of intense tracer uptake in multiple metastases in the liver and skeleton, consistent with stage IV disease.

Teaching point

^{18}F -DOPA is the imaging tracer of choice in neuroblastoma.

Keywords: Neuroblastoma, paediatric, ^{18}F -DOPA



Clinical indication for PET–CT: Glioblastoma, therapy evaluation

Clinical history

A 38 year old woman with grade IV glioblastoma, treated by surgery and adjuvant RT 12 months earlier and receiving bevacizumab, had an MRI study that showed reduction of the areas of Gd enhancement, suggestive of partial response.

PET–CT findings

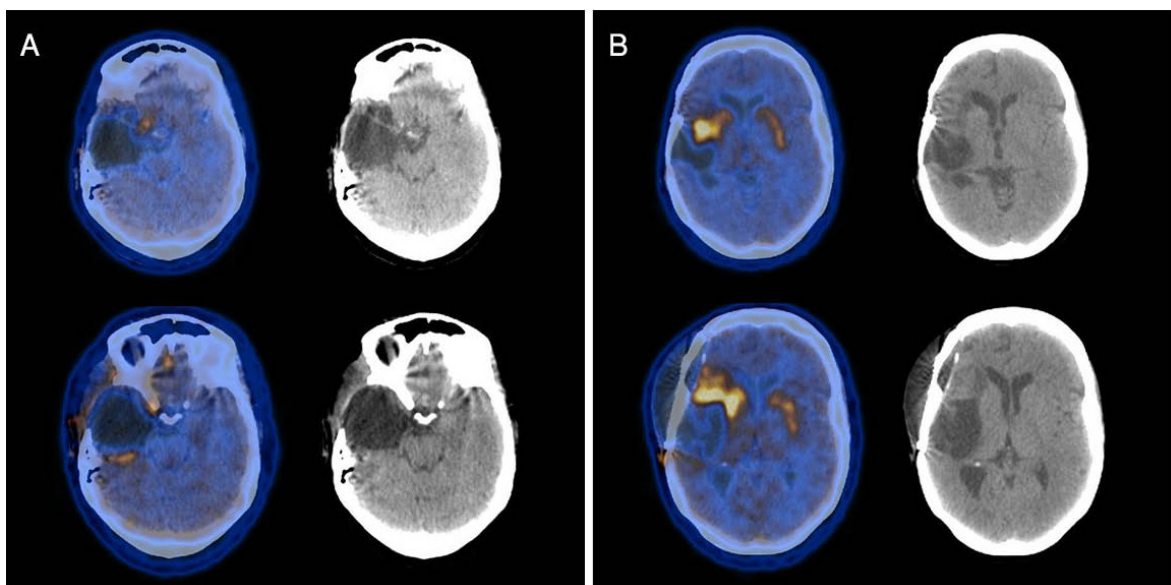
(A): baseline CT and fused transaxial slices of brain; (B): follow-up images of the same slices as in (A).

There is a new site of abnormal ^{18}F -DOPA uptake adjacent to post-surgical changes in the follow-up study as compared with the baseline study, consistent with disease progression.

Teaching point

It is difficult to evaluate response of brain tumours to therapy by MRI. The disease may progress without manifesting an increase in the size of the Gd enhanced tumour (pseudo-response). ^{18}F -DOPA PET–CT is a valuable method to assess treatment response in high grade gliomas.

Keywords: Glioma, tumour progression, pseudo-response, ^{18}F -DOPA



Clinical indication for PET–CT: Oligodendroglioma, evaluation after surgery

Clinical history

A 46 year old man with anaplastic oligodendroglioma was reassessed 3 months after surgery.

PET–CT findings

(A): baseline MIP and fused and CT transaxial slices of brain; (B): post-surgery images of the same slices as in (A).

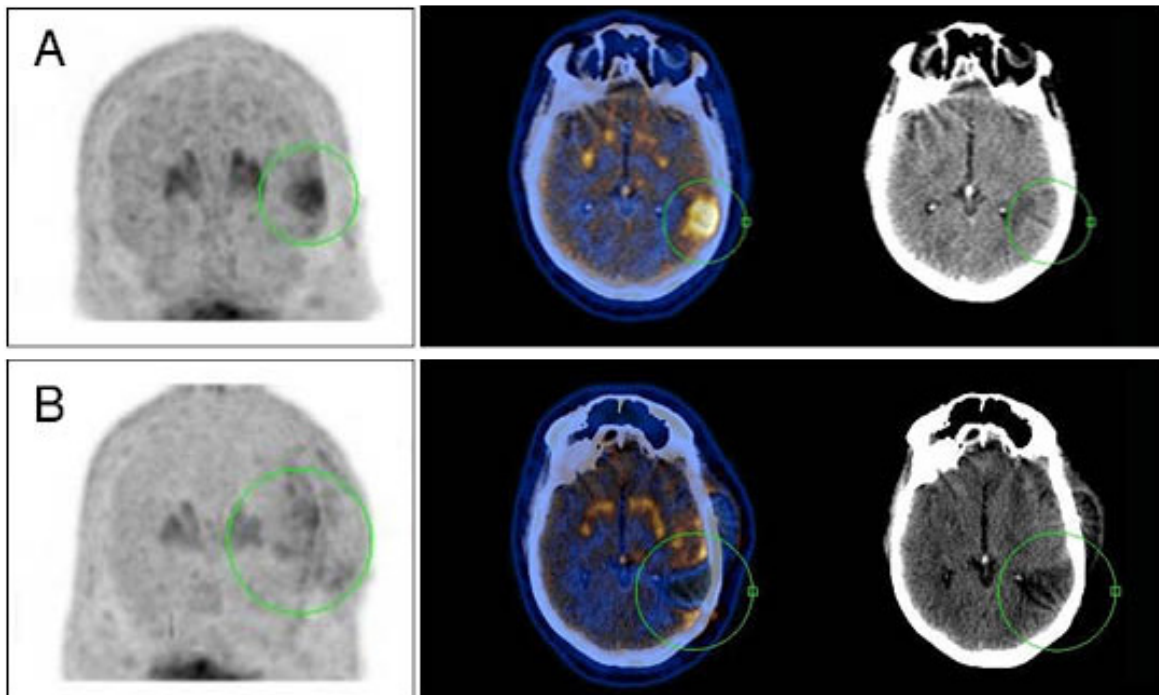
Prior to surgery there is highly increased tracer uptake by the tumour. After surgery there is only mild, slightly inhomogeneous ^{18}F -DOPA uptake surrounding the surgical cavity.

Follow-up: Follow-up at 6 months indicated no change.

Teaching point

Mild, homogenous ^{18}F -DOPA uptake observed after surgery should not be interpreted as recurrence.

Keywords: Surgery, pitfall, ^{18}F -DOPA



Clinical indication for PET–CT: Neuroblastoma, suspicion of relapse

Clinical history

A 2 year old patient with history of neuroblastoma presented with suspected relapse of the disease in a left paravertebral mass.

PET–CT findings

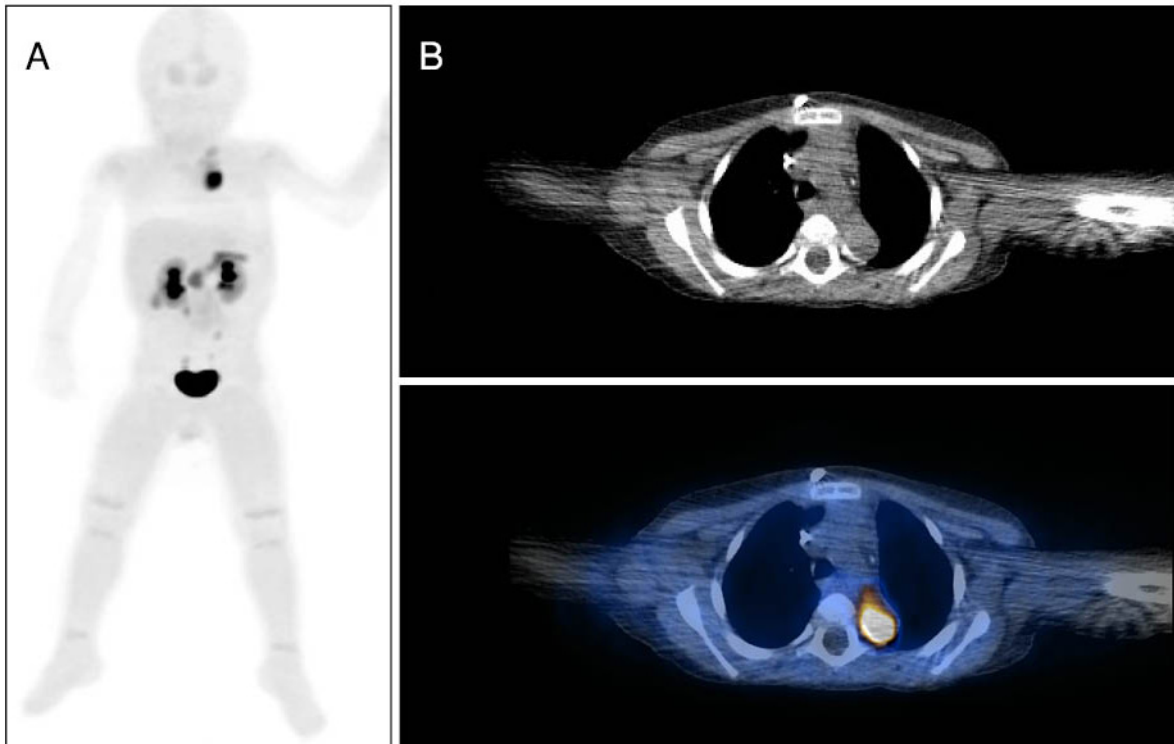
(A): MIP; (B): CT and fused transaxial slices of mid-thorax.

There is intense tracer uptake in a left paravertebral mass adjacent to the upper thoracic spine suggesting relapse. Biopsy confirmed recurrent neuroblastoma.

Teaching point

^{18}F -DOPA is the imaging tracer of choice in neuroblastoma. It has higher diagnostic accuracy in comparison with miBG scintigraphy, mainly due to the higher quality of PET–CT images as compared with SPECT.

Keywords: Neuroblastoma, paediatric, ^{18}F -DOPA



Clinical indication for PET–CT: MTC, suspected recurrence

Clinical history

A 76 year old patient with MTC, post-surgery, presented with high calcitonin serum levels (200 ng/mL).

PET–CT findings

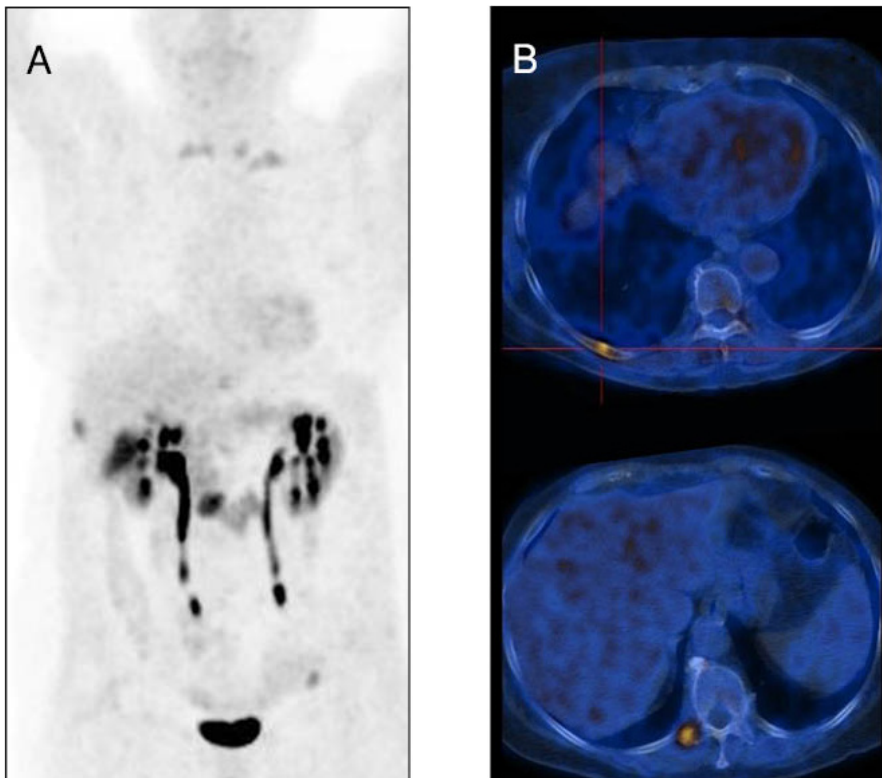
(A): MIP; (B): fused transaxial slices of mid-thorax and lower thorax.

There is intense tracer uptake in multiple bone lesions, including in ribs and vertebrae.

Teaching point

^{18}F -DOPA is the imaging tracer of choice in the detection of relapsed MTC.

Keywords: MTC, ^{18}F -DOPA



Clinical indication for PET–CT: MTC, suspected recurrence

Clinical history

A 56 year old patient with MTC, post-surgery, presented with suspected recurrence (due to calcitonin levels of 48 ng/mL).

PET–CT findings

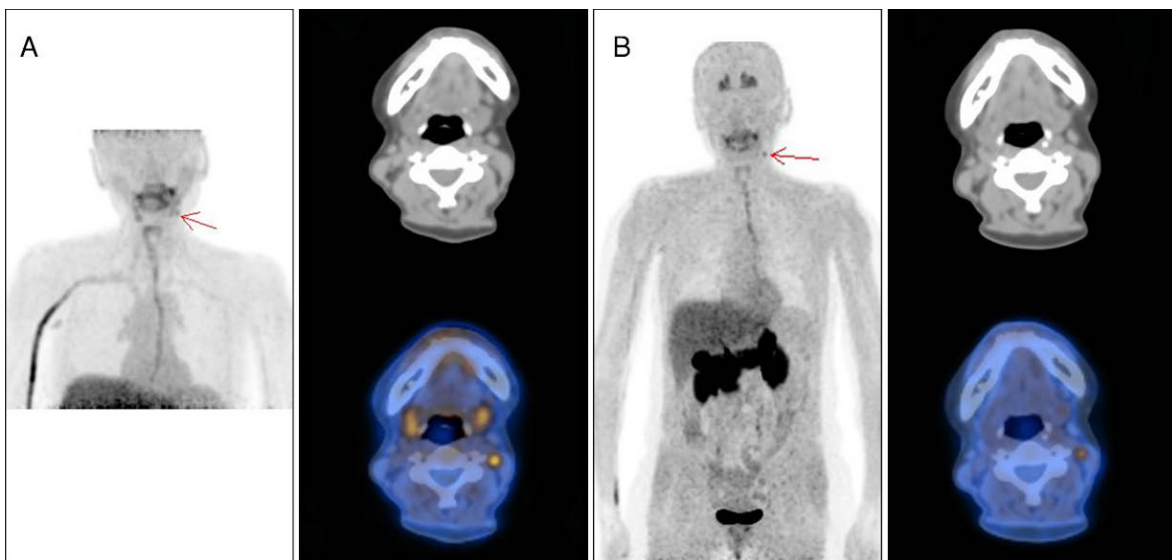
(A): early (10 min) regional study showing MIP, CT and fused transaxial slices of upper neck; (B): late (55 min) whole body study showing MIP, CT and fused transaxial slices at the same levels as in (A).

There is intense early tracer uptake in right parapharyngeal adenopathy (with a maximum standardized uptake value (SUV_{max}) of 3.5) decreasing in intensity in the late images (SUV_{max} 2.1) (arrows).

Teaching point

^{18}F -DOPA is the tracer of choice for detection of relapsed MTC. Performing early and late studies, and detecting fast washout, may help in the diagnosis of aggressive relapse.

Keywords: MTC, early images, ^{18}F -DOPA



Clinical indication for PET–CT: Astrocytoma grade II, follow-up after surgery

Clinical history

A 46 year old man with a history of astrocytoma grade II, treated by surgery 4 years and 2 years prior to current examination, was considered to have stable disease following clinical assessment and MRI.

PET–CT findings

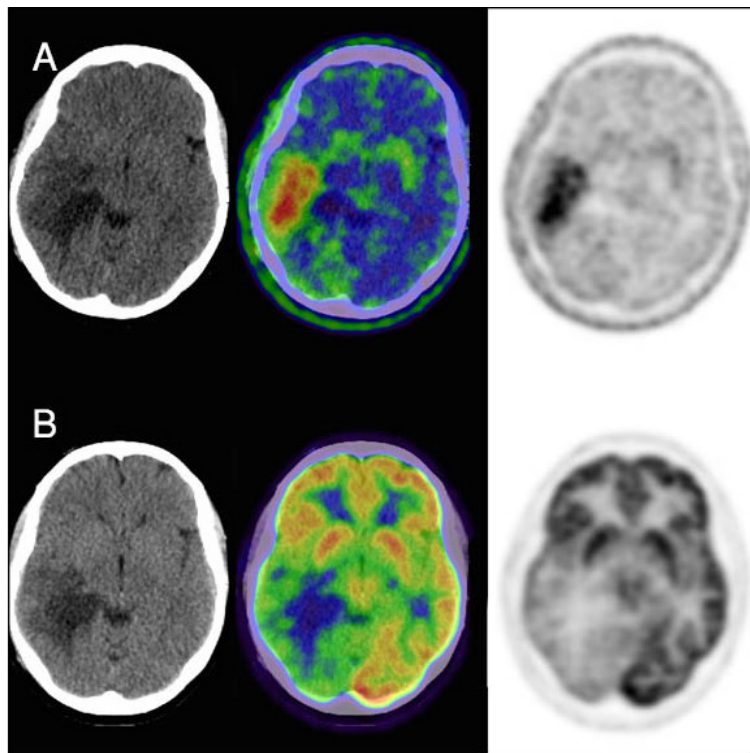
(A): ^{18}F -DOPA CT, fused and PET transaxial brain slices; (B): ^{18}F -FDG, same images at same level as in (A).

There is intense ^{18}F -DOPA uptake in the surgical bed in the left temporal area, with only mild uptake of ^{18}F -FDG. Watchful waiting was chosen at first, but after subsequent clinical deterioration, surgery was performed and recurrent astrocytoma was diagnosed.

Teaching point

^{18}F -DOPA can be used as an amino acid tracer in neuro-oncology.

Keywords: Glioma, ^{18}F -DOPA, ^{18}F -FDG



8. FLUOROESTRADIOL, FES (^{18}F)

8.1. GENERAL CHARACTERISTICS

Name: ^{18}F -fluoroestradiol (^{18}F -FES)

Synonyms: [^{18}F]FES; 16α -[^{18}F]fluoro- 17β -estradiol; [^{18}F]fluoroestradiol, fluoroestradiol

Radioisotope

^{18}F is a short half-life PET radioisotope (109.7 min) emitting positrons of E_{max} 1.656 MeV. Owing to the high chemical stability of C–F bonds in organic compounds as well as the high water solubility of F compounds, ^{18}F tracers usually exhibit suitable stability and biodistribution in humans. Although the F chemistry is complicated, the vast application of ^{18}F labelled compounds in nuclear medicine has led to development of efficient automated radiopharmaceutical production methods allowing large scale production of ^{18}F tracers for clinical use.

Radiosynthesis

^{18}F is routinely produced by proton irradiation of enriched ^{18}O water in biomedical cyclotrons, followed by ^{18}F -KF formation (Fig. 8.1). ^{18}F -FES was first synthesized by nucleophilic displacement of the triflate containing precursor using tetrabutylammonium ^{18}F -fluoride, followed by automated high performance liquid chromatography (HPLC) purification. A one pot synthesis of nucleophilic fluorination of a cyclic sulphone was later developed successfully with radiochemical yields of 30–45% and specific activity of 37 GBq/ μmol (1 Ci/ μmol) in 60–120 min, leading to suitable automated modules (50% radiochemical yields in 50–80 min) [48].

8.2. PHARMACOKINETICS

8.2.1. Physiological biodistribution and metabolism

After ^{18}F -FES administration, it is cleared from the blood and metabolized in 20 min with only 20% of intact tracer, mostly bound to plasma proteins. Liver uptake is rapid, and the metabolites appear in the blood as early as 5 min after injection. The main radioactive metabolites in the blood and urine are sulphate and glucuronide conjugates.

8.2.2. Mechanism of retention

^{18}F -FES binds to the oestrogen receptors (ERs) on the tumour cell surface as well as on intratumoural receptors in ER positive breast tumours. It has a proven value in the assessment of ER status of primary and metastatic breast cancer [48].

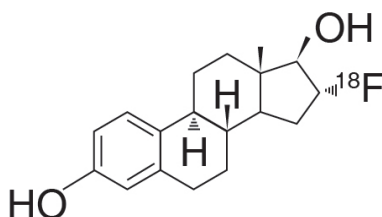


FIG. 8.1. Molecular structure of ^{18}F -fluoroestradiol.

8.4.2. Cases

Cases courtesy of A. Glaudemans, University Medical Centre Groningen, the Netherlands.

8.4.2.1. Case No. 8.1

Clinical indication for PET–CT: Metastatic breast cancer, predicting response to treatment

Clinical history

A 55 year old woman with a history of breast cancer (oestrogen receptor positive (ER+), human epidermal growth factor receptor 2 negative (HER2–)) had undergone lumpectomy followed by adjuvant chemotherapy and RT. Three years later the patient developed rapidly progressive bone metastases. The patient was referred to determine whether the bone metastases were ER+, in which case treatment with antihormonal drugs would be considered.

PET–CT findings

(A): low intensity MIP; (B): normal intensity MIP.

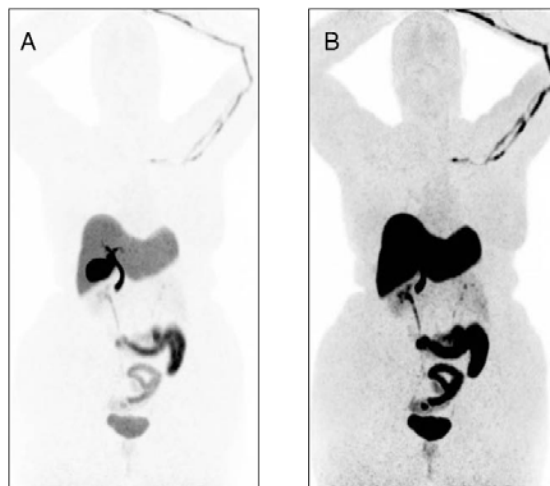
The normal biodistribution of ^{18}F -FES is demonstrated, with uptake in the liver, and excretion via the gallbladder and bile ducts to the intestines, and via the kidneys to the urinary bladder. There are no pathological findings. The known bone metastases do not show any ER expression.

Follow-up: Treatment with anti-hormonal drugs was cancelled and the patient was referred to chemotherapy.

Teaching points

In ^{18}F -FES PET–CT studies, the liver can be visualized by applying low intensity images.

Keywords: Breast cancer, therapy prediction, ^{18}F -FES normal biodistribution



Clinical indication for PET–CT: Breast cancer, staging

Clinical history

A 46 year old woman with right breast cancer (ER+) presented with palpable right axillary lymphadenopathy.

PET–CT findings

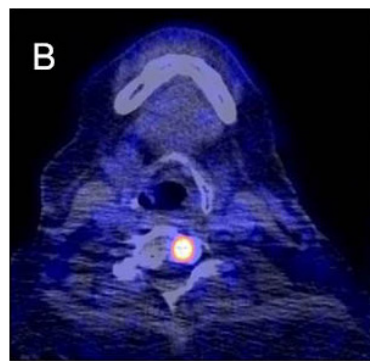
(A): MIP; (B): fused transaxial slice of upper neck.

There is increased tracer uptake in the right breast tumour and in several right axillary and retroclavicular LNs, confirming ER expression. There is an additional focal uptake in a cervical vertebra, confirming increased ER expression in a bone metastasis.

Teaching point

The disease was upstaged, leading to a change in treatment plan.

Keywords: Breast cancer, staging, treatment planning, ^{18}F -FES



Clinical indication for PET–CT: Breast cancer, restaging

Clinical history

A 63 year old woman with breast cancer had undergone lumpectomy followed by chemotherapy and RT. No anti-hormonal therapy had been given. The patient presented with complaints of fatigue and malaise. ^{18}F -FDG and ^{18}F -FES PET–CT were performed to restage the disease.

PET–CT findings

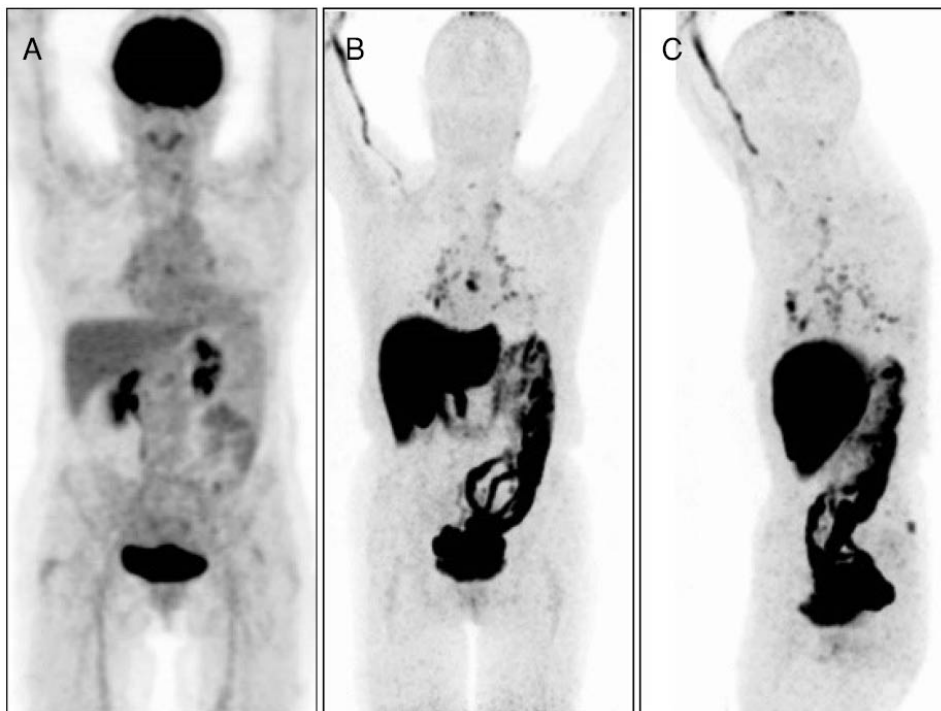
(A): ^{18}F -FDG MIP; (B): ^{18}F -FES anterior MIP; (C): ^{18}F -FES lateral MIP.

There is slightly increased ^{18}F -FDG uptake in reactive mediastinal and hilar LNs, and in a solitary lesion in the left iliac bone. ^{18}F -FES images demonstrate the presence of increased ER expression in multiple mediastinal and hilar LNs, and in the left iliac bone metastasis, suggestive of ER+ breast cancer.

Teaching point

ER status may change during the natural history of the tumour. In case of a diagnostic dilemma, ^{18}F -FES PET–CT may be useful for restaging. Evidence for recurrent metastatic disease with increased ER receptor expression may lead to a change in treatment plan.

Keywords: Breast cancer, restaging, treatment planning, ^{18}F -FES, ^{18}F -FDG



Clinical indication for PET–CT: Breast cancer

Clinical history

A 53 year old woman with a history of colon cancer (treated with hemicolectomy) and breast cancer (ER+, treated with surgery, chemotherapy and loco-regional RT) presented following a partial epileptic seizure with visual symptoms. MRI of the brain demonstrated an 18 mm lesion in the left occipital lobe. Biopsy could not be performed owing to the location of the lesion.

PET–CT findings

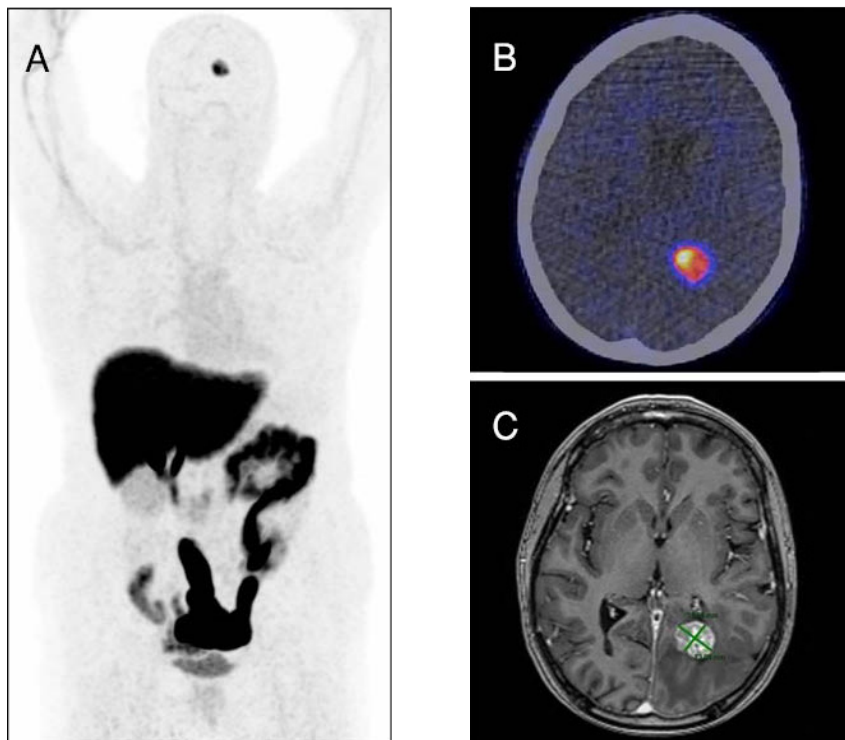
(A): MIP; (B): fused transaxial slice of brain; (C): corresponding MRI.

There is focal uptake in a solitary lesion in the brain, consistent with increased ER expression in a brain metastasis of breast cancer.

Teaching point

¹⁸F- FES PET–CT evidence for brain metastasis from breast cancer.

Keywords: Breast cancer, staging, ¹⁸F-FES



9. FLUOROETHYL-TYROSINE, FET (^{18}F)

9.1. GENERAL CHARACTERISTICS

Name: O-(2- ^{18}F fluoroethyl)-L-tyrosine (^{18}F -FET)

Synonyms: [^{18}F]FET, FET, F-18 FET

Radioisotope

^{18}F is a short half-life PET radioisotope (109.7 min) emitting positrons of E_{max} 1.656 MeV. Owing to the high chemical stability of C–F bonds in organic compounds as well as the high water solubility of F compounds, ^{18}F tracers usually exhibit suitable stability and biodistribution in humans. Although the F chemistry is complicated, the vast application of ^{18}F labelled compounds in nuclear medicine has led to development of efficient automated radiopharmaceutical production methods allowing large scale production of ^{18}F tracers for clinical use.

Radiosynthesis

Automated synthesis of this radiopharmaceutical is reported using a tosylated-L-tyrosine derivate already protected by a tert-butyl ester as a precursor for one-step nucleophilic ^{18}F fluorination in the presence of tetrabutylammonium hydrogen carbonate/carbonate (Fig. 9.1). It achieves a specific activity of 18 GBq/ μmol (0.49 Ci/ μmol) in 80 min, a radiochemical yield of 55–60% and >99% radiochemical purity [55].

9.2. PHARMACOKINETICS

9.2.1. Physiological biodistribution and metabolism

^{18}F -FET accumulation in all organs peaks within 5 min after the injection, followed by a decrease and plateau at approximately 20–60 min. The blood activity curve shows a biexponential pattern with a half-life of 40 min. Tracer uptake in the pancreas is of mild intensity, almost equivalent to that in the liver and spleen, and similar to that in the heart and stomach, with none higher than the blood pool activity (Fig. 9.2) [55]. The elimination route of the tracer explains the high intensity activity in the kidneys, ureters and urinary bladder, and the variable visualization of the gallbladder. There is no tracer accumulation in bone, bone marrow or intestines (Fig. 9.2, top). In the brain, concentration in the normal cortex increases continuously up to 40 min post-injection, but is, as a rule, very low. The transverse and superior sagittal sinuses are visualized in early phase images (Fig. 9.2, bottom).

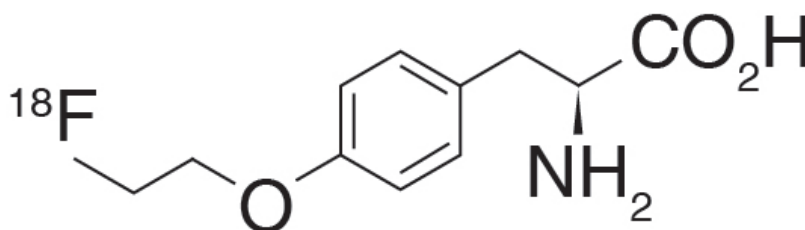


FIG. 9.1. Molecular structure of ^{18}F -fluoroethyl-tyrosine.

9.2.2. Mechanism of retention

Malignant cells develop overexpressed substance transporter systems to support energy supply, protein synthesis and cell division. The L-type amino acid transporter and Na⁺ dependent B0 systems manage the transport of various amino acids for final incorporation into proteins. Radiolabelled amino acids, including ¹⁸F-FET, are trapped in transformed cells, though they are not incorporated into proteins. They can be useful in brain tumour imaging based solely on amino acid transport.

9.2.3. Pharmacology and toxicology

No pharmacological and toxicological effects have been reported owing to low tracer concentration.

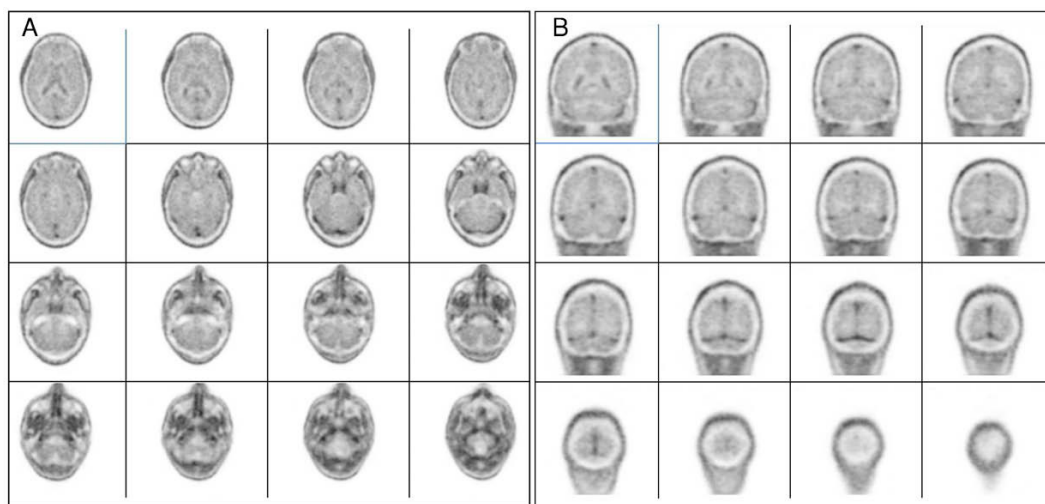
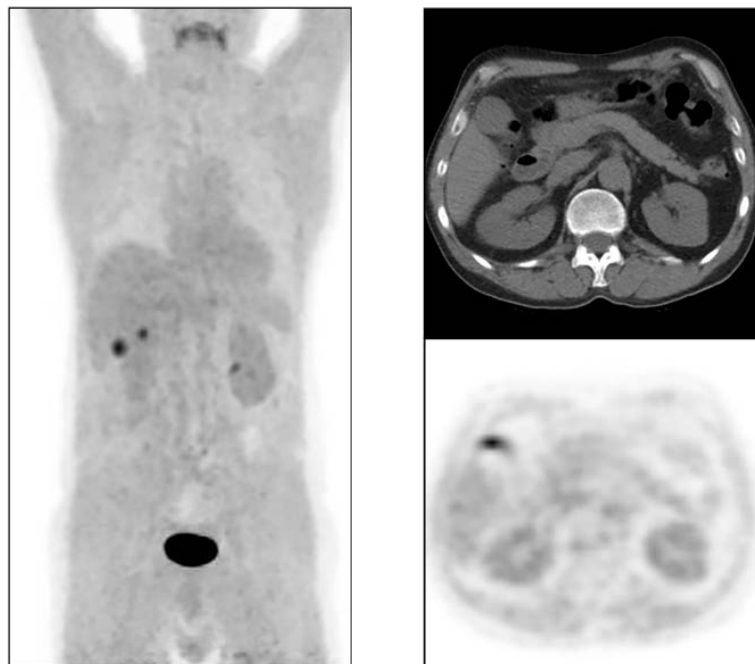


FIG. 9.2. Normal biodistribution of ¹⁸F-FET.

9.3. METHODOLOGY

9.3.1. Activity, administration, dosimetry

Studies have been performed following the IV injection of 400 MBq (10.8 mCi). Human dosimetry was estimated based on this dose at 70 and 200 min. The urinary bladder received the highest dose (0.060 mGy/MBq or 222 mrad/mCi). Other organs, such as the uterus (0.022 mGy/MBq or 81 mrad/mCi) and kidney (0.020 mGy/MBq or 74 mrad/mCi), received moderate doses. No increased uptake was seen in the liver, bone, intestine, lung, heart or pancreas. The effective dose was 0.0165 mSv/MBq (61 mrem/mCi). The effective dose based on biodistribution data from mice was estimated to be 0.009 mSv/MBq (33 mrem/mCi) [55].

9.3.2. Imaging protocol

A fasting period of at least 4 hours prior to administration of the radiotracer is suggested. Imaging is performed following the IV injection of 4–5 MBq/kg. Acquisition of the PET component includes a dynamic study of one bed position brain acquisition for 40 min, or a static protocol with an early, one bed position brain acquisition 10 min after injection, followed by a later study at 40–50 min after injection for a duration of 10 min. For the CT imaging protocol, see general comment in Section 1.3.

9.4. CLINICAL ASPECTS

9.4.1. Indications

¹⁸F-FET is an amino acid PET tracer used mainly in the diagnosis of CNS tumours. One of the great advantages of using ¹⁸F-FET compared to ¹⁸F-FDG for the diagnosis of brain tumours is the very low background in the healthy brain. Brain tumours demonstrate increased tracer uptake and therefore the tumour to background ratio is favourable, making the ¹⁸F-FET studies quite easy to read and interpret [56–60].

The most common clinical indication for ¹⁸F-FET is the identification of tumour recurrence in patients with unclear findings on MRI. Treatment related processes, such as fibrosis, necrosis or oedema, may occur, making the interpretation of conventional imaging studies equivocal. ¹⁸F-FET PET–CT is highly accurate for detection of viable tumour tissue.

¹⁸F-FET may also be used for early monitoring of response to different treatment options (e.g. chemotherapy, RT, targeted therapy). ¹⁸F-FET allows a more reliable distinction between pseudo- and real progression, and between pseudo- and real response, which are not always easy to recognize with MRI. Inclusion of ¹⁸F-FET imaging in the diagnostic workup improves patient management and avoids under- or over-treatment.

Early detection of malignant transformation of low grade to high grade tumours is of clinical importance because the initiation of a specific treatment depends mainly on the World Health Organization (WHO) grade. ¹⁸F-FET PET–CT allows non-invasive detection of malignant progression of low grade gliomas with high diagnostic accuracy.

¹⁸F-FET may also have a role in selected cases for biopsy target definition. Implementation of ¹⁸F-FET imaging in biopsy planning reduces the number of required trajectories in patients with brain tumours, especially in the presence of widespread MRI abnormalities, or in the presence of lesions located in high risk or functional areas.

Delineation of the extent of disease for RT planning is another clinical indication for ¹⁸F-FET imaging.

9.4.2. Cases

9.4.2.1. Case No. 9.1

Clinical indication for PET-CT: Evaluation of brain lesion

Clinical history

A 46 year old man with nausea and headache. MRI shows an infiltrating lesion with low Gd enhancement (A).

PET-CT findings

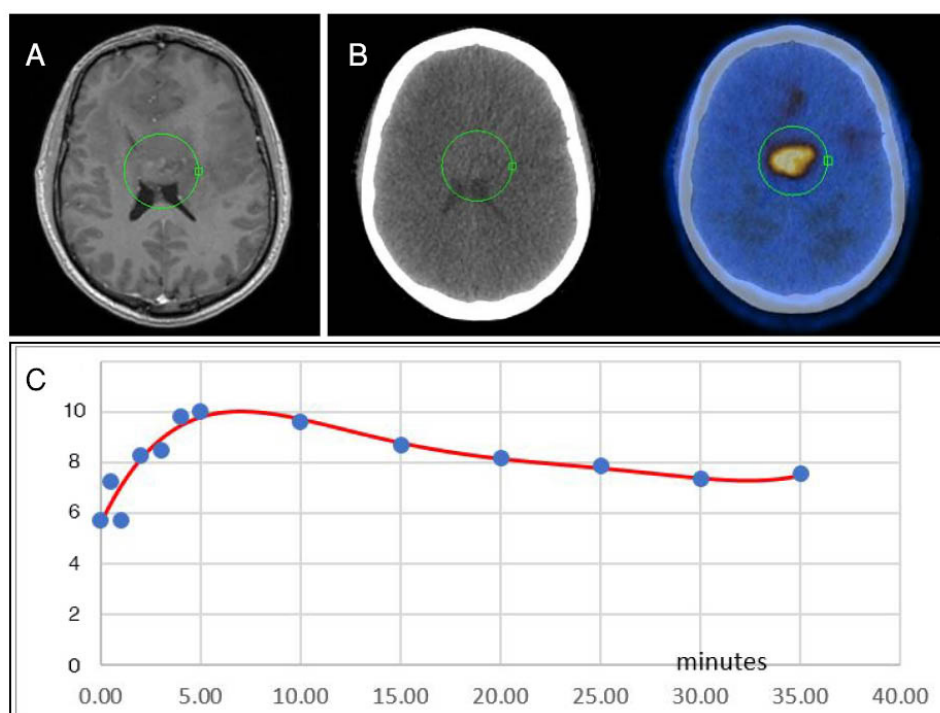
(A): MRI transaxial slices of brain; (B): CT and fused transaxial slices; (C): graph of uptake over time.

There is intense ^{18}F -FET uptake, with decreasing uptake during the 35 min examination (C). Surgery confirmed a high grade glioma.

Teaching point

Decreasing pattern of ^{18}F -FET uptake during the study and high tumour to background ratio generally indicate aggressive behaviour of the tumour.

Keywords: High grade glioma, ^{18}F -FET



Clinical indication for PET–CT: Evaluation of brain lesion

Clinical history

A 49 year old woman with seizures. MRI shows a ring enhancing lesion in the right parietal region (A).

PET–CT findings

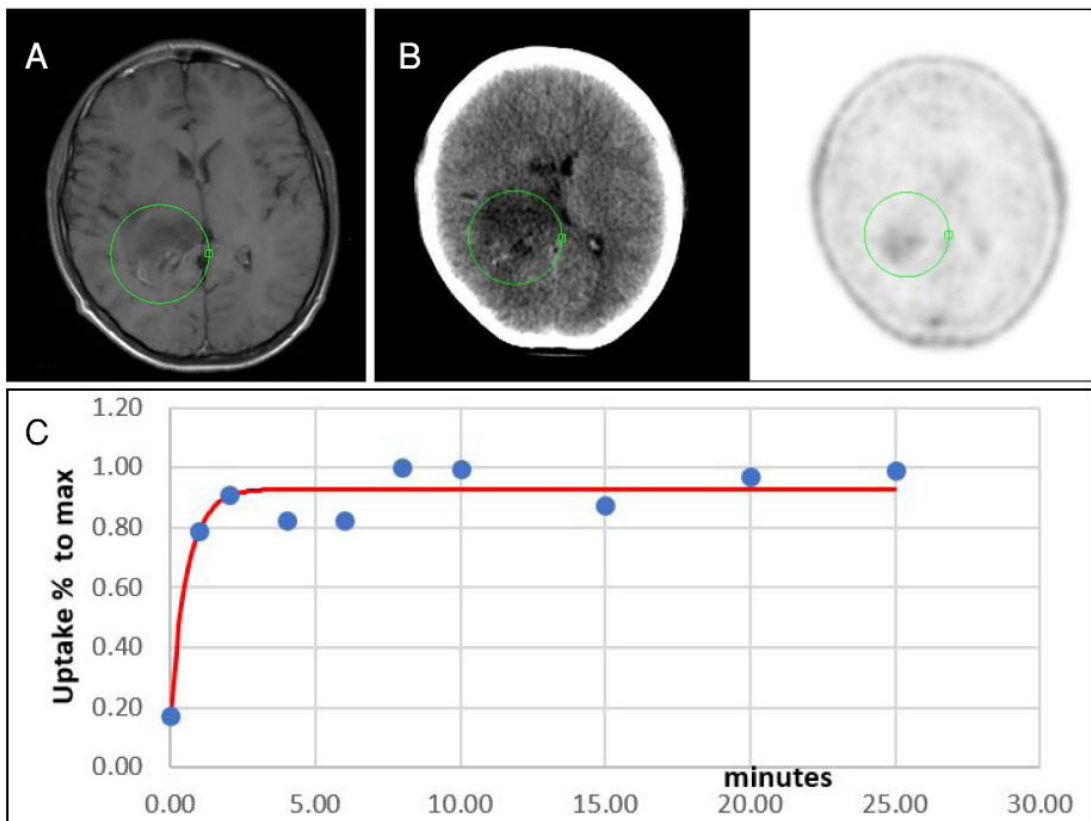
(A): MRI transaxial slices of brain; (B): CT and PET transaxial slices; (C): graph of uptake over time.

There is faint ^{18}F -FET uptake at the lesion with no decrease in intensity over the 25 min study (C). Surgery confirmed a low grade glioma.

Teaching point

A pattern of increasing ^{18}F -FET uptake (or at least no decrease in activity) over the study duration, as well as low tumour to background ratio, generally indicate lesions with better prognosis.

Keywords: Low grade glioma, ^{18}F -FET



Clinical indication for PET–CT: Characterization of brain lesion

Clinical history

A 46 year old woman with MRI showing an area of brain haemorrhage in the left parietal region with no apparent cause (A).

PET–CT findings

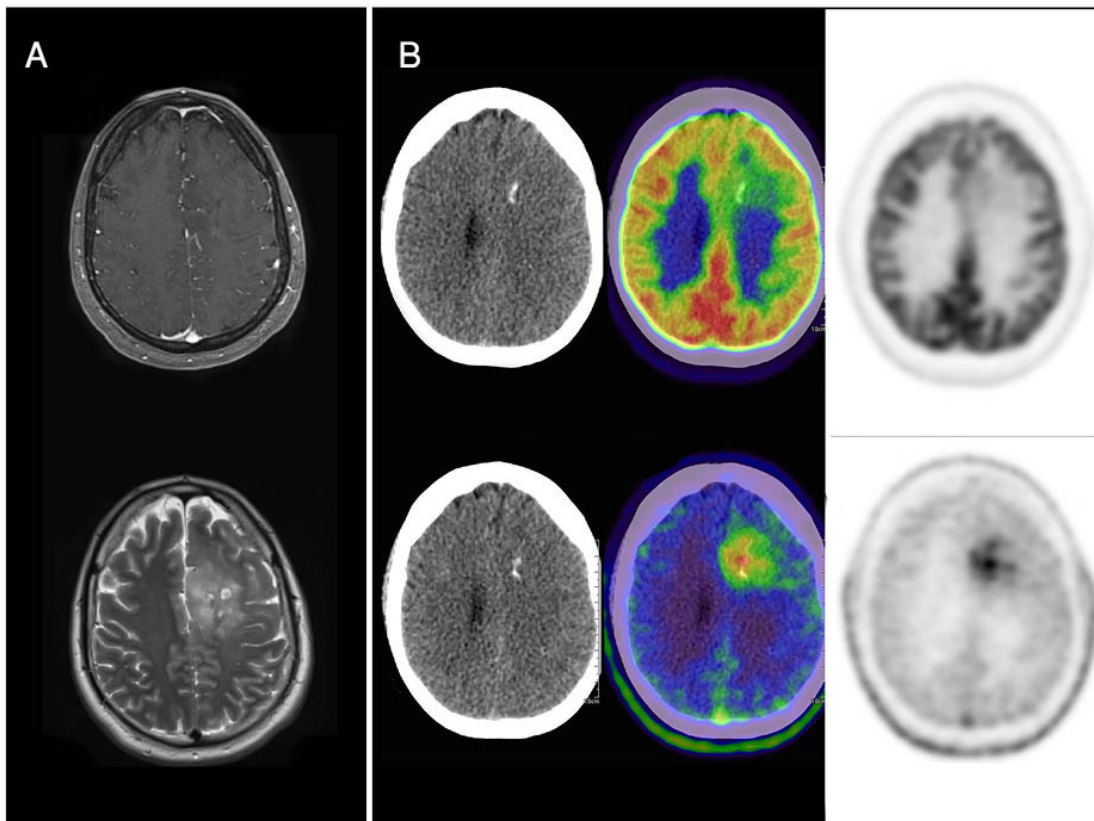
(A): MRI transaxial brain slices at two levels; (B): CT, fused and PET transaxial slices.

There is no ^{18}F -FET uptake in the lesion seen on MRI.

Teaching point

^{18}F -FET PET–CT may be helpful in finding the potentially underlying malignant cause of brain haemorrhage.

Keywords: Brain haemorrhage, ^{18}F -FET



Clinical indication for PET–CT: Characterization of brain lesion

Clinical history

A 46 year old woman with vascular malformation. MRI shows areas of signal changes due to recent radioembolization (A).

PET–CT findings

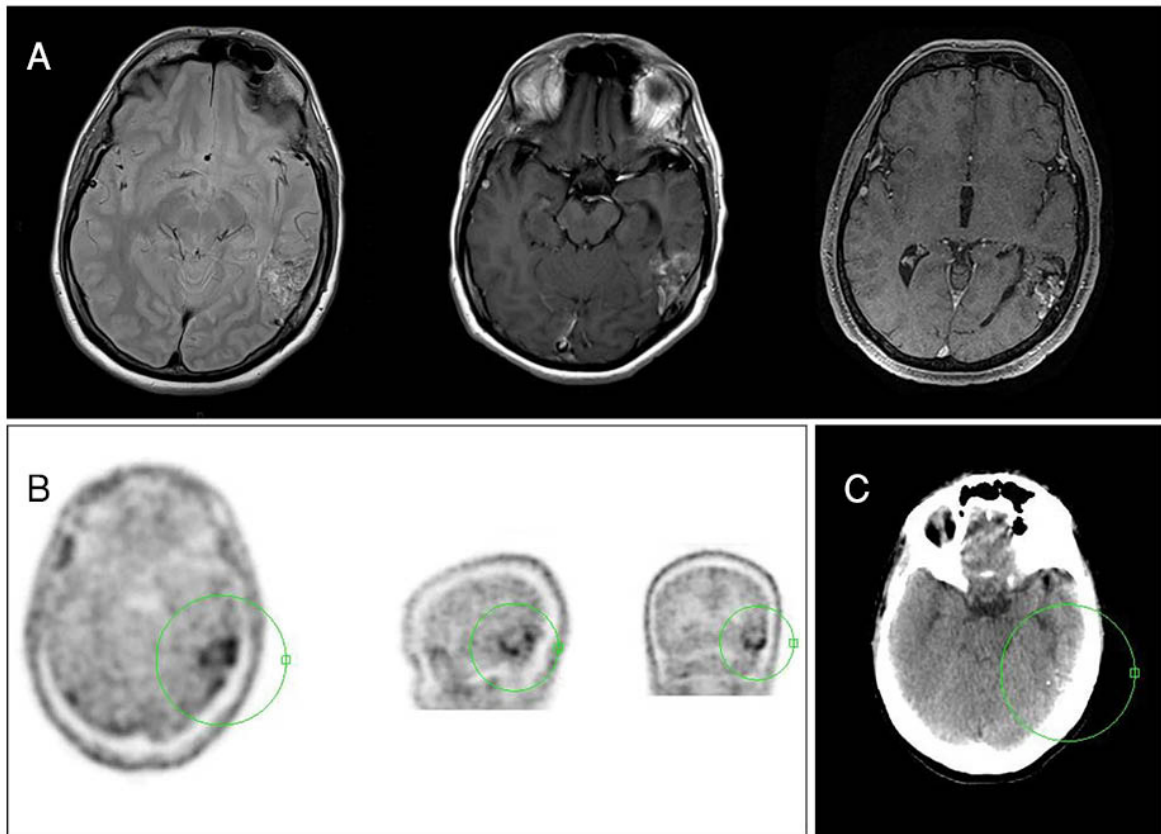
(A): MRI transaxial slices of brain; (B): PET transaxial, sagittal and coronal slices; (C): CT transaxial slice.

There is moderate tracer uptake in the known lesion.

Teaching point

Non-neoplastic brain lesions may show mild to moderate ^{18}F -FET uptake, comparable with the uptake intensity of low grade tumours.

Keywords: Benign brain lesion, ^{18}F -FET



Clinical indication for PET–CT: Evaluation of parietal brain mass

Clinical history

A 30 year old woman with partial complex seizure disorder. MRI shows a 3 cm mass in the left parietal lobe (see T2 weighted fluid-attenuated inversion recovery (FLAIR) images) without Gd enhancement.

PET–CT findings

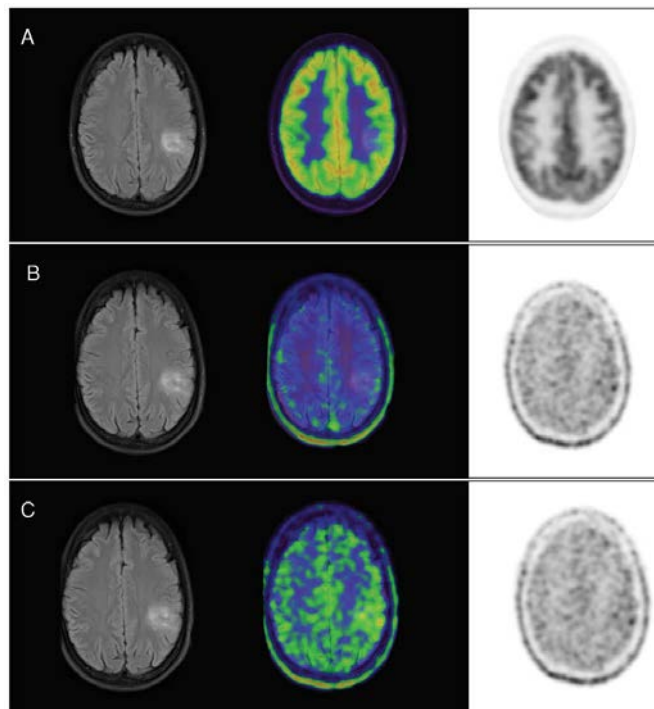
(A): ^{18}F -FDG MRI, fused and PET transaxial slices of brain; (B): early ^{18}F -FET MRI, fused and PET transaxial slices; (C): late ^{18}F -FET MRI, fused and PET transaxial slices.

There is no ^{18}F -FDG uptake (A), and no early ^{18}F -FET uptake is visible in the images taken 10 min post-injection (B). In the late ^{18}F -FET images, acquired 60 min post-injection, there is mild tracer uptake, with a maximum tumour to background ratio (TBR_{max}) ($\text{SUV}_{\text{max}}/\text{SUV}_{\text{mean}}$) of 2.2 in the lesion (C), consistent with low grade glioma. Surgery confirmed a grade II oligodendroglioma.

Teaching point

Up to 30% of low grade gliomas do not take up ^{18}F -FET. However, because uptake increases over time, using delayed images may help lower the number of false negative results.

Keywords: Oligodendroglioma, ^{18}F -FET, ^{18}F -FDG



Clinical indication for PET–CT: Characterization of brain lesion

Clinical history

A 56 year old man presented with an incidental finding on MRI of an area of signal change probably due to low grade tumour (A).

PET–CT findings

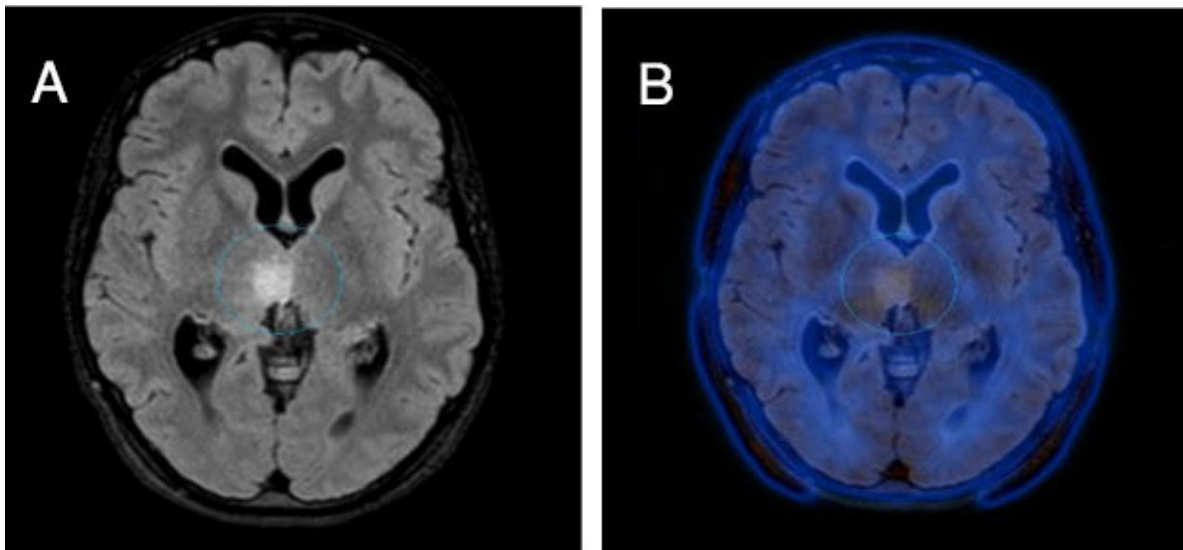
(A): MRI transaxial slice of brain; (B): fused transaxial slice.

There is no ^{18}F -FET uptake in the lesion seen on MRI. Surgery diagnosed grade II oligodendroglioma.

Teaching point

Absence of ^{18}F -FET uptake does not exclude tumours with an indolent course of disease.

Keywords: Low grade glioma, prognosis, ^{18}F -FET



Clinical indication for PET–CT: Evaluation of brain lesion

Clinical history

A 40 year old woman presented with partial complex seizure disorder. MRI shows an infiltrating lesion in the left frontal lobe without Gd enhancement (A).

PET–CT findings

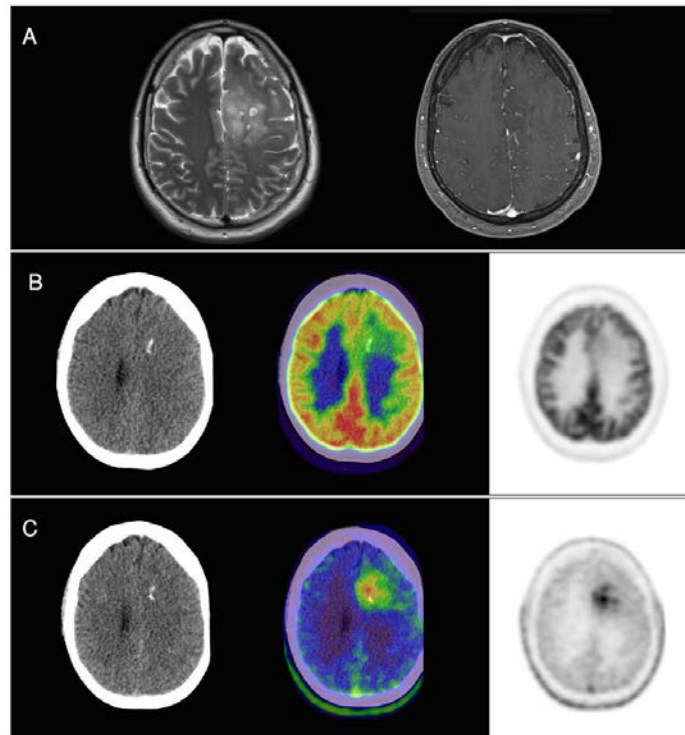
(A): MRI transaxial slices of brain; (B): ^{18}F -FDG CT, fused and PET slices; (C): ^{18}F -FET, early study, same slices as in (B).

There is mild ^{18}F -FDG uptake in the left frontal lesion (B). Intense ^{18}F -FET uptake, with a TBR_{max} ($\text{SUV}_{\text{max}}/\text{SUV}_{\text{mean}}$) of 3.4, is seen in the lesion (C). Surgery confirmed a grade II oligodendroglioma.

Teaching point

A TBR_{max} below 2.5 essentially excludes a grade IV glioma. On the other hand, low grade gliomas may display very intense uptake; therefore this study has high negative predictive value and lower positive predictive value.

Keywords: Oligodendroglioma, ^{18}F -FET, ^{18}F -FDG



Clinical indication for PET–CT: Evaluation of brain lesion

Clinical history

A 58 year old man with seizures and a large left frontal mass with no Gd enhancement on MRI.

PET–CT findings

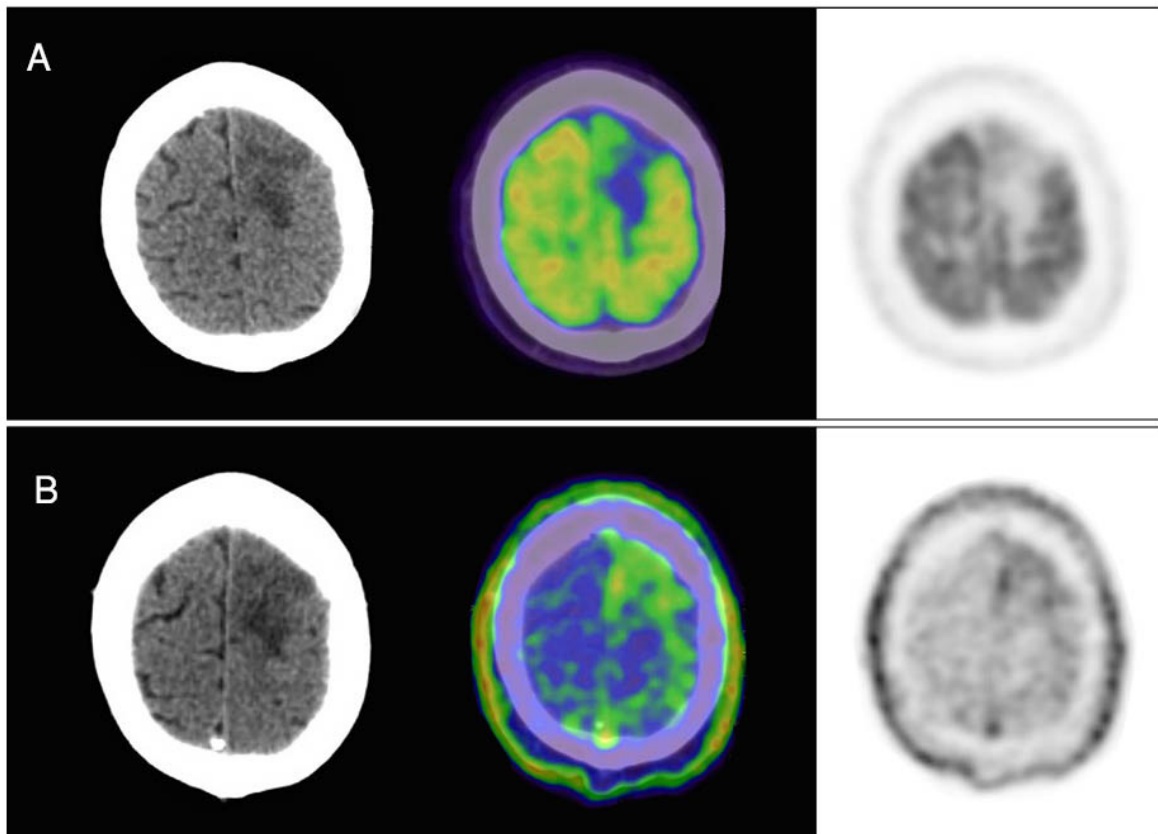
(A): ^{18}F -FDG CT, fused and PET transaxial slices of brain; (B): ^{18}F -FET, early study, same slices as in (A).

There is no increased ^{18}F -FDG uptake in the lesion (A). Mild early ^{18}F -FET uptake, TBR_{max} ($\text{SUV}_{\text{max}}/\text{SUV}_{\text{mean}}$) 2.6, is seen in the brain lesion (B). The findings are consistent with a glioma, most likely grade II. Surgery confirmed an oligodendroglioma with several anaplastic foci.

Teaching point

Gliomas tend to be heterogeneous. Grading the tumour according to the intensity of ^{18}F -FET is not reliable.

Keywords: Oligodendroglioma, ^{18}F -FET, ^{18}F -FDG



Clinical indication for PET–CT: Gliosarcoma, suspected recurrence

Clinical history

A 48 year old man with left temporal gliosarcoma treated by surgery and adjuvant chemoradiation 16 months earlier. Follow-up MRI shows a hyperintense T1w lesion (A).

PET–CT findings

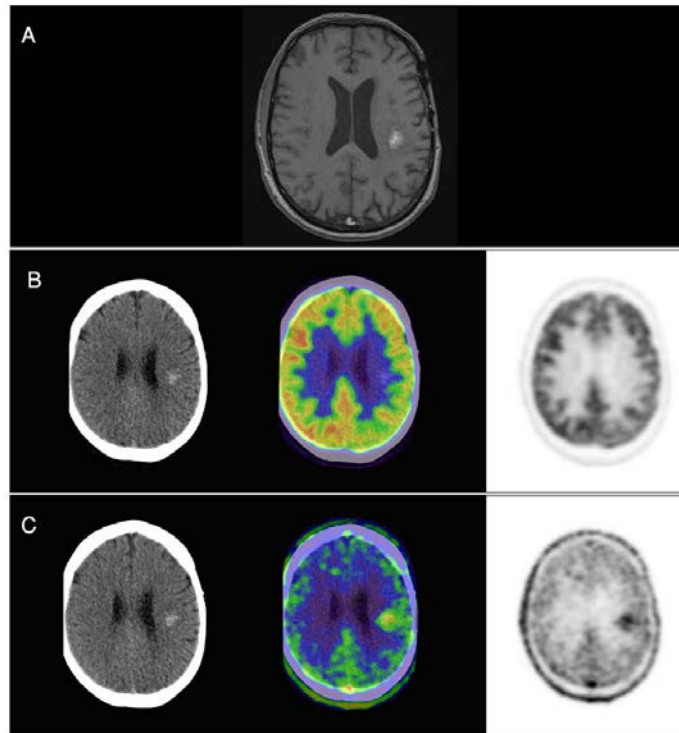
(A): MRI transaxial slice of brain; (B): ^{18}F -FDG CT, fused and PET transaxial slices; (C): ^{18}F -FET, same slices as in (B)

There is no significant ^{18}F -FDG uptake (B) in the left temporal region; however, there is intense ^{18}F -FET uptake, TBR_{max} ($\text{SUV}_{\text{max}}/\text{SUV}_{\text{mean}}$) 2.6, consistent with recurrent disease (C). The patient underwent RT with initial response but later progressed.

Teaching point

^{18}F -FET PET–CT is helpful in distinguishing recurrent glioma or metastases from post-radiation changes. A threshold of 2.1 for the TBR_{max} has been proposed.

Keywords: Recurrent glioma, radionecrosis, ^{18}F -FET, ^{18}F -FDG



Clinical indication for PET–CT: Extent of brain tumour recurrence

Clinical history

A 51 year old woman with a brain tumour was treated by surgery, followed by adjuvant chemoradiation for recurrence. MRI shows areas of signal changes due to the tumour recurrence in the temporal region (A).

PET–CT findings

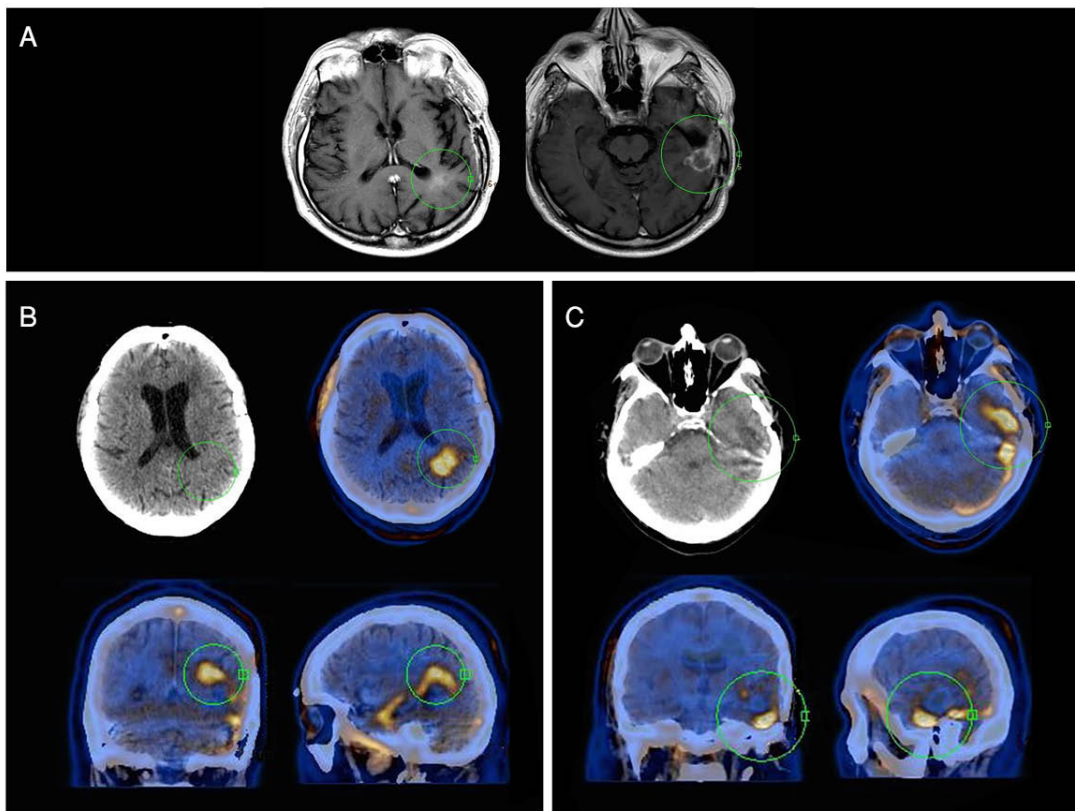
(A): MRI transaxial slices of brain; (B, C): CT transaxial slices and fused PET–CT slices in three planes (transaxial, coronal and sagittal).

There is an area of very high ^{18}F -FET uptake in the lesion, larger in size as compared with MRI findings.

Teaching point

^{18}F -FET PET–CT identifies recurrent tumour and defines with high accuracy the area of disease. This will give significant information for further treatment planning.

Keywords: Boundaries of disease recurrence, ^{18}F -FET



Clinical indication for PET–CT: Differentiating radiation injury from recurrence

Clinical history

A 55 year old woman with grade II–III oligoastrocytoma treated by surgery and adjuvant RT 13 months prior to current investigation. MRI shows a focal area of Gd enhancement (A) but no corresponding perfusion anomaly (B), which suggests radiation necrosis.

PET–CT findings

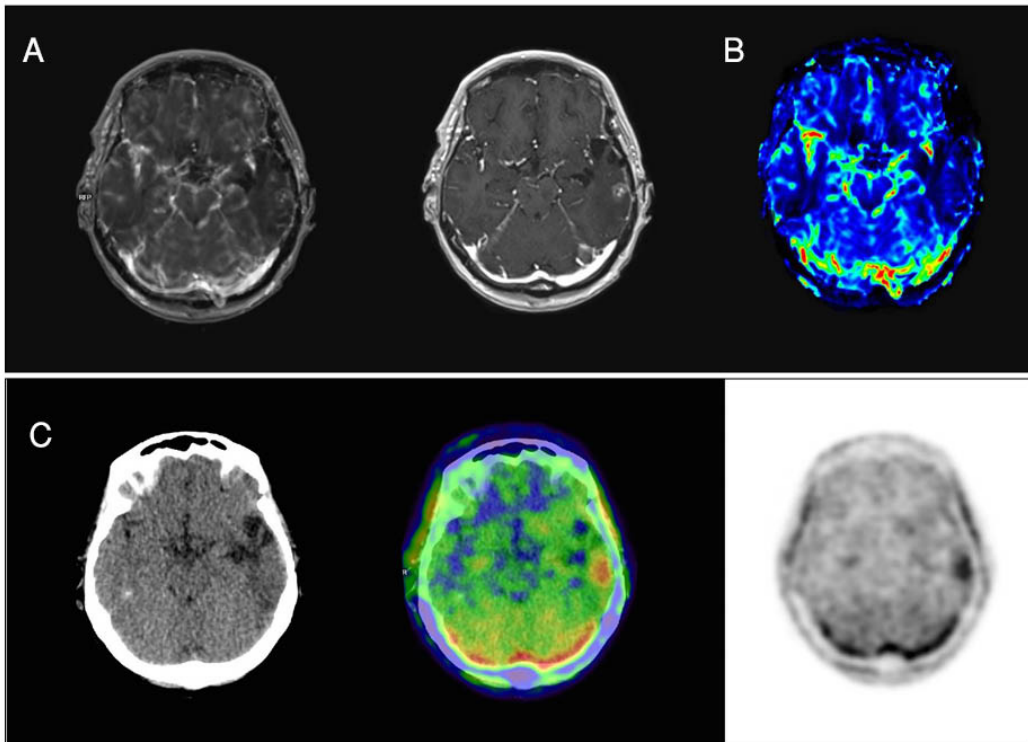
(A, B): MRI transaxial slices of brain; (C): CT, fused PET–CT and PET axial slices of brain.

There is intense tracer uptake in the Gd enhancing lesion, consistent with persistent or recurrent disease. Surgery revealed a grade II oligoastrocytoma.

Teaching point

^{18}F -FET PET–CT is helpful for distinguishing recurrent glioma or metastases from post-radiation changes. A threshold of 2.1 for the TBR_{max} has been proposed for the differential diagnosis.

Keywords: Recurrent glioma, radionecrosis, ^{18}F -FET



Clinical indication for PET–CT: Differentiating radiation injury from recurrence

Clinical history

A 31 year old man with grade III oligoastrocytoma treated by surgery and adjuvant RT 3 years earlier, followed by recurrence treated by surgery and radio-chemotherapy 8 months prior to current investigation.

PET–CT findings

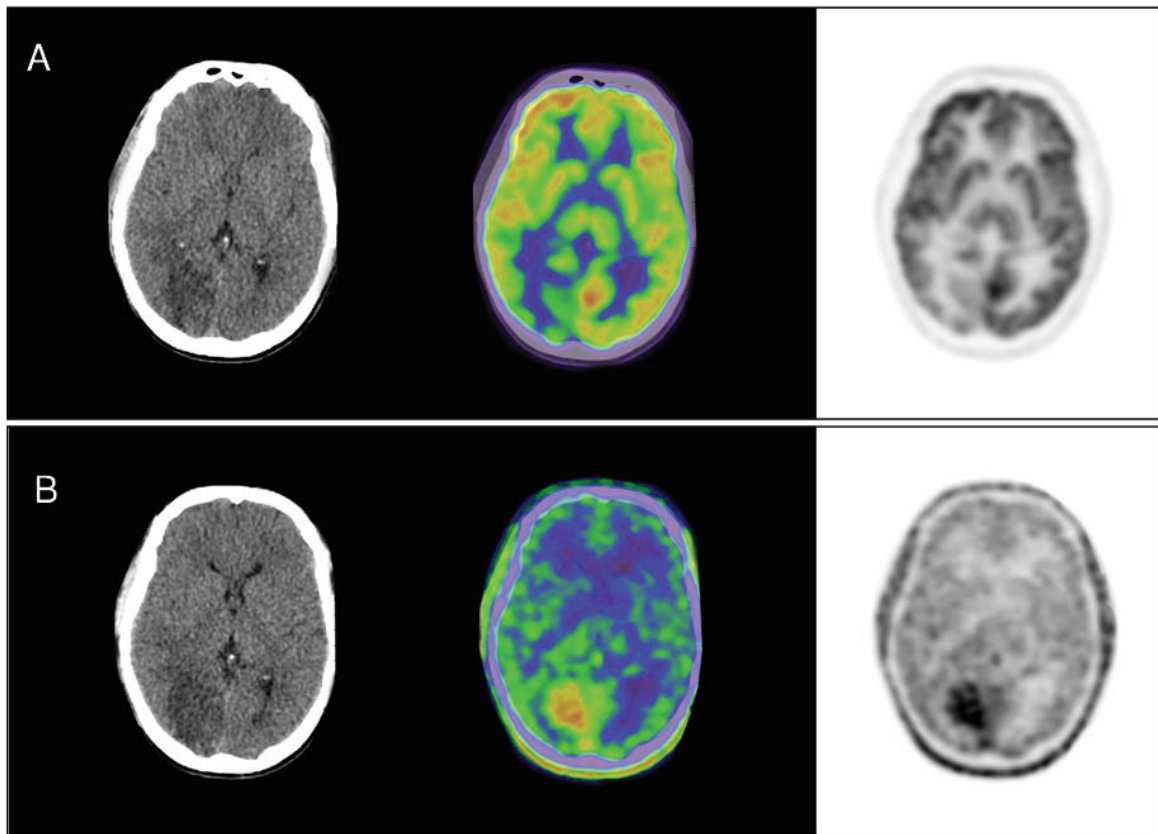
(A): ^{18}F -FDG CT, fused and PET transaxial slices of brain; (B): ^{18}F -FET, same slices as in (A).

There is mild ^{18}F -FDG uptake (A) and intense ^{18}F -FET uptake, TBR_{max} 3.4 (B), consistent with recurrent disease. Glioblastoma was excised at surgery.

Teaching point

^{18}F -FET PET–CT is helpful for differentiating recurrent glioma or metastases from post-radiation changes.

Keywords: Recurrent glioma, ^{18}F -FET, ^{18}F -FDG



Clinical indication for PET–CT: Differentiating radiation injury from recurrence

Clinical history

A 45 year old man with anaplastic oligodendroglioma treated by surgery and adjuvant RT 10 months earlier. MRI shows a very small area of Gd enhancement without any other signal changes (A).

PET–CT findings

(A): MRI transaxial slice of brain; (B): fused and CT transaxial slices; (C): MRI follow-up images.

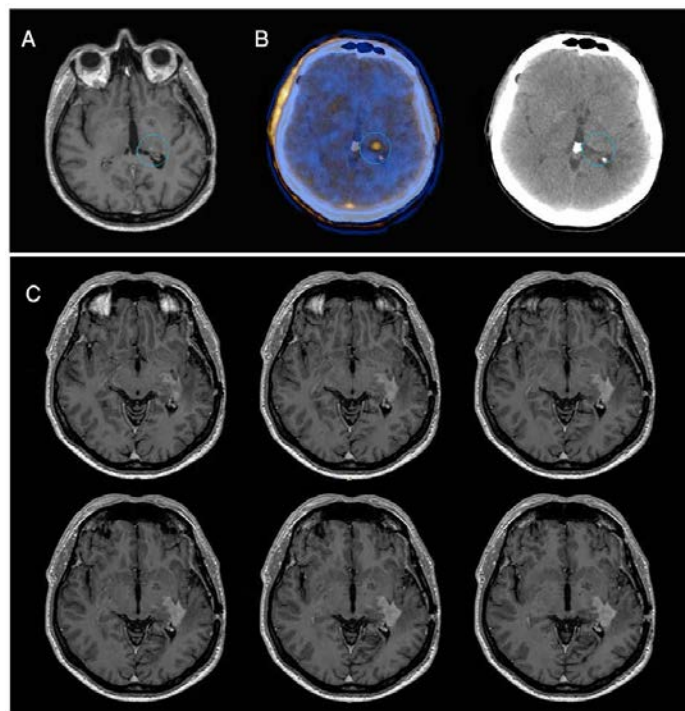
There is intense ^{18}F -FET uptake in the Gd enhancing lesion, consistent with recurrence.

Follow-up: MRI performed 3 months later shows disease progression (C).

Teaching point

In patients with high grade glioma, ^{18}F -FET PET–CT is helpful in characterizing very small, doubtful lesions seen on MRI and may thus shorten time to diagnosis.

Keywords: Recurrent glioma, ^{18}F -FET



Clinical indication for PET–CT: Suspicion of disease progression

Clinical history

A 51 year old woman, with glioblastoma grade IV treated by surgery and adjuvant RT 18 months earlier, receiving bevacizumab at the time of the investigation. MRI shows small areas of Gd enhancement suspected to reflect disease progression during treatment (A).

PET–CT findings

(A): MRI transaxial slices of brain; (B): fused transaxial slice; (C): MRI follow-up images.

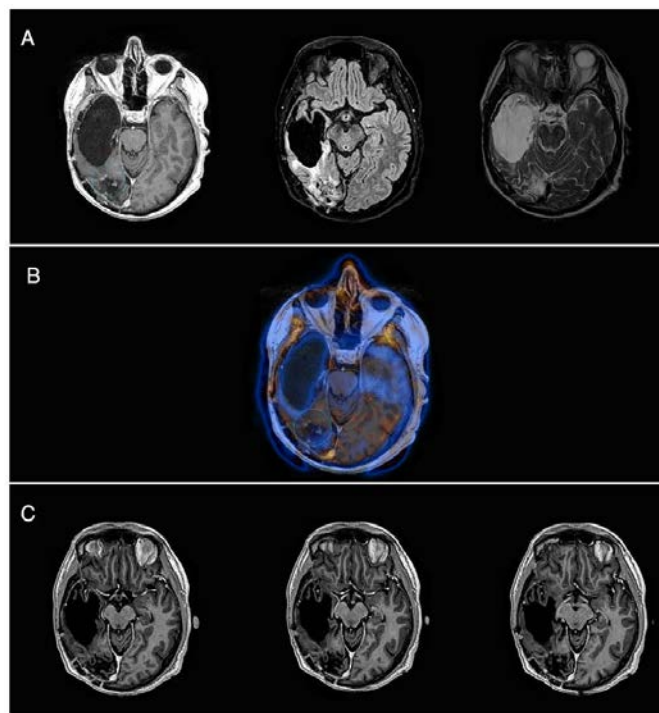
There is no tracer uptake in the Gd enhancing lesion.

Follow-up: MRI performed 2 months later shows reduction of areas of Gd enhancement (C).

Teaching point

¹⁸F-FET PET–CT is highly accurate in high grade gliomas. On MRI, recurrence is difficult to differentiate from pseudo-progression.

Keywords: Recurrent glioma, pseudo-progression, ¹⁸F-FET



Clinical indication for PET–CT: Differentiating radiation injury from recurrence

Clinical history

A 72 year old man with melanoma of the back and metastatic brain lesions treated with stereotactic radiation. MRI shows two areas of Gd enhancement in the right frontal (green arrow) and left parietal (red arrow) regions, suggestive of radiation necrosis (A).

PET–CT findings

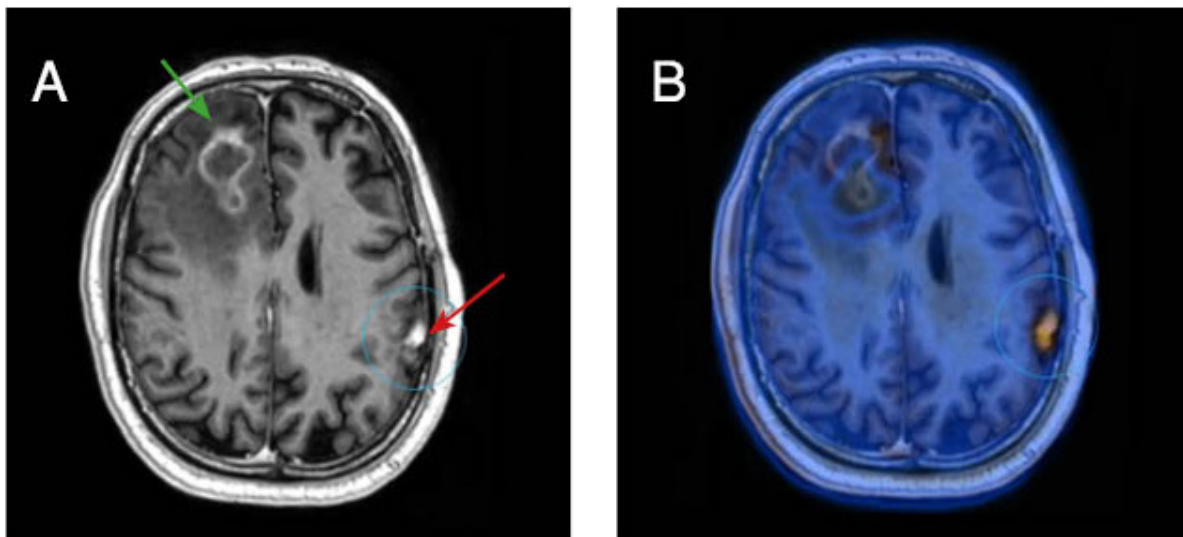
(A): MRI transaxial slice of brain; (B): fused transaxial slice.

There is intense tracer uptake in the Gd enhancing left parietal lesion consistent with persistent viable tumour. However, there is no ¹⁸F-FET uptake in the right frontal lesion.

Teaching point

¹⁸F-FET PET–CT is helpful for distinguishing metastases from post-radiation changes.

Keywords: Brain metastasis, radionecrosis, ¹⁸F-FET



Clinical indication for PET–CT: Suspected brain metastasis in patient with oesophageal cancer

Clinical history

A 61 year old man with newly diagnosed oesophageal carcinoma. MRI shows an area of Gd enhancement suspected to be a brain metastasis (A).

PET–CT findings

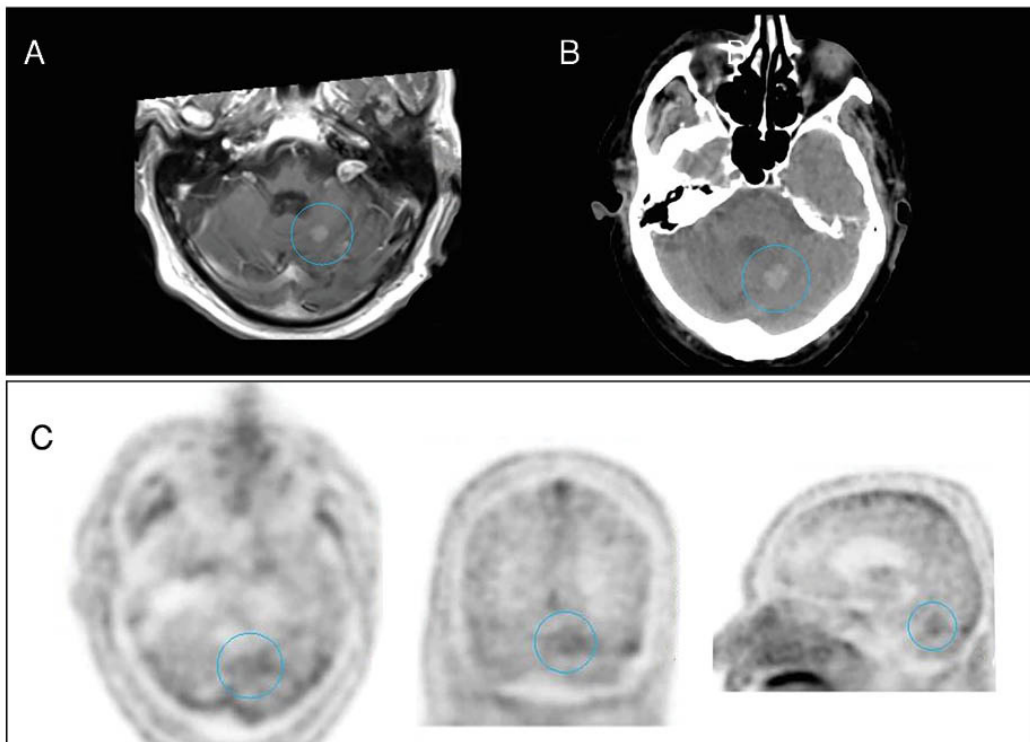
(A): MRI transaxial slice of brain; (B): CT transaxial slice; (C): PET slices in three planes.

There is very faint ^{18}F -FET uptake in the Gd enhancing lesion.

Teaching point

Literature regarding the accuracy of ^{18}F -FET imaging for the detection of secondary lesions is scarce. It appears that ^{18}F -FET PET–CT does not have a high enough sensitivity for the identification of brain metastases.

Keywords: Brain metastasis, ^{18}F -FET



10. FLUOROTHYMIDINE, FLT (¹⁸F)

10.1. GENERAL CHARACTERISTICS

Name: ¹⁸F-fluorothymidine (¹⁸F-FLT)

Synonyms: 3'-deoxy-3'-[¹⁸F]fluorothymidine; [¹⁸F]fluorothymidine, ¹⁸FLT, F-18 FLT.

Radioisotope

¹⁸F is a short half-life PET radioisotope (109.7 min) emitting positrons of E_{\max} 1.656 MeV. Owing to the high chemical stability of C–F bonds in organic compounds as well as the high water solubility of F compounds, ¹⁸F tracers usually exhibit suitable stability and biodistribution in humans. Although the F chemistry is complicated, the vast application of ¹⁸F labelled compounds in nuclear medicine has led to development of efficient automated radiopharmaceutical production methods allowing large scale production of ¹⁸F tracers for clinical use.

Radiosynthesis

Unlike ¹⁸F-FDG, the radiosynthesis of ¹⁸F-FLT can lead to many complex and potentially toxic by-products, and therefore ¹⁸F-FLT has to be purified. The most reliable purification is by HPLC, but some recent papers describe solid phase extraction strategies. A reliable technique for radiosynthesis of ¹⁸F-FLT has been developed based on ¹⁸F displacement of a protected nosylate precursor (Fig. 10.1). A simple three step process was used to prepare 370 MBq (radiochemically pure, specific activity 37 GBq/μmol in 100 min, 13% radiochemical yield). In addition, a fully automated method for the synthesis of ¹⁸F-FLT has also been developed, with 50% radiochemical yield, by modifying a commercial ¹⁸F-FDG synthesizer and its disposable fluid pathway [61–65].

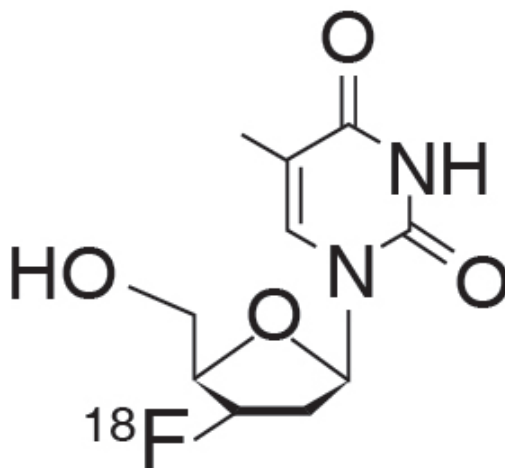


FIG. 10.1. Molecular structure of ¹⁸F-fluorothymidine.

10.2. PHARMACOKINETICS

10.2.1. Physiological biodistribution and metabolism

While ^{18}F -FLT does not complete the full nucleoside biochemical pathway, conjugated ^{18}F -FLT is cleared via the kidneys and excreted in the urine, enabling the visualization of the kidneys, ureter and bladder. There is intense tracer uptake in the bone marrow and moderate to intense activity uptake in the liver. The spleen shows only faint uptake and the brain is not visualized (Fig. 10.2) [61–65].

10.2.2. Mechanism of retention

^{18}F -FLT is an analogue of the nucleoside thymidine (deoxythymidine), however substitution of the 3'-F atom prevents it from further entering the regular biochemical pathway. ^{18}F -FLT is transported actively from the blood into cells and is further phosphorylated by thymidine kinase 1 without incorporation into DNA. The activity accumulated in the cells is proportional to thymidine kinase 1 activity as well as to cellular proliferation.

10.2.3. Pharmacology and toxicology

Pharmacology and toxicology were initially assessed for non-radioactive FLT when it was investigated as an antiviral drug. FLT had unacceptable toxicity at much greater doses than those used for the radioactive tracer. The United States National Cancer Institute investigational new drug application indicates that an ^{18}F -FLT dose of 2.59 MBq/kg with a maximal activity of 185 MBq (5 mCi) shows no evidence of toxicity or complications attributable to its intravenous administration.



FIG. 10.2. Normal biodistribution of ^{18}F -FET.

10.3. METHODOLOGY

10.3.1. Activity, administration, dosimetry

Typical IV injected activities range between 185 and 370 MBq (5 to 10 mCi). The United States National Institutes of Health requires a radiochemical purity of no less than 95% as well as no more than 5 µg of non-radioactive FLT and no more than 5 µg of other UV absorbing impurities.

The effective dose equivalent is reported at 0.028 ± 0.012 mSv/MBq for the standard adult male and 0.033 ± 0.012 mSv/MBq for the standard adult female. The critical organ is the urinary bladder wall and the dose depends on the voiding schedule, 0.18 mGy/MBq in males with voiding at 6 hours, and 0.08 mGy/MBq with voiding at 2 and 6 hours post injection [61–65].

10.3.2. Imaging protocol

Patient preparation does not require any specific dietary restrictions. Imaging is performed after the IV administration of 2–3 MBq/kg, following an uptake period of 50–60 min. Acquisition of the PET component is performed with 2–3 mins/bed position. For the CT imaging protocol, see general comments in Section 1.3.

10.4. CLINICAL ASPECTS

10.4.1. Indications

¹⁸F-FLT is a marker for tumour cell proliferation [66]. ¹⁸F-FLT is phosphorylated by thymidine kinase 1. The activity of this enzyme is elevated during cell mitosis, and therefore ¹⁸F-FLT uptake reflects cell proliferation in cancer tissue. After treatment, such as chemotherapy, RT or biological treatment, ¹⁸F-FLT imaging reflects the presence of residual active tumour tissue in which the treatment was not effective.

According to this rationale, the clinical use of ¹⁸F-FLT is mainly to assess early response to treatment and for early identification of patients who did not respond. Although ¹⁸F-FLT has not entered routine clinical practice, many investigational studies have been published. The main fields of investigation are head and neck cancers [67], non-small cell lung cancer (NSCLC) [68], breast cancer [69], haematological malignancies [70, 71] as well as gastric and oesophageal cancer [72].

10.4.2. Cases

10.4.2.1. Case No. 10.1

Clinical indication for PET–CT: Non-Hodgkin lymphoma, staging

Clinical history

A 52 year old patient with newly diagnosed diffuse large B-cell non-Hodgkin lymphoma.

PET–CT findings

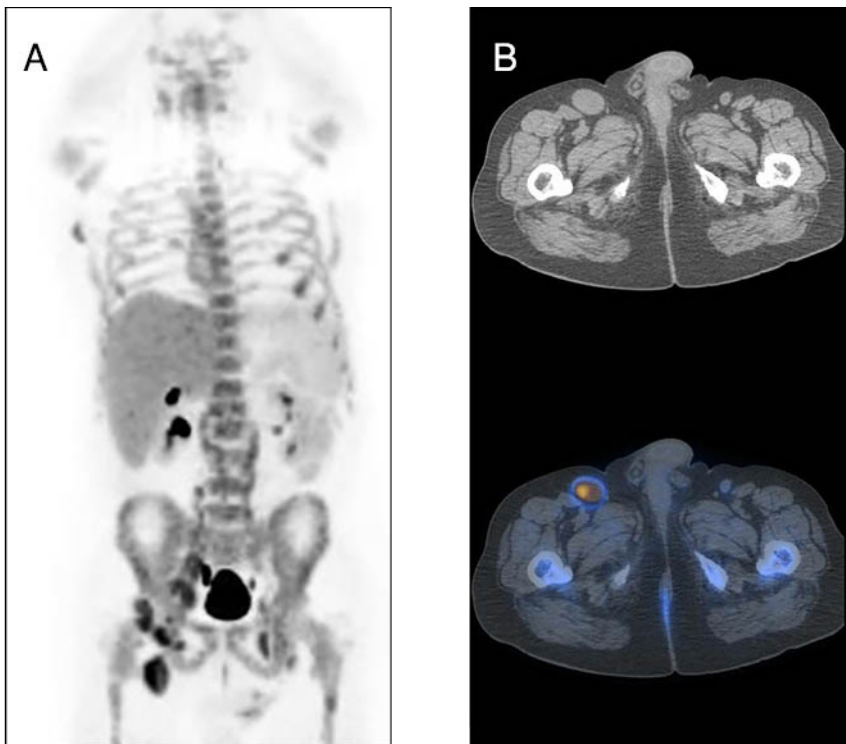
(A): MIP; (B): CT and fused transaxial slices at the inguinal level.

There is intense tracer uptake in enlarged bilateral inguinal and right iliac LNs.

Teaching point

^{18}F -FLT can be positive in lymphoma. The degree of ^{18}F uptake seems to correlate with outcome.

Keywords: Lymphoma, ^{18}F -FLT



Clinical indication for PET–CT: NSCLC, restaging

Clinical history

A 57 year old patient with NSCLC who progressed after first line chemotherapy was referred for a baseline study before therapy with Nivolumab.

PET–CT findings

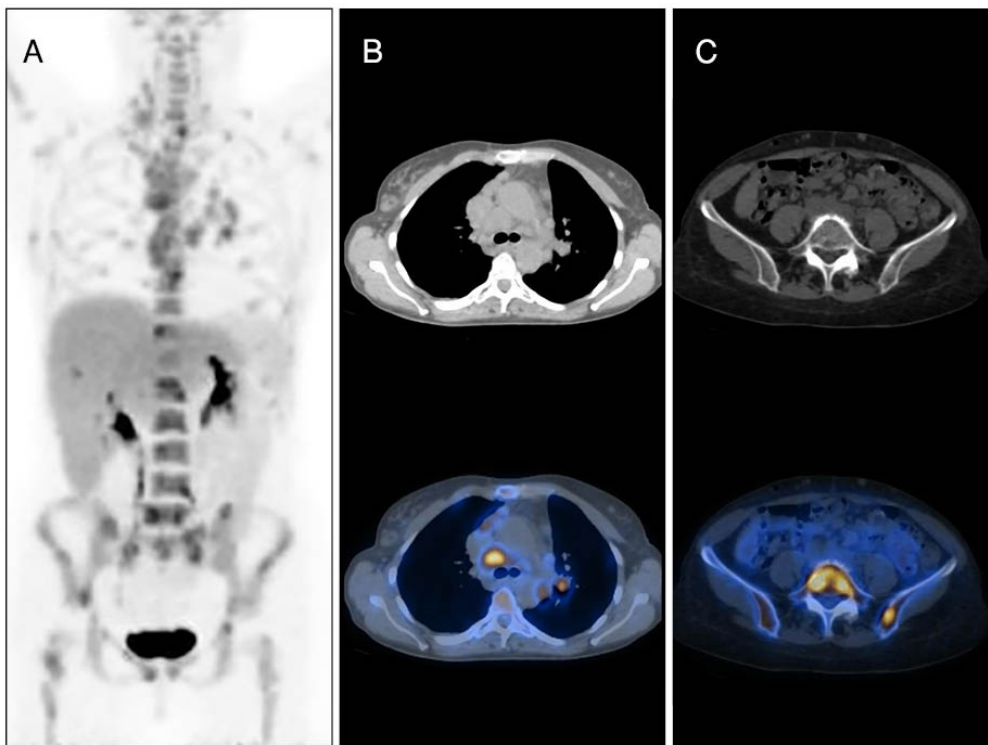
(A): MIP; (B): CT and fused slices of thorax; (C): CT and fused slices of pelvis.

There is intense tracer uptake in a left lung lesion, as well as in mediastinal LNs and small bone metastases.

Teaching point

¹⁸F-FLT may show intense uptake in NSCLC. The baseline investigation is useful to assess response to future therapies.

Keywords: NSCLC, ¹⁸F-FLT



11. FLUCICLOVINE, FACBC (^{18}F)

11.1. GENERAL CHARACTERISTICS

Name: ^{18}F -fluciclovine (^{18}F -FACBC)

Synonyms: Anti-1-amino-3- ^{18}F fluorocyclobutane-1-carboxylic acid; [^{18}F]FACBC

Radioisotope

^{18}F is a short half-life PET radioisotope (109.7 min) emitting positrons of E_{max} 1.656 MeV. Owing to the high chemical stability of C–F bonds in organic compounds as well as the high water solubility of F compounds, ^{18}F tracers usually exhibit suitable stability and biodistribution in humans. Although the F chemistry is complicated, the vast application of ^{18}F labelled compounds in nuclear medicine has led to development of efficient automated radiopharmaceutical production methods allowing large scale production of ^{18}F tracers for clinical use.

Radiosynthesis

Similar to the two step process for ^{18}F -FDG radiosynthesis, ^{18}F -FACBC can be produced by nucleophilic fluorination of syn-1-t-butyl-carbamate-3-trifluoromethanesulfonyloxy-1-cyclobutane-1-carboxylic acid methyl ester with ^{18}F -KF/Kryptofix 222 and subsequent hydrolysis and purification leading to a radiosynthesis yield of 12% and a radiochemical purity of 99% in 60 min (Fig 11.1). An automated radiosynthesis of anti- ^{18}F -FACBC is also reported with a yield of 24%, radiochemical purity of 99% and specific activity of 137–192 GBq/mmol [73–76].

11.2. PHARMACOKINETICS

11.2.1. Physiological biodistribution and metabolism

No specific metabolic pathway has been identified for ^{18}F -FACBC. On early images, at 1 min after tracer administration, there is intense tracer uptake in the liver and pancreas, moderate uptake in salivary and pituitary glands, in the bowel and in bone marrow, and faint uptake in the spleen and muscles. Only minor brain and lung uptake is observed, lower than that of the blood pool (Fig. 11.2(A)). On delayed studies, bone marrow activity decreases while muscle activity increases (Fig. 11.2(B)). Urinary excretion causes visualization of the kidneys and proximal ureters [73–76].

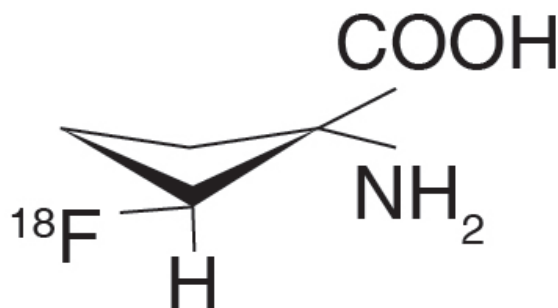


FIG. 11.1. Molecular structure of ^{18}F -fluciclovine.

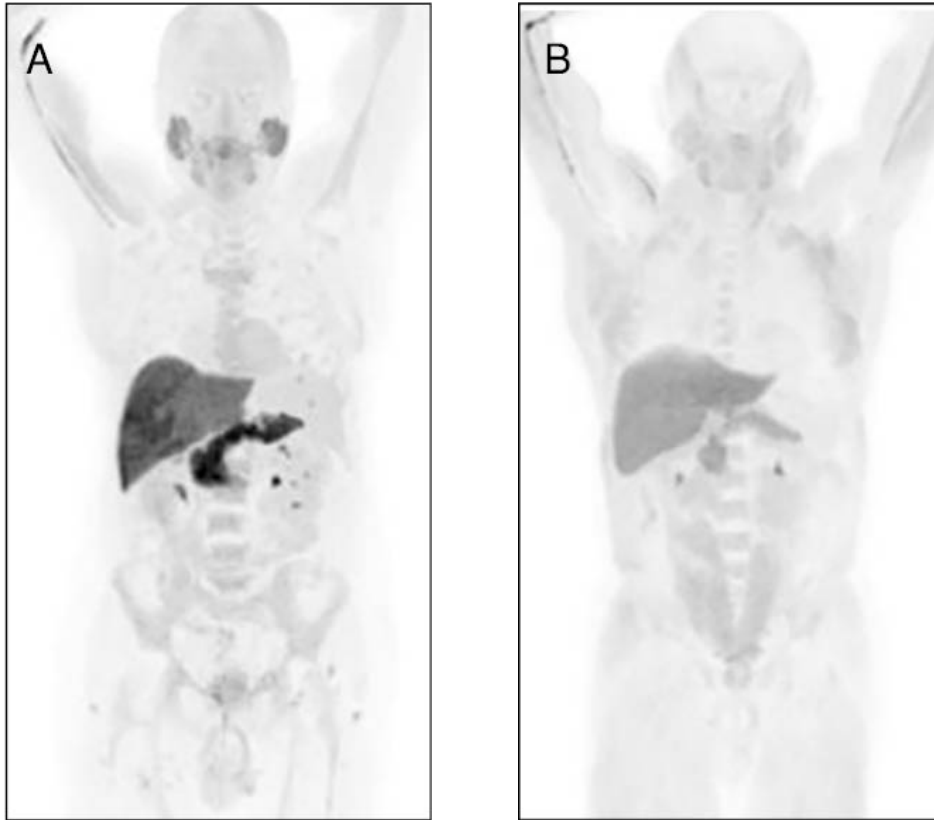


FIG. 11.2. Normal biodistribution of ^{18}F -fluciclovine in two patients.

11.2.2. Mechanism of retention

As a non-natural amino acid, ^{18}F -FACBC is not metabolized. It accumulates intracellularly in high concentrations. Its uptake is directed through both the L-type transporter and the energy dependent A-type transporter.

11.2.3. Pharmacology and toxicology

No notable adverse effect on the CNS, cardiovascular system and respiratory functions have been reported. High safety margins were achieved and the product is well tolerated in all patients [73–76].

11.3. METHODOLOGY

11.3.1. Activity, administration, dosimetry

Activities of 335–8200 MBq/mL (9–221 mCi/mL) at calibration time and date are available in 30 mL multidose vials. The administered activity for a patient is 370 MBq (10 mCi) through an IV bolus. The biodistribution data show that the liver receives the highest dose of radioactivity, followed by the pancreas, heart wall, kidneys and spleen. The effective dose equivalent is 0.016 4 mSv/MBq (60.6 mrem/mCi).

11.3.2. Imaging protocol

The patient has to fast for 4 hours. Imaging is performed following the IV injection of a tracer dose of 3–4 MBq/kg and an uptake period of 1–2 min. It is suggested to administer ^{18}F -FACBC with the patient already positioned on the tomograph's bed. Acquisition of the PET component starts from the pelvis for an acquisition time of 2–3 min/bed position. For the CT imaging protocol, see general comment in Section 1.3.

11.4. CLINICAL ASPECTS

11.4.1. Indications

^{18}F -FACBC is mainly used in prostate cancer although some other malignancies have been also studied, including breast cancer and primary brain tumours [77–79]. In prostate cancer, the main indications are similar to those for radiolabelled choline or PSMA. ^{18}F -FACBC PET–CT studies are performed for detection of the primary cancer, to guide biopsy, for staging intermediate risk/high risk patients, and for restaging BCR.

11.4.2. Cases

11.4.2.1. Case No. 11.1

Clinical indication for PET–CT: Prostate cancer, staging

Clinical history

A 62 year old patient with newly diagnosed prostate cancer, stage T3a, Gleason score 4+3, PSA 9.8 ng/mL.

PET–CT findings

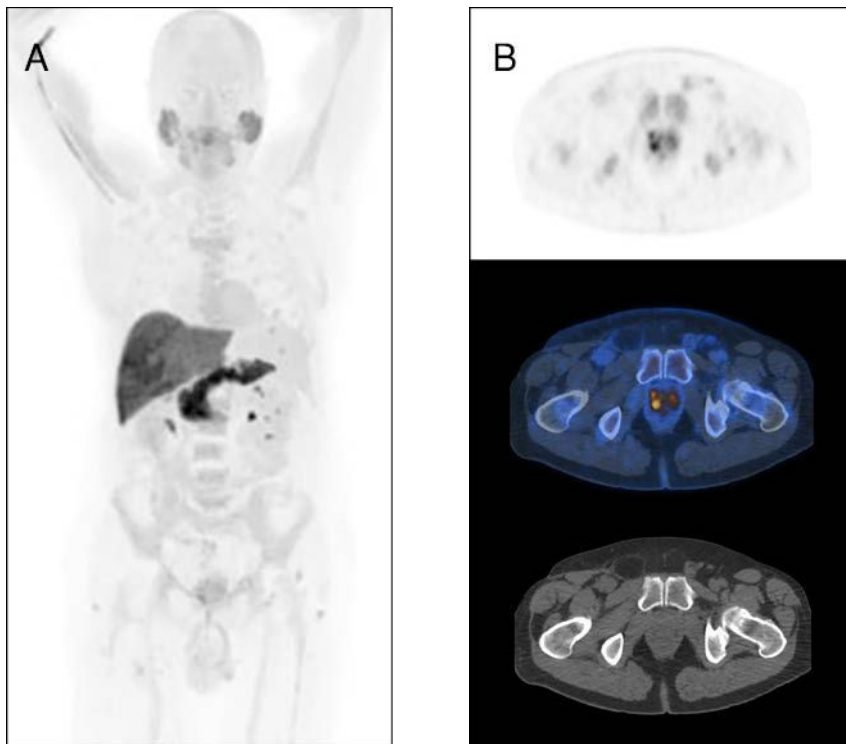
(A): MIP; (B): PET, fused and CT transaxial slices of pelvis.

There is focal intense tracer uptake in the right lobe of the prostate. No nodal or distant metastases are visible.

Teaching point

^{18}F -FACBC is useful in staging high risk prostate cancer.

Keywords: Prostate cancer, staging, ^{18}F -FACBC



11.4.2.2. Case No. 11.2

Clinical indication for PET–CT: Prostate cancer, staging

Clinical history

A 61 year old patient with newly diagnosed prostate cancer, stage T3b, Gleason score 4+4, PSA 12 ng/mL.

PET–CT findings

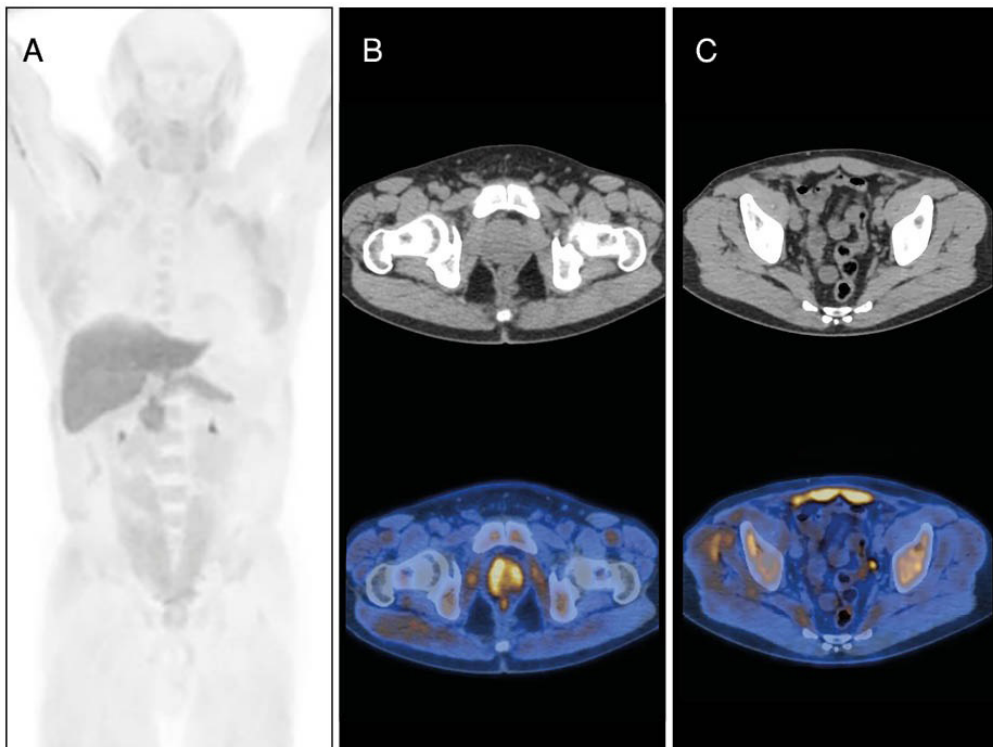
(A): MIP; (B, C): CT and fused transaxial slices at two levels of pelvis.

There is intense tracer uptake in an enlarged prostate gland (B) and focal uptake in a small (7 mm) left iliac LN metastasis (C).

Teaching point

^{18}F -FACBC is useful in staging high risk prostate cancer. The presence of LN metastases at presentation is common in high risk patients. Note the intensity of uptake despite the small size of the LN.

Keywords: Prostate cancer, staging, ^{18}F -FACBC



Clinical indication for PET–CT: Prostate cancer, staging

Clinical history

A 72 year old patient with newly diagnosed prostate cancer, stage T3a, Gleason score 4+4, PSA 28 ng/mL.

PET–CT findings

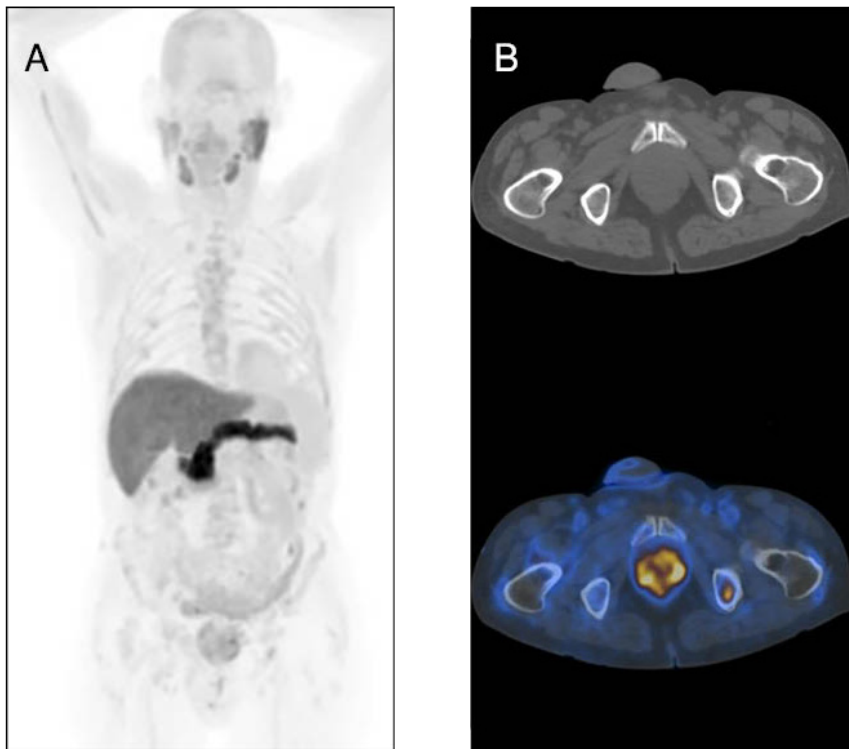
(A): MIP; (B): CT and fused transaxial slices of pelvis.

There is intense tracer uptake in an enlarged prostate gland and an additional focal uptake in a small osteoblastic metastasis in the left ischium.

Teaching point

^{18}F -FACBC is useful in staging high risk prostate cancer. The incidence of bone lesions in prostate cancer at presentation is relatively rare, but higher in patients with high risk tumours.

Keywords: Prostate cancer, staging, ^{18}F -FACBC



11.4.2.4. Case No. 11.4

Clinical indication for PET–CT: Prostate cancer, BCR

Clinical history

A 64 year old patient with prostate cancer BCR, with PSA 0.9 ng/mL.

PET–CT findings

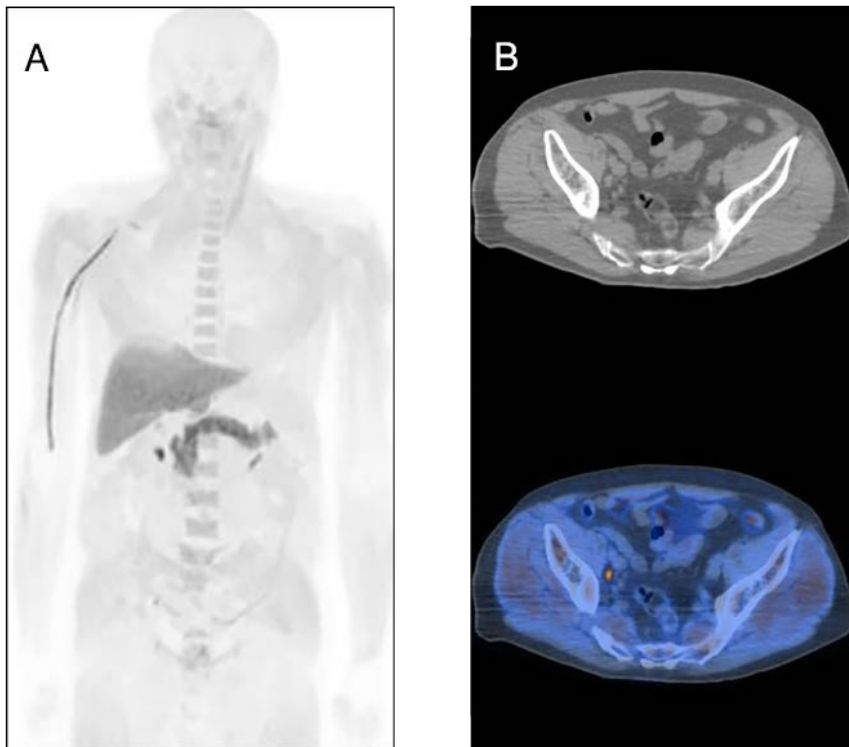
(A): MIP; (B): CT and fused transaxial slices of pelvis.

There is faint tracer uptake in a small (9 mm) right iliac LN (B).

Teaching point

Small LN metastases may be ^{18}F -FACBC positive. The presence of oligometastatic disease indicates that the patient is a candidate for aggressive therapy, such as salvage RT or salvage pelvic LND.

Keywords: Prostate cancer, BCR, ^{18}F -FACBC



11.4.2.5. Case No. 11.5

Clinical indication for PET–CT: Prostate cancer, BCR

Clinical history

A 71 year old patient with prostate cancer BCR, PSA 1.0 ng/mL and PSA dt 8.6 months.

PET–CT findings

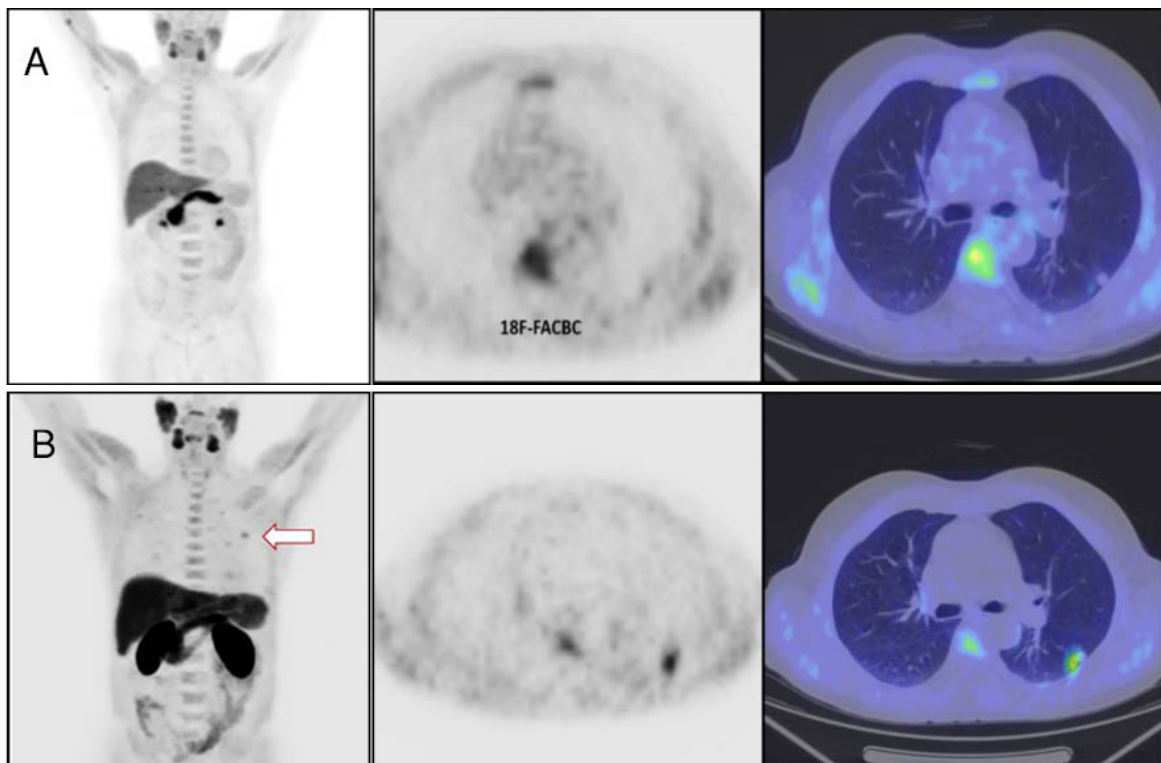
(A): ^{18}F -FACBC MIP, PET and fused transaxial slices of mid-thorax; (B): ^{18}F -choline MIP and same slices at same level as (A).

There are no areas of increased ^{18}F -FACBC uptake in the thorax, while on CT there is a 10 mm left lung nodule (A). ^{18}F -choline imaging performed one week later shows moderate tracer uptake in the lung lesion (B). Biopsy of the lung lesion diagnosed a metastasis of prostate cancer.

Teaching point

^{18}F -FACBC may be false negative in small lung metastases of prostate cancer.

Keywords: Prostate cancer, lung metastasis, ^{18}F -FACBC



11.4.2.6. Case No. 11.6

Clinical indication for PET–CT: Prostate cancer, BCR

Clinical history

A 71 year old patient with prostate cancer BCR, post-radical prostatectomy, PSA 2.1 ng/mL.

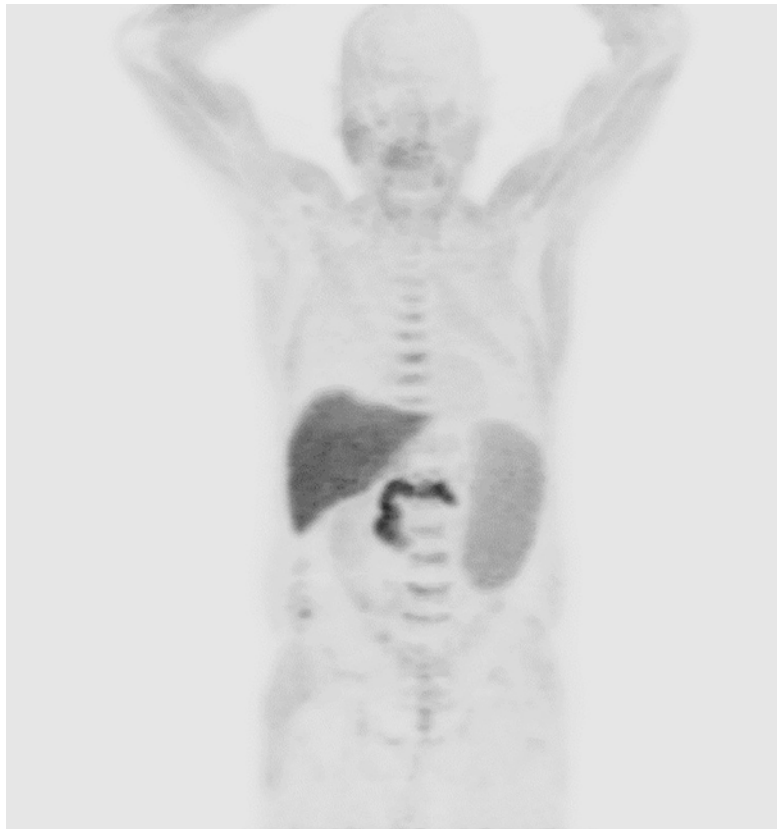
PET–CT findings

The image (MIP) shows low intensity abnormal tracer uptake in an enlarged spleen. The patient was further diagnosed with idiopathic myelofibrosis.

Teaching point

^{18}F -FACBC can show positive results in haematological conditions, such as myelofibrosis.

Keywords: Prostate cancer, myelofibrosis, ^{18}F -FACBC



Clinical indication for PET–CT: Prostate cancer, BCR

Clinical history

A 58 year old patient with prostate cancer BCR, with PSA 0.4 ng/mL.

PET–CT findings

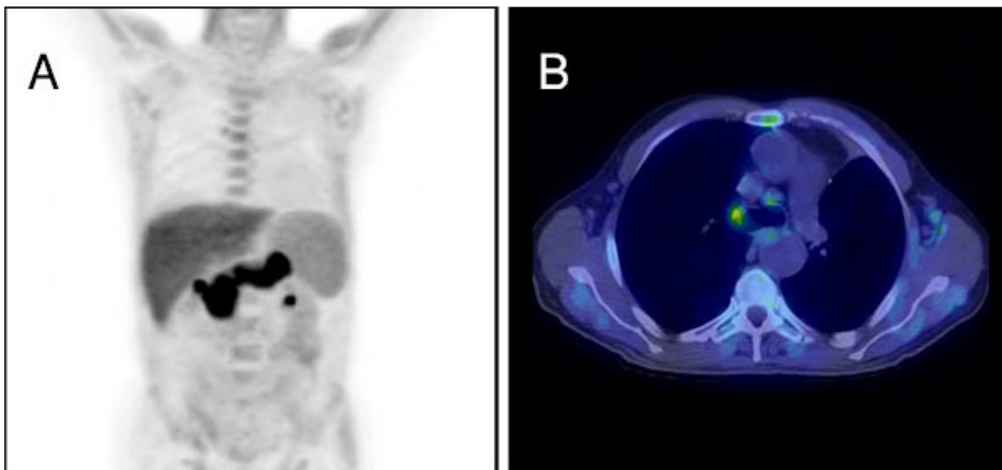
(A): MIP; (B): fused transaxial slice of mid-thorax.

There is low intensity increased tracer uptake in mediastinal LNs. Biopsy diagnosed chronic lymphocytic leukaemia.

Teaching point

^{18}F -FACBC can show positive results in haematological conditions, such as chronic lymphocytic leukaemia.

Keywords: Prostate cancer, leukaemia, ^{18}F -FACBC



12. FMISO (^{18}F)

12.1. GENERAL CHARACTERISTICS

Name: [^{18}F]fluoromisonidazole (^{18}F -MISO)

Synonyms: [^{18}F]FMISO; 1-(2-nitroimidazolyl)-3- ^{18}F fluoro-2-propanol; ^1H -1-(3- ^{18}F fluoro-2-hydroxypropyl)-2-nitroimidazole.

Radioisotope

^{18}F is a short half-life PET radioisotope (109.7 min) emitting positrons of E_{max} 1.656 MeV. Owing to the high chemical stability of C–F bonds in organic compounds as well as the high water solubility of F compounds, ^{18}F tracers usually show suitable stability and biodistribution in humans. Although the F chemistry is complicated, the vast application of ^{18}F labelled compounds in nuclear medicine has led to development of efficient automated radiopharmaceutical production methods allowing large scale production of ^{18}F tracers for clinical use.

Radiosynthesis

At least two methods for ^{18}F -MISO production have been described. The most promising method seems to be a nucleophilic substitution of the tosylate leaving group by ^{18}F -fluoride on a tetrahydropyranyl-protected precursor (NITTP), with hydrolysis of the protecting group, which can be automated using either HPLC or Sep-Paks for the purification of the radiotracer (Fig. 12.1). This method results in a chemical yield of $\leq 40\%$, radiochemical purity of $\geq 97\%$ and specific activity of 34 TBq/mmol [80, 81].

12.2. PHARMACOKINETICS

12.2.1. Physiological biodistribution and metabolism

Under normal oxygen tension, MISO is metabolized primarily in the liver to its demethylated form, but ^{18}F -MISO is not a substrate for this reaction. Additionally, approximately 7% is conjugated to glucuronide, and a small amount (less than 5%) is converted to aminoimidazole. Substantial amounts

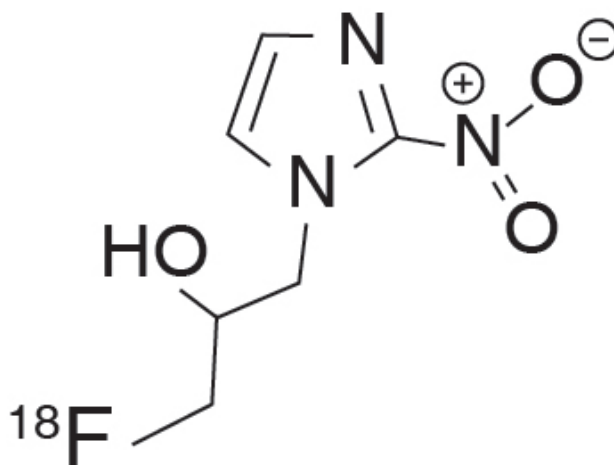


FIG. 12.1. Molecular structure of [^{18}F]fluoromisonidazole.

of MISO are recoverable in faeces. Faecal bacteria are able to reduce misonidazole only in the absence of oxygen. At treatment doses, the plasma half-life of both ^{18}F -MISO and MISO ranges from 8 to 17.5 hours. Parent molecule and glucuronide metabolites are primarily excreted in the urine. ^{18}F -MISO studies normally show intense tracer uptake in the bowel, probably due to the presence of anaerobic bacteria, and activity of moderate intensity in muscles and in the thyroid, spleen, pancreas, heart, lung and kidney. Low and variable ^{18}F -MISO uptake is demonstrated in the brain, indicating that the tracer is freely diffusible across the blood–brain barrier. Uptake in the liver is variable. The tracer is excreted via the kidneys (Fig. 12.2) [80, 81].

12.2.2. Mechanism of retention

^{18}F -MISO is relatively hydrophilic and diffuses across cell membranes, showing a passive distribution in normal tissues, owing to the presence of the nitro group. The molecule is then reduced in hypoxic cellular media ($p\text{O}_2 \leq 2\text{--}3$ mmHg) and binds selectively to macromolecules within hypoxic cells.

12.2.3. Pharmacology and toxicology

The maximum dose to humans reported in imaging protocols is 1 mg/kg or 70 mg for a 70 kg subject. This is about 0.1% of the projected median lethal dose. No adverse events have been reported. Total patient imaging doses of the current radiopharmaceutical formulation contain up to 15 μg of fluoromisonidazole and less than 35 μg of other nitroimidazole derivatives. This is less than 0.001% of the projected median lethal dose.



FIG. 12.2. Normal biodistribution of ^{18}F -FMISO.

12.3. METHODOLOGY

12.3.1. Activity, administration, dosimetry

The IV administered activity is 3.7 MBq/kg (0.1 mCi/kg). Calculated total body dose for a 70 kg man injected with 3.7 MBq/kg is 0.013 mGy/MBq, and for a 57 kg woman it is 0.016 mGy/MBq. Effective dose equivalents are 0.013 mSv/MBq for men and 0.014 mSv/MBq for women. The majority (97%) of the injected activity is homogeneously distributed in the body, leaving only 3% for urinary excretion. Doses to smaller organs that could not be directly determined by visualization, such as the lens, were calculated assuming average total body concentrations. The absence of tracer visualization in these organs suggests a lack of increased accumulation [82–97].

12.3.2. Imaging protocol

The patient has to fast for at least 2 hours prior to the study. Imaging is performed after the IV administration of 6 MBq/kg and an uptake period of 3–4 hours. The acquisition protocol for the PET component includes, for the early study at 15 min, 3 frames of 300 seconds each, and a delayed acquisition at 3 or 4 hours post-injection. For the CT imaging protocol, see general comments in Section 1.3.

12.4. CLINICAL ASPECTS

12.4.1. Indications

When present in tumours, ischaemia is associated with poor prognosis, increased invasion rate, higher incidence of metastases and resistance to chemoradiation. In hypoxic cells, ^{18}F -MISO is reduced and binds selectively to macromolecules. ^{18}F -MISO is relatively hydrophilic and diffuses across cell membranes. PET–CT with ^{18}F -MISO has been used as a non-invasive method for detecting and characterizing hypoxia in several malignancies. In brain tumours, the degree of ^{18}F -MISO uptake is related to the response to treatment and prognosis. The degree of uptake can be used to discriminate between high grade and low grade gliomas. In squamous cell cancer of the head and neck, ^{18}F -MISO can be a predictor of outcome to RT. Higher ^{18}F -MISO uptake has been associated with worse prognosis and shorter survival. In NSCLC, detection of hypoxic tumour areas with ^{18}F -MISO could allow modification of the planned RT fields and dose optimization. Higher ^{18}F -MISO uptake has been associated with incomplete response to treatment and increased risk of recurrence. In ER+ breast cancer, ^{18}F -MISO PET–CT can predict primary resistance to hormone therapy [82–97].

12.4.2. Cases

12.4.2.1. Case No. 12.1

Clinical indication for PET–CT: High grade glioblastoma, suspected recurrence

Clinical history

A 15 year old boy with high grade glioblastoma, post-subtotal resection, subsequently treated with RT and temozolomide. MRI showed changes related to right frontal craniotomy, a hypodense subjacent area in the surgical bed (gliosis), and persistence of an expansive lesion in the thalamus (A).

PET–CT findings

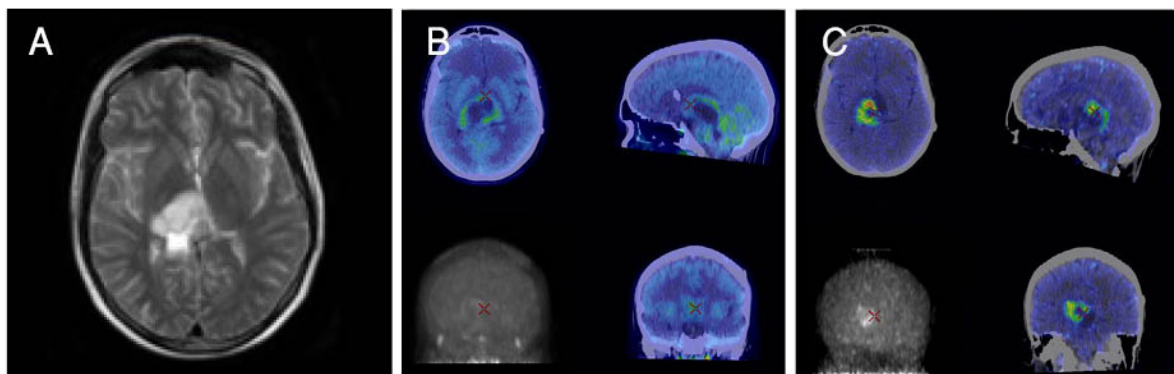
(A): MRI transaxial slice of brain; (B): ^{11}C -methionine, MIP and fused slices in three planes; (C): ^{18}F -MISO, same images at same levels as in (B).

There is a right thalamic lesion crossing the midline and reaching the left mesencephalon, with faint peripheral ^{11}C -methionine uptake. Despite the low intensity uptake, the findings are suspicious for residual active tumour or relapse (B). In the ^{18}F -MISO study there is tracer uptake at the margins of the surgical bed, coinciding with the ^{11}C -methionine study, but more prominent uptake in the central, anterior and right lateral areas, consistent with a hypoxic area in the lesion.

Teaching point

^{18}F -MISO is a hypoxia biomarker whose clinical relevance in cancer patients is still controversial. Its main application is for ‘in vivo’, non-invasive hypoxia identification. This may lead to better RT planning, since oxygenation in tumour tissue influences response to treatment, with a much higher radiation dose necessary to achieve the same therapeutic effect in hypoxic tumours. Additionally, ^{18}F -MISO also has the potential to become a prognostic biomarker.

Keywords: Glioblastoma, hypoxia, ^{18}F -MISO, ^{11}C -methionine



13. FAZA (¹⁸F)

13.1. GENERAL CHARACTERISTICS

Name: ¹⁸F-FAZA

Synonyms: ¹⁸FAZA; [¹⁸F]fluoroazomycinarabinofuranoside; 1-(5-[¹⁸F]fluoro-5-deoxy- α -D-arabinofuranosyl)-2-nitroimidazole.

Radioisotope

¹⁸F is a short half-life PET radioisotope (109.7 min) emitting positrons of E_{\max} 1.656 MeV. Owing to the high chemical stability of C–F bond in organic compounds as well as the high water solubility of the compounds, ¹⁸F tracers usually show suitable stability and biodistribution in humans. Although the F chemistry is complicated, the vast application of ¹⁸F labelled compounds in nuclear medicine has led to development of efficient automated radiopharmaceutical production methods allowing large scale production of ¹⁸F tracers for clinical use.

Radiosynthesis

¹⁸F-FAZA can be readily synthesized under standard nucleophilic substitution conditions (Kryptofix 222 and K₂CO₃), followed by hydrolysis of the protective acetyl groups using 1-(2,3-di-O-acetyl-5-O-tosyl- α -D-arabinofuranosyl)-2-nitroimidazole and ¹⁸F-fluoride (Fig. 13.1). An automated synthesis method was also recently developed, providing a radiochemical yield of 20.7% \pm 3.5% and absolute yield of 9.8 \pm 2.3 GBq in 50 min.

13.2. PHARMACOKINETICS

13.2.1. Mechanism of retention

2-nitroimidazole compounds are postulated to undergo reduction in hypoxic conditions, forming highly reactive oxygen radicals that subsequently bind covalently to macromolecules inside the cells (see also section on ¹⁸F-MISO). While FMISO has slow clearance kinetics and a high lipophilicity, resulting

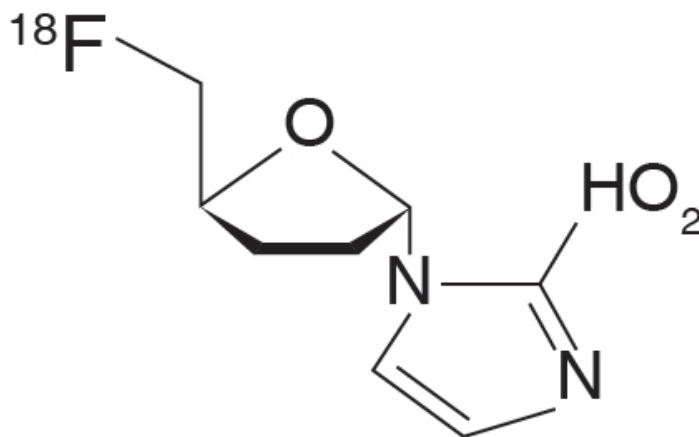


FIG. 13.1. Molecular structure of ¹⁸F-FAZA.

in substantially high background on PET scans, ^{18}F -FAZA is a 2-nitroimidazole with a sugar addition moiety showing more water solubility and better pharmacokinetics.

13.3. METHODOLOGY

13.3.1. Activity, administration, dosimetry

The IV administered activity is 371 ± 32 MBq (range: 277–427 MBq). The critical organ is the urinary bladder wall, with maximum radiation absorbed doses of 0.047 ± 0.008 mGy/MBq and 0.067 ± 0.007 mGy/MBq based respectively on 2 and 4 hour voiding intervals. The effective dose for standard male and female patients is 0.013 ± 0.004 mSv/MBq and 0.014 ± 0.004 mSv/MBq, respectively, depending on the voiding schedule. The effective dose equivalent for ^{18}F -FAZA is 0.015 mSv/MBq.

13.3.2. Imaging protocol

The patient does not have to fast. Imaging is performed following the IV administration of 370 MBq and an uptake period of 120 min. The acquisition of the PET component moves from mid-thigh to brain with 5 min/bed position. For the CT imaging protocol, see general comments in Section 1.3.

13.4. CLINICAL ASPECTS

13.4.1. Indications

The tracer was investigated at the University Medical Centre Groningen, the Netherlands. Three studies have been published using this experimental tracer to assess the amount of hypoxia in malignant tumours of the head and neck and of the lung [1–3, 98–100]. Because it is at the investigational stage, the tracer is not routinely used in clinical practice.

13.4.2. Cases

13.4.2.1. Case No. 13.1

Clinical indication for PET–CT: Oropharyngeal cancer, serial studies assessing the dynamics of tumour hypoxia during chemoradiation

Clinical history

A 67 year old male with prostate cancer and bladder cancer (previously treated curatively) presented with pain in his left ear and difficult swallowing. A large tumour mass at the left side of the base of the tongue was visualized. Biopsy diagnosed locally advanced (stage IV, cT3N2bM0) squamous cell carcinoma of the base of the tongue. A multidisciplinary tumour board recommended primary chemoradiation. Prior to starting treatment, the patient agreed to participate in a study to assess tumour hypoxia before and during treatment using ^{18}F -FAZA PET–CT.

PET–CT findings

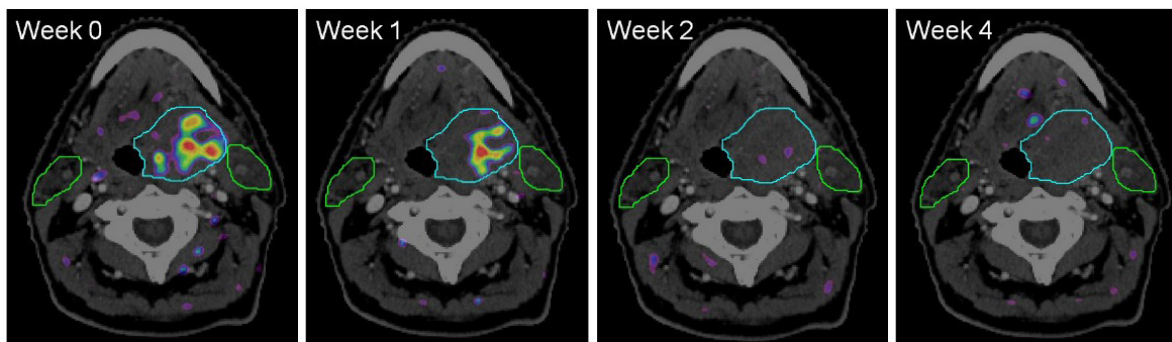
Images (fused transaxial slices) show the four ^{18}F -FAZA PET–CT studies performed in this patient. The first study was performed just prior to the start of chemoradiation (week 0) and showed a large area of tracer uptake in the primary tumour, representing the hypoxic area. Subsequently, three additional studies were performed during chemoradiation: at week 1 the area of hypoxia was still large but smaller and at a slightly different location than at baseline; at weeks 2 and 4 no hypoxia could be detected.

Follow-up: Two months after chemoradiation the patient had a complete response with no visualization of the tumour. Five years after treatment there were still no signs of recurrence of metastatic disease.

Teaching point

^{18}F -FAZA PET–CT is suitable to evaluate tumour hypoxia before and during treatment in patients with head and neck cancer. Tumour hypoxia can change rapidly during therapy, and therefore it is very difficult to adapt RT based on hypoxia imaging.

Keywords: Head and neck cancer, RT, hypoxia, ^{18}F -FAZA



14. EXENDIN (⁶⁸Ga)

14.1. GENERAL CHARACTERISTICS

Name: ⁶⁸Ga-exendin-4

Synonyms: ⁶⁸Ga labelled [1,4,7-tris (carboxymethyl)-10-(2'-hydroxypropyl)-1,4,7,10 tetraazacyclododecane]-VS-Cys⁴⁰-exendin-4; ⁶⁸Ga-DOTA-Ahx-Lys⁴⁰-exendin-4.

Radioisotope

⁶⁸Ga is a short half-life PET radioisotope (67.7 min) emitting positrons of E_{\max} 1.9 MeV. It is usually obtained from a ⁶⁸Ge generator. The parent isotope, ⁶⁸Ge, has a half-life of 271 days and can be easily utilized for in-hospital production of ⁶⁸Ga.

Radiosynthesis

The ⁶⁸Ga labelling of DO3A-VS-Cys⁴⁰-exendin-4 is performed using an automated synthesizer coupled with a generator (Fig. 14.1). The non-decay corrected radiochemical yield is 43% ± 2% with radiochemical purity of over 90% wherein the individual impurity signals in a HPLC chromatogram do not exceed 5% [101–105].

14.2. PHARMACOKINETICS

14.2.1. Physiological biodistribution and metabolism

According to current knowledge, no direct healthy human metabolism studies have been reported for ⁶⁸Ga-exendin-4. However, based on European Association of Nuclear Medicine guidelines on DOTA conjugated peptides, it appears to be rapidly cleared from the blood. Arterial elimination of the radiopharmaceutical and its metabolites is biexponential. No radioactive metabolites are detected after 4 hours in the serum or urine.

14.2.2. Mechanism of retention

This radiopharmaceutical is a glucagon-like peptide-1 (GLP-1) agonist having high affinity for GLP-1 receptor, with retention in the GLP-1 receptor positive organs and tumours [101–105].

14.2.3. Pharmacology and toxicology

No comprehensive toxicological studies on DOTA-exendin-4 have been reported. The human experience using exendin-4 in therapy involves twice daily doses ($2 \times 10 \mu\text{g}$) for 3 months in adolescents with severe obesity, without any side effects. There is evidence that the mass quantity of the reported PET studies (7–25 μg) is within the acceptable range for patients with life threatening malignancies whose treatment may benefit from the use of the proposed PET–CT procedure [101–105].

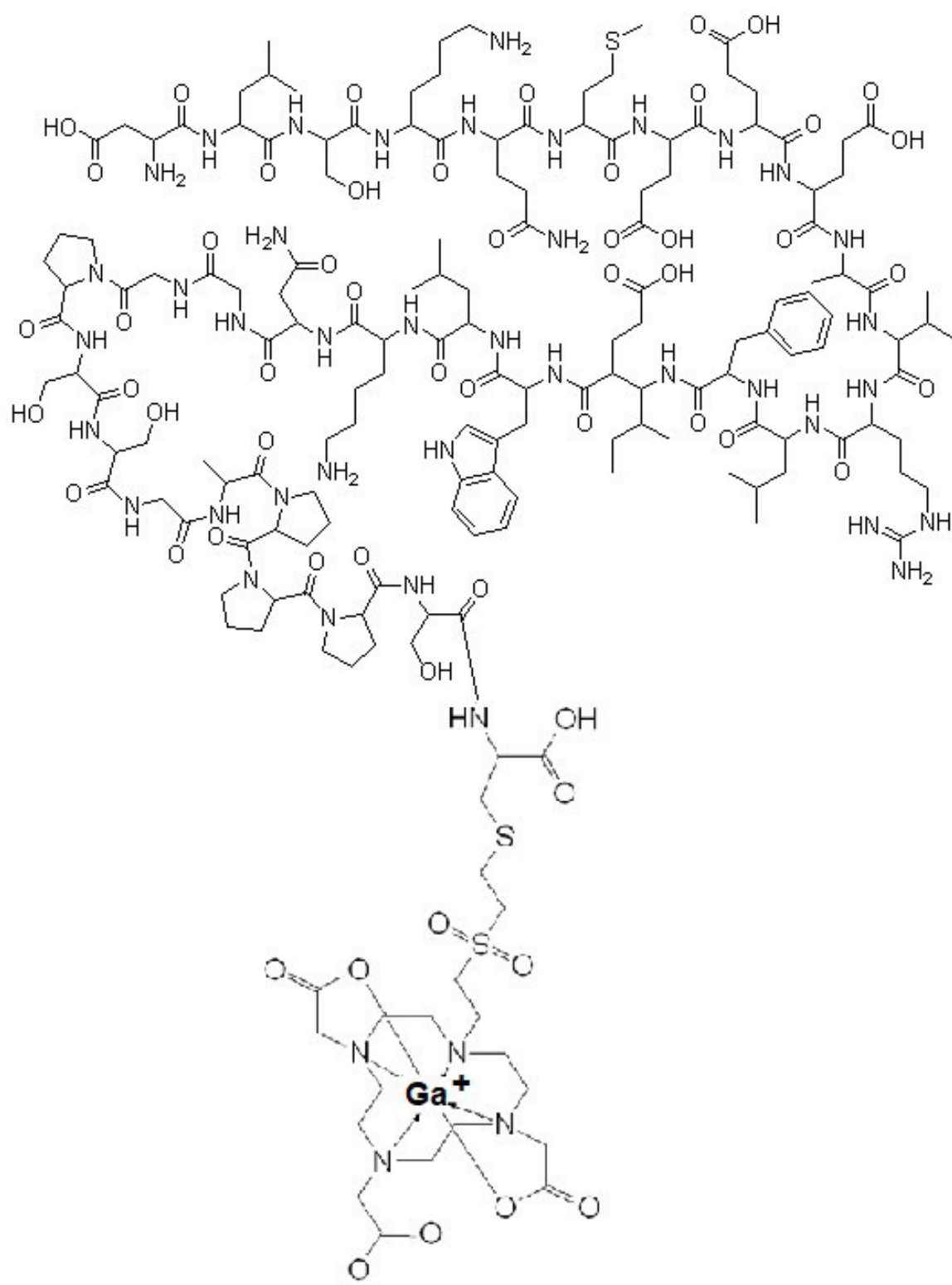


FIG. 14.1. Molecular structure of ^{68}Ga -exendin-4.

14.3. METHODOLOGY

14.3.1. Activity, administration, dosimetry

⁶⁸Ga-NOTA-exendin-4 (18.5–185 MBq, 7–25 µg) is administered via IV injection over 2–3 min. It was observed in biodistribution studies that the radiation dose to the kidneys is a concern with respect to potential repeat studies in humans. The absorbed dose to the kidneys was the limiting factor in laboratory animals as well as in humans; the yearly kidney limiting dose is 150 mGy. More than 200 MBq can be administered yearly in a patient, allowing for repeated (2–4 times) scanning. This could enable longitudinal clinical PET studies of GLP-1 receptor in the pancreas, transplanted islets or insulinoma [101–105].

14.3.2. Imaging protocol

Patient preparation requires a fasting period of at least 4 hours. Imaging is performed after the IV administration of 80–100 MBq and an uptake period of 1–2 hours. Acquisition of the PET component moves from pelvis to liver dome, with 2 mins/bed position. For the CT imaging protocol, see general comments in Section 1.3.

14.4. CLINICAL ASPECTS

14.4.1. Indications

The technique was investigated at the Radboud University Medical Center, Nijmegen, the Netherlands [101–105]. ⁶⁸Ga-exendin can be used for in vivo targeting of GLP-1 receptor expressing beta cell derived tumours, such as insulinomas. Previous and ongoing studies indicate a higher sensitivity and specificity as compared with triple phase CT, MRI, endoscopic US and somatostatin receptor PET–CT. Because it is at the investigational stage, this study is not routinely performed in clinical practice.

14.4.2. Cases

14.4.2.1. Case No. 14.1

Clinical indication for PET–CT: Suspected insulinoma

Clinical history

A 41 year old male suffering from hypoglycaemic episodes for 2 years was hospitalized after losing consciousness. A fasting test resulted in a positive Whipple's triad with a plasma glucose level of 1.7 mmol/L, a plasma insulin level of 35 mU/L and neuroglycopenic symptoms. MRI and ^{68}Ga -DOTATOC PET–CT performed over the following months did not show any abnormalities in the pancreas.

PET–CT findings

(A): ^{68}Ga -DOTATOC transaxial fused slices of liver and pancreas; (B): ^{68}Ga -exendin, same slices as in (A).

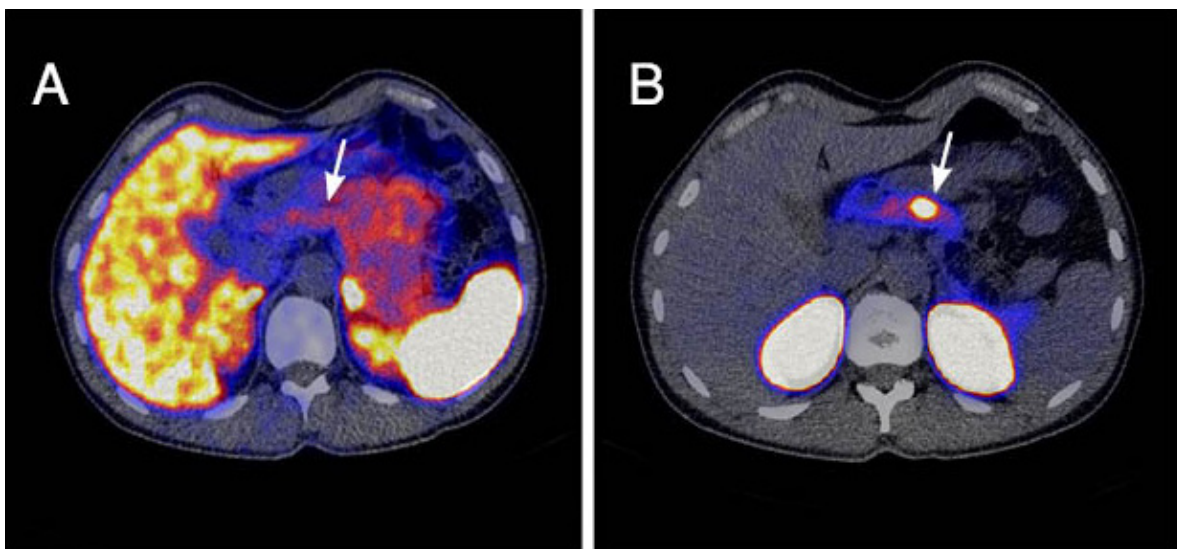
On ^{68}Ga -exendin imaging a GLP-1 receptor positive lesion was clearly demonstrated in the body of the pancreas (B, arrow).

Follow-up: The patient underwent partial pancreatectomy and an insulinoma was found. The patient has had no hypoglycaemic episodes since the surgery.

Teaching point

GLP-1 receptor imaging with ^{68}Ga -exendin PET–CT shows high potential for the detection of insulinomas, especially in the case of negative conventional imaging procedures.

Keywords: Insulinoma, GLP-1 receptor, ^{68}Ga -exendin



15. 5-HYDROXYTRYPTOPHAN, HTP (^{11}C)

15.1. GENERAL CHARACTERISTICS

Name: ^{11}C -5-hydroxytryptophan (^{11}C -HTP)

Synonyms: [^{11}C]5-HTP, 5-HTP PET, ^{11}C -5-HTP; ^{11}C -HTP (hydroxytryptamine)

Radioisotope

^{11}C is a short half-life PET radioisotope (20.4 min) emitting positrons of E_{max} 0.970 MeV. Owing to the abundance of carbon in the chemistry of life and biomolecules, ^{11}C radiopharmaceuticals demonstrate identical behaviour to natural compounds, allowing tracing of biological processes.

Radiosynthesis

In 2006, a multienzymatic synthesis of enantiomerically pure [^{11}C]-L-5-HTP from [^{11}C]methyl iodide (Fig. 15.1) was developed on a robotic system, providing a radiochemical yield at end of bombardment of 24% and specific activity of 44 000 GBq/mmol in 50 min. However the multienzymatic reaction steps made the yields small [106, 107].

15.2. PHARMACOKINETICS

15.2.1. Physiological biodistribution and metabolism

A kinetic analysis of the uptake of ^{11}C -HTP demonstrated an increase during the first few minutes followed by a washout and a stabilization of the tissue/blood ratio at about 2 min. There is a gradual increase in the transport rate during the first 20 to 30 min, after which a constant level is achieved. ^{11}C -HTP goes through decarboxylation and is stored in vesicles, followed by release into the extracellular environment. ^{11}C -serotonin is thereafter degraded and eventually excreted as urinary 5-hydroxyindole acetic acid [106, 107].

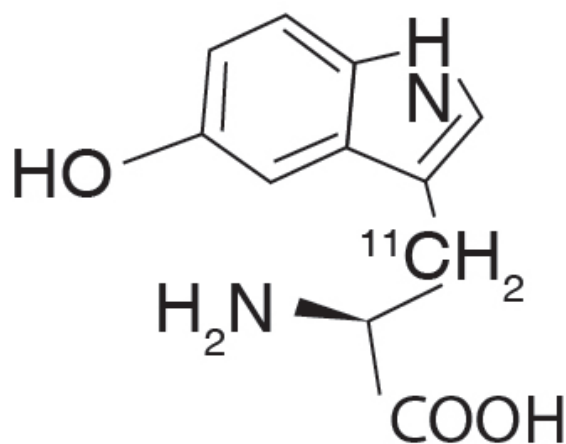


FIG. 15.1. Molecular structure of ^{11}C -5-hydroxytryptophan.

15.2.2. Mechanism of retention

¹¹C-HTP is taken up into NET cells followed by decarboxylation to serotonin by an enzyme called aromatic amino acid decarboxylase. The resulting end-product, serotonin, is transported into storage vesicles through the vesicular monoamine transporter as well as through the metabolic pathway of serotonin [106, 107].

15.2.3. Pharmacology and toxicology

5-HTP has been used in management of cases of depression. A typical dose of 5-HTP is in the range of 300–500 mg taken daily without any side effects. ¹¹C-HTP is used at tracer level and far below the pharmaceutical intake.

15.3. METHODOLOGY

15.3.1. Activity, administration, dosimetry

The IV administered activity is 140–521 MBq (mean 381 MBq). No data on the dosimetry of ¹¹C-HTP could be found.

15.3.2. Imaging protocol

Patients have to fast for at least 4 hours prior to administration of the radiopharmaceutical. Imaging is performed after an uptake period of 1 hour for a PET component acquisition time of 2 mins/bed position. The CT imaging protocol is discussed in the general comments in Section 1.3.

15.4. CLINICAL ASPECTS

15.4.1. Indications

Before the breakthrough of somatostatin labelled receptor ligands suited for PET imaging, ¹⁸F-DOPA and ¹¹C-HTP were considered superior for evaluation of NETs as compared with ¹¹¹In labelled octreotide and/or CT. While ¹⁸F-DOPA reflects the catecholaminergic pathway, ¹¹C-HTP is related to the serotonergic pathway. However, while both tracers were useful for the detection of NETs, because of the complexity of the ¹¹C-HTP synthesis, ¹⁸F-DOPA was routinely preferred, except for the detection of pancreatic islet tumours. In the latter, ¹¹C-HTP PET–CT proved to be superior as compared with ¹⁸F-DOPA because the dopaminergic pathway seems to be dysfunctional. With the advent of ⁶⁸Ga labelled somatostatin receptor ligands, the additional information they made available for radionuclide therapy made PET–CT imaging using ¹⁸F-DOPA obsolete in the general clinical practice of managing patients with NETs. The same applies for the use of ¹¹C-HTP PET–CT in pancreatic islet cell tumours. This section on ¹¹C-HTP was nevertheless included as an illustration of its normal distribution and of past evidence. It is noteworthy that preclinical research on its potential as a marker of serotonin synthesis in the brain and hence in different neuropsychiatric conditions also proved fruitless [108–110].

15.4.2. Cases

15.4.2.1. Case No. 15.1

Clinical indication for PET–CT: Small bowel NET, restaging after surgery

Clinical history

A 51 year old man underwent partial resection of the ileum in which pathology examination revealed 18 foci of NET. The patient was referred to exclude residual sites of active NET.

PET–CT findings

MIP.

The physiological distribution of the tracer is demonstrated, with homogeneous uptake throughout the pancreas and excretion by the kidneys to the urinary bladder. There are no sites of pathological tracer activity.

Follow-up: No further treatment was indicated for this patient. Three years after surgery no remnant of relapse has been found

Teaching point

The distribution pattern is normal.

Keywords: NET, ^{11}C -HTP, normal biodistribution



Clinical indication for PET–CT: NET of the pancreas, staging

Clinical history

A 65 year old woman complained of frequently recurring urinary bladder infection. US of the abdomen revealed a lesion in the tail of the pancreas as well as multiple liver lesions. Retrospectively, the patient also complained of increased sweating during mild exercise, but without flushing. Tissue analysis of one of the liver lesions confirmed a metastasis from a grade 1 NET originating in the pancreas.

PET–CT findings

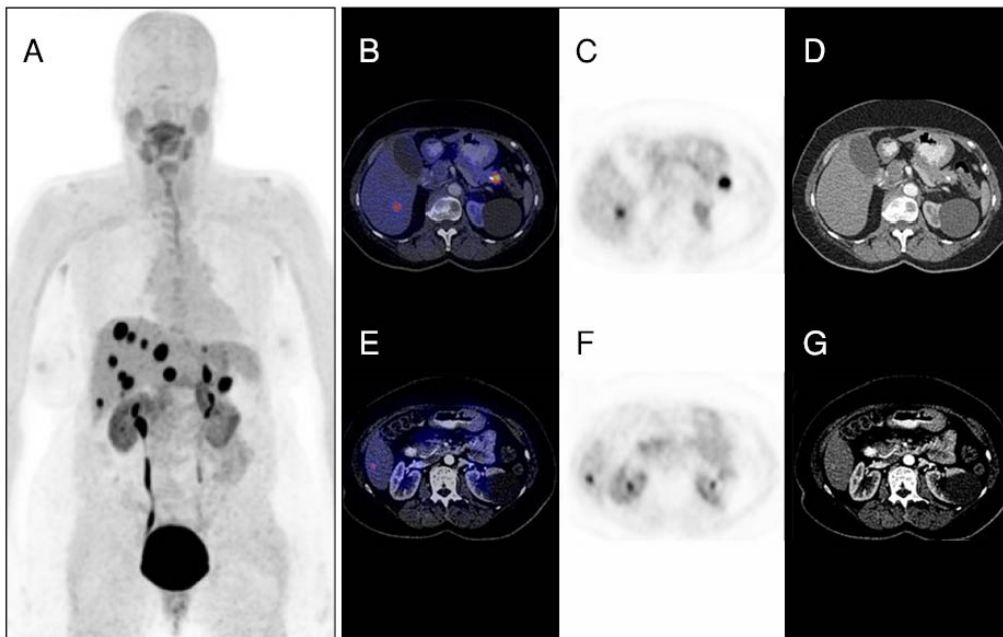
(A): MIP; (B–D): transaxial fused, PET and contrast enhanced CT of the upper abdomen; (E–G): same images as in (B–D), mid-abdomen.

There are multiple sites of intense tracer uptake in the upper abdomen, including high uptake in a calcified lesion with some enhancement in the tail of the pancreas (B–D). Additional sites of intense focal tracer uptake are seen in hypodense liver lesions with slight arterial enhancement on CT (E–G). Because of the initial lack of complaints no treatment was started. Two years later the patient showed disease progression, with onset of flushing and diarrhoea. Treatment with somatostatin analogue showed good response for an additional 2 years.

Teaching points

^{11}C -HTP is sensitive for the detection of pancreatic NETs.

Keywords: NET, pancreas, ^{11}C -HTP



16. METHIONINE (^{11}C)

16.1. GENERAL CHARACTERISTICS

Name: ^{11}C -methionine

Synonyms: [^{11}C]MET; L-[methyl- ^{11}C]methionine; 2-amino-4-[^{11}C]methylsulfanyl-butanoic acid; l-[S-methyl ^{11}C]methionine

Radioisotope

^{11}C is a short half-life PET radioisotope (20.4 min) emitting positrons of E_{max} 0.970 MeV. Owing to the abundance of carbon in the chemistry of life and biomolecules, ^{11}C radiopharmaceuticals demonstrate identical behaviour to natural compounds, allowing tracing of the biological processes.

Radiosynthesis

A continuous flow procedure has been automated for the synthesis of ^{11}C -methyl iodide from $^{11}\text{C}\text{-CO}_2$ and L-[methyl ^{11}C]methionine from ^{11}C -methyl iodide and L-S-benzyl-homocysteine in 20 min for a yield of >30%, 44 mCi or 1.62 MBq ^{11}C -methionine (Fig. 16.1), with specific activity of 3.3 Ci/mmol (122 GBq/mmol) and radiochemical purity of >96%. In a second automated method, without HPLC purification, a solid phase supported ^{11}C -methylation of L-homocysteine thiolactone on Al_2O_3 is employed for a yield of 10.2 GBq (276 mCi) and radiochemical purity >99% [80, 111–114].

16.2. PHARMACOKINETICS

16.2.1. Physiological biodistribution and metabolism

^{11}C -methionine biodistribution at 20 min after administration shows intense tracer uptake in the pituitary gland, the choroid plexus, confluence of sinuses, Waldeyer's ring, lacrimal and salivary glands, as well as in the liver, spleen and pancreas. Moderate tracer uptake is seen in the bone marrow and kidneys. Faint tracer uptake is found in the brain (Fig. 16.2(A)). Low, variable uptake is seen in the bowel. In most cases, no radioactive urine is detected in the ureters or bladder. Testicular, bone marrow and left ventricular uptake increases with age (Fig. 16.2(B, C)). Intracellular ^{11}C -methionine will either undergo integration into protein or incorporation of its methyl group into DNA and other compounds. Metabolites include serine and cysteine [80, 111–114].

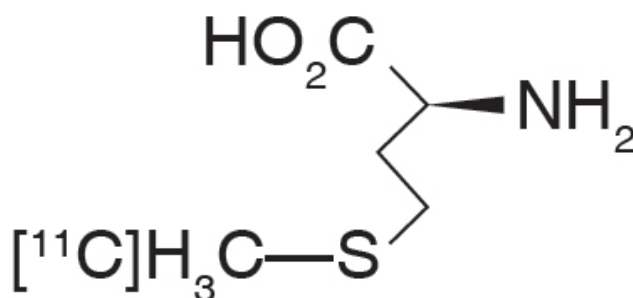


FIG. 16.1. Molecular structure of ^{11}C -methionine.

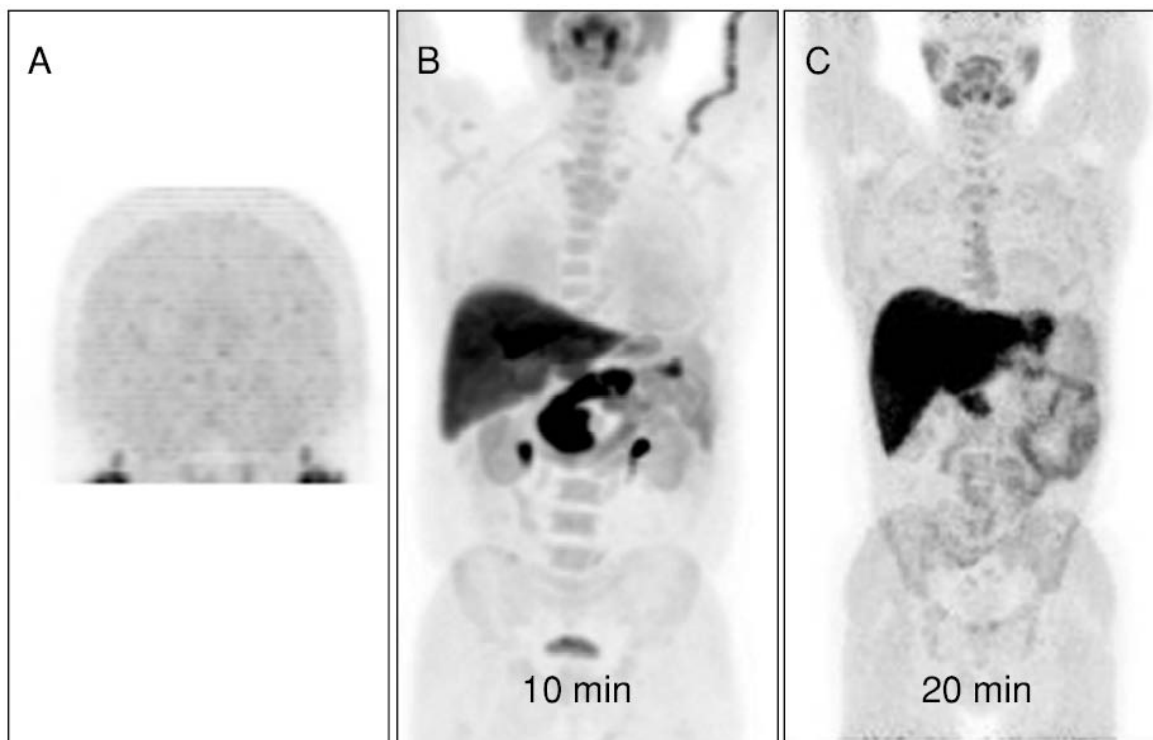


FIG. 16.2. Normal biodistribution of ^{11}C -methionine in the brain (A) and in the body 10 min (B) and 20 min (C) after injection.

16.2.2. Mechanism of retention

^{11}C -methionine, as a natural amino acid, is transported into cells by various transporters, and is incorporated into proteins in small portions. It is also incorporated into lipids, RNA and DNA. Being an essential amino acid, it is involved in the synthesis of proteins as well as in the synthesis and regulation of DNA.

16.2.3. Pharmacology and toxicology

Methionine is a natural amino acid found in living organisms and food. Nutritional and metabolic studies have employed the D and DL isomers of methionine, both below and above the required dose. No adverse effects have been reported in adults and children. ^{11}C -methionine is administered at tracer level and far below the dietary intake [80, 111–114].

16.3. METHODOLOGY

16.3.1. Activity, administration, dosimetry

An activity with a mean dose of 210–500 MBq is administered via IV injection. The organs that receive the highest absorbed doses are the bladder wall (0.027 mGy/MBq, 100 mrad/mCi), pancreas (0.019 mGy/MBq, 70 mrad/mCi), liver (0.018 mGy/MBq, 66 mrad/mCi) and kidneys (0.011 mGy/MBq, 41 mrad/mCi). The effective dose calculated for a 70 kg standard man is 0.0053 mSv/MBq (20 mrem/mCi) [115–126].

16.3.2. Imaging protocol

16.3.2.1. Brain imaging

Patient preparation requires a fasting period of at least 4 hours. Imaging is performed immediately after the IV administration of 3 MBq/kg. Acquisition of the PET component comprises 5 frames, at 1 min, 2 min, 3 min, 9 min and 20 min, for a total of 35 min. For the CT component imaging protocol, see general comments in Section 1.3.

16.3.2.2. Whole body imaging

Patient preparation requires a fasting period of at least 4 hours. Imaging is performed after the IV administration of 6 MBq/kg and an uptake period of 10–20 min. Acquisition of the PET component moves from the neck to the mediastinum (the base of the heart), with 4 min/bed position. For the CT imaging protocol, see general comments in Section 1.3. Because of the many potential sites of ectopic PTAs it is necessary to acquire images up to the lower mediastinum. Delayed acquisition at 20 or 40 min (Fig. 16.2(C)) should be included in the protocol when early acquisition is negative.

16.4. CLINICAL ASPECTS

16.4.1. Indications

16.4.1.1. Clinical applications

The main application for PET–CT with ^{11}C -methionine is in brain tumours, specifically gliomas that present with increased protein metabolism. This is in contrast to normal tissues that show low tracer uptake. Clinical indications for ^{11}C -methionine PET–CT imaging in brain tumours include diagnosis, biopsy and treatment planning, as well as the differential diagnosis between tumour recurrence and radiation necrosis. It can also diagnose pseudo-progression, a process in which combined RT and temozolomide can cause vasodilation, blood–brain barrier disruption and oedema. On MRI this process manifests as an increase in the size of Gd-enhanced lesions. The degree of uptake of ^{11}C -methionine correlates with tumour aggressiveness, reported to be related to overall survival.

In parathyroid gland imaging, $^{99\text{m}}\text{Tc}$ -sestaMIBI scintigraphy is the technique of choice in the pre-surgical location of PTAs. It is limited, however, by the size and location of these lesions. Clinical indications for ^{11}C -methionine PET–CT of the parathyroid glands include detection of PTAs and assessment of suspected recurrence after parathyroidectomy. ^{11}C -methionine PET–CT has improved the detection of PTAs in cases when other imaging techniques are negative, with a sensitivity of 83% and a specificity of 100%, including ectopic PTAs. The mediastinum is one of the most common sites for ectopic PTAs; other locations including the high cervical, intrathyroidal and retro-oesophageal regions, and the carotid and thyroglossal duct. The mechanism by which PTAs capture ^{11}C -methionine is not completely known. It is presumed to be related to the synthesis of pre-pro-PTH, which is a PTH precursor [116, 120, 121]. ^{11}C -methionine PET–CT provides images that reflect the metabolic activity of the parathyroid glands with high resolution.

Although the normal distribution of the tracer, with high uptake in the salivary glands, liver, pancreas and bone marrow, may present a problem in the study of tumours outside the brain, ^{11}C -methionine PET–CT has been also used in tumours of the head and neck, thymus, oesophagus and lung, as well as lymphoma and myeloma [116, 120, 121].

The main limitation to extend the use of ^{11}C -methionine PET–CT is the short half-life of ^{11}C , which restricts its use to centres with an on-site cyclotron.

16.4.2. Cases

16.4.2.1. Case No. 16.1

Clinical indication for PET–CT: Oligoastrocytoma, suspected relapse

Clinical history

A 41 year old male with a left frontal grade III oligoastrocytoma, partially removed, subsequently treated with RT and chemotherapy, had an epileptic crisis 3 years later. MRI showed growth of the residual tumour, and a new focus outside the surgical bed. Chemotherapy was instituted. Follow-up MRI performed one year later showed tumour growth, a nodule in the lateral wall of the surgical cavity, as well as multiple Gd-positive foci in the left frontal lobe and one in the right anterior parasagittal region, with a difficult differential diagnosis between gliosis and relapse (A).

PET–CT findings

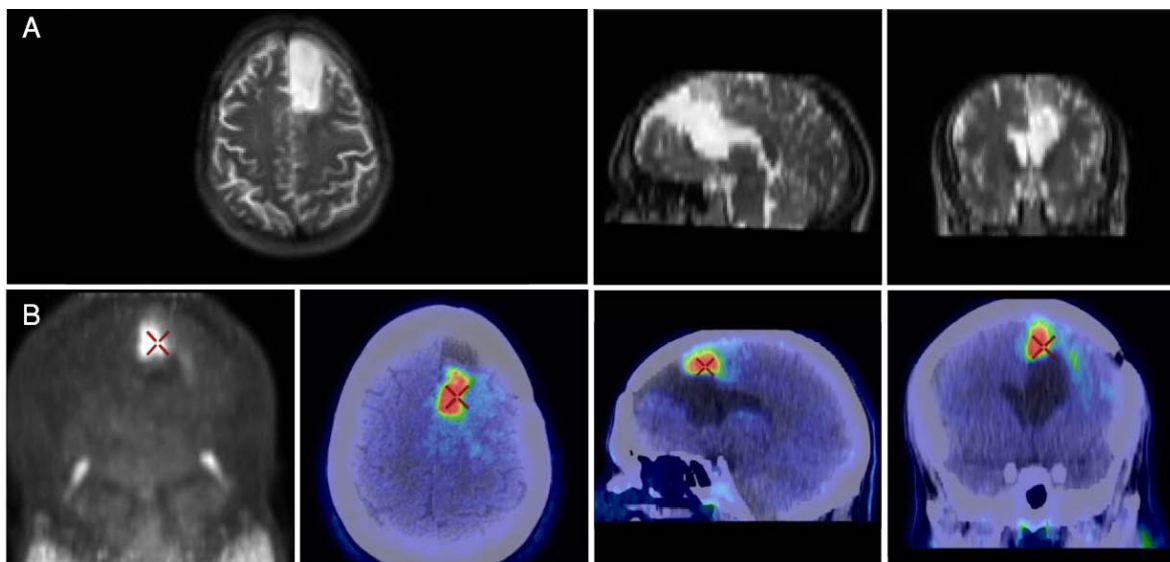
(A): MRI images of brain, three planes; (B): MIP and fused images, three planes.

There is intense ^{11}C -methionine uptake in the left frontal lobe consistent with tumour relapse, extending into the adjacent white matter. There is no evidence of tumour activity in the right hemisphere.

Teaching point

^{11}C -methionine imaging plays a complementary role in patients with brain tumours and indeterminate MRI results, allowing early differentiation between recurrence and radionecrosis.

Keywords: Oligoastrocytoma, relapse, gliosis, ^{11}C -methionine



Clinical indication for PET–CT: Astrocytoma grade III, suspected relapse

Clinical history

Patient with left frontal astrocytoma grade III had undergone surgery followed by RT. Follow-up MRI raised the suspicion of relapse.

PET–CT findings

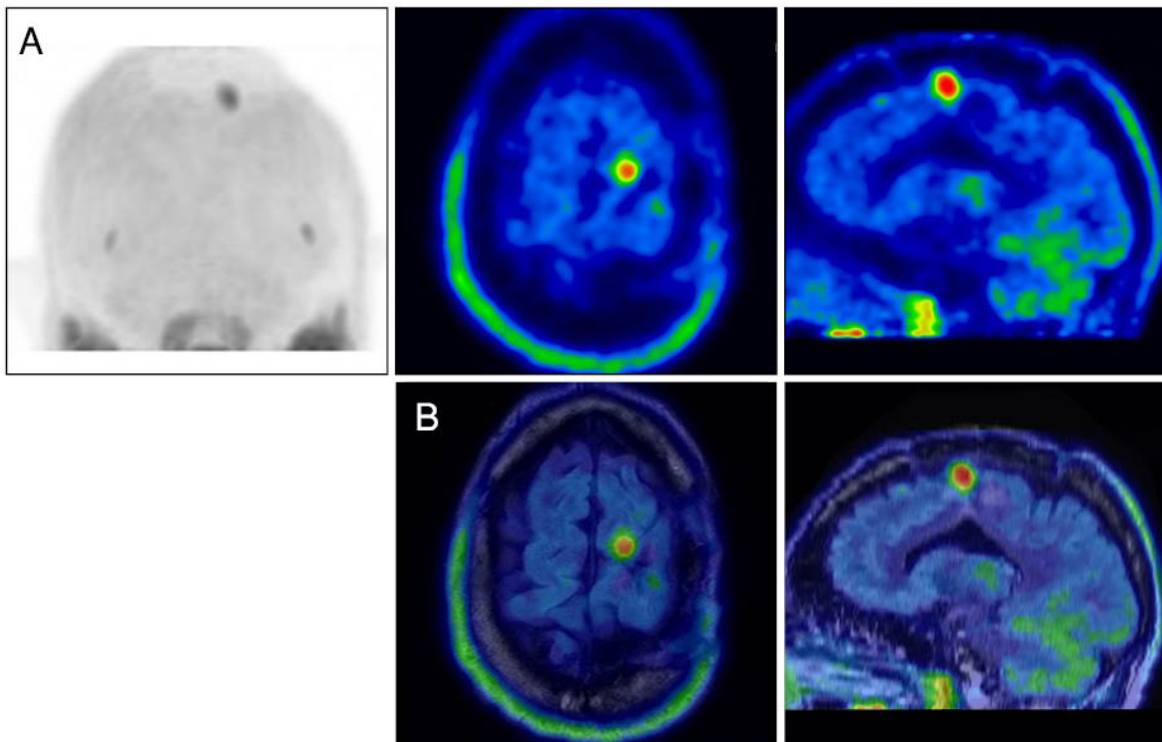
(A): MIP, and transaxial and sagittal PET slices; (B): fused PET–MRI in same planes.

There is increased tracer uptake in the left fronto-parietal region, consistent with relapse of the tumour in the lesion seen on MRI.

Teaching point

¹¹C-methionine imaging can discriminate, with good accuracy, between the presence of relapse and post-surgical or radiation changes.

Keywords: Astrocytoma, relapse, RT, ¹¹C-methionine



Clinical indication for PET–CT: Astrocytoma, suspected relapse

Clinical history

Patient with left frontal astrocytoma grade III had undergone surgery followed by RT. Follow-up MRI findings could not discriminate between relapse and post-RT changes (A).

PET–CT findings

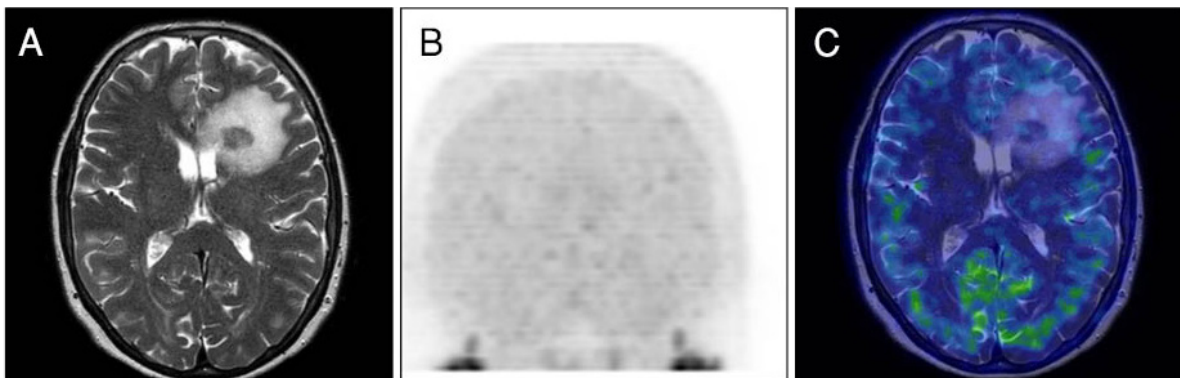
(A): MRI transaxial slice of brain; (B): MIP; (C): fused PET–MRI transaxial slice.

There are no areas of increased tracer uptake in the left frontal lobe, thus there is no evidence for tumour relapse.

Teaching point

¹¹C-methionine imaging can discriminate with good accuracy between the presence of relapse and post-surgical or radiation changes.

Keywords: Astrocytoma, RT, ¹¹C-methionine



Clinical indication for PET–CT: Glioblastoma grade II, post-operative assessment

Clinical history

A 25 year old female had undergone surgery with macroscopically complete resection of right frontal glioblastoma. MRI T2-FLAIR shows heterogeneous hyperintensity (A) and T1 using Gd showed peripheral contrast enhancement surrounding the surgical bed. The patient is referred to differentiate surgical changes from residual tumour.

PET-CT findings

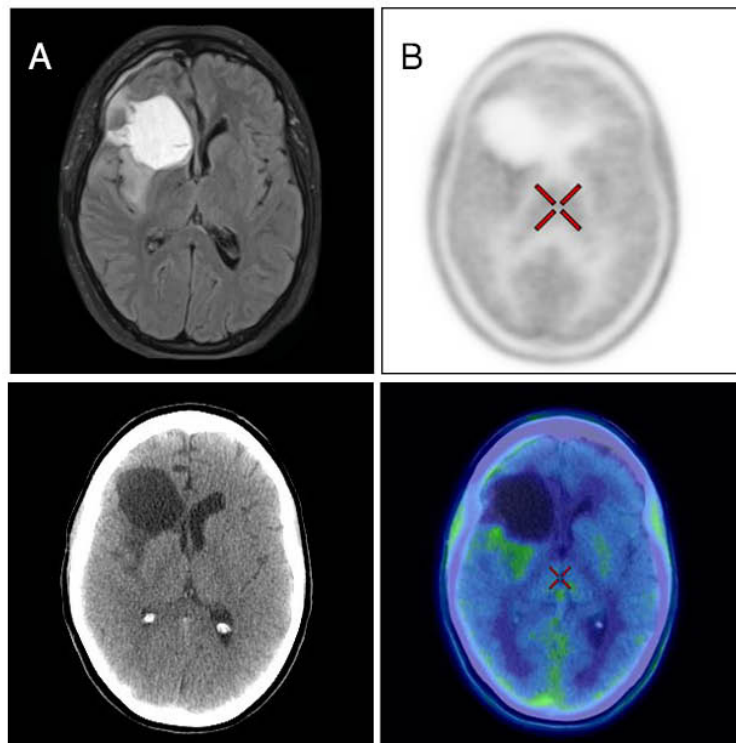
(A): MRI transaxial slice of brain; (B): PET, fused and CT transaxial slices.

There is low intensity peripheral tracer uptake at the posterior aspect of the surgical field, consistent with post-operative inflammatory reaction.

Teaching points

Reactive gliosis and inflammatory changes may show uptake of ¹¹C-methionine, due to the active tracer transport into inflammatory cells, and to the alteration of the blood–brain barrier.

Keywords: Glioblastoma, surgery, reactive gliosis, ¹¹C-methionine



Clinical indications for PET-CT: Suspected PTA, incidental finding

Clinical history

A 72 year old female with multinodular goitre, HPT and hypercalcaemia, had a negative ^{99m}Tc-sestaMIBI scintigraphy.

PET-CT findings

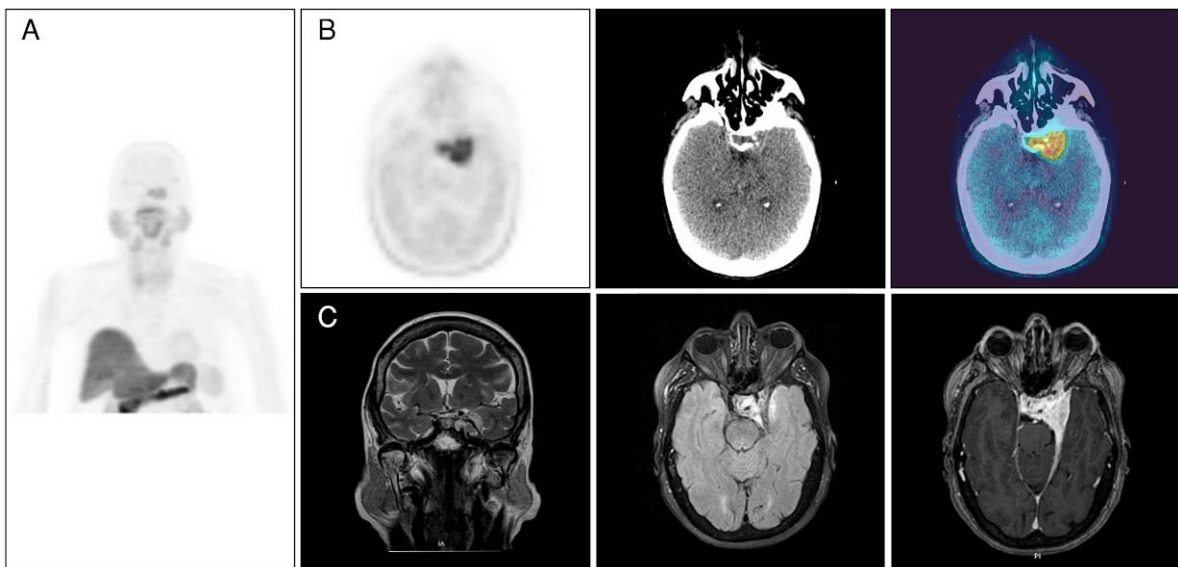
(A): MIP; (B): PET, CT and fused transaxial slices of head; (C): MRI coronal and transaxial slices.

There is a focus of abnormal tracer activity in the left base of the skull extending into the adjacent bone, consistent with a meningioma. MRI (C) confirmed the diagnosis.

Teaching point

Meningioma, the most common primary brain tumour, demonstrates uptake of ¹¹C-methionine; this is higher in intensity in large lesions and in those located at the base of the skull. The degree of uptake does not correlate with tumour aggressiveness.

Keywords: Meningioma, incidental finding, ¹¹C-methionine



Clinical indication for PET–CT: Primary HPT

Clinical history

A 74 year old female patient with a history of chronic renal failure and multinodular goitre presented with serum PTH of 68 pg/mL. ^{99m}Tc-sestaMIBI scan showed a multinodular goitre extending into the thorax, with moderately increased uptake in a nodule in the left thyroid lobe and no evidence of hyperfunctioning parathyroid tissue. The patient was referred to localize hyperfunctioning parathyroid tissue.

PET–CT findings

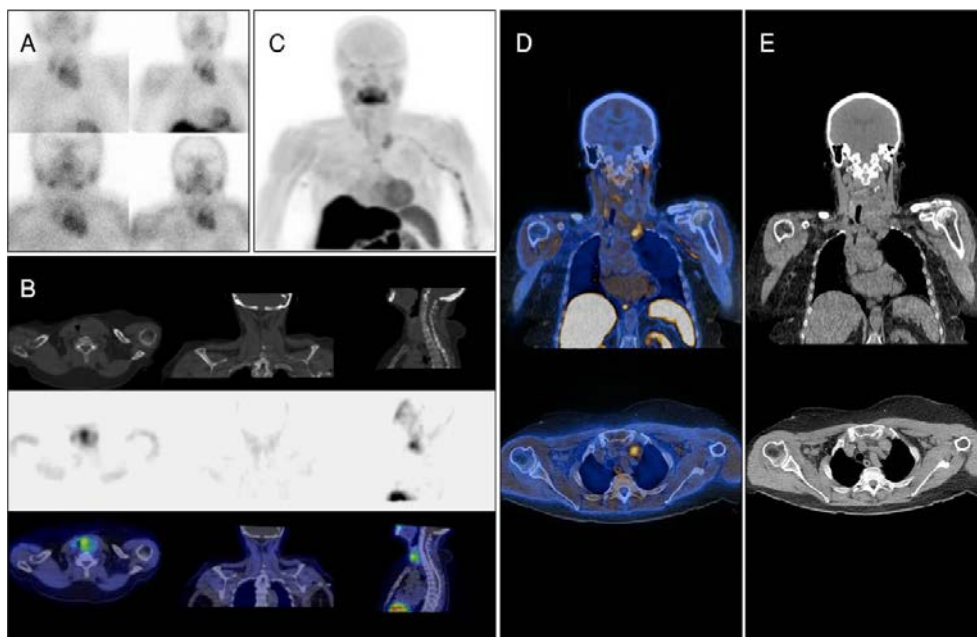
(A): ^{99m}Tc-sestaMIBI planar images of thorax, 10 min and 2 hours after the injection; (B): CT, ^{99m}Tc-sestaMIBI SPECT and SPECT–CT images of thorax; (C): ¹¹C-methionine PET MIP; (D): ¹¹C-methionine PET–CT fused coronal and transaxial slices; (E): CT coronal and transaxial slices.

The study revealed a multinodular goitre with a large mass in the left lobe, displacing the trachea to the right. In the lower, anterolateral aspect of this mass, there is focal ¹¹C-methionine uptake in a nodule without a clear plane of cleavage with the thyroid, suggesting a left PTA. Left thyroid lobectomy confirmed an intrathyroidal PTA.

Teaching point

¹¹C-methionine PET–CT can diagnose and precisely localize PTA in the majority of patients with primary HPT, including those with negative contrast US and ^{99m}Tc-sestaMIBI SPECT.

Keywords: HPT, intrathyroidal PTA, ¹¹C-methionine



Clinical indication for PET–CT: Parathyroid cancer, suspected relapse

Clinical history

A 23 year old female patient with parathyroid cancer resected 3 years earlier presented with rising PTH levels and hypercalcaemia. ^{99m}Tc -sestaMIBI scintigraphy was negative. US showed an undetermined nodule adjacent to the trachea.

PET–CT findings

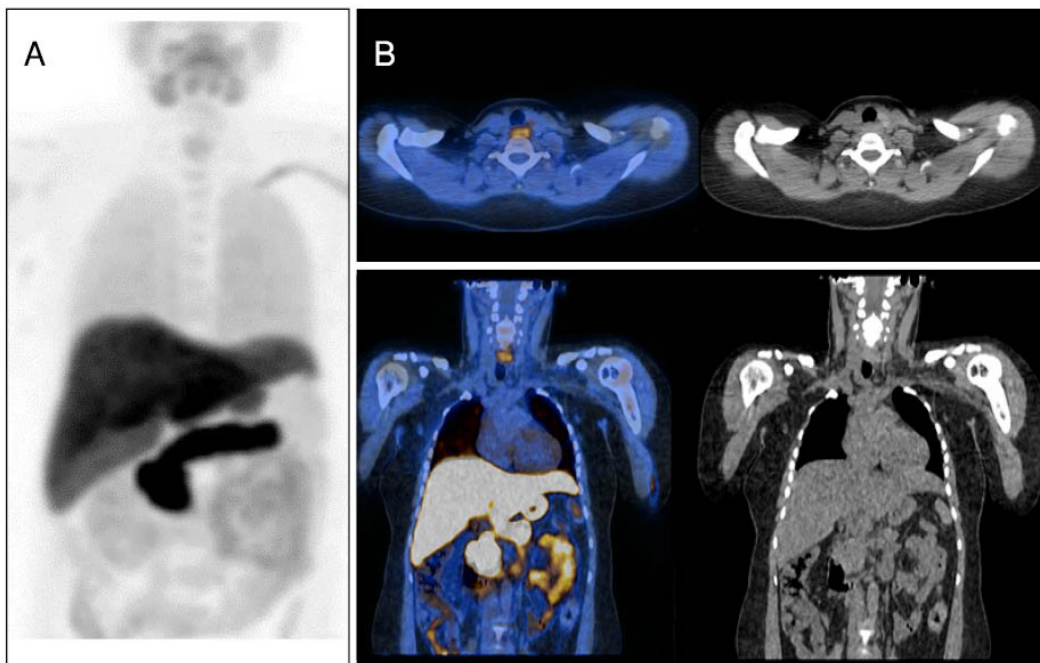
(A): MIP; (B): fused and CT transaxial and coronal slices of neck and chest.

There is increased tracer uptake in the lower neck, adjacent to, and behind the trachea, suggesting hyperfunctioning parathyroid tissue due to cancer relapse. Surgery confirmed the diagnosis.

Teaching point

^{11}C -methionine PET–CT is a complementary imaging technique that can help localize PTA or parathyroid carcinoma in patients with negative ^{99m}Tc -sestaMIBI studies.

Keywords: Parathyroid cancer, ^{11}C -methionine



Clinical indication for PET–CT: Localization of a PTH producing lesion

Clinical history

A 70 year old man presented with elevated serum Ca (3.2 mmol/L) and PTH (40 pmol/L), and osteoporosis. A PTA was suspected. Pre-operative imaging for localization of the adenoma showed a right side paratracheal mass, 2 cm on US and 4 × 4 cm, with cystic appearance, on CT. Fine needle cytology from this lesion showed no malignant cells. There was no tracer uptake on an ¹⁸F-FDG PET–CT study. A dual phase ^{99m}Tc-sestaMIBI scan showed increased uptake on the medial side of the right lower thyroid pole. ¹¹C-methionine PET–CT was requested for definitive localization of a PTH producing lesion.

PET–CT findings

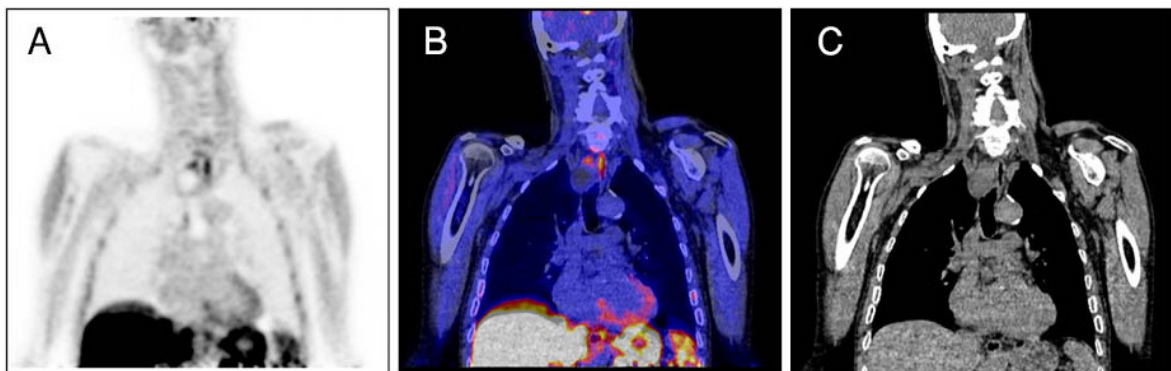
(A): PET coronal slice of thorax; (B): fused slice; (C): CT slice.

There is increased tracer uptake in the upper mediastinum, on the medial superior border of a cystic lesion, on the right side of the trachea. Surgery consisted of extirpation en bloc, with hemithyroidectomy and LND of the central compartment on the right side. Pathology examination revealed a pT3N0 parathyroid carcinoma.

Teaching point

¹¹C-methionine PET–CT cannot distinguish between benign and malignant parathyroid lesions. Because primary HPT is far more frequently caused by a hyperfunctioning benign PTA, diagnosis of parathyroid carcinoma is made, as a rule, only after tissue sampling, in this case at surgery.

Keywords: Parathyroid carcinoma, surgery, ¹¹C-methionine



Clinical indication for PET–CT: Adenoid cystic carcinoma of the submandibular gland, staging

Clinical history

Patient with a newly diagnosed adenoid cystic carcinoma of the right submandibular gland was referred for presurgical staging.

PET–CT findings

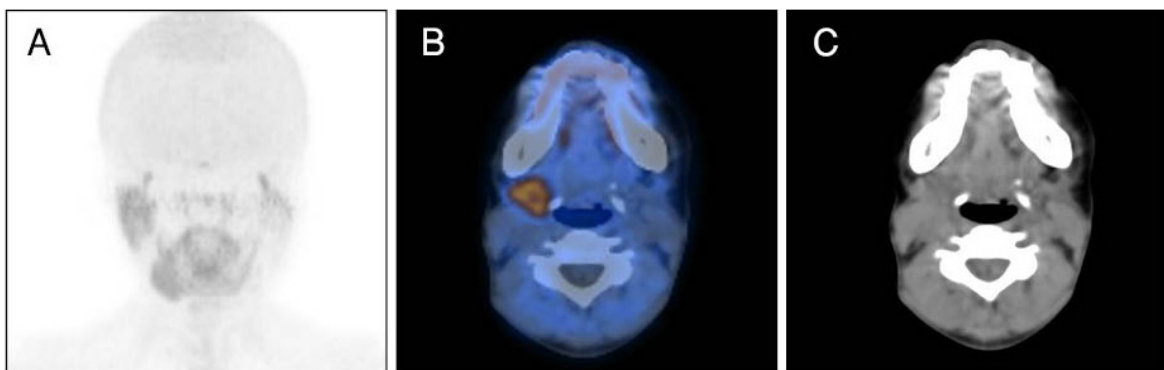
(A): MIP; (B): fused transaxial slice of salivary glands; (C): CT slice.

There is increased tracer uptake in the right submandibular gland, with no significant activity in LNs.

Teaching point

¹¹C-methionine PET–CT is performed prior to proton therapy to exclude the presence of LN metastases.

Keywords: Adenoid cystic carcinoma, staging, RT planning, ¹¹C-methionine



Clinical indication for PET–CT: Parathyroid cancer, suspected relapse

Clinical history

A 54 year old patient with previous history of testicular cancer, epidermoid scalp carcinoma and parathyroid carcinoma with capsular invasion, post-parathyroidectomy, was referred for follow-up in view of a negative ^{99m}Tc -sestaMIBI scintigraphy.

PET–CT findings

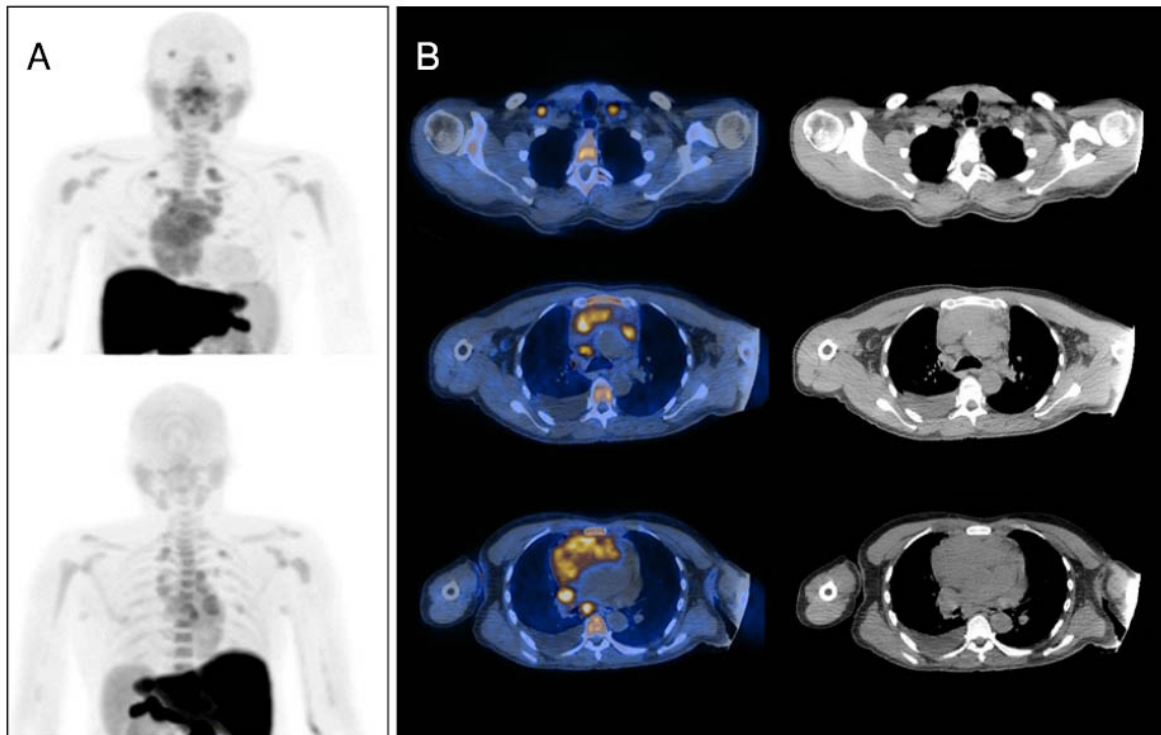
(A): MIP; (B): fused transaxial and coronal slices of thorax; (C): CT, same slices as in (B).

There is intense tracer uptake in a large mass involving the mediastinum, as well as in cervical, supraclavicular and mediastinal LNs. Biopsy from supraclavicular LNs indicated Hodgkin lymphoma.

Teaching point

Lymphoma can be ^{11}C -methionine avid.

Keywords: Parathyroid cancer, lymphoma, ^{11}C -methionine



17. SODIUM FLUORIDE, NaF (^{18}F)

17.1. GENERAL CHARACTERISTICS

Name: ^{18}F -sodium fluoride (^{18}F -NaF)

Synonyms: Na^{18}F , F-18 NaF

Radioisotope

^{18}F is a short half-life PET radioisotope (109.7 min) emitting positrons of E_{max} 1.656 MeV. Owing to the high chemical stability of C–F bond in organic compounds as well as the high water solubility of F compounds, ^{18}F tracers usually show suitable stability and biodistribution in humans. Although the F chemistry is complicated, the vast application of ^{18}F labelled compounds in nuclear medicine has led to development of efficient automated radiopharmaceutical production methods allowing large scale production of ^{18}F tracers for clinical use.

Radiosynthesis

After proton bombardment of ^{18}O water in commercial cyclotrons for production of various ^{18}F radiopharmaceuticals, elution of the ^{18}F adsorbing membrane using normal saline yields high quantities of ^{18}F -NaF (Fig. 17.1).

17.2. PHARMACOKINETICS

17.2.1. Physiological biodistribution and metabolism

Fluoride ions are deposited in the bone matrix and reflect both bone remodelling and blood flow. The uptake of fluoride ions is higher in osteoblastic processes, while purely osteolytic lesions have lower uptake, or none at all. The target organ is the bone, but approximately 20% is excreted through



FIG. 17.1. Normal biodistribution of ^{18}F -NaF: MIP in antero-posterior and lateral views.

the kidney in the urine in the first 1–2 hours. While overall the biodistribution is similar to that of ^{99m}Tc -diphosphonates, skeletal uptake of ^{18}F -NaF is twice as high as compared with ^{99m}Tc labelled compounds. Blood clearance of ^{18}F -NaF is faster and the bone to background ratio of ^{18}F -fluoride is much higher (Fig. 17.2) [127, 128].

17.2.2. Mechanism of retention

After IV injection, ^{18}F -NaF rapidly equilibrates within the extracellular fluid space and fluorine is extracted and incorporated into hydroxyapatite crystals. First-pass extraction from bone capillaries is about 100%. Approximately 20% is then rapidly excreted in the urine and only 10% remains in the blood in patients with normal kidney function [127, 128].

17.2.3. Pharmacology and toxicology

No pharmacological and toxicological effects have been reported, owing to low tracer concentration and availability of ^{18}F in carrier-added form. Furthermore, as the injected dose of NaF is very low, there are no pharmacological concerns.

17.3. METHODOLOGY

17.3.1. Activity, administration, dosimetry

^{18}F -NaF is administered as an IV bolus, typically in an activity of 185–370 MBq (5–10 mCi). Paediatric activity is weight based: 2.1 MBq/kg (0.06 mCi/kg). The dose critical organ in adults is the urinary bladder, which receives 0.22 mGy/MBq (0.81 rad/mCi). The effective dose for adults is estimated at 0.024 mSv/MBq (0.089 rem/mCi) [127, 128].

17.3.2. Imaging protocol

Patient preparation does not require any special diet, however good hydration is important. Imaging is performed after the IV administration of 50–200 MBq and an uptake period of 20–60 min. The urinary bladder should be emptied just before scanning. Acquisition of the PET component includes a true whole body study with 2–3 min/bed position. For the CT imaging protocol, see general comments in Section 1.3.

17.4. CLINICAL ASPECTS

17.4.1. Indications

Clinical indications are the same as for ^{99m}Tc labelled diphosphonate bone scintigraphy. PET–CT is more sensitive than bone scintigraphy, including SPECT, for most indications for which side by side comparisons have been performed. The choice of PET or SPECT depends on the availability of the radiopharmaceutical and PET–CT devices, and costs.

17.4.2. Cases

17.4.2.1. Case No. 17.1

Clinical indication for PET–CT: Prostate cancer, staging

Clinical history

A 64 year old man with newly diagnosed prostate cancer was referred for staging.

PET–CT findings

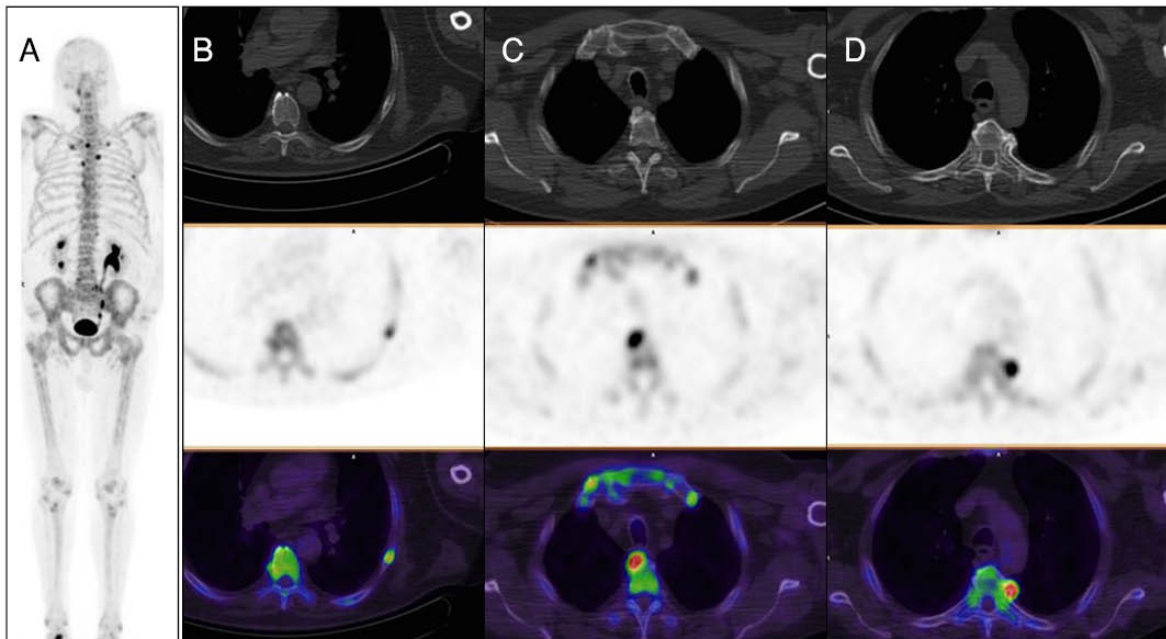
(A): MIP; (B–D): CT, PET and fused transaxial slices at various levels of the thorax.

There are foci of increased tracer uptake in an osteoblastic bone metastasis in the sixth left rib (B) and in degenerative changes and osteophytes in thoracic vertebrae (C, D).

Teaching point

Bone remodelling is seen with high contrast in both malignant and non-malignant skeletal lesions. ^{18}F -NaF may be used as a substitute for bone scintigraphy.

Keywords: Prostate cancer, metastasis, ^{18}F -NaF



Clinical indication for PET–CT: Breast cancer, staging

Clinical history

A 60 year old woman with newly diagnosed breast cancer (ductal adenocarcinoma, ER+, progesterone receptor positive (PR+), HER2–), and positive sentinel LNs, was referred for staging.

PET–CT findings

(A): MIP; (B): CT, PET and fused transaxial slices of upper chest; (C): follow-up ^{99m}Tc-MDP bone scan.

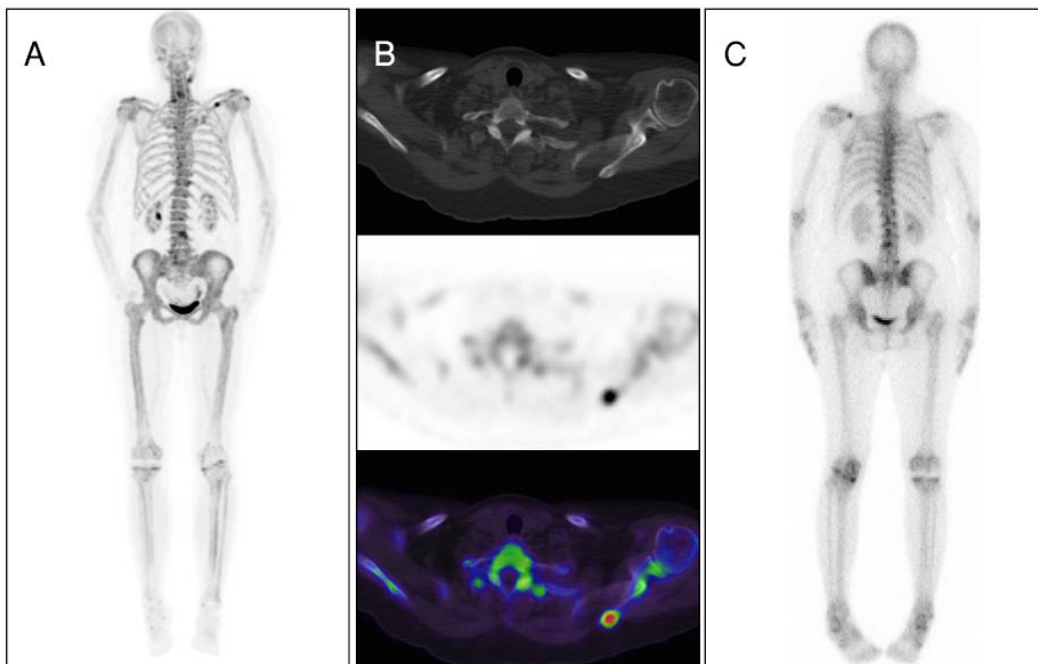
There is a single focus of increased tracer activity in the spine of the left scapula, with no corresponding abnormality on CT. The patient was on tamoxifen and no further changes to the treatment protocol were made.

Follow-up: ^{99m}Tc-MDP bone scan performed 5 years later showed no change (C).

Teaching point

Solitary bone metastases are infrequent. In spite of the fact that bone SPECT or PET studies can detect bone metastases early, reporting such solitary lesions in the absence of corresponding CT abnormalities should be done with caution.

Keywords: Breast cancer, single bone lesion, ¹⁸F-NaF



Clinical indication for PET–CT: Breast cancer, staging

Clinical history

A 55 year old woman with newly diagnosed breast cancer (ductal adenocarcinoma, ER+, PR+, HER2–).

PET–CT findings

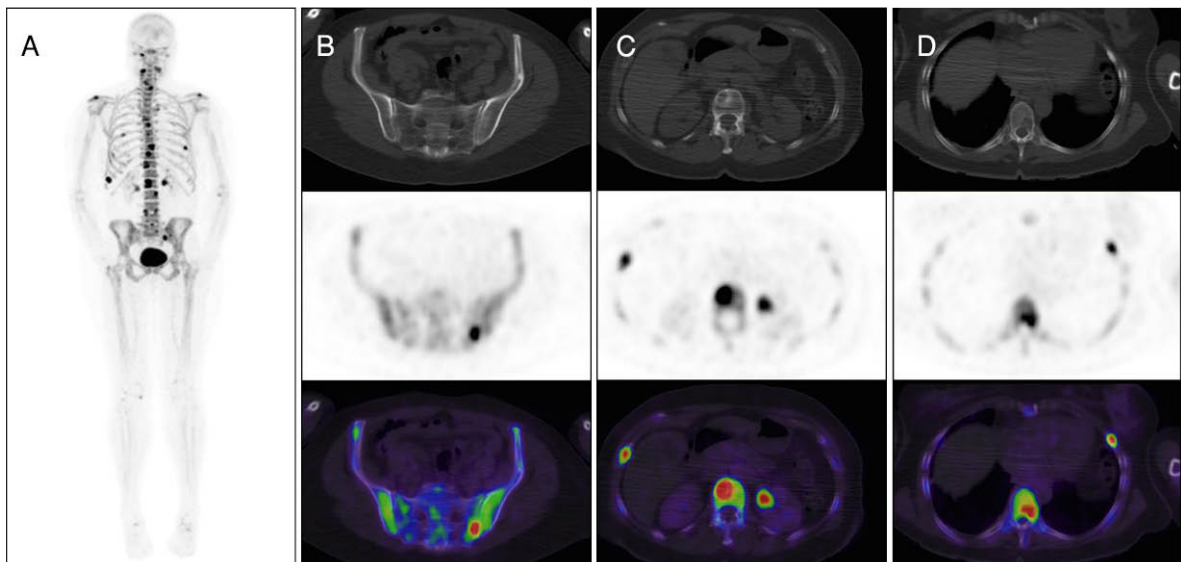
(A): MIP; (B): CT, PET, and fused transaxial slices of pelvis; (C, D): CT, PET, and fused transaxial slices of chest.

There are multiple foci of increased tracer uptake, consistent with disseminated bone metastases. Note the heterogeneity of the CT patterns: some lesions are osteolytic (B), others are sclerotic (C) or do not show any CT abnormality (D).

Teaching point

The sensitivity of ^{18}F -NaF PET–CT is higher for sclerotic metastases, but increased tracer uptake may be seen in lytic lesions as well.

Keywords: Breast cancer, bone metastases, ^{18}F -NaF



Clinical indication for PET–CT: Recurrent breast cancer, treatment response

Clinical history

A 44 year old woman with breast cancer presented with diffuse skeletal pain.

PET–CT findings

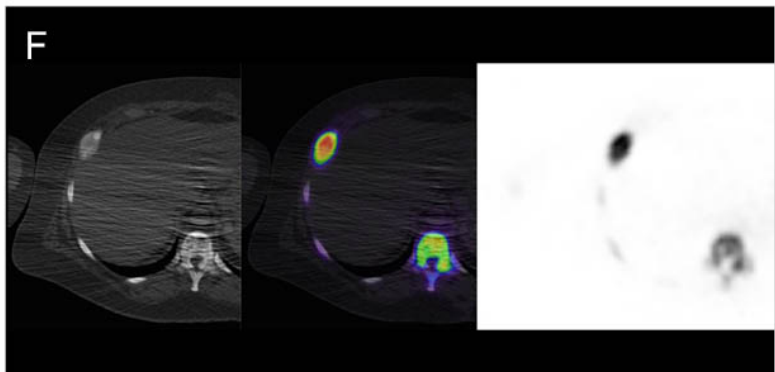
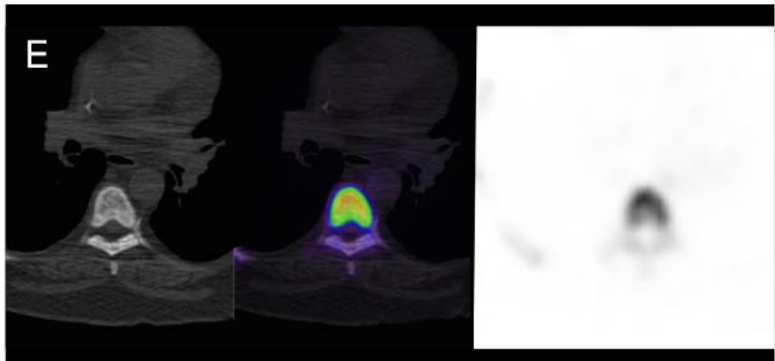
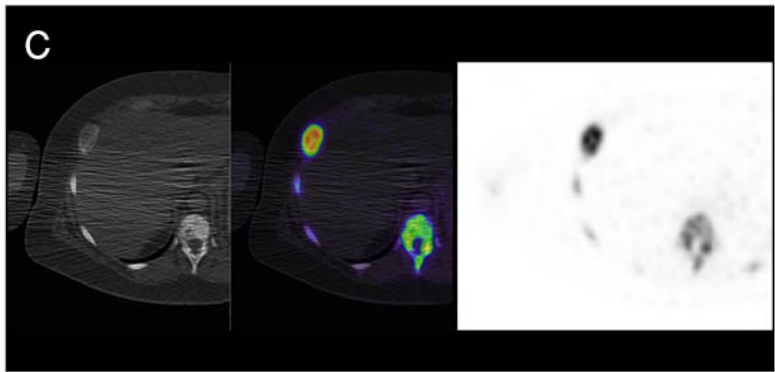
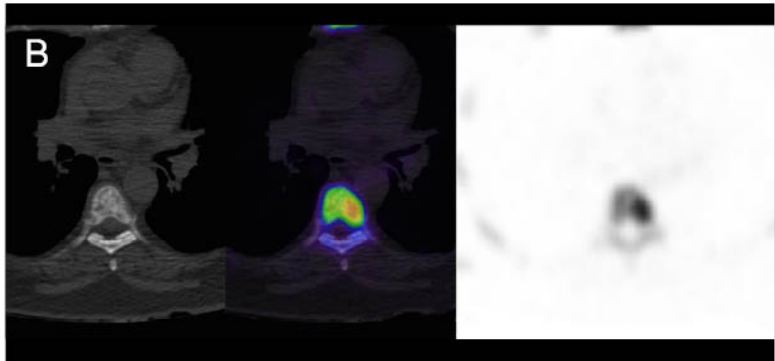
(A–C): images before treatment. (A): MIP; (B): CT, fused and PET transaxial slices of mid-thorax; (C): CT, fused and PET transaxial slices of lower thorax. (D–F): similar images after treatment.

Before treatment there are multiple foci of increased tracer uptake, consistent with disseminated metastatic bone involvement (A). After 5 months of chemotherapy, ^{18}F -NaF uptake becomes more homogeneous (D). While some foci in the thoracic spine are no longer seen (B, E), the overall result remains unchanged on PET, while CT demonstrates increasingly sclerotic lesions (C, F).

Teaching point

In many cases, response of bone metastases to treatment can be only indirectly assessed by ^{18}F -NaF PET, in combination with analysis of the CT patterns of lesions.

Keywords: Breast cancer, bone metastases, response to chemotherapy, ^{18}F -NaF



Clinical indication for PET–CT: Recurrent breast cancer

Clinical history

A 78 year old woman with a history of breast cancer, 17 years earlier, presented with pain in her left hip. CT showed a lytic lesion in the left ilium.

PET–CT findings

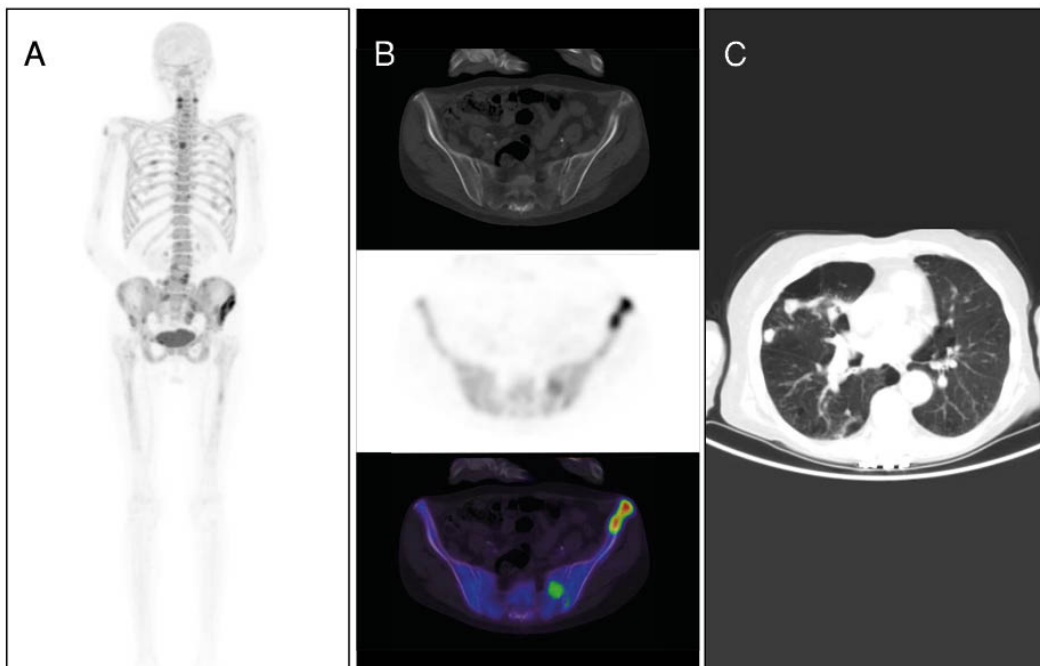
(A): MIP; (B): CT, PET and fused transaxial slices of pelvis; (C): CT transaxial slice of thorax.

There is a focus of intense increased activity in the lytic lesion in the left ilium. Additional tracer-avid lesions are seen in both the axial and appendicular skeleton, consistent with disseminated bone metastases. Low dose CT also shows multiple lung metastases (C).

Teaching point

Whole body ^{18}F -NaF PET is highly sensitive for bone metastases. The component may provide additional relevant information.

Keywords: Breast cancer, bone and lung metastases, ^{18}F -NaF



Clinical indication for PET–CT: Multiple myeloma

Clinical history

A 65 year old woman with newly diagnosed myeloma.

PET–CT findings

(A): MIP; (B, C, D): CT, fused and PET transaxial slices of cervical, dorsal and lumbar spine, respectively; (E): CT, PET and fused coronal and transaxial slices of femur; (F): CT transaxial slice of thorax; (G): follow-up ^{18}F -FDG PET–CT image.

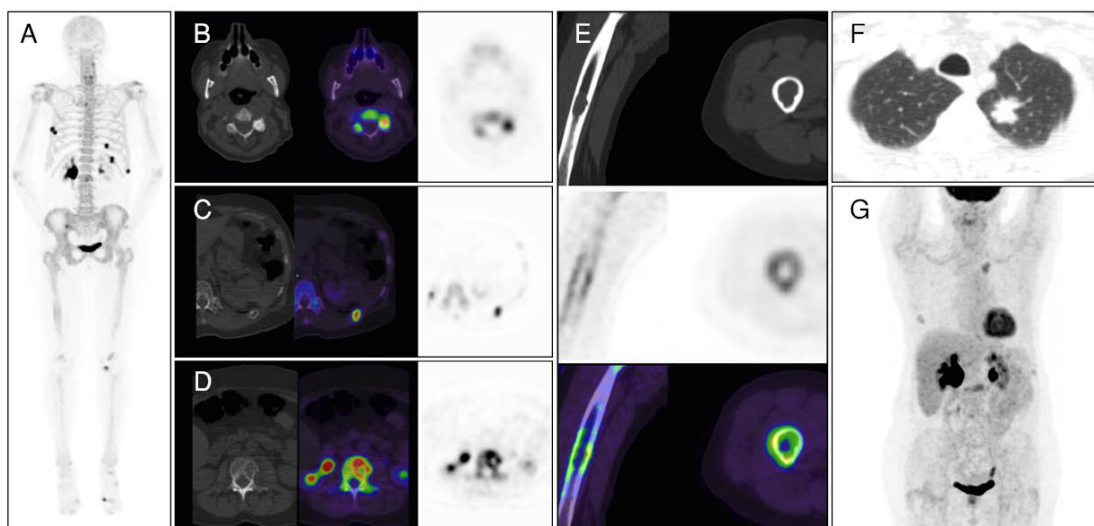
There are multiple foci of increased tracer uptake corresponding to osteolytic lesions in lumbar vertebrae and ribs as well as to degenerative changes in the cervical spine (C, D). Mildly increased uptake bordering bone marrow infiltration is seen in the right femur (E). In addition, low dose CT shows a spiculated lung nodule in the left upper lobe (F).

Follow-up: ^{18}F -FDG PET–CT (G) was positive for the lung nodule, which was shown to be adenocarcinoma, and some of the bone lesions.

Teaching point

The use of ^{18}F -NaF is not normally advised for this indication, however the exam is frequently informative in multiple myeloma. Indeed, ^{18}F -NaF lacks specificity but the concomitant CT findings improve the positive predictive value. The CT component can provide additional relevant information.

Keywords: Breast cancer, multiple myeloma, osteolytic lesion, ^{18}F -NaF



Clinical indication for PET–CT: Breast cancer, restaging

Clinical history

A 72 year old woman with infiltrating ductal breast cancer (ER+, PR–, HER2–) complained of diffuse bone pain. ^{99m}Tc-MDP bone scintigraphy showed no evidence of bone metastases.

PET–CT findings

(A): ^{99m}Tc-MDP bone scintigraphy (anterior view); (B): ¹⁸F-NaF MIP; (C): MRI (coronal, T2 weighted) of the pelvic region.

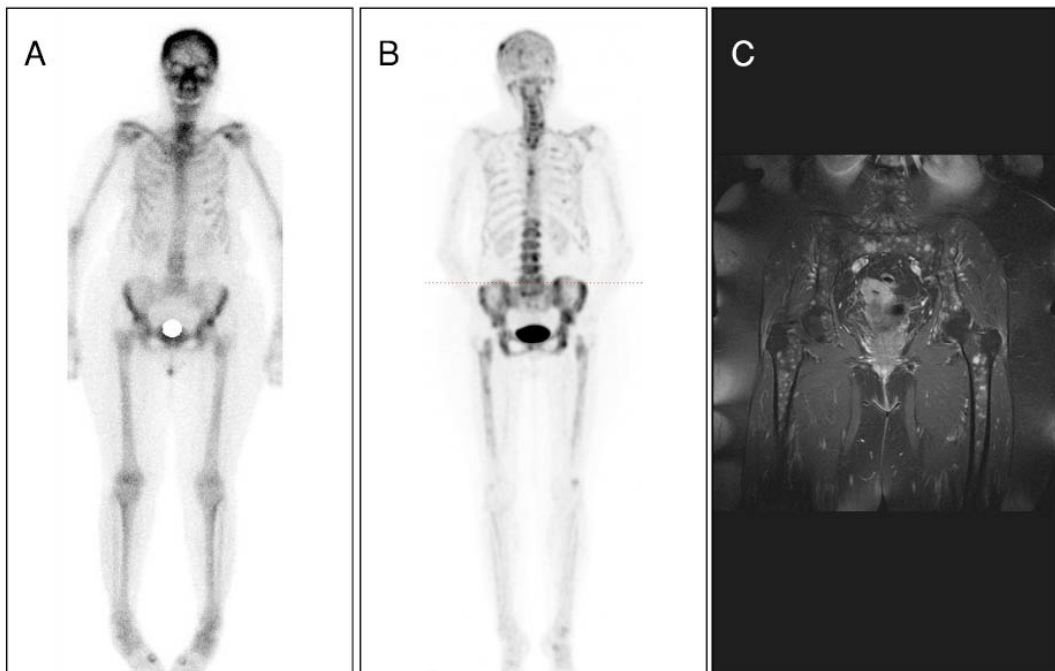
MIP shows highly heterogeneous tracer uptake in the skull, spine, pelvic grid and femurs, consistent with metastatic bone marrow involvement (B).

Follow-up: MRI confirmed the presence of multiple small metastases (C).

Teaching point

¹⁸F-NaF is more sensitive than planar bone scintigraphy.

Keywords: Breast cancer, small bone metastases, ¹⁸F-NaF



18. SODIUM IODIDE, NaI (^{124}I)

18.1. GENERAL CHARACTERISTICS

Name: I-124 sodium iodide ($^{124}\text{I-NaI}$)

Synonyms: I-124 NaI

Radioisotope

^{124}I is a long half-life PET radioisotope (4.18 days) emitting positrons of E_{max} 2.138 MeV and 1.535 MeV, usually obtained from biomedical cyclotrons via proton irradiation of ^{124}Te .

Radiosynthesis

There are various methods of ^{124}I production. The $^{124}\text{Te}(p, n)$ reaction gives the purest form of ^{124}I using 9–14 MeV protons. Enriched ^{124}Te is irradiated followed by thermodistillation with high recovery yield. No-carrier-added iodide is collected in the form of $^{124}\text{I-NaI}$ in NaOH solution (pH of 8.5) [129, 130].

18.2. PHARMACOKINETICS

18.2.1. Physiological biodistribution and metabolism

Apart from thyroid tissue, physiological uptake of radioiodine also occurs in a variety of tissues with functional sodium iodide symporter expression, including salivary and lacrimal glands, stomach, choroid plexus, ciliary body of the eye, skin, placenta, lactating mammary gland and thymus, and, to a lesser extent, the prostate, ovary, adrenal gland, lungs and heart. The liver is the major organ metabolizing radioiodinated thyroglobulin released from functioning thyroid tissues. Retention of radioiodine can occur as a result of structural or functional changes in any part of the body located along the route of radiotracer excretion or blood pooling [129, 130]. $^{124}\text{I-NaI}$ imaging performed at 1 hour after tracer administration shows uptake in the oesophagus and stomach (Fig. 18.1(A)), decreasing in intensity on images acquired at 24 hours (Fig. 18.1(B)).

After retention of iodine in the thyroid, a coupling reaction leads to synthesis of T4 and T3 hormones catalysed by thyroid peroxidase followed by storage inside the thyroid follicles. The proteases solve the follicles and T4 and T3 are free to diffuse via the basal surface into the bloodstream mostly in protein bound forms. The physical half-life of radioiodine does not permit formation of hormones.

18.2.2. Mechanism of retention

Iodide is transported actively into the cells via the sodium iodide symporter at the basolateral membrane of thyrocytes, then enters the colloid on the apical membrane, located on the opposite side. In the colloid, iodide is oxidized and bound to thyroglobulin via the enzyme thyroid peroxidase. It then either remains in the colloid or exits the cell as the final product [129, 130].

18.2.3. Pharmacology and toxicology

No direct pharmacology or toxicology data are available for $^{124}\text{I-NaI}$. However, in this context, iodine is used at the tracer level, far from the level toxic for humans.

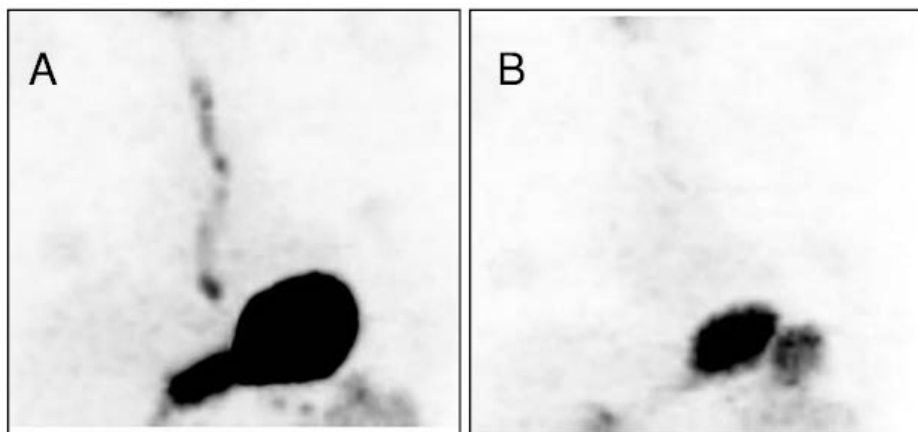


FIG. 18.1. Normal biodistribution of $^{124}\text{I-NaI}$ at 10 min and 2 h.

18.3. METHODOLOGY

18.3.1. Activity, administration, dosimetry

Before use, the solution is filtered using a membrane filter bacterial filter (0.22 μm) and diluted with sterile saline. Diagnostic ^{124}I imaging is performed after IV administration of 74 MBq of ^{124}I . The effective dose of ^{124}I depends on thyroid uptake: it is 0.095 mSv/MBq with a thyroid uptake of 0% (i.e. following thyroid ablation) and it increases to 1.5 mSv/MBq with a thyroid uptake of 35% (i.e. other patients). The total radiation exposure has been calculated at 7.0 mSv for a dose of 74 MBq ^{124}I . This radiation exposure due to ^{124}I is only a fraction of the total radiation exposure that results from the therapeutic use of ^{131}I (340 mSv for 5550 MBq) [131–134].

18.3.2. Imaging protocol

Patient preparation does not require any special diet. Imaging is performed with two time point acquisitions, at 1 and 24 hours after the administration of 1 MBq/kg. Acquisition of the PET component is from head to mid-thigh with 3–5 min/bed position. For the CT imaging protocol, see general comments in Section 1.3. For dosimetry purposes, sequential imaging is performed at five time points, at approximately 1–2, 24, 48, 72 and 96 hours after tracer administration [133].

18.4. CLINICAL ASPECTS

18.4.1. Indications

$^{124}\text{I-NaI}$ is available in only few centres worldwide. It may have some useful clinical applications in thyroid cancer. It may be an ideal tracer for dosimetry before personalized treatment with ^{131}I in patients with metastatic thyroid cancer [131]. The main advantage of $^{124}\text{I-NaI}$ is based on the better spatial resolution of PET compared to gamma camera imaging obtained with ^{131}I [133, 134]. $^{124}\text{I-NaI}$ PET–CT has a high sensitivity in the detection of small metastases in thyroid carcinoma. It is therefore superior to diagnostic ^{131}I planar whole body scintigraphy [133] and has a high prognostic value [132]. It could also potentially be useful in treatment planning in thyroid cancer.

18.4.2. Cases

18.4.2.1. Case No. 18.1

Clinical indication for PET–CT: Thyroid cancer, suspected recurrence

Clinical history

A 32 year old female with thyroid cancer and thyroglobulin levels at 38 ng/mL and increasing, scheduled for ^{131}I treatment.

PET–CT findings

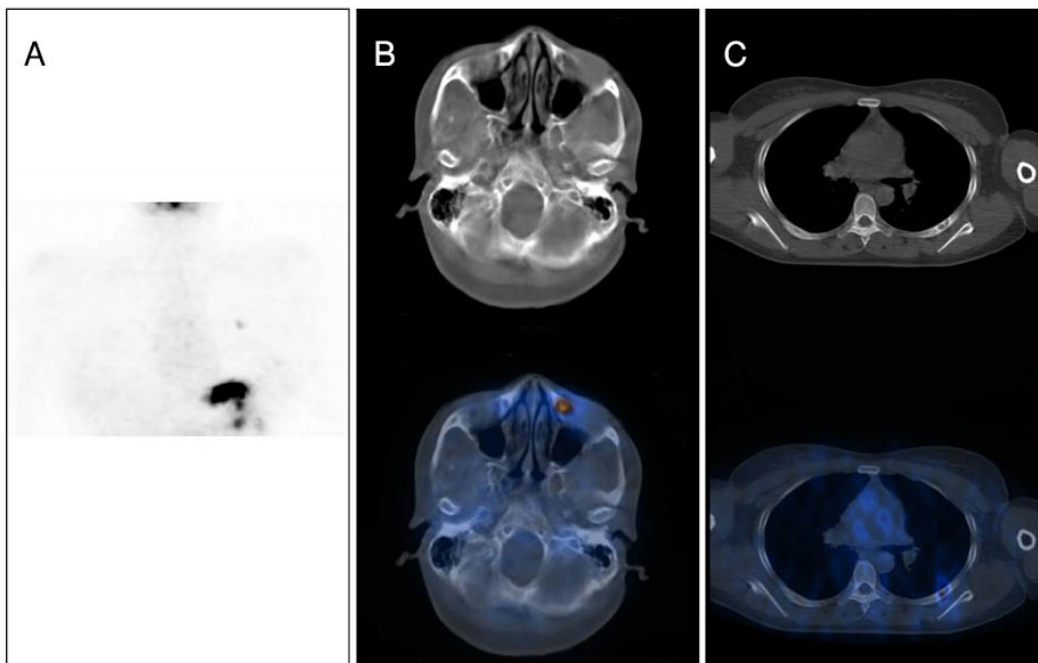
(A): MIP; (B): CT and fused transaxial slices of skull; (C): CT and fused transaxial slices of thorax.

At 24 hours there is increased focal uptake in two small lytic bone lesions in the left maxillary bone (B) and the left seventh rib (C).

Teaching point

^{124}I is very sensitive for detecting small metastatic lesions from thyroid cancer.

Keywords: Thyroid cancer, restaging, ^{124}I -Na



Clinical indication for PET–CT: Thyroid cancer, staging and risk stratification prior to thyroid ablation and PET based dosimetry for planning ^{131}I ablation

Clinical history

A 30 year old woman with T3mN1Mx papillary thyroid cancer, who presented initially with palpable nodules in the right thyroid lobe and right supraclavicular region, underwent total thyroidectomy and central LND followed by right lateral LND. PET–CT was performed 4 weeks after surgery, under thyroid-stimulating hormone stimulation with two image acquisitions at 24 and 96 hours.

PET–CT findings

(A): MIP; (B–D): fused transaxial slices at multiple levels of the neck; (E, F): ^{131}I whole body scintigraphy follow-up images.

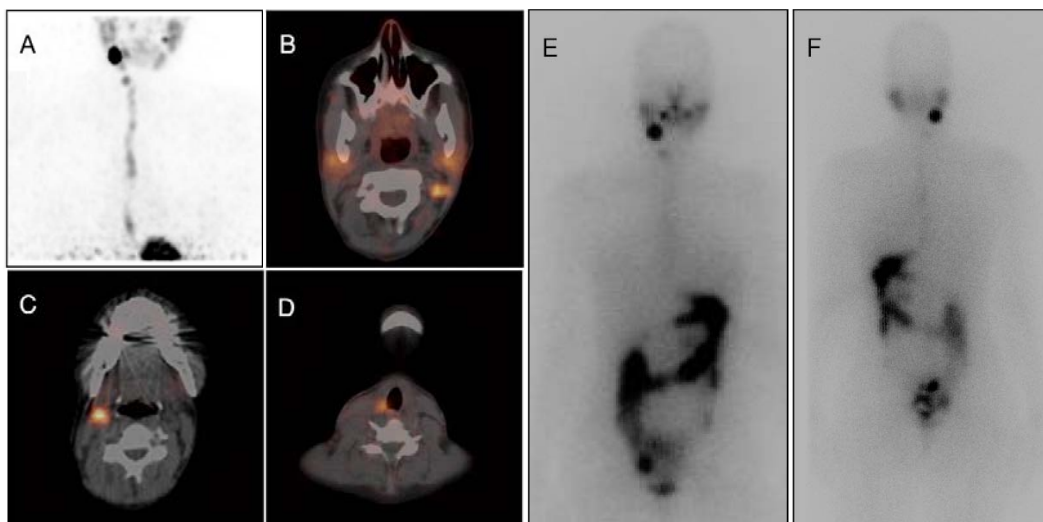
There is increased focal tracer uptake in one 8 mm right cervical level II LN, in three small left cervical level II LNs, and in right paratracheal remnant thyroid tissue.

Follow-up: The patient received a standard dose of 2775 MBq ^{131}I as ablation on the same day the 96 hour PET–CT study was performed. ^{131}I whole body scintigraphy was performed on days 1 and 9 after ablation (E, F) and shows focal uptake in the right jaw angle and the right side of the thyroid bed.

Teaching point

^{124}I PET–CT has a high sensitivity for detection of thyroid remnants and metastases in the pre-therapeutic workup in preparation for ^{131}I therapy. It can enable visualization of additional LNs, leading to better nodal staging, and thus guide management decisions on alternative treatment options [132, 135–144].

Keywords: Thyroid cancer, nodal metastases, ^{124}I -NaI



Clinical indication for PET–CT: Thyroid cancer, pre-ablative assessment and risk stratification and PET based dosimetry for planning ^{131}I ablation therapy

Clinical history

A 62 year old woman with T2N0Mx papillary thyroid cancer presented with a multinodular goitre and a cold nodule on ^{123}I thyroid scintigraphy. Fine needle aspiration of the cold nodule showed differentiated thyroid cancer. The patient underwent near total thyroidectomy. PET–CT was performed 3.5 weeks after surgery.

PET–CT findings

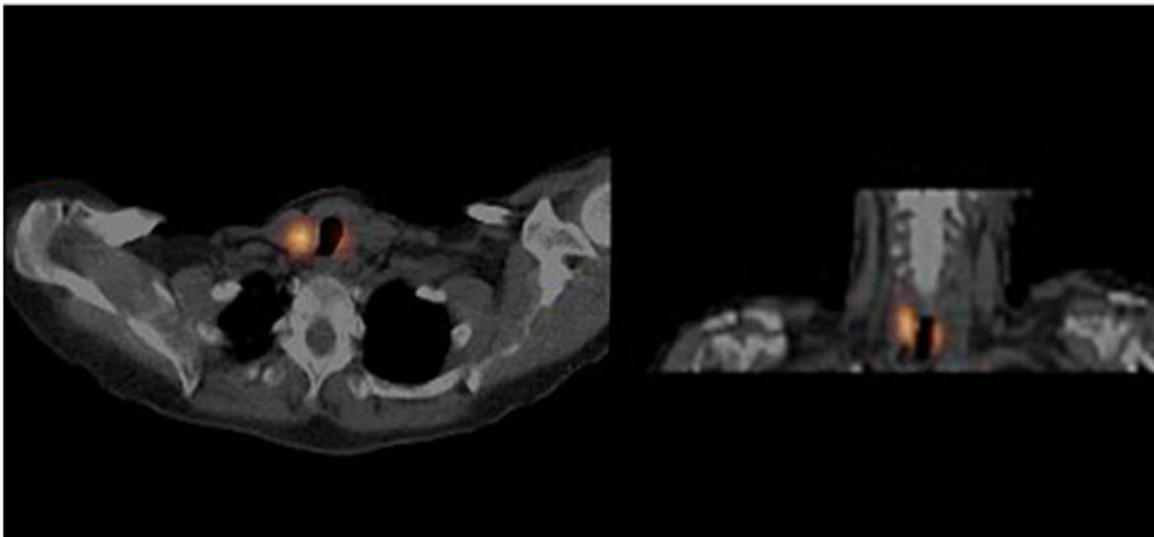
(Left): transaxial fused slices of neck; (right): coronal slices.

There is increased tracer uptake in bilateral paratracheal thyroid tissue remnants. Using a conventional thyroid formula, absorbed ^{131}I doses were calculated from the ^{124}I -NaI data (uptake at 24 and 96 hours, effective $T_{1/2}$ and lesion volumes). The absorbed doses were at least four times higher than the dose generally considered to be sufficient [132, 135–144].

Teaching point

^{124}I PET–CT provides more detailed diagnostic information than common diagnostic investigation and also offers dosimetry based personalized treatment of remnants.

Keywords: Thyroid cancer, pre-treatment dosimetry, ^{124}I -NaI



19. PSMA LIGAND (⁶⁸Ga)

19.1. GENERAL CHARACTERISTICS

Name: ⁶⁸Ga-PSMA-11

Synonyms: ⁶⁸Ga labelled Glu-NH-CO-NH-Lys(Ahx)-HBED-CC; ⁶⁸Ga labelled Glu-urea-Lys(Ahx)-HBED-CC; ⁶⁸Ga-PSMA ligand Glu-urea-Lys(Ahx)-HBED-CC; ⁶⁸Ga-PSMA ligand Glu-urea-Lys(Ahx)-HBED-CC; [⁶⁸Ga]prostate specific membrane antigen 11; ⁶⁸Ga-HBED-CC-PSMA; ⁶⁸Ga labelled Glu-NH-CO-NH-Lys(Ahx)-HBED-CC; gallium-68 PSMA ligand; Glu-urea-Lys(Ahx)-HBED-CC; PSMA-HBED-CC GA-68

Radioisotope

⁶⁸Ga is a short half-life PET radioisotope (67.7 min) emitting positrons of E_{\max} 1.9 MeV. It is usually obtained from a ⁶⁸Ge generator. The parent isotope ⁶⁸Ge has a half-life of 271 days and can be easily utilized for in-hospital production of generator produced ⁶⁸Ga.

Radiosynthesis

The tracer can be prepared using commercially available synthesizers (Fig. 19.1) and cassettes under good manufacturing practice conditions with radiochemical purity of 97.3% ± 0.7% (sum of two diastereomers) in 20 min and radiochemical yield of 87% ± 4% (decay corrected). The final formulated batches met all acceptance criteria prior to release for human use and were successfully evaluated in patients [145–149].

19.2. PHARMACOKINETICS

19.2.1. Physiological biodistribution and metabolism

In human subjects injected with ⁶⁸Ga-PSMA, intense uptake is noted in the lacrimal and salivary glands, as well as in the liver, spleen, jejunum and kidneys. Tracer activity can be found in vocal cords, pancreas, stomach, rectum, bone marrow and testes. Variable uptake is found in calcified choroid plexus, thyroid and adrenal nodules, axillary LNs and celiac ganglia, and occasional in osteophytes and gallbladder. There is almost no uptake in the brain (Fig. 19.2). ⁶⁸Ga-PSMA ligands are excreted foremost via the urinary system and collected in the urinary bladder. A small proportion is cleared through the hepatobiliary system [145–149]. No direct studies on the metabolites are available.

19.2.2. Mechanism of retention

PSMA, a tumour associated antigen and type II transmembrane protein, is expressed on the membrane of prostatic epithelial cells, and overexpressed on prostate tumour cells. Upon IV administration of ⁶⁸Ga-PSMA, the Glu-urea-Lys (Ahx) moiety targets and binds to PSMA expressing tumour cells. Upon internalization, PSMA expressing tumour cells can be detected during PET imaging [145–149].

19.2.3. Pharmacology and toxicology

No direct human toxicity studies are available. However, it was shown that for 86 µg PSMA-11 per kg body weight single dose administered IV in rats, acute toxicity was below the no-observed-adverse-effect level (NOAEL). Based on the referenced study, a safety factor of 1000 can be assumed for a

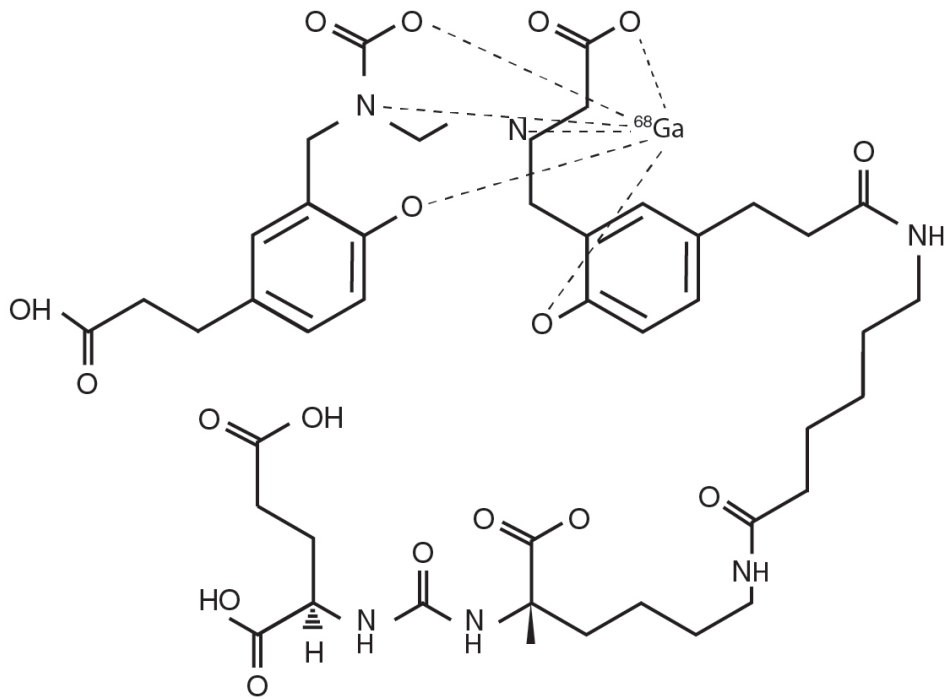


FIG. 19.1. Molecular structure of ^{68}Ga -PSMA.



FIG. 19.2. Normal biodistribution of ^{68}Ga -PSMA.

maximum human dose of PSMA-11 of 6.3 nmol or 6 µg per injection for a standardized patient of 70 kg body weight at a maximal concentration of 0.6 µg/mL [148].

19.3. METHODOLOGY

19.3.1. Activity, administration, dosimetry

⁶⁸Ga-PSMA is administered via IV route in an activity of 1.8–2.2 MBq (0.049–0.060 mCi) per kg body weight. The highest tracer uptake was observed in the kidneys, liver, upper large intestine and urinary bladder. Mean organ doses are: kidneys 0.262 ± 0.098 mGy/MBq, liver 0.031 ± 0.004 mGy/MBq, upper large intestine 0.054 ± 0.041 mGy/MBq and urinary bladder 0.13 ± 0.059 mGy/MBq. The calculated mean effective dose is 0.023 ± 0.004 mSv/MBq (0.085 ± 0.015 rem/mCi) [148, 150–155].

19.3.2. Imaging protocol

Patients have to fast for 4 hours. Imaging is performed following the IV administration of 1.5–2.5 MBq/kg and an uptake period of 60–100 min. Acquisition of the PET component starts from the pelvis, with 2–3 min/bed position. For the CT imaging protocol, see general comments in Section 1.3.

19.4. CLINICAL ASPECTS

19.4.1. Indications

The main clinical applications of ⁶⁸Ga-PSMA PET–CT are for prostate cancer. Similar to radiolabelled choline, this study can be performed for intraprostatic detection of a primary tumour, especially in association with MRI or using hybrid PET–MRI [150]. The study can also be of value for nodal staging in patients with newly diagnosed intermediate or high risk primary tumours according to the main risk factors, Gleason score, T stage and PSA values [151]. This is particularly helpful to decide on the most appropriate surgical option, or to direct patients showing multimetastatic spread of the disease to a different type of treatment, such as RT or ADT. ⁶⁸Ga-PSMA PET–CT is also performed for restaging of BCR, defined as an increase in PSA levels up to 0.2 ng/mL after radical prostatectomy, or 2.0 ng/mL after RT [152]. ⁶⁸Ga-PSMA PET–CT can differentiate between local and distant relapse and identify patients with oligometastatic disease, potentially treatable with salvage treatments, as compared to those affected by disseminated metastatic spread who are candidates for ADT. Appropriate use of ⁶⁸Ga-PSMA PET–CT led to a change in the decision making process in up to half of patients with prostate cancer [153]. ⁶⁸Ga-PSMA PET–CT plays a major role in the selection of metastatic castrate resistant prostate cancer patients who may benefit from systemic treatment with ²²³Ra or other radioligand treatment using β emitters such as ¹⁷⁷Lu-PSMA or α emitters such as ²²⁵Ac-PSMA [154, 155].

19.4.2. Cases

19.4.2.1. Case No. 19.1

Clinical indication for PET–CT: Prostate cancer, staging

Clinical history

A 56 year old man with newly diagnosed prostate cancer, Gleason score 4+5, PSA 14 ng/mL, candidate for radical prostatectomy.

PET–CT findings

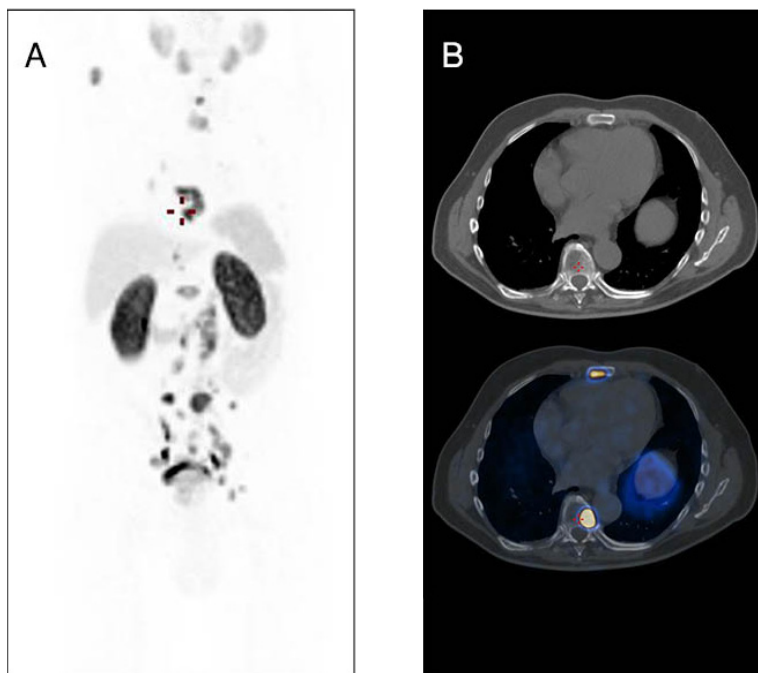
(A): MIP; (B): CT and fused transaxial slices of lower thorax.

There is intense tracer uptake in the prostate and in multiple foci in LNs and bones.

Teaching point

In high risk patients, a whole body imaging test such as ^{68}Ga -PSMA PET–CT can localize distant metastases to LNs or bones. In this case, based on the results of this study, the patient received ADT.

Keywords: Prostate cancer, staging, ^{68}Ga -PSMA



Clinical indication for PET–CT: Prostate cancer, BCR

Clinical history

A 62 year old man with prostate cancer, Gleason score 4+4, post-radical prostatectomy, presented with PSA 0.7 ng/mL, PSA dt 5 months, and TTR 24 months. He was a candidate for salvage RT to the prostatic fossa.

PET–CT findings

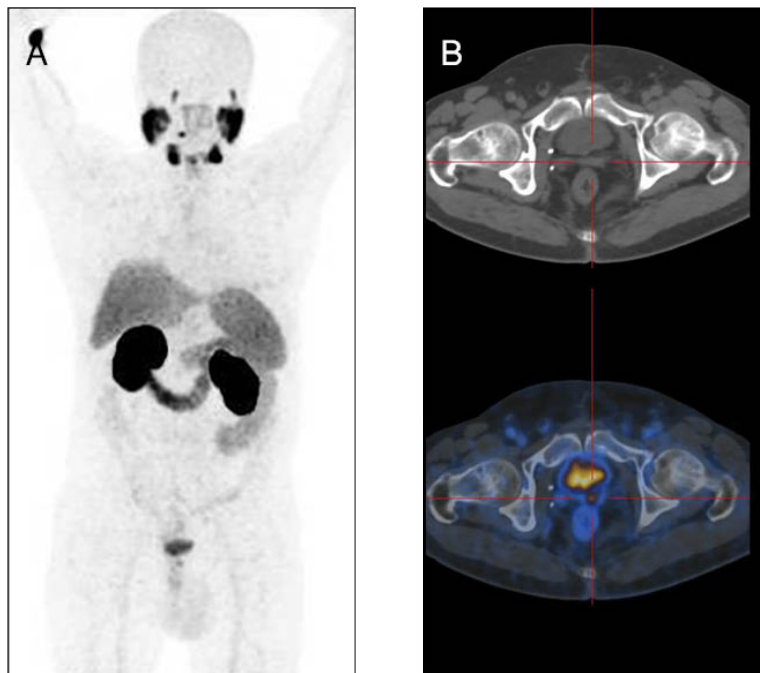
(A): MIP; (B): CT and fused transaxial slices of pelvis.

There is a single focus of increased tracer uptake in the prostatic fossa, confirmed by biopsy as local relapse.

Teaching point

⁶⁸Ga-PSMA can diagnose local relapse. The presence of radioactive urine may cause pitfalls. In this case, ⁶⁸Ga-PSMA PET–CT showed the presence of a single focus of increased uptake with no additional findings. Following the ⁶⁸Ga-PSMA study, the patient was referred for salvage RT to the pelvis.

Keywords: Prostate cancer, local relapse, ⁶⁸Ga-PSMA



19.4.2.3. Case No. 19.3

Clinical indication for PET–CT: Prostate cancer, BCR

Clinical history

A 68 year old man with prostate cancer, pT3N0Mx, Gleason score 4+5, post-radical prostatectomy followed by adjuvant external beam RT, presented with PSA 2.49 ng/mL and PSA dt 8 months.

PET–CT findings

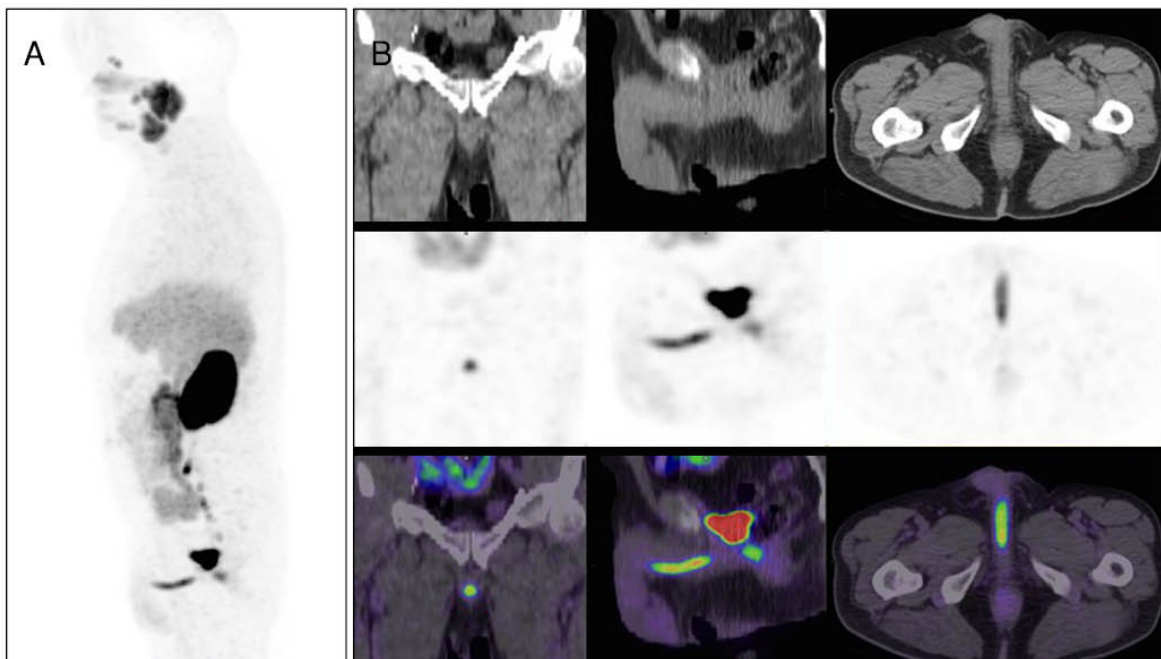
(A): sagittal MIP; (B): CT, PET and fused coronal, sagittal and transaxial slices of pelvis.

There is a small focus of tracer uptake in the prostatic fossa and the urethra, due to radioactive urine, with no evidence of recurrent disease (note that the patient complained of frequent urinary incontinence during physical exertion).

Teaching point

In patients who have undergone surgery, focal uptake related to radioactive urine should be recognized and distinguished from recurrent disease. Urinary radioactivity is in the mid-line and follows the urethra.

Keywords: Prostate cancer, pitfall, ⁶⁸Ga-PSMA



Clinical indication for PET–CT: Prostate cancer, BCR

Clinical history

A 64 year old man with prostate cancer, Gleason score 4+4, post-radical prostatectomy, presented with PSA 0.7 ng/mL, PSA dt 6 months and TTR 12 months. He was a candidate for salvage RT to the prostatic fossa.

PET–CT findings

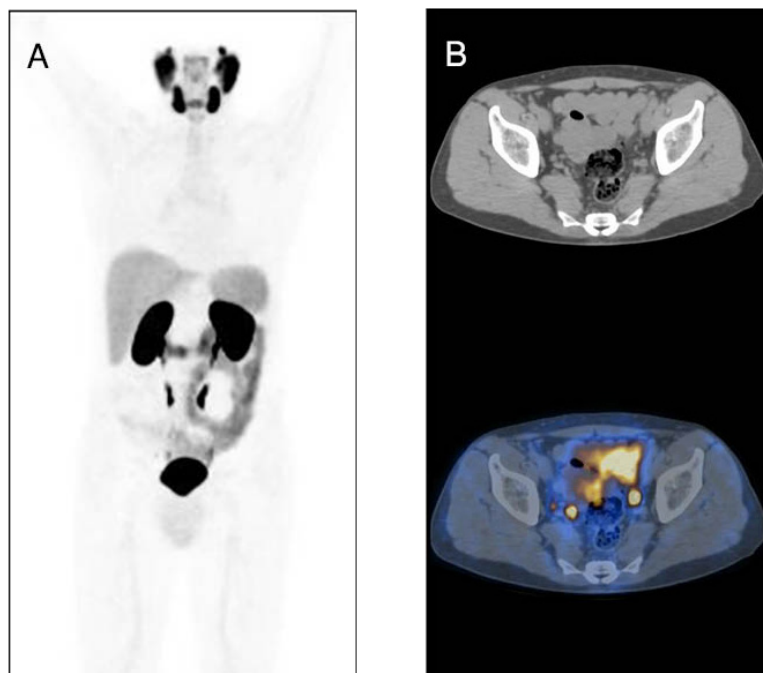
(A): MIP; (B): CT and fused transaxial slices of pelvis.

There is a single focus of increased tracer uptake in an 8 mm right external iliac LN.

Teaching point

⁶⁸Ga-PSMA is very sensitive for detection of small metastatic LNs. A single nodal metastasis, precisely localized, is potentially curable with aggressive treatment. In this case, following the ⁶⁸Ga-PSMA study, the single metastasis was included in the radiation field.

Keywords: Prostate cancer, LN relapse, ⁶⁸Ga-PSMA



Clinical indication for PET–CT: Prostate cancer, BCR

Clinical history

A 72 year old man with prostate cancer, Gleason score 4+5, post-radical prostatectomy, presented with PSA 0.4 ng/mL, PSA dt 6 months and TTR 10 months. He was a candidate for salvage RT to the prostatic fossa.

PET–CT findings

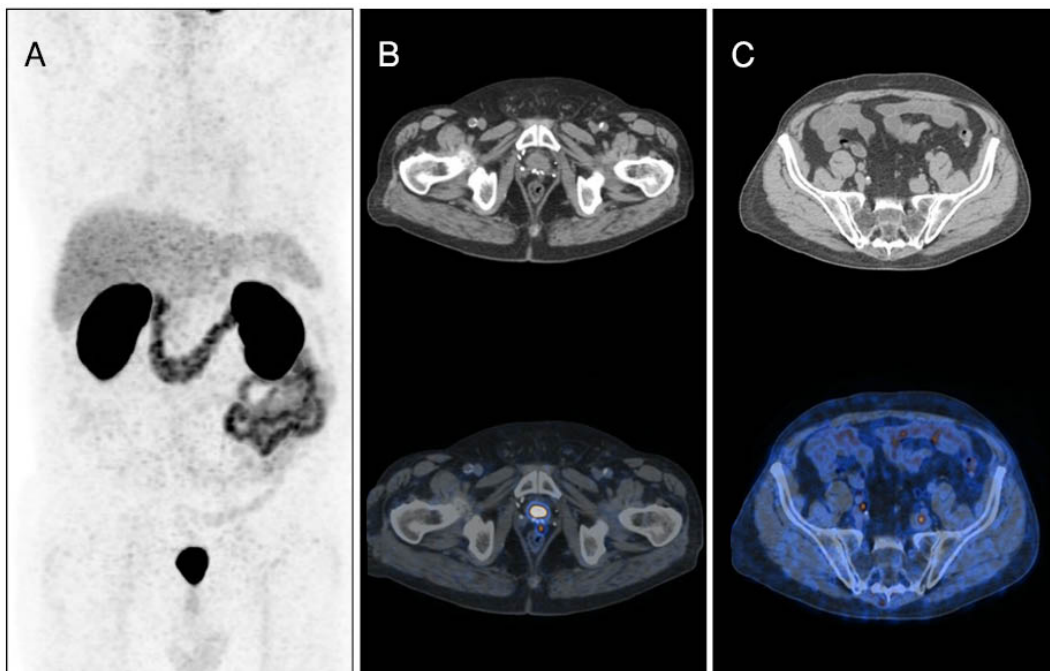
(A): MIP; (B, C): CT and fused transaxial slices at two levels of pelvis.

There are two foci of increased tracer uptake: in the prostatic fossa and in a 7 mm right common iliac LN.

Teaching point

⁶⁸Ga-PSMA PET–CT is very sensitive for the detection of small lesions in the pelvis. In this case, the study detected both local relapse and a single nodal metastasis, both potentially treatable with aggressive treatment. Following the ⁶⁸Ga-PSMA study both sites of disease were included in the radiation field.

Keywords: Prostate cancer, local and LN relapse, ⁶⁸Ga-PSMA



Clinical indication for PET–CT: Prostate cancer, BCR

Clinical history

A 64 year old man with prostate cancer, Gleason score 4+5, post-radical prostatectomy, presented with PSA 1.9 ng/mL, PSA dt 6 months and TTR 28 months.

PET–CT findings

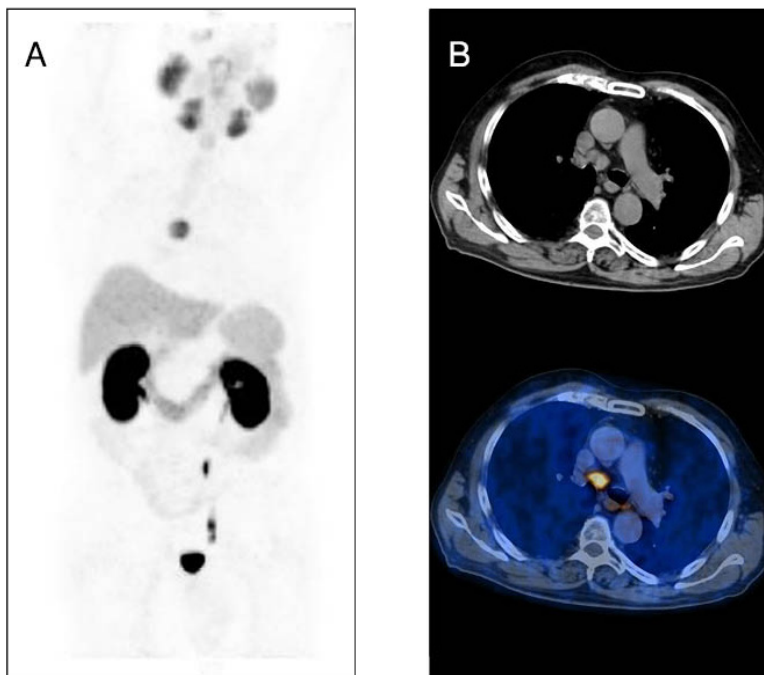
(A): MIP; (B): CT and fused transaxial slices of mid-thorax.

There is focal tracer uptake in an enlarged, 24 mm, precarinal LN. Transbronchial biopsy confirmed a prostate cancer metastasis.

Teaching point

⁶⁸Ga-PSMA PET–CT showed the presence of a single metastasis in a thoracic LN. Although infrequent in prostate cancer, mediastinal nodal metastases may occur. Following the ⁶⁸Ga-PSMA study the patient was referred for ADT.

Keywords: Prostate cancer, distant LN metastasis, ⁶⁸Ga-PSMA



Clinical indication for PET–CT: Prostate cancer, BCR

Clinical history

A 72 year old man with prostate cancer, Gleason score 4+3, post-radical prostatectomy, was examined during treatment with abiraterone because of increasing PSA levels (127 ng/mL). The patient was a candidate for ²²³Ra-chloride treatment.

PET–CT findings

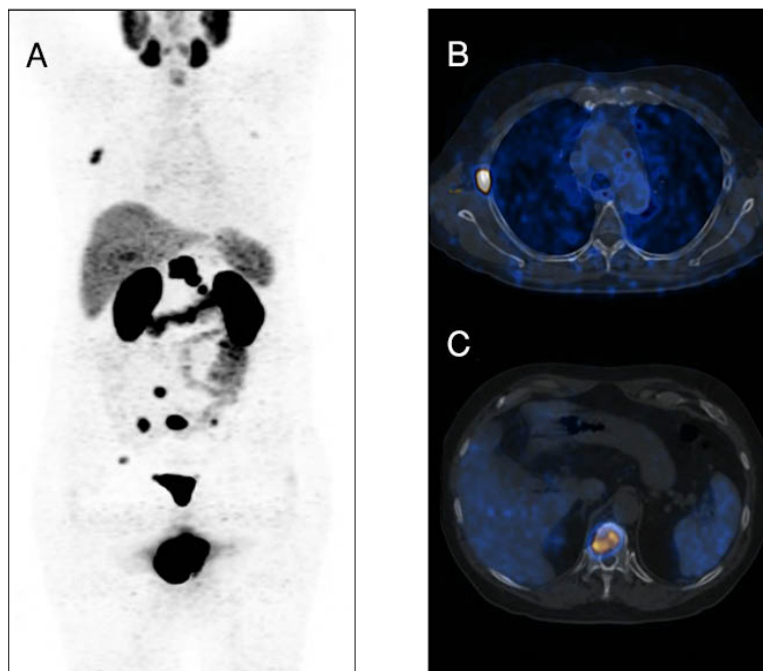
(A): MIP; (B): fused transaxial slices at mid-thoracic and mid-abdominal levels.

There are multiple foci of increased tracer uptake in the bones, with no evidence for nodal or visceral metastases. Following the study, the patient was referred for ²²³Ra-chloride treatment.

Teaching point

⁶⁸Ga-PSMA PET–CT should be always performed in patients eligible for ²²³Ra-chloride treatment, to confirm the presence of bone lesions and exclude the presence of nodal or visceral metastases.

Keywords: Prostate cancer, bone metastases, ⁶⁸Ga-PSMA



Clinical indication for PET–CT: Prostate cancer, BCR

Clinical history

A 72 year old patient with prostate cancer, Gleason score 3+4, stage T3aN0MxR1, presented with PSA 0.21 ng/mL.

PET–CT findings

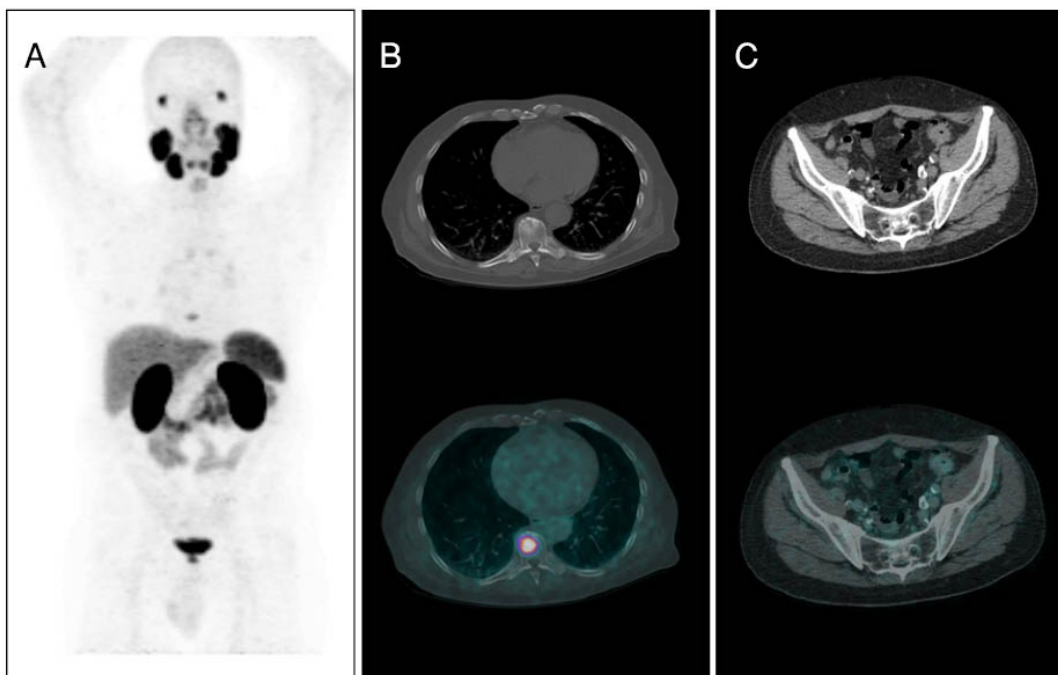
(A): MIP; (B, C): CT and fused transaxial slices of thorax and pelvis.

There is intense tracer uptake in an osteoblastic bone metastasis in the T-10 vertebral body. There is also faint uptake in a subcentimetre left sacral LN.

Teaching point

The prostate lymphatics drain into the periprostatic, subcapsular network, from which three groups of ducts originate: the ascending ducts from the cranial prostate draining into the external iliac LNs, the lateral ducts running to the hypogastric LNs and the posterior ducts draining from the caudal prostate to the subaortic sacral LNs of the promontory. Morphological criteria used by conventional imaging techniques underestimate the presence of malignancy in LNs. ⁶⁸Ga-PSMA PET–CT has a higher sensitivity for the detection of subcentimetre nodal metastases in patients with BCR.

Keywords: Prostate cancer, bone and small nodal metastases, ⁶⁸Ga-PSMA



Clinical indication for PET–CT: Prostate cancer, BCR

Clinical history

A 67 year old man with prostate cancer, Gleason score 4+3, post-radical prostatectomy, presented with increasing PSA (114 ng/mL) during enzalutamide treatment.

PET–CT findings

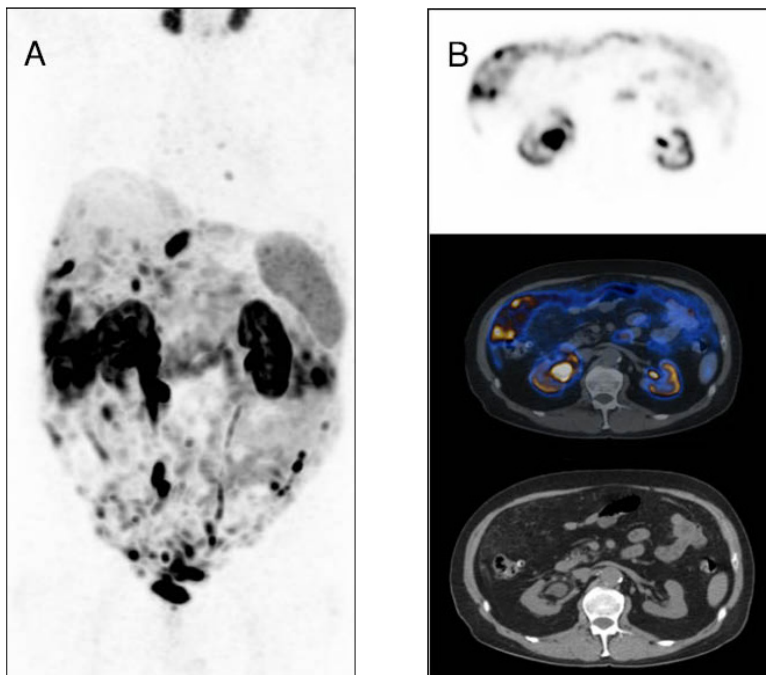
(A): MIP; (B): PET, fused and CT slices of mid-abdomen.

There are multiple foci of tracer uptake in the peritoneum, the liver capsule and mediastinal LNs.

Teaching point

⁶⁸Ga-PSMA PET–CT can show peritoneal invasion in patients with prostate cancer. Peritoneal metastases are rare in prostate cancer, especially in the absence of skeletal or other visceral metastases. The metastatic patterns and mechanisms of tumour dissemination of prostate cancer have traditionally been explained by the mechanical theory of dissemination through the lympho-vascular channels or, alternatively, through the “seed and soil” hypothesis.

Keywords: Prostate cancer, peritoneal metastases, ⁶⁸Ga-PSMA



Clinical indication for PET–CT: Prostate cancer, BCR

Clinical history

A 66 year old patient with prostate cancer, Gleason score 3+4, stage T3N0M0, post-radical prostatectomy and following a previous recurrence treated with ADT. The patient presented with PSA 8.8 ng/mL. Contrast enhanced CT showed bladder wall thickening, suspicious for relapse.

PET–CT findings

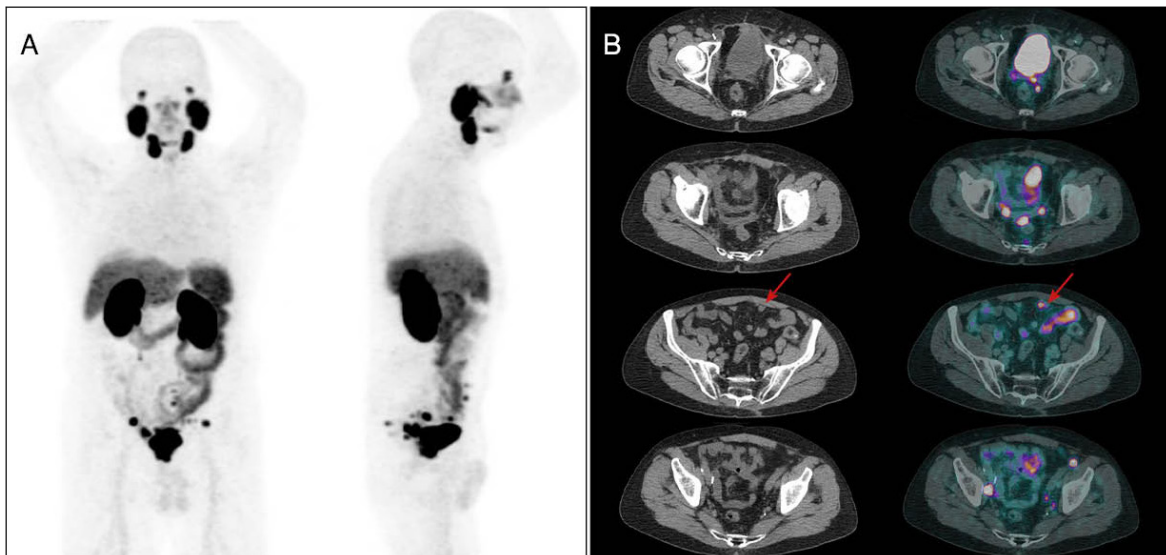
(A): MIP; (B): CT and fused transaxial slices at multiple levels of pelvis.

There is intense tracer uptake in nodules adjacent to the bladder, as well as in the peritoneum (arrows), consistent with tumour implants.

Teaching point

Peritoneal metastases, with or without ascites, represent an advanced stage of aggressive prostate cancer.

Keywords: Prostate cancer, peritoneal metastases, ⁶⁸Ga-PSMA



Clinical indication for PET–CT: Prostate cancer, BCR

Clinical history

A 67 year old patient with prostate cancer treated with primary RT presented with PSA 37 ng/mL.

PET–CT findings

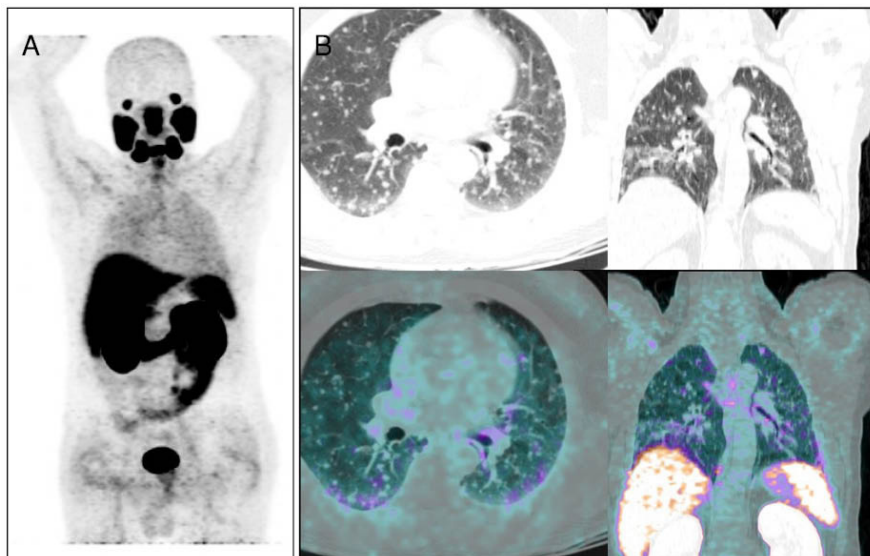
(A): MIP; (B): CT and fused transaxial and coronal slices of thorax.

There is diffuse tracer uptake in multiple pulmonary nodules, ranging from a few millimetres to 1 cm in diameter. In addition, there is also increased ⁶⁸Ga-PSMA uptake in the prostate, suggesting local recurrence.

Teaching point

The usual pattern of metastatic spread in prostate cancer is through the lymphatic pathways. Lung metastases are often found at autopsy, and such metastases are the second most common type of metastatic spread, after skeletal lesions. They usually occur concomitantly with LN and bone metastases, or in the context of multiple organ involvement. Isolated pulmonary metastases are very rare. There are two radiological patterns of pulmonary metastasis in prostate cancer. The lymphangitic pattern, secondary to infiltration of pulmonary lymphatic vessels, is the most common pattern in prostate cancer and presents as a thickening of the interlobular connective tissue, the peribroncho-vascular interstitium and/or the subpleural interstitium, which can sometimes be nodular. The second, less common, pattern is the haematogenous pattern, with solitary or multiple lung nodules of different size.

Keywords: Prostate cancer, lung metastases, ⁶⁸Ga-PSMA



Clinical indication for PET–CT: Prostate cancer, BCR

Clinical history

A 68 year old patient diagnosed with prostate cancer, post-radical prostatectomy, presented with PSA 0.39 ng/mL.

PET–CT findings

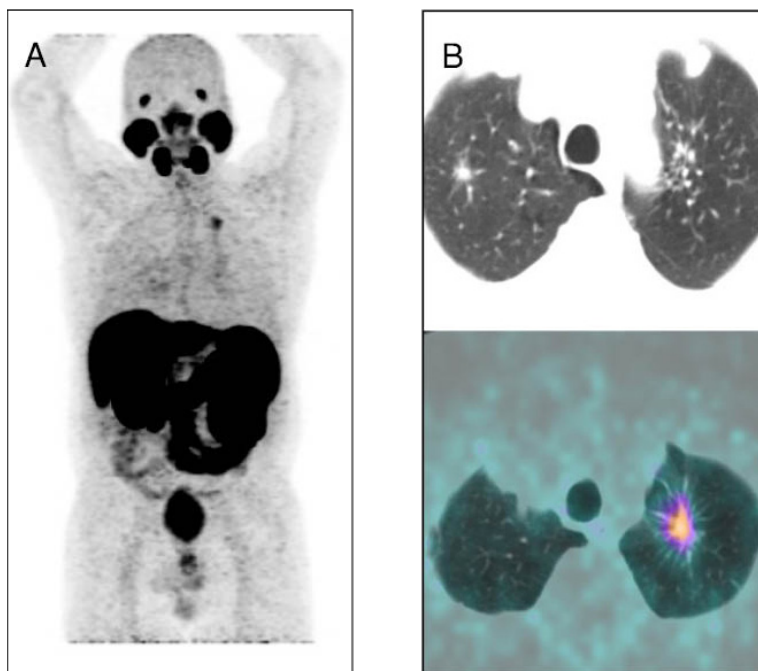
(A): MIP; (B): CT and fused transaxial slices of upper thorax.

There is tracer uptake in a pulmonary nodule with irregular margins and spiculated edges in the left upper lobe. Biopsy diagnosed primary lung adenocarcinoma.

Teaching point

The presence of irregular margins and spiculation in a lung lesion on CT is highly suspicious for malignancy. ⁶⁸Ga-PSMA uptake related to tumour neovasculature can be the cause for visualization in non-prostatic solid malignancies such as squamous cell carcinoma, glioma, and lung or breast cancer. In the future, these tumours could be targets for anti-tumour therapy.

Keywords: Prostate cancer, primary lung cancer, ⁶⁸Ga-PSMA



Clinical indication for PET–CT: Prostate cancer, BCR

Clinical history

A 64 year old patient with prostate cancer, Gleason score 3+4, post-radical prostatectomy, with perineural invasion and negative surgical margins, presented with PSA 0.2 ng/mL and PSA dt 6 months.

PET–CT findings

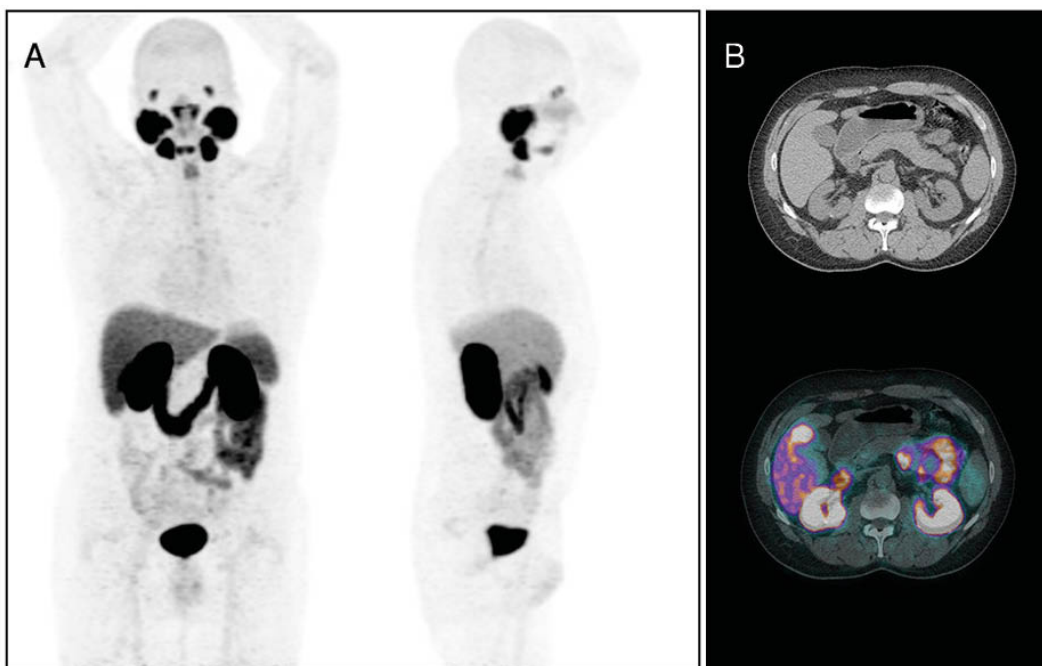
(A): coronal and saggital MIP; (B): CT and fused transaxial slices of mid-abdomen.

There is a focal area of tracer uptake in the liver, segment 4B, consistent with a metastasis.

Teaching point

Autopsy of 1589 patients diagnosed with prostate cancer found metastases in the bone in 90%, in the lungs in 46%, in the liver in 25%, in the pleura in 21% and in adrenal glands in 13% of cases. Isolated hepatic metastases in prostate cancer are rare. In this case, there was no evidence of disease in other organs and the patient was referred for surgery.

Keywords: Prostate cancer, liver metastasis, ⁶⁸Ga-PSMA



Clinical indication for PET–CT: Prostate cancer, BCR

Clinical history

A 65 year old man with prostate cancer, Gleason score 4+3, stage pT2cN0Mx, post-radical prostatectomy followed by RT two years later because of an imaging-negative relapse, presented with PSA 6.06 ng/mL and PSA dt 9 months.

PET–CT findings

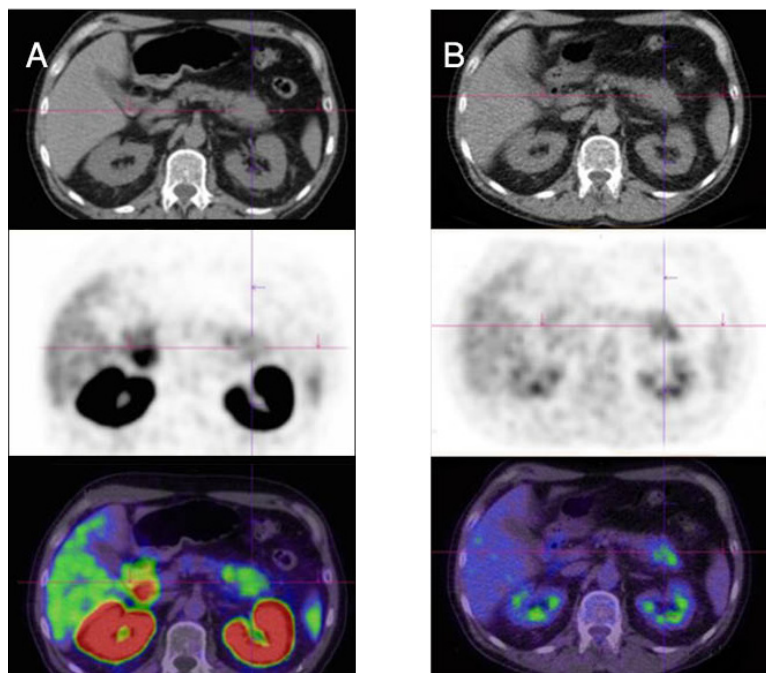
(A): ^{68}Ga -PSMA CT, PET and fused transaxial slices of upper abdomen; (B): ^{18}F -FDG slices at the same levels.

There is a focus of increased ^{68}Ga -PSMA uptake in a 4 cm mass in the tail of the pancreas (A). ^{18}F -FDG PET–CT also shows increased uptake in the same lesion (B). Surgery diagnosed a mildly differentiated pancreatic adenocarcinoma (pT3N1). There was no evidence of prostate cancer relapse. PSA was 5.15 and 6.18 ng/mL 6 and 12 months later, respectively.

Teaching point

PSMA may be expressed in a wide variety of primary tumours, in addition to prostate adenocarcinoma.

Keywords: Prostate cancer, pancreatic adenocarcinoma, ^{68}Ga -PSMA



Clinical indication for PET–CT: Prostate cancer, BCR

Clinical history

A patient with prostate cancer, post-RT as primary treatment, followed by BCR treated with ADT, presented with PSA 3.1 ng/mL.

PET–CT findings

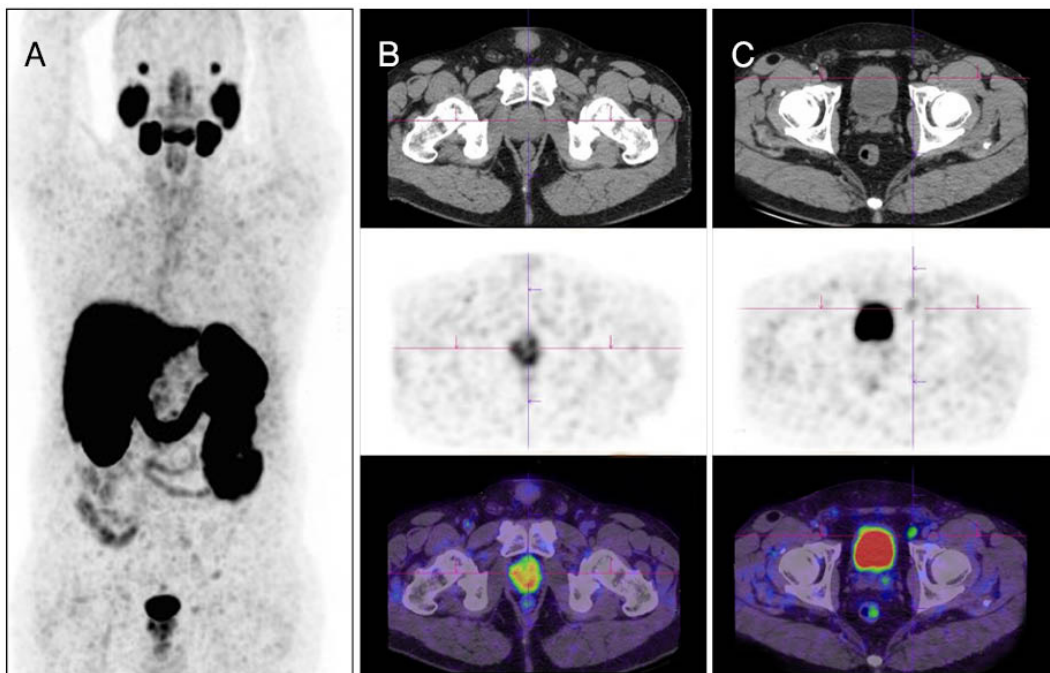
(A): MIP; (B, C): CT, PET and fused transaxial slices at two levels of pelvis.

There is faint tracer uptake in a 3 mm right sacral LN and a right iliac LN.

Teaching point

Internal and external iliac LNs, and obturator LNs, are the stations most frequently involved in metastatic spread of prostate carcinoma. Metastases to presacral and common iliac LNs are rare. ⁶⁸Ga-PSMA PET–CT has a high sensitivity for the detection of subcentimeter nodal metastases in BCR.

Keywords: Prostate cancer, nodal metastases, ⁶⁸Ga-PSMA



Clinical indication for PET–CT: Prostate cancer, BCR

Clinical history

An 81 year old patient with prostate cancer state after RT and ADT as primary treatment, presented with PSA 23 ng/mL.

PET–CT findings

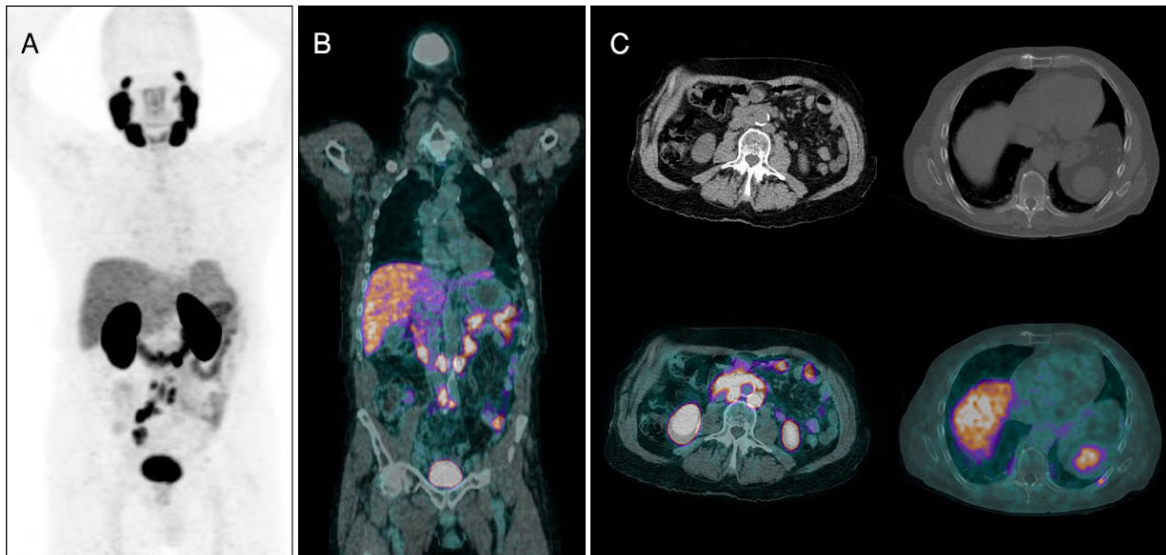
(A): MIP; (B): fused coronal slice; (C): CT and fused transaxial slices of lower abdomen and lower thorax.

There is intense tracer uptake in enlarged iliac and retroperitoneal LNs and an additional focal uptake in the 9th left rib, consistent with metastatic spread.

Teaching point

⁶⁸Ga-PSMA is useful to localize the site of recurrence as well as to identify distant metastases, with optimized subsequent treatment tailoring.

Keywords: Prostate cancer, metastases, ⁶⁸Ga-PSMA



Clinical indication for PET–CT: Prostate cancer, BCR

Clinical history

A 68 year old patient with prostate cancer, post-radical prostatectomy, presented with PSA 1.0 ng/mL. ^{99m}Tc-MDP bone scintigraphy (A) shows intense tracer uptake in the left pelvis.

PET–CT findings

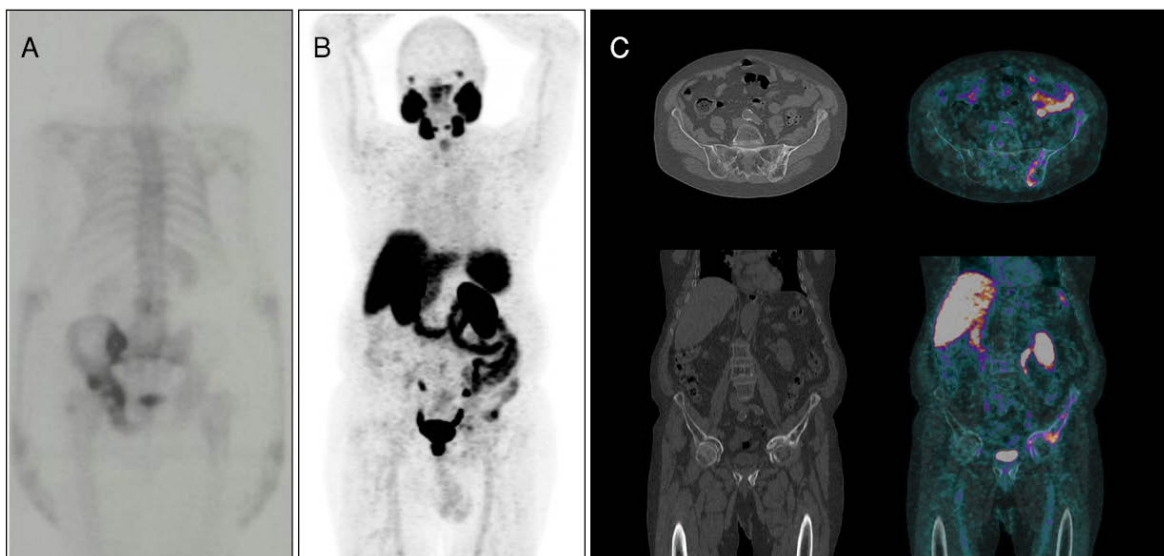
(A): ^{99m}Tc-MDP bone scintigraphy; (B): MIP; (C): CT and fused transaxial and coronal slices.

There is cortical thickening and sclerosis of the right iliac bone on CT, with partially increased, inhomogeneous ⁶⁸Ga-PSMA uptake, consistent with Paget’s disease.

Teaching point

⁶⁸Ga-PSMA uptake by benign processes such as Paget’s disease has been reported. In these cases tracer uptake is related to osseous remodelling and increased vascularization.

Keywords: Prostate cancer, Paget’s disease, ⁶⁸Ga-PSMA



Clinical indication for PET–CT: Prostate cancer, BCR

Clinical history

A 65 year old man with prostate cancer, Gleason score 4+4, post-radical prostatectomy, presented with PSA 0.21 ng/mL, PSA dt 8.2 months and TTR 28 months.

PET–CT findings

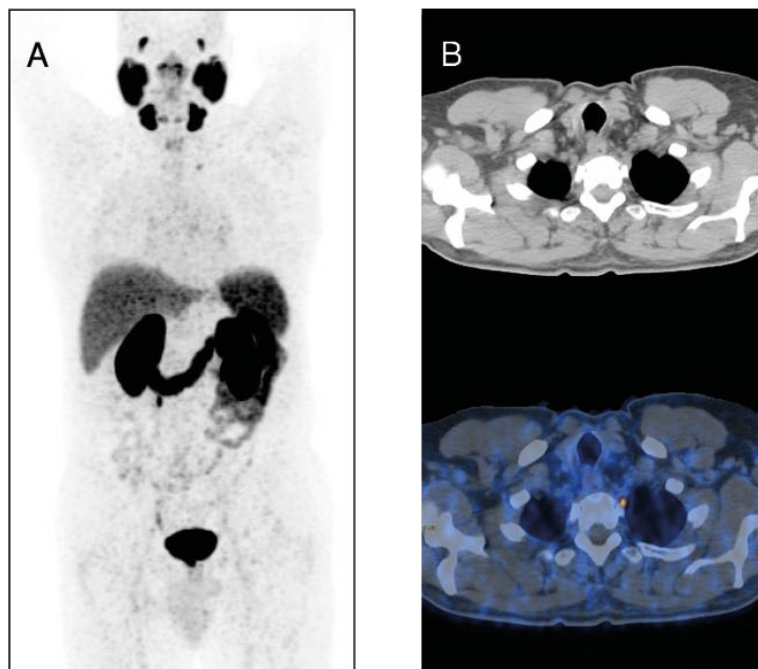
(A): MIP; (B): CT and fused transaxial slices of upper thorax.

There is faint tracer uptake in a left cervical ganglion.

Teaching point

This finding does not represent malignancy and should be recognized by the low intensity of ^{68}Ga -PSMA uptake and by its shape and location on CT.

Keywords: Prostate cancer, cervical ganglion, ^{68}Ga -PSMA



Clinical indication for PET–CT: Prostate cancer, BCR

Clinical history

A 75 year old man with prostate cancer, Gleason score 4+3, post-radical prostatectomy, presented with PSA 0.5 ng/mL and PSA dt 6.2 months.

PET–CT findings

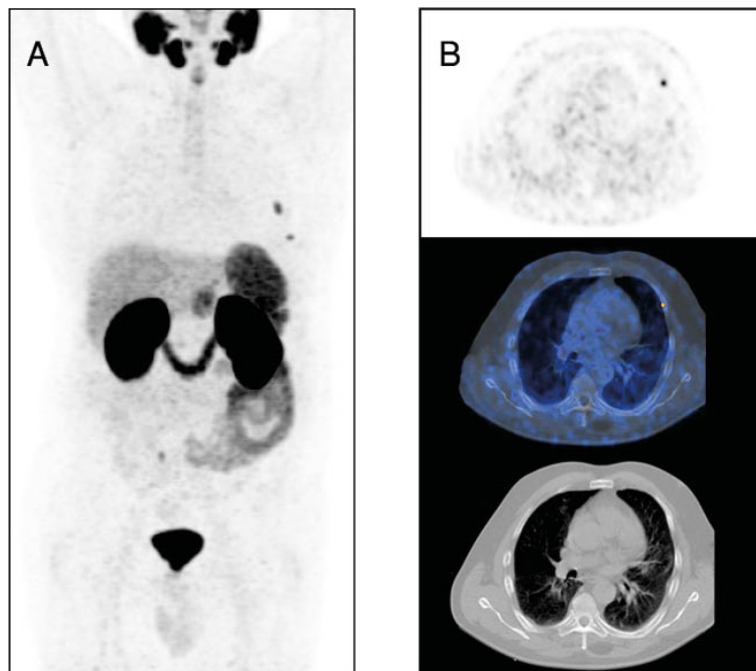
(A): MIP; (B): PET, fused and CT transaxial slices of mid-thorax.

There is faint tracer uptake in a left rib, consistent with a healing fracture seen on CT.

Teaching point

Fractures with callus formation can show increased PSMA expression.

Keywords: Prostate cancer, fracture, ⁶⁸Ga-PSMA



Clinical indication for PET–CT: Prostate cancer, BCR

Clinical history

A 75 year old man with prostate cancer, Gleason score 4+4, post-radical prostatectomy, presented with PSA 0.8 ng/mL, PSA dt 6 months and TTR 18 months.

PET–CT findings

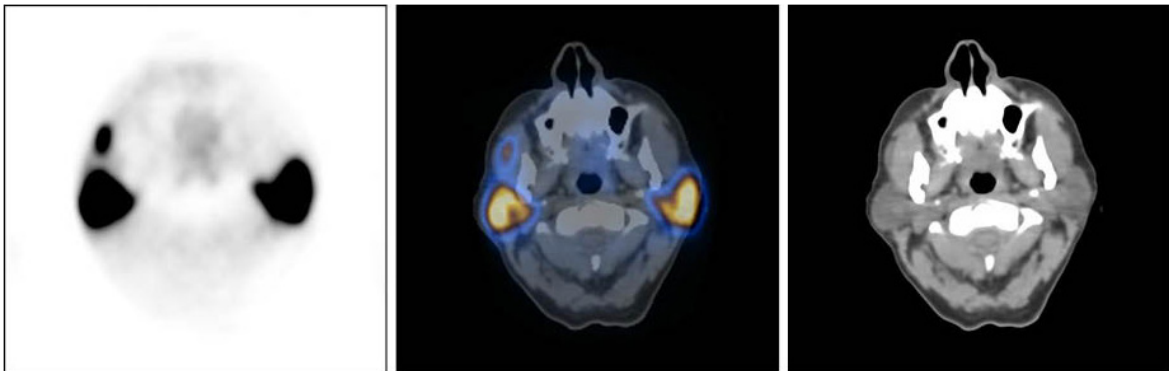
PET, fused and CT slices of head.

There is intense tracer uptake, adjacent and lateral to the right masseter muscle, consistent with an accessory parotid gland.

Teaching point

Accessory parotid glands are a relatively common finding and can be recognised by the location and intensity of tracer uptake.

Keywords: Prostate cancer, accessory salivary gland, ⁶⁸Ga-PSMA



20. SOMATOSTATIN ANALOGUES (⁶⁸Ga)

20.1. GENERAL CHARACTERISTICS

Name: ⁶⁸Ga-DOTA-peptide

Synonyms: ⁶⁸Ga labelled (1,4,7,10-tetraazacyclododecane-N, N', N'', N'''-tetraacetic acid)-1-somatostatin ligands ⁶⁸Ga-DOTA-somatostatins:

- ⁶⁸Ga labelled (1,4,7,10-tetraazacyclododecane-N, N', N'', N'''-tetraacetic acid)-1-(d)-Phe1-Thy3-octreotate (DOTATATE)
- ⁶⁸Ga labelled (1,4,7,10-tetraazacyclododecane-N, N', N'', N'''-tetraacetic acid)-1-(d)-Phe1-Thy3-octreotide (DOTATOC)
- ⁶⁸Ga labelled (1,4,7,10-tetraazacyclododecane-N, N', N'', N'''-tetraacetic acid)-1-NaI3-octreotide (DOTANOC)

Radioisotope

⁶⁸Ga is a short half-life PET radioisotope (67.7 min) emitting positrons of E_{\max} 1.9 MeV. It is usually obtained from a ⁶⁸Ge generator. The parent isotope ⁶⁸Ge has a half-life of 271 days and can be easily utilized for in-hospital production of generator produced ⁶⁸Ga.

Radiosynthesis

⁶⁸Ga labelling of DOTA-somatostatins is performed via a small scale laboratory method as well as an automated method using a synthesizer coupled with a ⁶⁸Ge generator usually eluted using 0.1 M HCl followed by a pre-concentration and/or pre-purification in some cases. Purified ⁶⁸Ga is then directly eluted into the reaction vial containing DOTA-somatostatin heated to 90–100°C for 10–15 min. This is followed by reverse phase column purification and further dilution with normal saline. The tracer is then passed through a 0.22 μm filter to get a sterile preparation for injection. Radiolabelling yields of >95% can usually be achieved within 15 mins [156–159].

20.2. PHARMACOKINETICS

20.2.1. Physiological biodistribution and metabolism

All ⁶⁸Ga-DOTA-conjugated peptides, such as ⁶⁸Ga-DOTANOC (Fig. 20.1), are rapidly cleared from the blood. Arterial elimination of activity is biexponential, and no radioactive metabolites are detected after 4 hours in the serum or urine. Maximum renal activity after injection averages <50% of the uptake by the spleen. Excretion is almost entirely through the kidneys. At 60 min after injection there is moderate uptake in the pituitary gland and intense uptake in the lacrimal and salivary glands, liver, pancreas, spleen and adrenals (Fig. 20.2). Tracer uptake in the uncinate process of the pancreas, when present, has a variable pattern, ranging from mild diffuse, intense diffuse or focal to diffuse inhomogeneous, and this should be recognized as a potential pitfall (Fig. 20.3).

20.2.2. Mechanism of retention

Synthetic somatostatin peptides have a long biological half-life. They show strong and specific affinity for somatostatin receptors located on the cellular surface of neuroendocrine tumours. The three

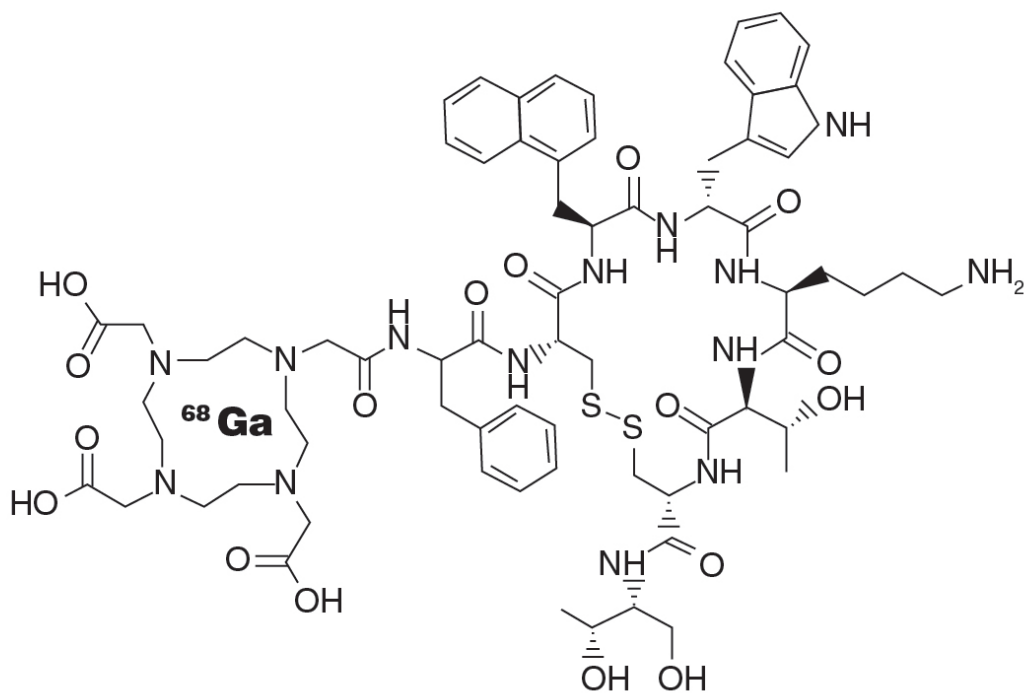


FIG. 20.1. Molecular structure of ^{68}Ga -DOTANOC.



FIG. 20.2. Normal biodistribution of ^{68}Ga -DOTA-peptide.

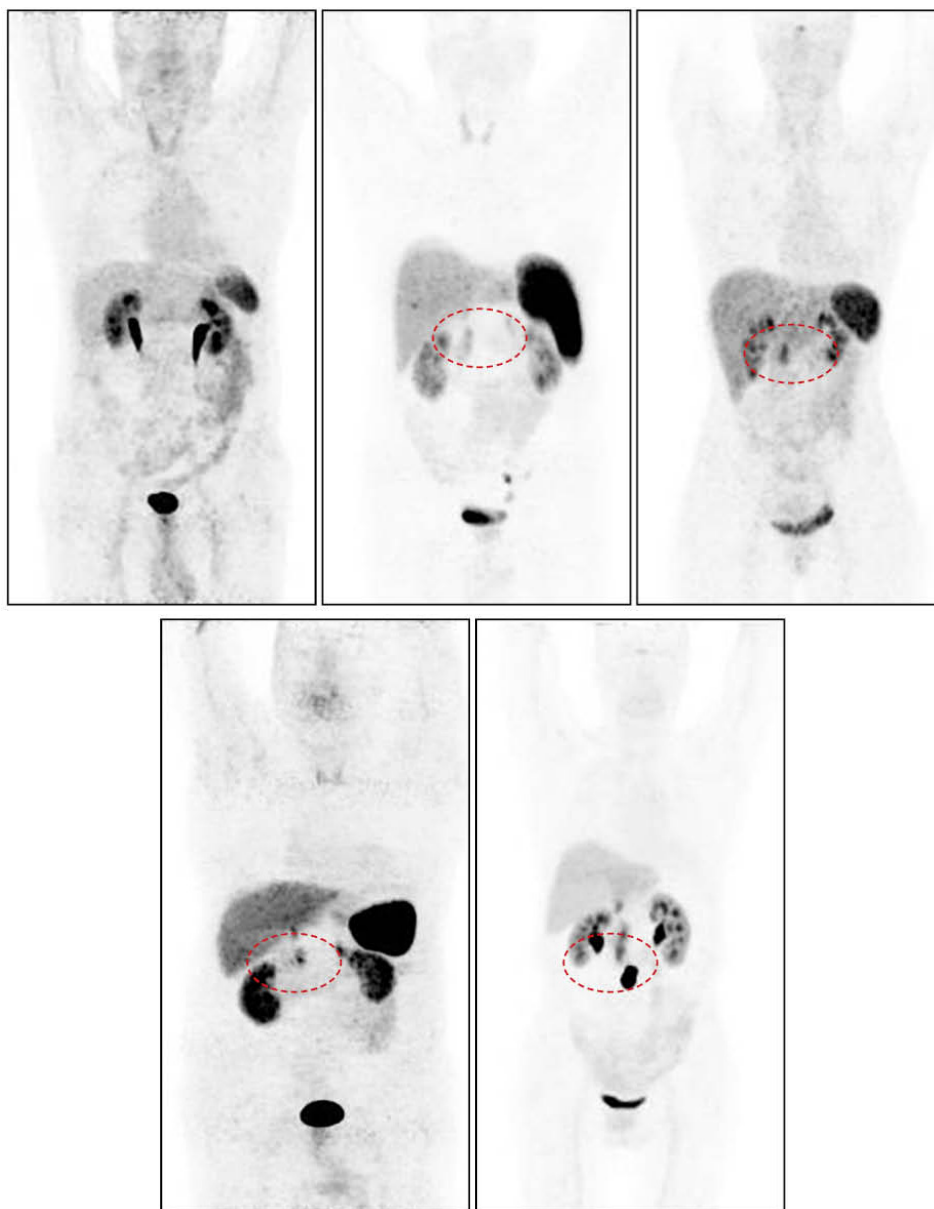


FIG. 20.3. Five variants of normal biodistribution of ⁶⁸Ga-DOTA-peptide.

well known agents used clinically, DOTATATE, DOTATOC and DOTANOC, have different affinities for receptor subtypes (Table 20.1).

⁶⁸Ga-DOTANOC has high affinity for somatostatin receptor subtypes 2, 3, and 5, suggesting a wider receptor binding profile than ⁶⁸Ga-DOTATATE and ⁶⁸Ga-DOTATOC, which are selective essentially only for subtype 2 receptors (Table 20.1).

20.2.3. Pharmacology and toxicology

The studies performed in humans using ⁶⁸Ga-somatostatin provide strong evidence that the mass quantity of the investigational drug ($\leq 50 \mu\text{g}$) is within the acceptable range for patients with life threatening malignancies whose treatment may benefit from the use of the proposed PET-CT imaging procedure.

TABLE 20.1. DIFFERENT AFFINITY PROFILES FOR SOMATOSTATIN RECEPTOR SUBTYPES 1–5

Name	SSTR1 ^a	SSTR2 ^a	SSTR3 ^a	SSTR4 ^a	SSTR5 ^a
⁶⁸ Ga-DOTATATE	>10 000	0.2 ± 0.5	>1 000	300 ± 140	377 ± 18
⁶⁸ Ga-DOTATOC	>10 000	2.5 ± 0.5	613 ± 140	>1 000	73 ± 21
⁶⁸ Ga-DOTANOC	>10 000	1.9 ± 0.4	40 ± 5.8	270 ± 74	7.2 ± 1.6

^a SSTR: somatostatin receptor.

20.3. METHODOLOGY

20.3.1. Activity, administration, dosimetry

The injected activity ranges between 111 and 259 MBq (3–7 mCi) depending on the patient's body weight. An activity of 185 MBq (5 mCi) per 70 kg is used. A one time activity of 185 MBq ⁶⁸Ga-somatostatin administered to a patient for the investigational study results in an effective dose of approximately 5 mSv (500 mrem). There is an additional 1.5 to 5.9 mSv from the CT (10–40 mAs) for an average body habitus. In total, this results in an effective dose of approximately 6.5 to 10.9 mSv [156–159].

20.3.2. Imaging protocol

Patient preparation does not require any dietary restrictions. Imaging is performed following IV administration of 2 MBq/kg and an uptake period of 60 min. Acquisition of the PET component is from mid-thigh to head with 2–3 min/bed position. For the CT imaging protocol, see general comment in Section 1.3.

20.4. CLINICAL ASPECTS

20.4.1. Indications

⁶⁸Ga-DOTA-conjugated peptide PET–CT is used for management of patients with NETs, at staging to localize primary tumours and metastases, for restaging during follow-up to detect residual, recurrent or progressive disease, to determine somatostatin receptor status and thus select patients with metastatic disease for peptide receptor radionuclide therapy, and finally to monitor response to therapy [159].

20.4.2. Cases

20.4.2.1. Case No. 20.1

Clinical indication for PET–CT: Suspected NET

Clinical history

A patient with incidentally found high values of chromogranin A (525 ng/L).

PET–CT findings

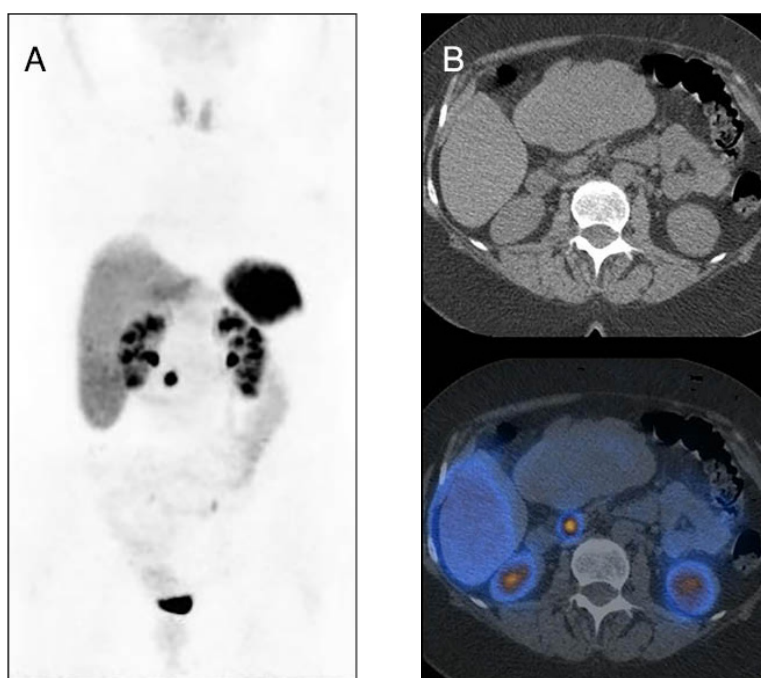
(A): MIP; (B): CT and fused transaxial slices of mid-abdomen.

There is increased focal ^{68}Ga -DOTANOC uptake in a solid, round nodule, 18 mm in diameter, in the uncinate process of the pancreas. Surgery diagnosed a primary NET of the pancreas, G2 (Ki-67 4%).

Teaching point

The focal uptake should not be confused with physiologically increased uptake in the uncinate process of the pancreas, in which case no significant findings are observed on CT.

Keywords: NET of pancreas, uncinate process, ^{68}Ga -DOTANOC



Clinical indication for PET–CT: Suspicion of pancreatic NET

Clinical history

A 50 year old woman with a hypervascular lesion in the pancreas, incidentally found on contrast enhanced CT (A, arrow).

PET–CT findings

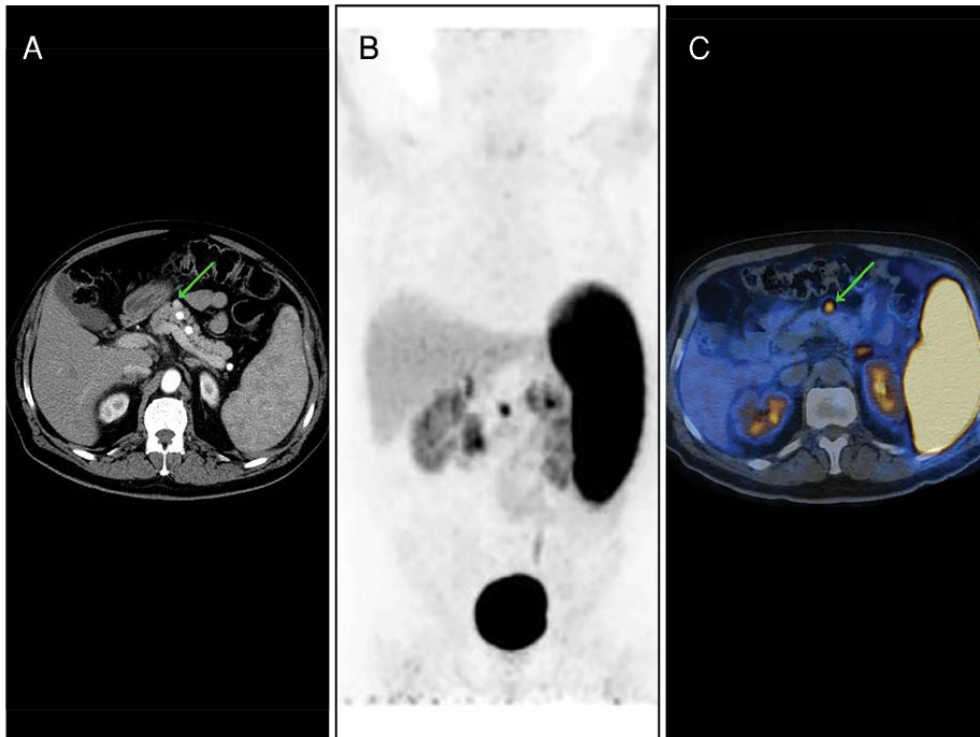
(A): contrast enhanced CT transaxial slice of mid-abdomen; (B): MIP; (C): fused transaxial slice of mid-abdomen.

There is a focal area of increased ^{68}Ga -DOTANOC uptake in the pancreas, corresponding to the known CT finding. At surgery, a well differentiated NET (Ki-67 2%) with high expression of somatostatin receptor analogues was diagnosed.

Teaching point

^{68}Ga -DOTANOC PET–CT has very high sensitivity for detection of well differentiated NETs, including very small lesions.

Keywords: Well differentiated NET, ^{68}Ga -DOTANOC



Clinical indication for PET–CT: Evaluation of a pancreatic lesion

Clinical history

A 48 year old man with clinical suspicion of insulinoma because of episodes of hypoglycaemia and a lesion in the pancreatic body detected on MRI (A).

PET–CT findings

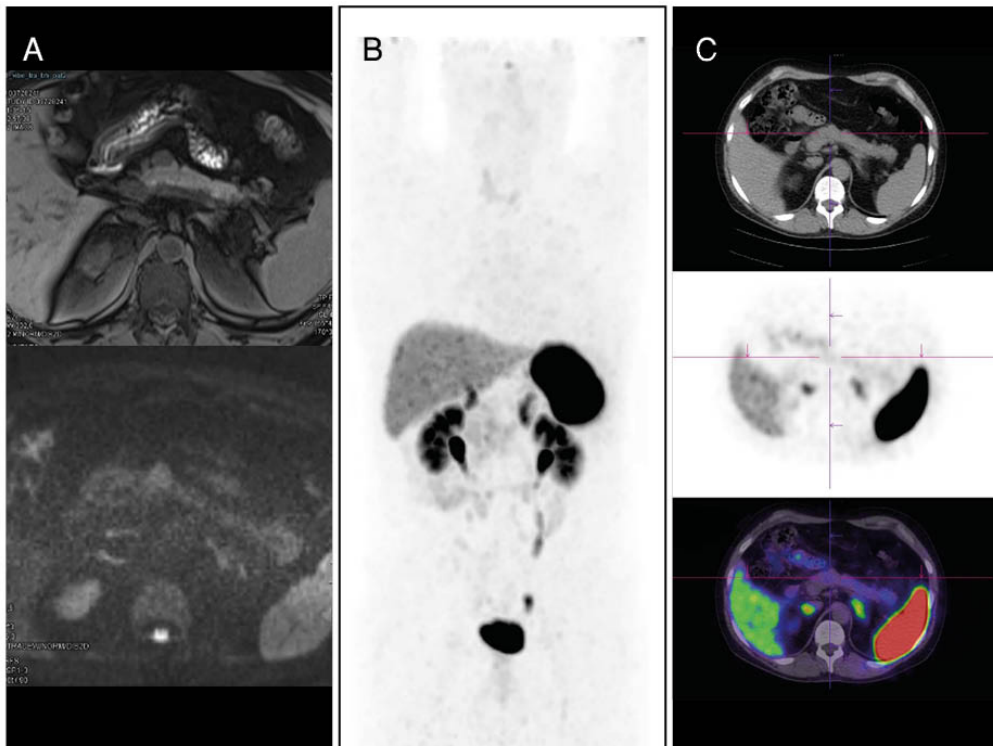
(A): MRI slice of mid-abdomen; (B): MIP; (C): CT, PET and fused transaxial slices of mid-abdomen.

No abnormal ⁶⁸Ga-DOTANOC uptake is seen in the pancreatic lesion. Insulinoma, however, was confirmed at surgery.

Teaching point

The sensitivity of ⁶⁸Ga-DOTA-peptides is variable, depending on the tumour type. In particular, sensitivity is lowest for insulinomas.

Keywords: Insulinoma, ⁶⁸Ga-DOTANOC



Clinical indication for PET–CT: Suspected pancreatic NET

Clinical history

A 58 year old patient with an incidental pancreatic lesion found on CT.

PET–CT finding

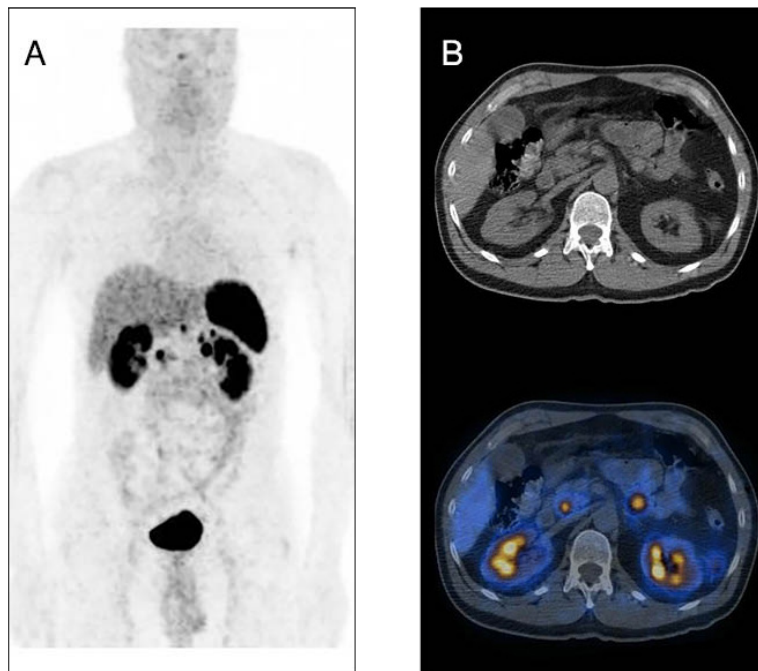
(A): MIP; (B): CT and fused transaxial slices of mid-abdomen.

There is increased focal ^{68}Ga -DOTANOC uptake in the head of the pancreas and in a peripancreatic LN, adjacent to the tail of the pancreas. At surgery, a well differentiated NET, G1 (Ki-67 2%), was diagnosed.

Teaching point

^{68}Ga -DOTANOC PET–CT allows accurate diagnosis and staging of NET.

Keywords: NET of pancreas, diagnosis, staging, ^{68}Ga -DOTANOC



Clinical indication for PET–CT: Evaluation of an incidentally found liver lesion, suspected to be a metastasis

Clinical history

A 52 year old male with an incidentally detected, single liver lesion in the left lobe, shown on US, suspected to represent a metastasis of unknown primary tumour.

PET–CT findings

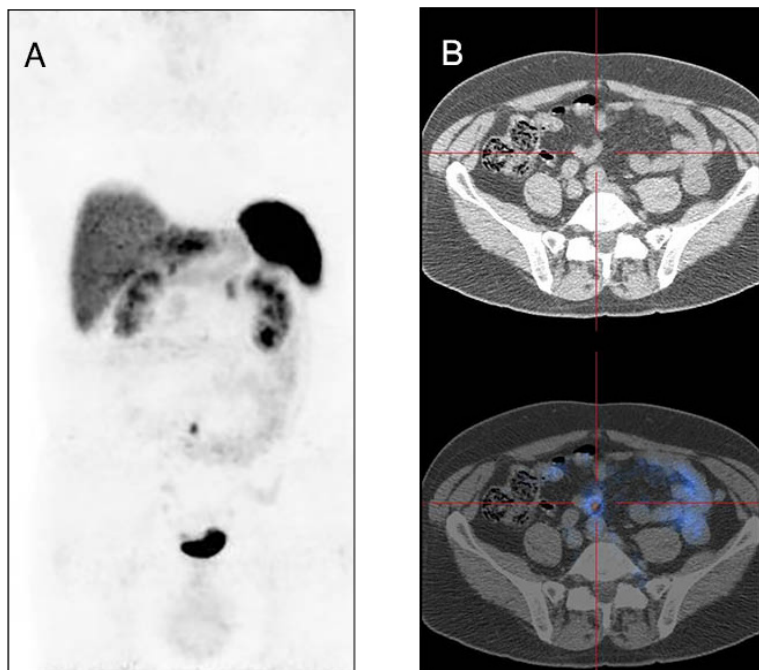
(A): MIP; (B): CT and fused transaxial slices of lower abdomen.

There is increased focal ^{68}Ga -DOTANOC uptake in an ileal loop, suspected to be the primary tumour (red marker), and in the known lesion in the left lobe of the liver, consistent with a metastasis. At surgery, well differentiated NET, G1 (Ki-67 2%), was diagnosed.

Teaching point

^{68}Ga -DOTANOC PET–CT is the imaging method of choice in cases of metastatic unknown primary tumour, when conventional imaging methods are negative and a NET is suspected.

Keywords: Unknown primary NET, ileum, ^{68}Ga -DOTANOC



Clinical indication for PET–CT: Suspected NET on ^{18}F -FDG PET–CT

Clinical history

A 70 year old patient with a history of non-Hodgkin lymphoma had a follow-up ^{18}F -FDG PET–CT that showed mesenteric LNs with desmoplastic reaction on the CT component, with no abnormal tracer uptake, highly suggestive of NET (A).

PET–CT findings

(A): ^{18}F -FDG PET–CT MIP, CT and fused transaxial slices of lower abdomen; (B): ^{68}Ga -DOTATATE, same slices as in (A).

There is intense ^{68}Ga -DOTATATE uptake in mesenteric LNs, and also in the primary tumour in the small bowel.

Teaching point

Nodal lymphoma involvement does not usually show mesenteric desmoplastic reaction on CT, which is typical for small bowel carcinoid.

Keywords: NET, mesenteric nodal metastases, ^{68}Ga -DOTATATE



Clinical indication for PET–CT: Multiple liver lesions on US and CT, suspected to be metastases

Clinical history

A 60 year old man showing multiple liver lesions on US and CT, suspected to be metastases of an unknown primary site.

PET–CT findings

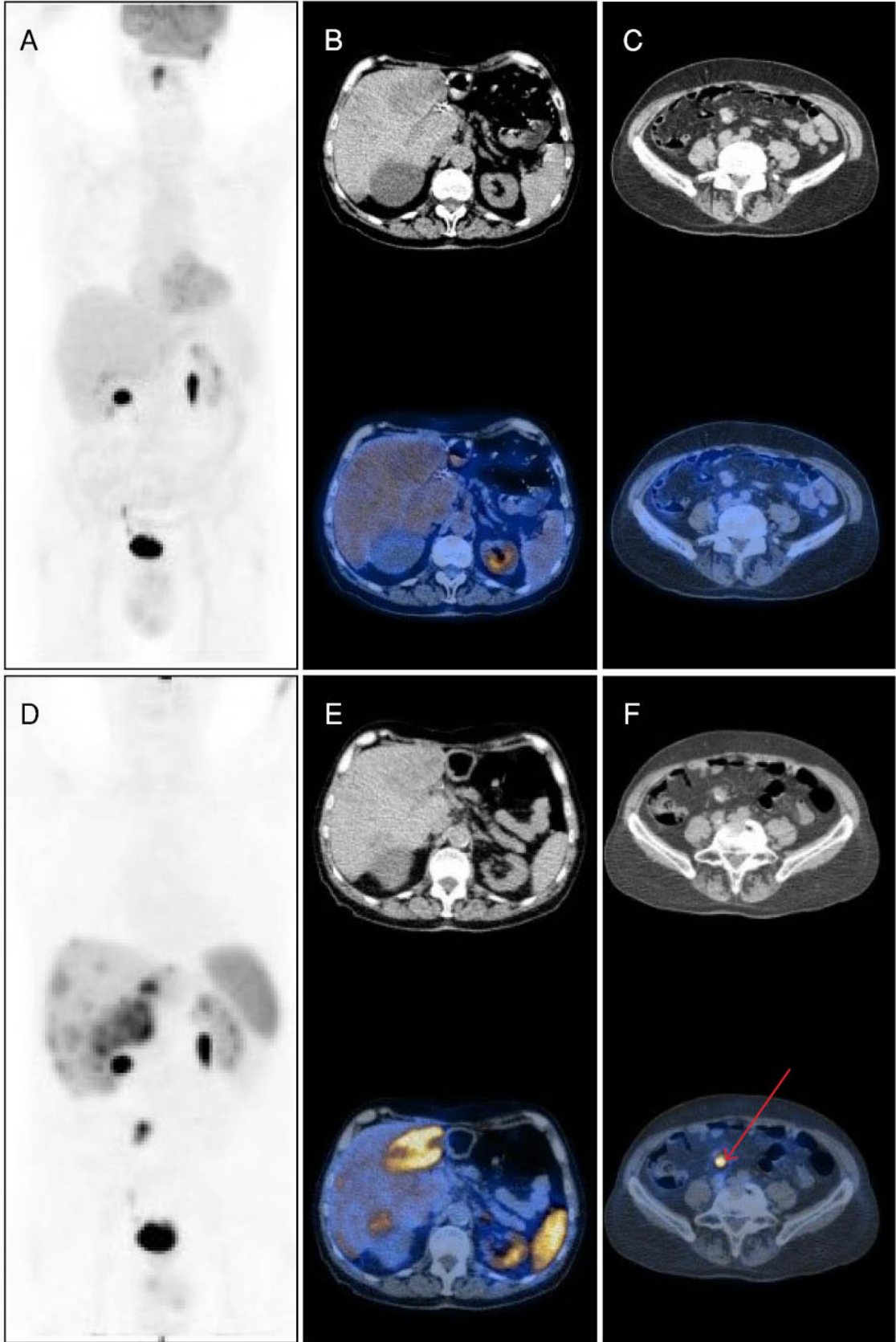
(A–C): ^{18}F -FDG MIP and transaxial CT and fused slices of upper abdomen and pelvis; (D–F): ^{68}Ga -DOTANOC, same slices as in (A–C).

There is no ^{18}F -FDG uptake in the liver or bowel (A–C). ^{68}Ga -DOTANOC PET–CT shows increased uptake in multiple liver lesions and a focal uptake in a loop of the ileum, suspected to be the primary tumour (F, red arrow). At surgery, a well differentiated NET, G1 (Ki-67 2%), was diagnosed.

Teaching point

PET–CT is the imaging method of choice in cases of metastatic cancer of unknown primary origin, and specifically ^{68}Ga -DOTA-peptides are the tracers of choice in cases of suspected NET of the abdomen. ^{18}F -FDG may be negative, especially in well differentiated NETs (G1).

Keywords: Unknown primary origin, ileum, ^{68}Ga -DOTANOC, ^{18}F -FDG



Clinical indication for PET–CT: Endobronchial carcinoid, staging

Clinical history

A 33 year old man with persistent cough and wheezing, not responsive to bronchodilators, had a CT that showed an endobronchial node in the left main bronchus. Bronchoscopy biopsy diagnosed carcinoid.

PET–CT findings

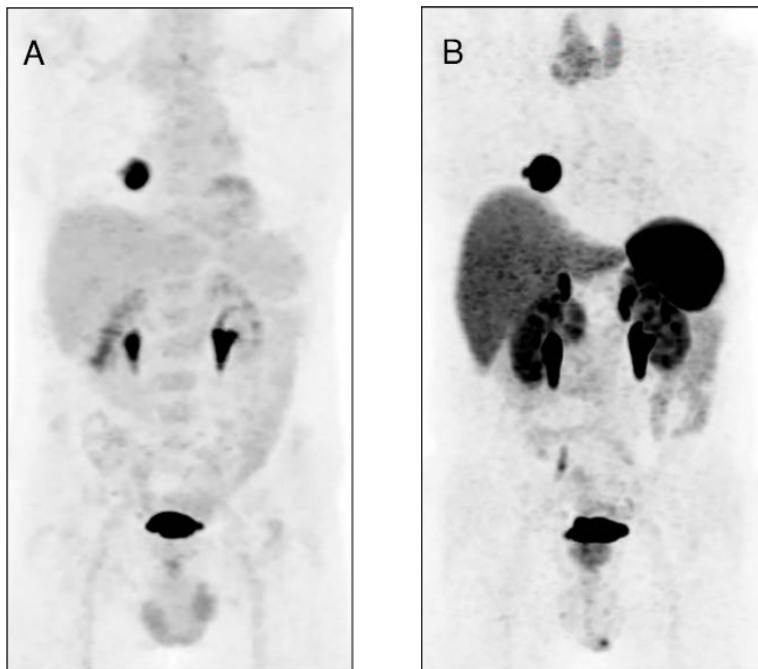
(A): ^{18}F -FDG MIP; (B): ^{68}Ga -DOTATATE MIP.

There is abnormal ^{68}Ga -DOTATATE uptake in a nodular lesion protruding into the left main bronchus, consistent with the known primary tumour. There is additional focal uptake in the left adrenal gland (C), confirmed by MRI to be an adenoma.

Teaching point

Endobronchial carcinoid is, as a rule, a well differentiated tumour, and thus shows high ^{68}Ga -DOTATATE uptake. Adrenal adenomas can be ^{68}Ga -DOTATATE avid.

Keywords: Endobronchial carcinoid, adrenal adenoma, ^{68}Ga -DOTATATE



Clinical indication for PET–CT: NET of the pancreas, staging

Clinical history

Incidentally found NET of the pancreas, G2 (Ki-67 5%).

PET–CT findings

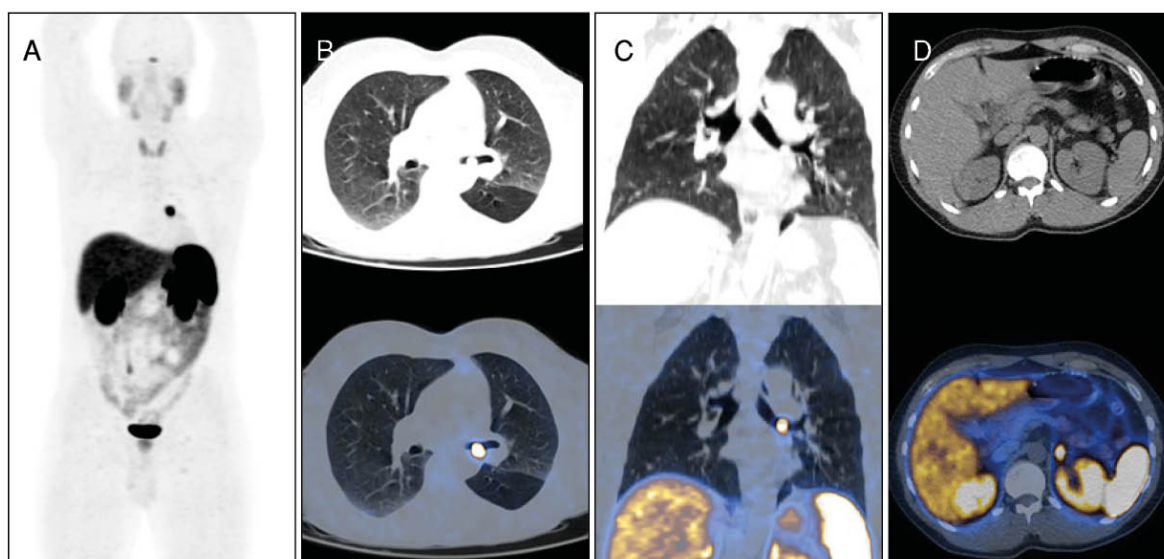
(A): ^{68}Ga -DOTANOC MIP; (B): CT and fused transaxial and coronal slices of thorax; (C): CT and fused transaxial slices of abdomen.

There are multiple areas of increased ^{68}Ga -DOTANOC uptake in the pancreas, liver and abdominal LNs (A). Note also focal uptake in 5 mm left supraclavicular LN (B).

Teaching point

^{68}Ga -DOTA-peptides can show very intense uptake even in small lesions, such as a LN in this case. The intensity of uptake depends on the number of receptors expressed by the tissue.

Keywords: NET, staging, ^{68}Ga -DOTANOC



Clinical indication for PET–CT: Primary NET of lung, staging

Clinical history

A patient with a lung mass was referred for ^{18}F -FDG imaging for staging. Subsequent biopsy diagnosed a moderately differentiated NET, G2 (Ki-67 8%). The patient was then referred for a second PET–CT study with ^{68}Ga -DOTANOC for staging.

PET–CT findings

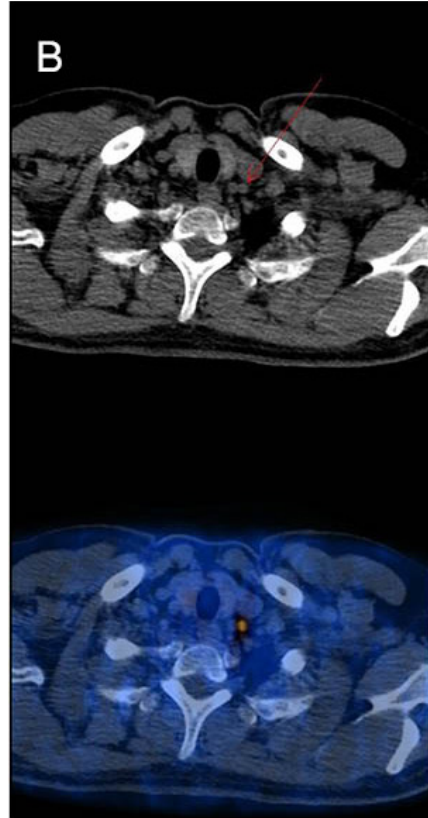
(A): ^{68}Ga -DOTANOC MIP; (B): CT and fused transaxial images.

There is increased focal ^{18}F -FDG uptake in the right lung nodule with no additional findings (A). ^{68}Ga -DOTANOC also shows intense uptake in the lung lesion, as well as in the thyroid, related to known De Quervin thyroiditis (B).

Teaching point

^{18}F -FDG and ^{68}Ga -DOTA-peptides can both be positive in G2 NETs, mainly in large tumours that can show variable grades of differentiation. Moreover, inflammatory cells within the lesion can also cause ^{18}F -FDG uptake. A positive ^{18}F -FDG study is an indicator of bad prognosis. Note the intense uptake of ^{68}Ga -DOTANOC in the thyroid due to the presence of a granulomatous disease.

Keywords: Lung NET, tissue characterization, thyroiditis, ^{68}Ga -DOTANOC, ^{18}F -FDG



Clinical indication for PET–CT: Moderately differentiated NET of pancreas (Ki-67 8%), staging

Clinical history

A 68 year old man with metastatic pancreatic NET was referred for staging.

PET–CT findings

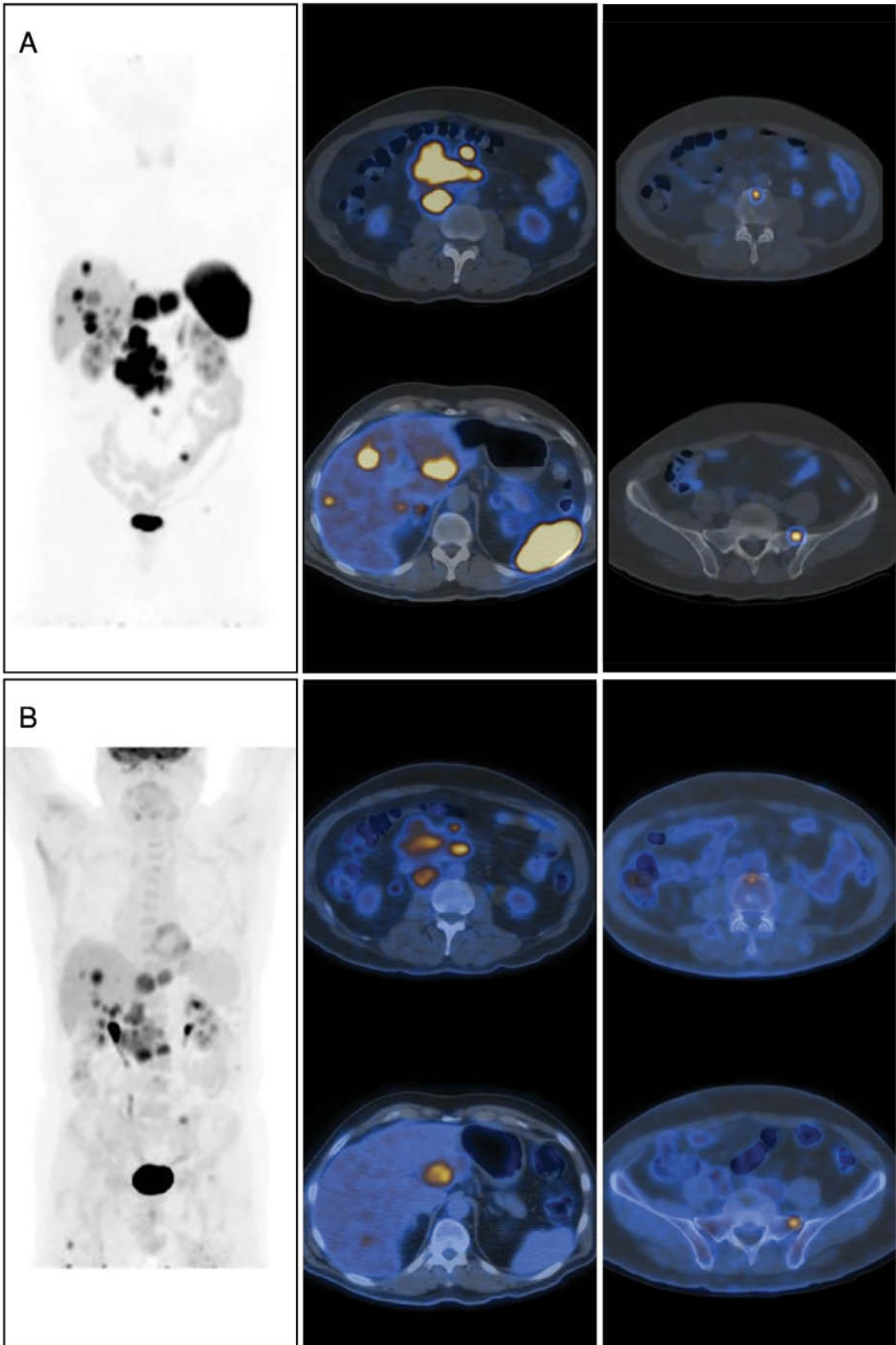
(A): ^{68}Ga -DOTANOC MIP, CT and fused transaxial slices of upper abdomen and pelvis; (B): ^{18}F -FDG, same slices as in (A).

^{68}Ga -DOTANOC shows intense pathologic uptake in the known pancreatic primary tumour and in known nodal and liver metastases, and also identifies previously unknown bone lesions (A). ^{18}F -FDG confirms the pathologic uptake in the pancreas, LNs, and some of the known liver and bone lesions (B).

Teaching point

The combined use of ^{18}F -FDG and ^{68}Ga -DOTANOC PET–CT studies provides complementary information regarding the different biological disease characteristics. This can be important for accurate selection of patients scheduled for radionuclide therapy as well as for assessment of outcome.

Keywords: NET, staging, ^{68}Ga -DOTANOC, ^{18}F -FDG



Clinical indication for PET–CT: MTC, staging

Clinical history

A 70 year old man with newly diagnosed MTC and suspicion of distant metastases on CT.

PET–CT findings

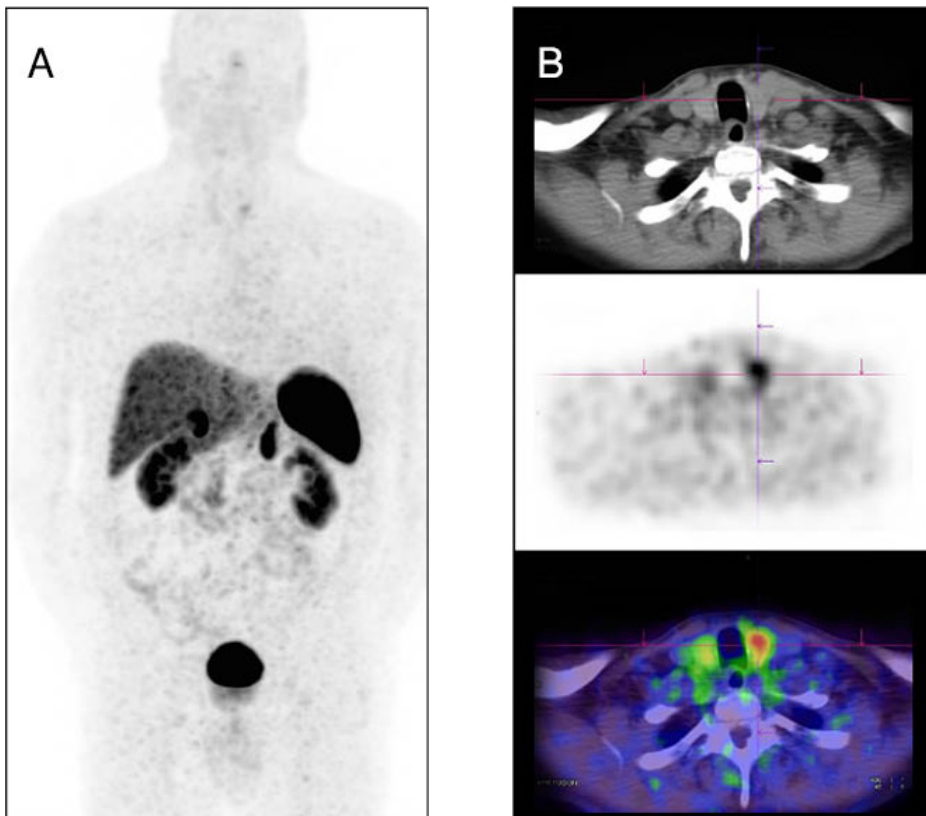
(A): MIP; (B): CT, PET and fused transaxial slices of lower neck.

There is increased ^{68}Ga -DOTANOC uptake of moderate intensity in the known tumour in the left lobe of the thyroid, with no additional findings.

Teaching point

PET–CT with ^{68}Ga -DOTA-peptides may be helpful in the staging of MTC, even though uptake can be variable.

Keywords: Medullary thyroid cancer, ^{68}Ga -DOTANOC



Clinical indication for PET-CT: Metastatic NET, potential eligibility for peptide receptor radionuclide therapy

Clinical history

A 63 year old man with pancreatic NET, with metastases seen on CT (A).

PET-CT findings

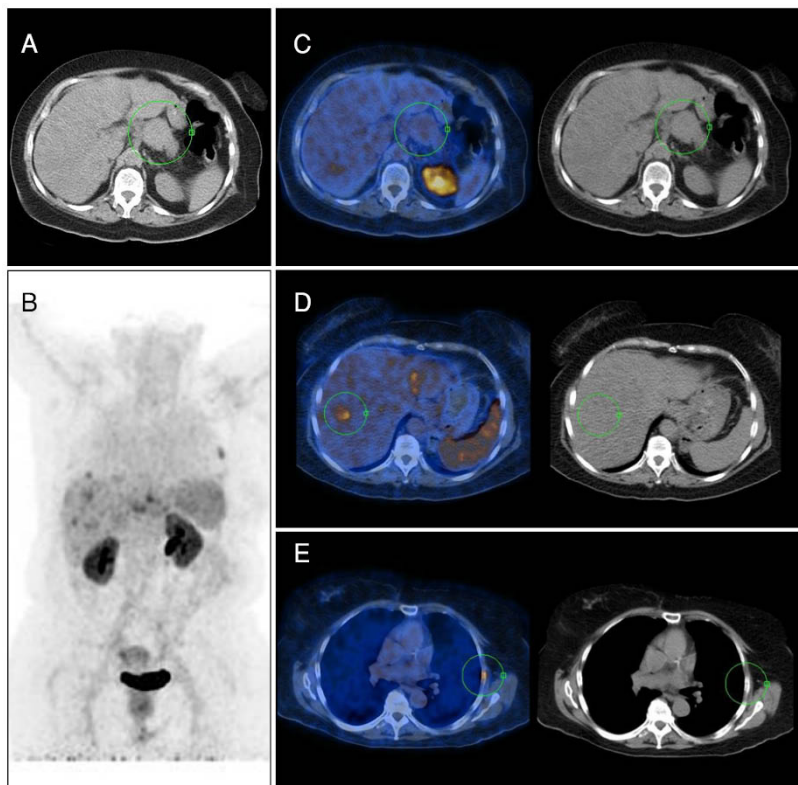
(A): CT transaxial slice of abdomen; (B): MIP; (C-E): fused and CT transaxial slices of upper and mid-abdomen and thorax.

There is almost no somatostatin receptor analogue uptake in the pancreatic NET (C), and only low uptake in the liver metastases (D) and in a previously unknown bone lesion (E).

Teaching point

⁶⁸Ga-DOTANOC PET-CT is mandatory for identifying candidates for peptide receptor radionuclide therapy. Patients with low tracer uptake may not benefit from this therapeutic approach.

Keywords: Radionuclide therapy, ⁶⁸Ga-DOTANOC



Clinical indication for PET–CT: Metastatic NET of pancreas, baseline prior to treatment

Clinical history

A 59 year old patient with NET of the pancreas, with liver and bone metastases, was referred for baseline evaluation to further assess response to somatostatin therapy.

PET–CT findings

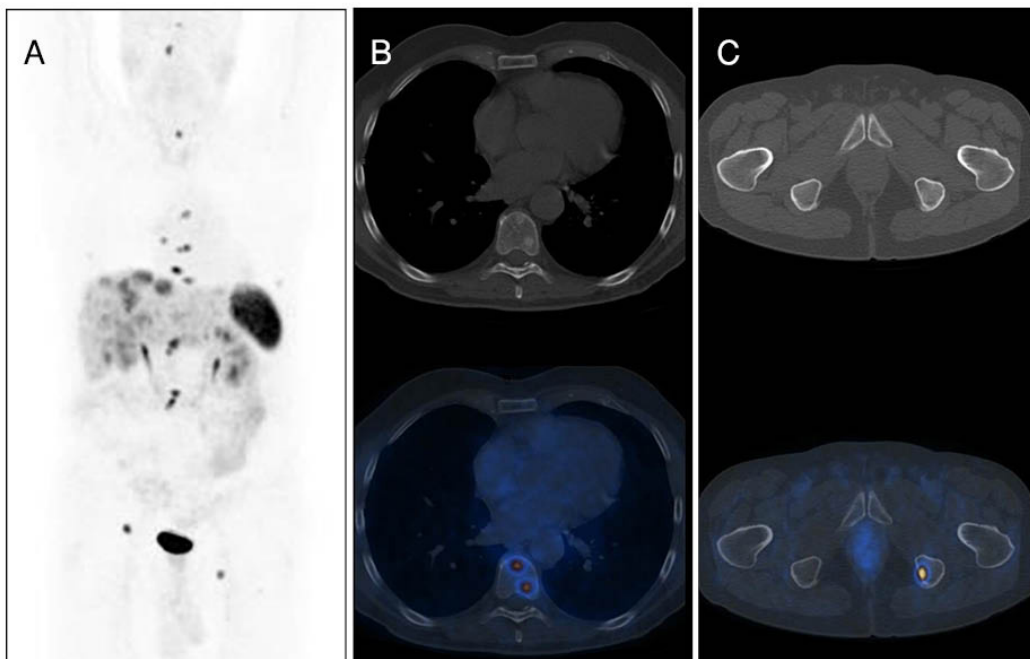
(A): MIP; (B): CT and fused transaxial slices of mid-thorax; (C) same images at level of pelvis.

There are multiple foci of increased ⁶⁸Ga-DOTANOC uptake in the liver and bone.

Teaching point

The presence of increased tracer uptake in multiple small lesions makes the patient a candidate for systemic treatment with ¹⁷⁷Lu-DOTA-peptides. Note the absence of any significant CT findings in the bone metastases.

Keywords: ⁶⁸Ga-DOTANOC, ¹⁷⁷Lu-DOTA-peptide treatment



Clinical indication for PET–CT: NET of pancreas, monitoring response to peptide receptor radionuclide therapy

Clinical history

Same patient as in Case 20.14. Repeat ^{68}Ga -DOTANOC PET–CT was performed after 6 cycles of ^{177}Lu -DOTA-peptide treatment.

PET–CT findings

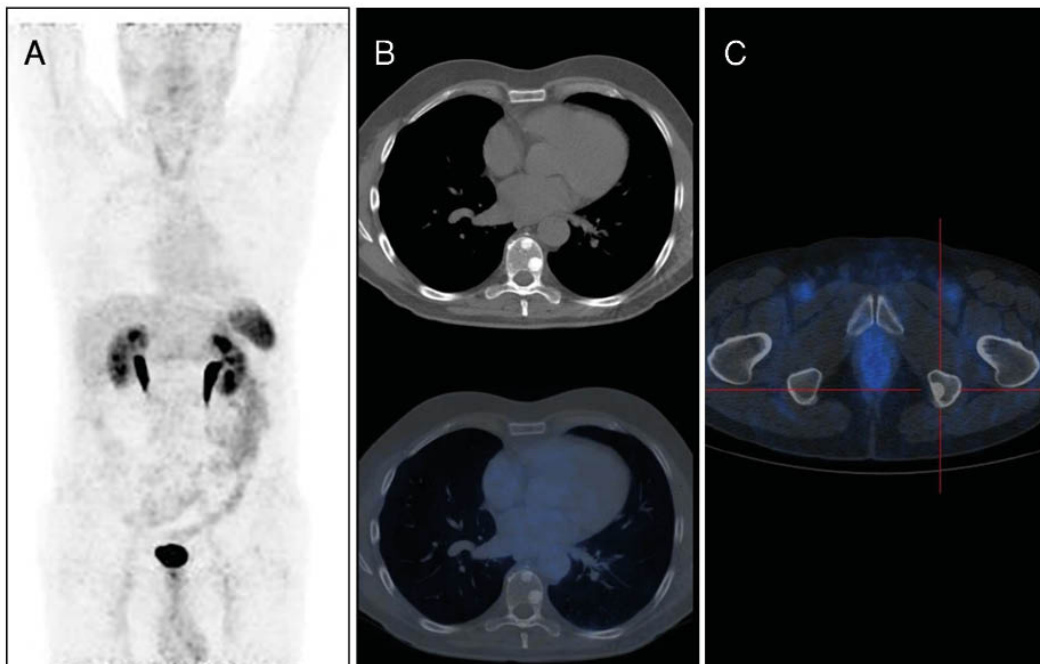
(A): MIP; (B): CT and fused transaxial slices of mid-thorax; (C): fused transaxial slice of pelvis.

No areas of abnormal ^{68}Ga -DOTANOC activity are seen. Note the new osteoblastic bone lesions on CT, a characteristic sign of response to treatment. However, without a comparison with the baseline PET–CT (see Case 20.14) the significance of these CT findings may have been difficult to interpret. A baseline study is mandatory in order to increase the accuracy of post-treatment evaluation.

Teaching point

A pre-treatment study is of value to assess therapeutic response.

Keywords: Treatment response assessment, ^{68}Ga -DOTANOC



Clinical indication for PET–CT: Meningioma, RT planning

Clinical history

A 70 year old man with a meningioma of the base of skull was referred prior to RT planning.

PET–CT findings

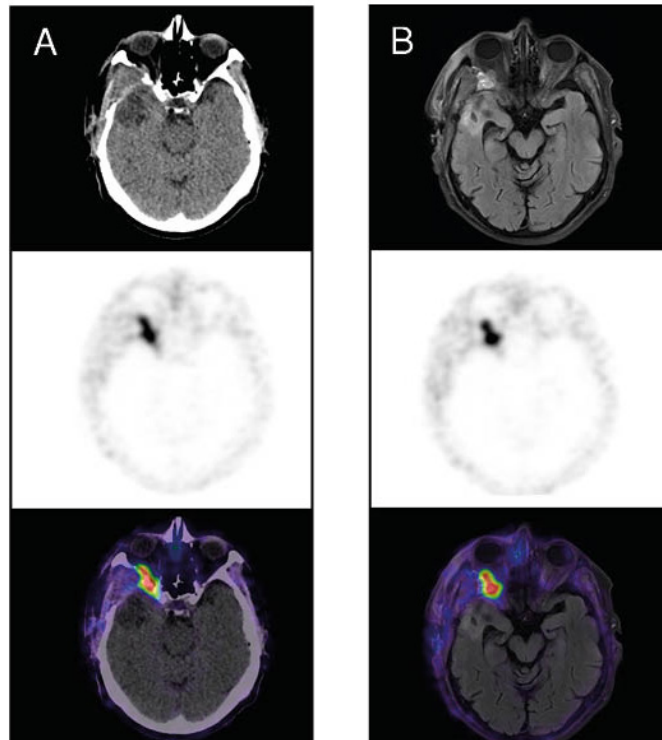
(A): CT, PET and fused transaxial slices of head; (B): MRI, PET and fused PET, same slices as in (A).

There is intense ^{68}Ga -DOTATATE uptake in the right sphenoidal bone with an extension into the orbital cavity, corresponding to the known meningioma. The lesion in bone is more precisely delineated than with MRI.

Teaching point

^{68}Ga -DOTA-peptide PET–CT allows for a precise delineation of the target volume of the skull base meningioma, which is often complex to achieve with a combination of CT and MRI.

Keywords: Meningioma, RT planning, ^{68}Ga -DOTATATE



Clinical indication for PET–CT: Paraganglioma, suspected recurrence

Clinical history

A 39 year old patient with a previous history of paraganglioma. Follow-up CT raised the suspicion of a relapse in thorax.

PET–CT findings

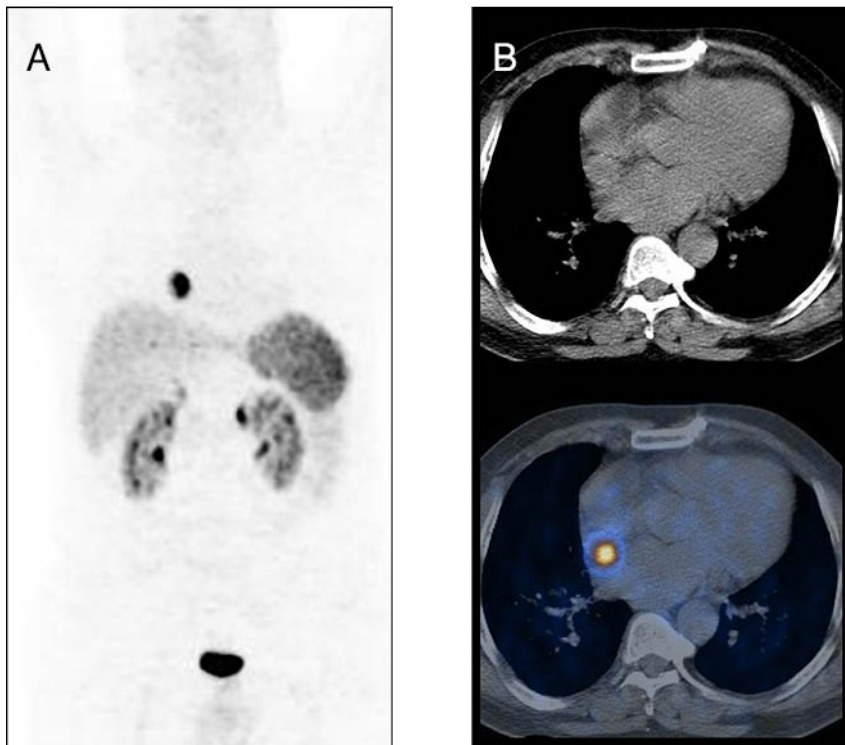
(A): MIP; (B): CT and fused transaxial slices of mid-thorax.

There is intense focal ⁶⁸Ga-DOTANOC uptake in a para-caval, round lesion. Note the high tumour to background ratio.

Teaching point

⁶⁸Ga-DOTANOC is the imaging method of choice to diagnose paraganglioma. In most cases the diagnosis is facilitated by the high tumour to background ratio.

Keywords: Paraganglioma, ⁶⁸Ga-DOTANOC



Clinical indication for PET–CT: NET of pancreas, suspected relapse

Clinical history

A 63 year old man with known pancreatic NET.

PET–CT findings

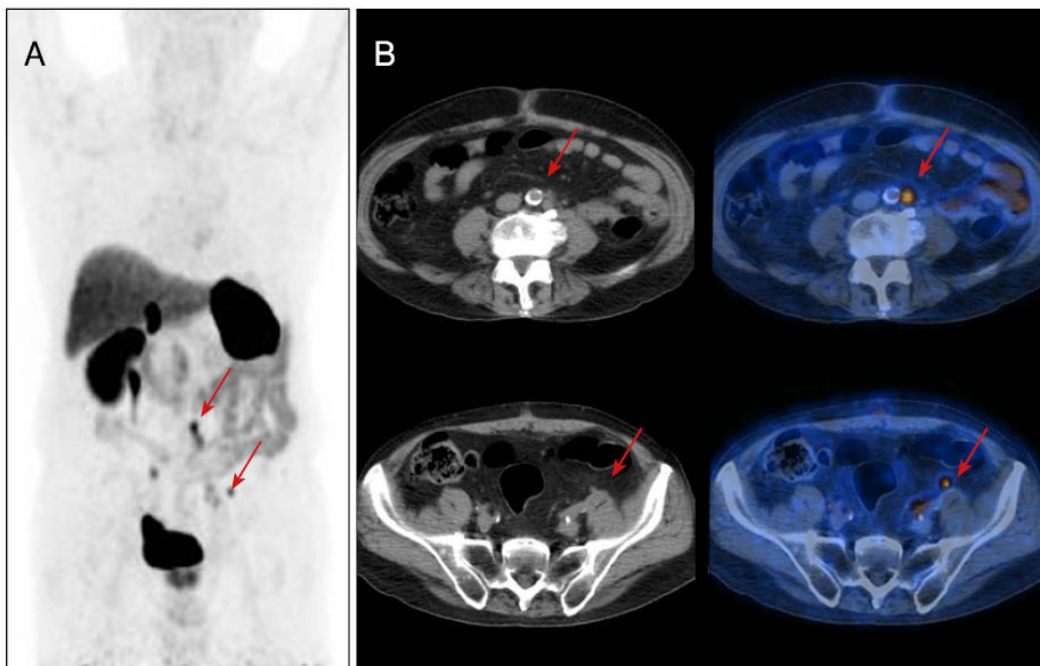
(A): MIP; (B): CT and fused transaxial slices of lower abdomen and pelvis.

There is intense ^{68}Ga -DOTANOC uptake in small (up to 8 mm) LNs (arrows), consistent with recurrence.

Teaching point

^{68}Ga -DOTANOC PET–CT has a higher sensitivity for detection of relapse than other imaging modalities.

Keywords: NET, LN relapse, ^{68}Ga -DOTANOC



Clinical indication for PET–CT: NET of pancreas, suspected relapse

Clinical history

A 63 year old man with well differentiated pancreatic NET (Ki-67 2%). Follow-up CT detected a suspicious lesion in the liver (A). The patient was referred for restaging.

PET–CT findings

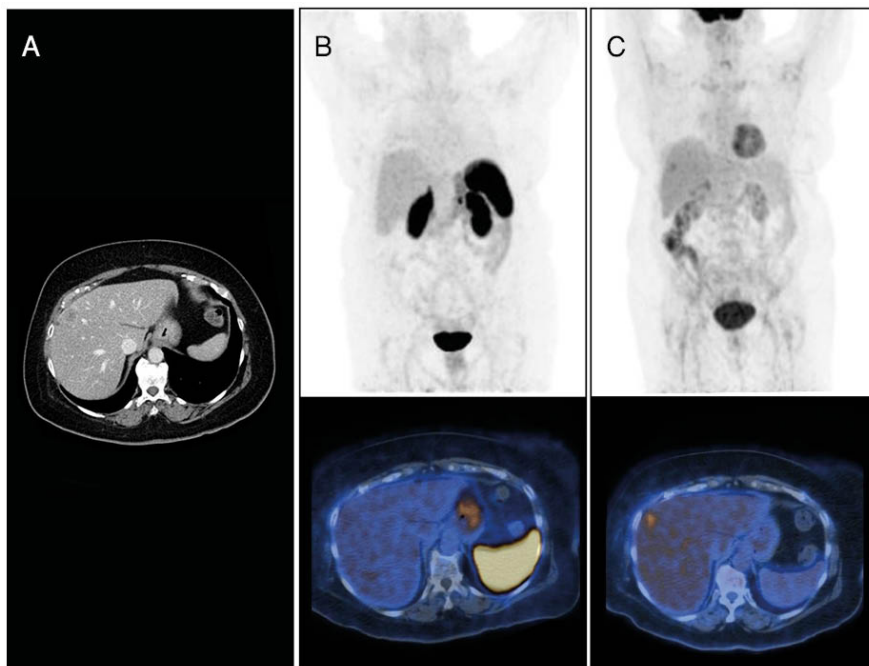
(A): CT image of upper abdomen; (B): ^{68}Ga -DOTANOC MIP and fused transaxial slice of upper abdomen; (C): ^{18}F -FDG, same images as in (B).

Only physiological ^{68}Ga -DOTANOC activity is demonstrated, with no evidence of liver relapse (B). ^{18}F -FDG shows mild pathologic uptake in the liver, confirming metastatic involvement (C).

Teaching point

The discrepancy between the positive ^{18}F -FDG and negative ^{68}Ga -DOTANOC studies in this case is probably due to the dedifferentiation of the tumour between the time of Ki-67 evaluation and imaging. Negative ^{68}Ga -DOTANOC PET–CT does not exclude recurrence.

Keywords: NET dedifferentiation, ^{68}Ga -DOTANOC



Clinical indication for PET–CT: NET, follow-up

Clinical history

A 70 year old man with NET, treated with octreotide.

PET–CT findings

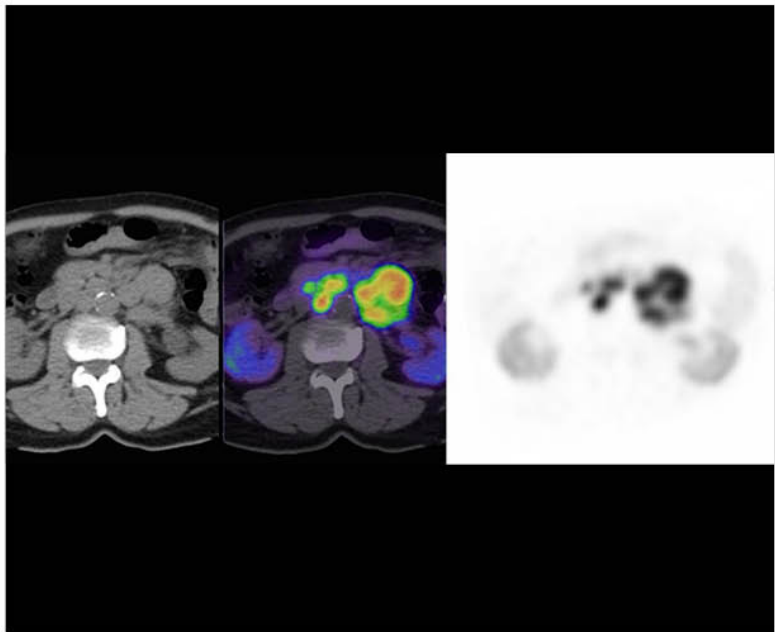
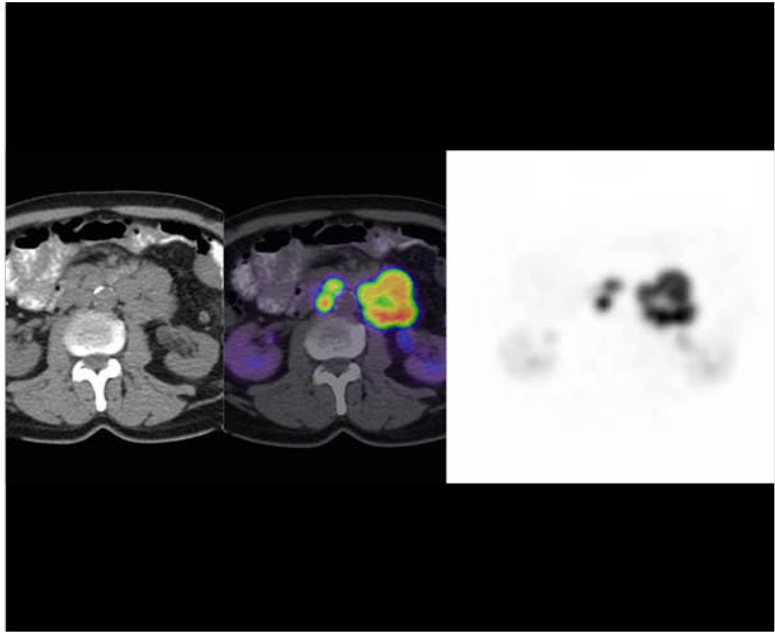
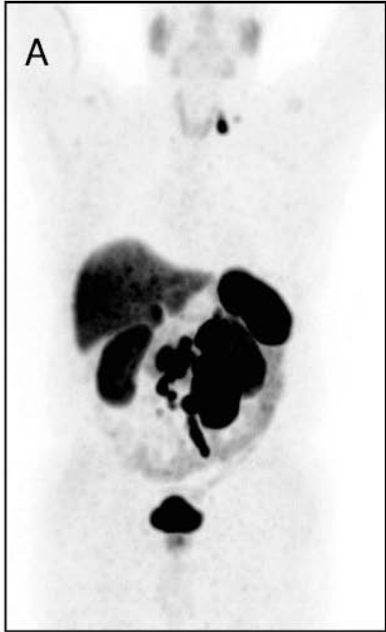
(A): ^{68}Ga -DOTATATE MIP, and CT, PET and fused transaxial slices of upper abdomen; (B): ^{68}Ga -DOTANOC, same slices as in (A).

^{68}Ga -DOTATATE and ^{68}Ga -DOTANOC performed 1 year apart show similar uptake in the NET lesions, but the uptake in liver, salivary glands and thyroid is higher with ^{68}Ga -DOTATATE (A).

Teaching point

The diagnostic performance of various ^{68}Ga -DOTA-peptides is very similar, with slight differences in their biodistribution.

Keywords: NET, ^{68}Ga -DOTANOC, ^{68}Ga -DOTATATE



Clinical indication for PET–CT: NET, follow-up

Clinical history

A 68 year old woman with NET of the midgut and liver metastases, treated with octreotide.

PET–CT findings

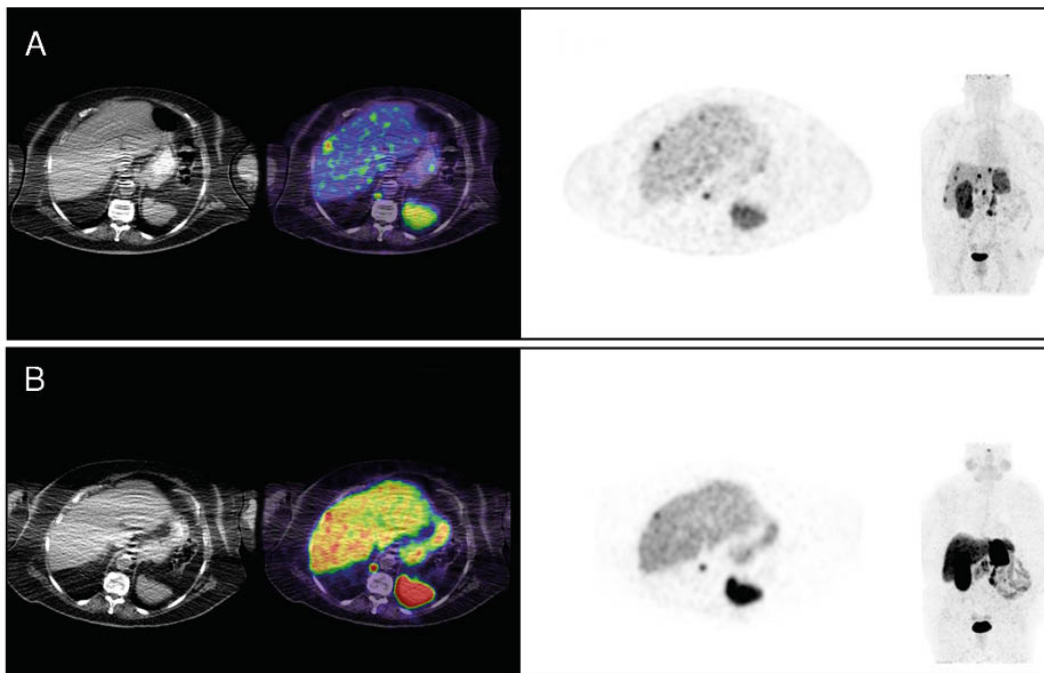
(A): ^{68}Ga -DOTANOC CT, fused and PET transaxial slices of mid-abdomen and MIP; (B): ^{68}Ga -DOTATATE, same slices as in (A).

The two studies performed 8 months apart show similar uptake in the metastatic lesions. However, due to the higher physiologic liver uptake in the ^{68}Ga -DOTATATE study, more metastases are identified with ^{68}Ga -DOTANOC.

Teaching point

Small liver metastases can be detected with higher sensitivity with ^{68}Ga -DOTANOC than with ^{68}Ga -DOTATATE.

Keywords: NET, liver metastases, ^{68}Ga -DOTANOC, ^{68}Ga -DOTATATE



Clinical indication for PET–CT: Recurrent gastrinoma

Clinical history

A 30 year old woman with history of gastrinoma presented with increasing levels of chromogranin A.

PET–CT findings

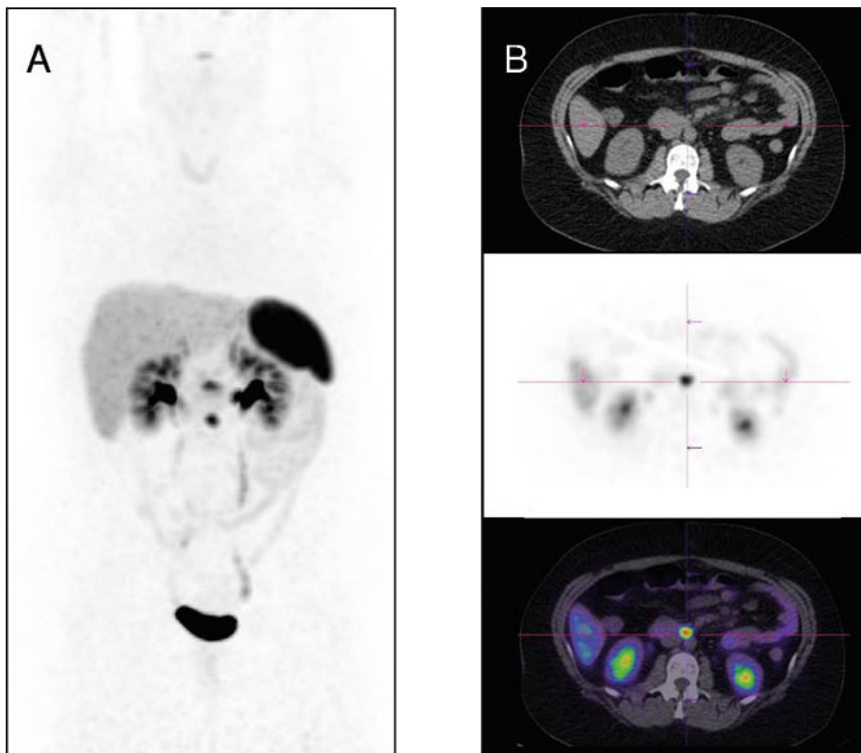
(A): MIP; (B): CT, PET and fused transaxial slices of mid-abdomen.

There is increased ^{68}Ga -DOTANOC uptake in a small retroperitoneal LN, consistent with relapse.

Teaching point

PET–CT with ^{68}Ga -DOTA-peptides is highly sensitive for detecting and staging recurrent NET.

Keywords: Gastrinoma, ^{68}Ga -DOTANOC



Clinical indication for PET–CT: Recurrent MTC

Clinical history

A 56 year old man with MTC, post-thyroidectomy, presented with progressive increase in calcitonin levels (up to 19 200 ng/L).

PET–CT findings

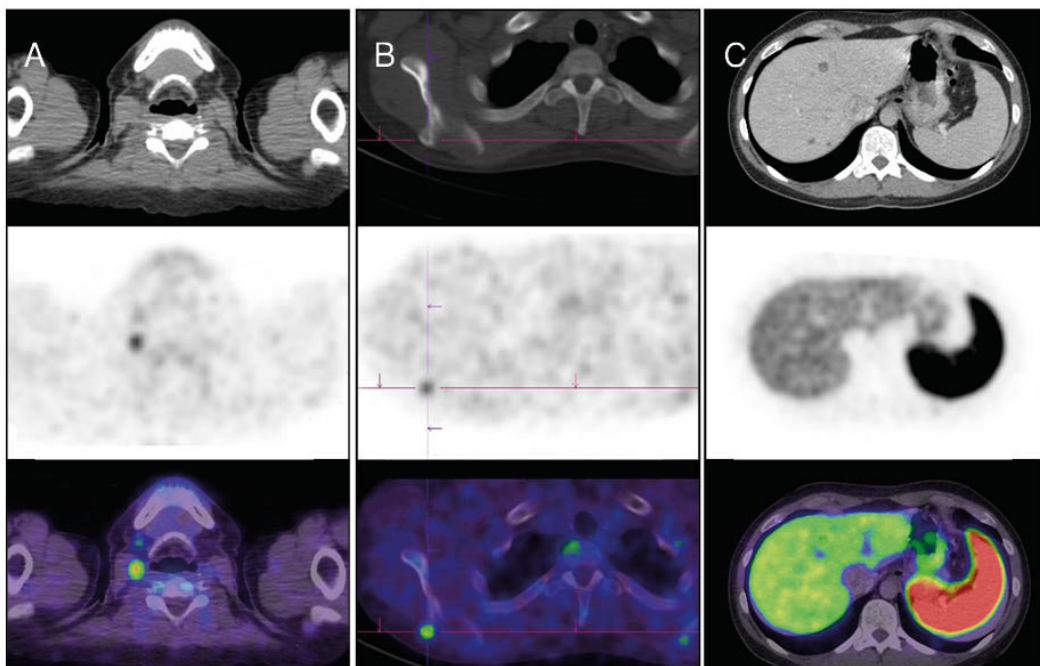
(A): CT, PET and fused transaxial slices of neck; (B): same images at level of thorax, (C): same images at level of liver.

There is increased ^{68}Ga -DOTANOC in a cervical LN and in a lesion in the right scapula. Additional metastases are seen on the diagnostic CT, but due to the high background uptake they are not identified on the PET component.

Teaching point

Although whole body PET–CT is capable of identifying metastases in various locations, when the tracer uptake intensity is low, such as in this case, lesions in organs with high background activity may be missed.

Keywords: MTC, metastases, ^{68}Ga -DOTANOC



Clinical indication for PET–CT: Lung carcinoid, post-operative restaging

Clinical history

A 60 year old man with lung carcinoid was referred for restaging after surgery.

PET–CT findings

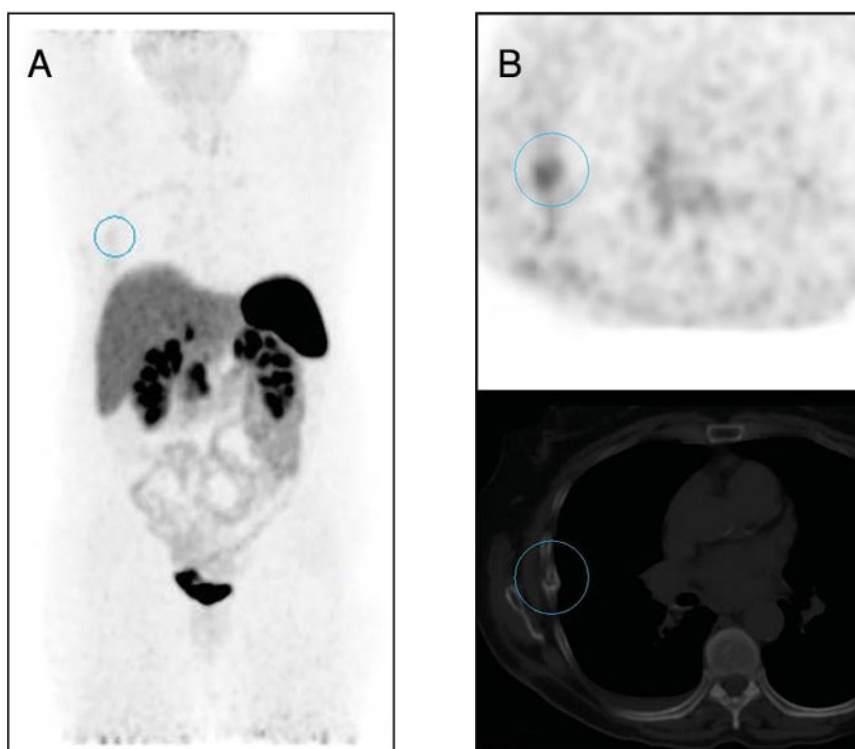
(A): MIP, (B): PET and CT transaxial slices of mid-thorax.

There is faint focal ^{68}Ga -DOTATOC uptake in a rib fracture seen on CT.

Teaching point

^{68}Ga -DOTATOC is not specific for NETs. Benign lesions may also show uptake.

Keywords: Rib fracture, ^{68}Ga -DOTATOC



Clinical indication for PET–CT: NET of pancreas, suspected recurrence

Clinical history

A 51 year old woman with a pancreatic NET resected 3 years earlier presented with elevated chromogranin A levels.

PET–CT findings

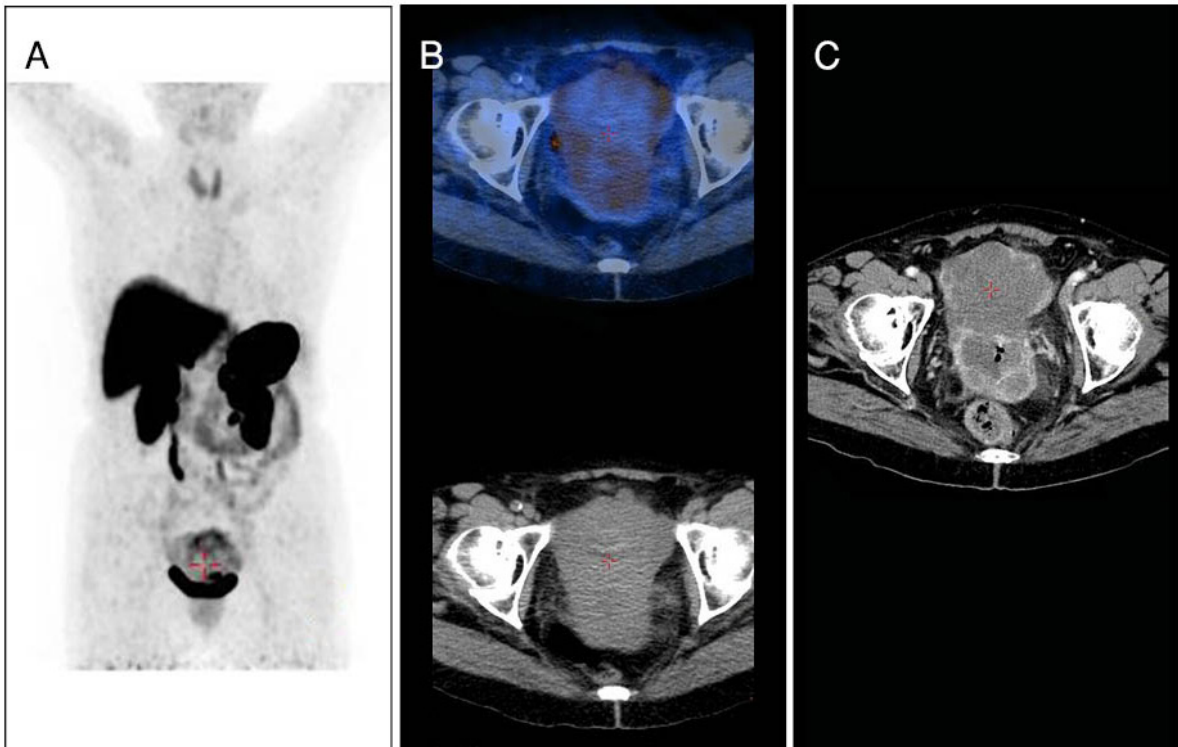
(A): MIP; (B): CT and fused transaxial slices of pelvis; (C): contrast enhanced CT transaxial slice of pelvis.

There is moderate expression of somatostatin receptor analogues in the uterus. Contrast enhanced CT (C) suggested an adenocarcinoma of the uterus, which was confirmed at surgery.

Teaching point

⁶⁸Ga-DOTANOC PET–CT is not specific for NETs. Other tumours such as, in this case, adenocarcinoma of the uterus, can show uptake.

Keywords: Adenocarcinoma of uterus, ⁶⁸Ga-DOTANOC



Clinical indication for PET–CT: Bronchial carcinoid, restaging

Clinical history

A 46 year old woman with bronchial carcinoid.

PET–CT findings

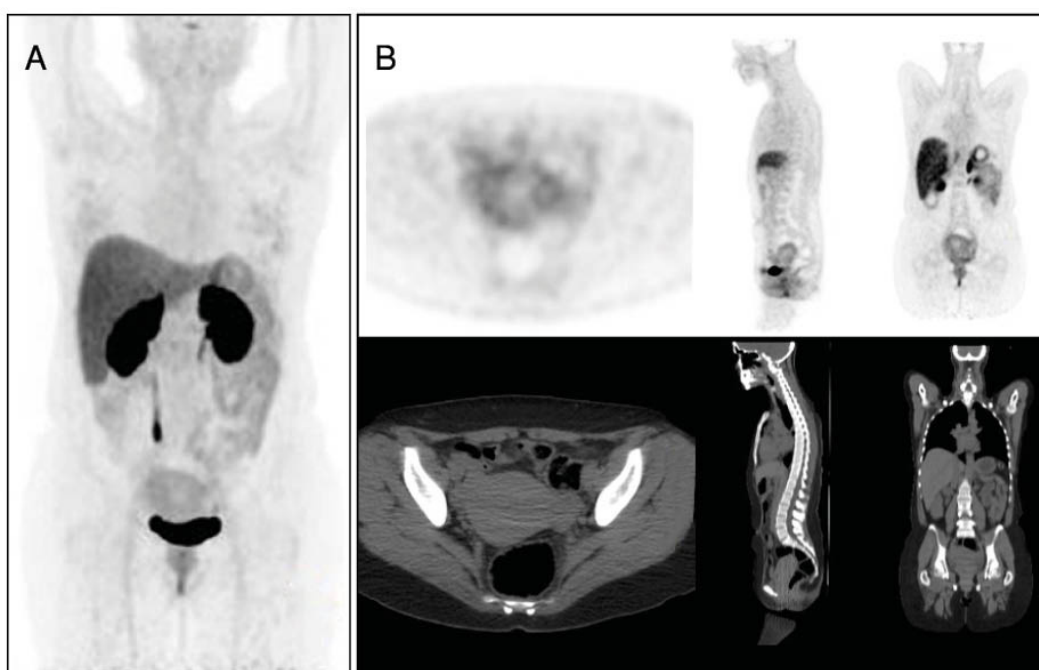
(A): MIP; (B): transaxial, coronal, sagittal PET and CT.

There is mild ^{68}Ga -DOTANOC uptake in the uterus in a patient with known leiomyomatosis uteri.

Teaching point

Myomatous uterus in pre-menopausal women is a potential pitfall in ^{68}Ga -DOTANOC PET–CT.

Keywords: Leiomyomatosis uteri, ^{68}Ga -DOTANOC



Clinical indication for PET–CT: Suspected NET (increased pancreatic polypeptide)

Clinical history

A 17 year old man with known Von Hippel–Lindau disease presented with increased levels of pancreatic polypeptide.

PET–CT findings

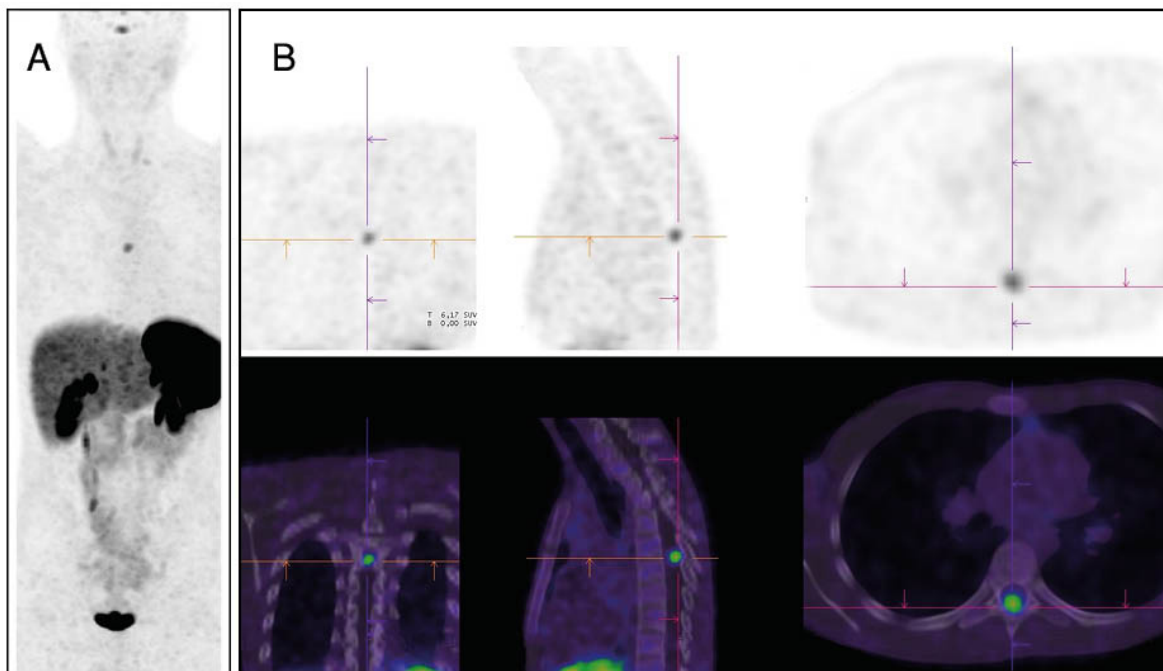
(A): MIP; (B): PET and fused coronal, sagittal and transaxial slices of thorax.

There is intramedullary focal ^{68}Ga -DOTANOC uptake in the T8 vertebra. MRI further identified a hemangioblastoma.

Teaching point

Hemangioblastomas are lesions that consistently display high uptake of ^{68}Ga -DOTA-peptides.

Keywords: Hemangioblastoma, ^{68}Ga -DOTANOC



Clinical indication for PET–CT: Midgut NET, post-operative follow-up

Clinical history

A 69 year old woman with a history of NET resected one year earlier, and a right upper lobe lung adenocarcinoma treated by chemoradiation 4 years earlier.

PET–CT findings

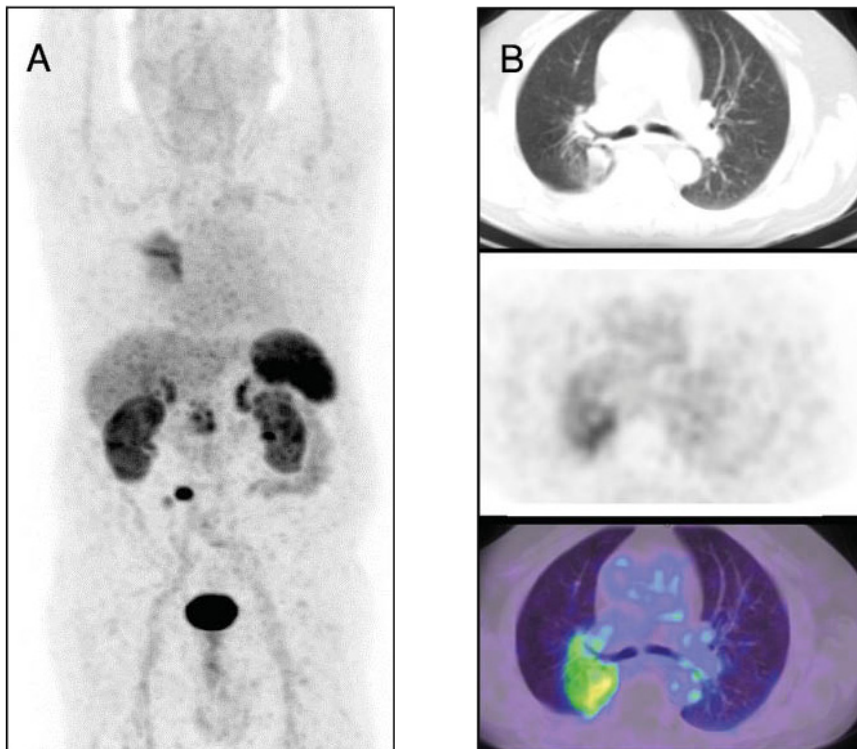
(A): MIP; (B): CT, PET and fused transaxial slices of mid-thorax.

There is abnormal ⁶⁸Ga-DOTANOC uptake in multiple sites of recurrent disease, as well as moderately increased uptake in the previously irradiated right lung parenchyma.

Teaching point

⁶⁸Ga-DOTA-peptides are taken up by various inflammatory conditions, such as post-radiation changes.

Keywords: NET, post-radiation changes, ⁶⁸Ga-DOTANOC



Clinical indication for PET–CT: NET of pancreas, restaging after surgery

Clinical history

A 57 year old woman with NET of the tail of pancreas (G1), post-spleno-pancreatectomy, was referred for suspected relapse in a peripancreatic LN.

PET–CT findings

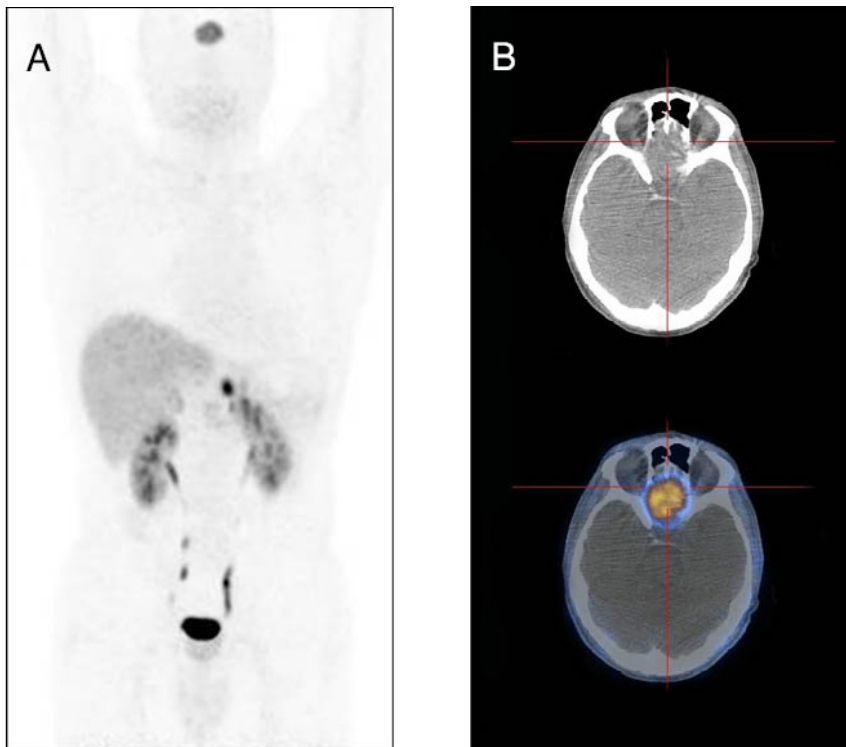
(A): MIP; (B): CT and fused transaxial slices of base of skull.

There is increased ^{68}Ga -DOTANOC uptake in a peripancreatic LN, consistent with relapse. In addition, there is intense uptake in a large lesion at the base of the skull, consistent with a meningioma (B). Note the high target to background ratio in the brain.

Teaching point

Increased ^{68}Ga -DOTANOC uptake is found in meningiomas. In case of doubtful findings with conventional imaging, ^{68}Ga -DOTA-peptides may improve diagnostic accuracy.

Keywords: Meningioma, ^{68}Ga -DOTANOC



Clinical indication for PET–CT: Suspected NET of pancreas

Clinical history

A 65 year old man with a suspected NET of the pancreas.

PET–CT findings

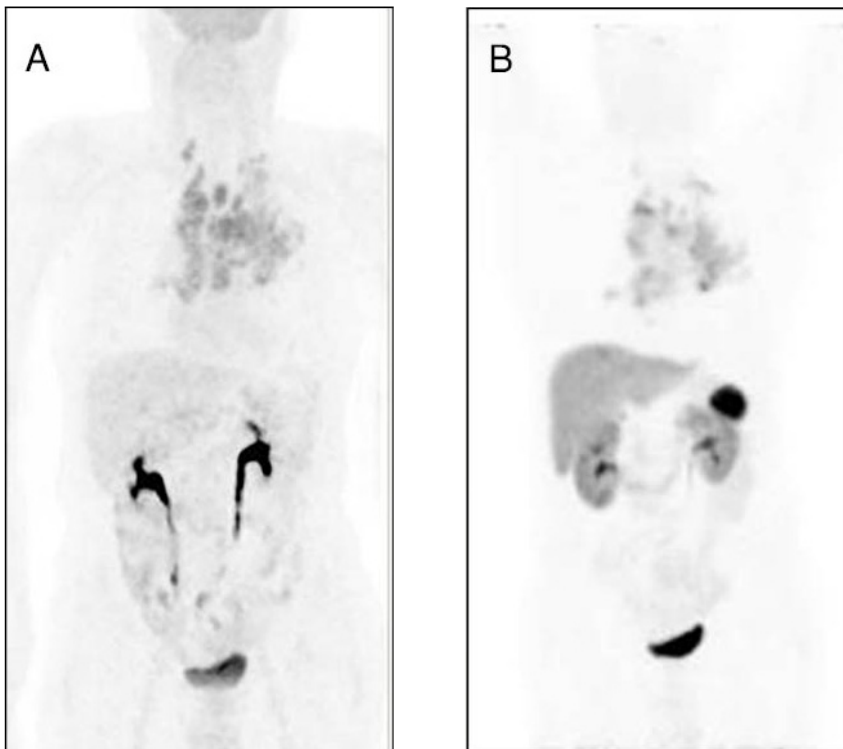
(A): ^{18}F -FDG MIP; (B): ^{68}Ga -DOTANOC MIP.

There is intense, symmetric ^{18}F -FDG uptake in mediastinal LNs, and no significant abnormal activity in the pancreas (A). There is similar, increased, symmetrical ^{68}Ga -DOTANOC uptake in mediastinal LNs, and no significant activity in the pancreas (B).

Teaching point

Increased uptake of ^{68}Ga -DOTANOC can be observed in chronic inflammatory processes since activated lymphocytes may overexpress SSTR. Chronic inflammatory processes can also demonstrate increased ^{18}F -FDG uptake.

Keywords: Chronic inflammation, ^{68}Ga -DOTANOC, ^{18}F -FDG



Clinical indication for PET–CT: Suspected carcinoid of right bronchus

Clinical history

A 62 year old patient with a suspected carcinoid of the right bronchus on CT.

PET–CT findings

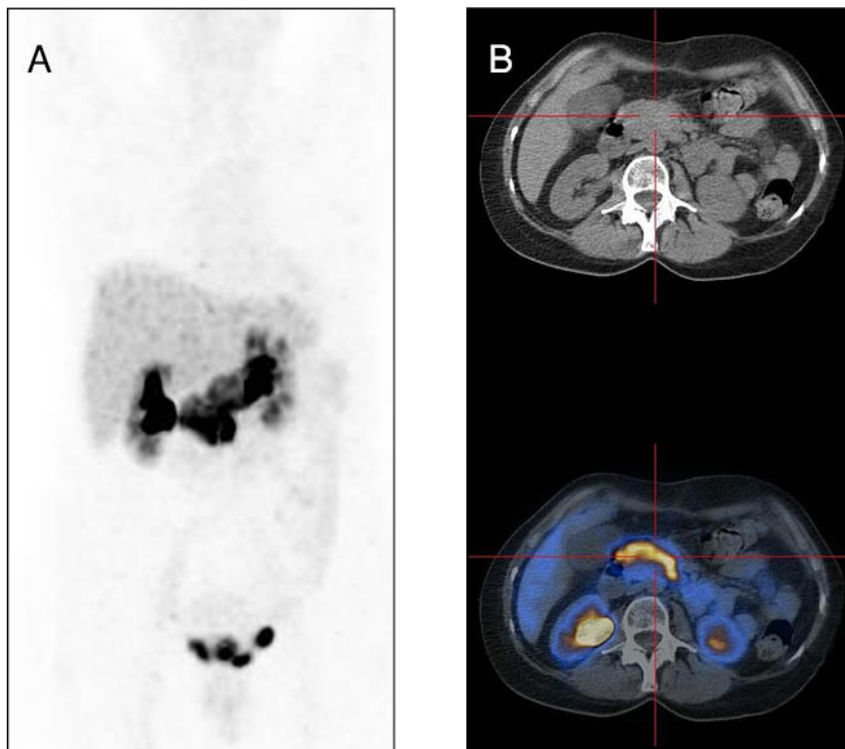
(A): MIP; (B): CT and fused transaxial slices of upper abdomen.

There is intense, inhomogeneous, increased ^{68}Ga -DOTANOC uptake in the pancreas, consistent with pancreatitis, a chronic inflammatory process. No significant uptake is seen in the right bronchus.

Teaching point

Increased uptake of ^{68}Ga -DOTANOC can be observed in chronic inflammation, since activated lymphocytes may overexpress SSTR.

Keywords: Chronic pancreatitis, ^{68}Ga -DOTANOC



21. TRASTUZUMAB (^{89}Zr)

21.1. GENERAL CHARACTERISTICS

Name: ^{89}Zr -trastuzumab

Synonyms: ^{89}Zr -Df-Bz-NCS-trastuzumab; ^{89}Zr labelled trastuzumab

Radioisotope

^{89}Zr is a long half-life PET radioisotope (78.4 hours) emitting positrons of E_{max} 395.5 keV, usually obtained from biomedical cyclotrons at proton energy of 14 MeV using natural ^{89}Y targets.

Radiosynthesis

^{89}Zr -trastuzumab is prepared for clinical use with a radiolabelling efficiency of $77.6\% \pm 3.9\%$, radiochemical purity of $98.1\% \pm 1.1\%$ and specific activity of 67.2 ± 2.4 MBq/mg (Fig. 21.1). The labelled monoclonal antibody was reported to be stable at 4°C with $<0.1\%$ degradation/day for up to 7 days [11, 80, 160–170].

21.2. PHARMACOKINETICS

21.2.1. Physiological biodistribution and metabolism

There are no direct reports on the metabolism of ^{89}Zr -trastuzumab, however it has been shown that trastuzumab is metabolized to peptides and amino acids. The elimination process in humans is complex and specifically mediated by epithelial cells. It depends on factors such as genetics and the clinical status of the patient. Trastuzumab binds to HER-2 and is metabolized intracellularly. The consequence of intracellular binding explains the dose dependent, non-linear elimination. The biological half-life of trastuzumab is approximately 28 days. The washout period is up to 24 weeks after cessation of trastuzumab treatment. The renal excretion of trastuzumab is very low [11, 80, 160, 161].

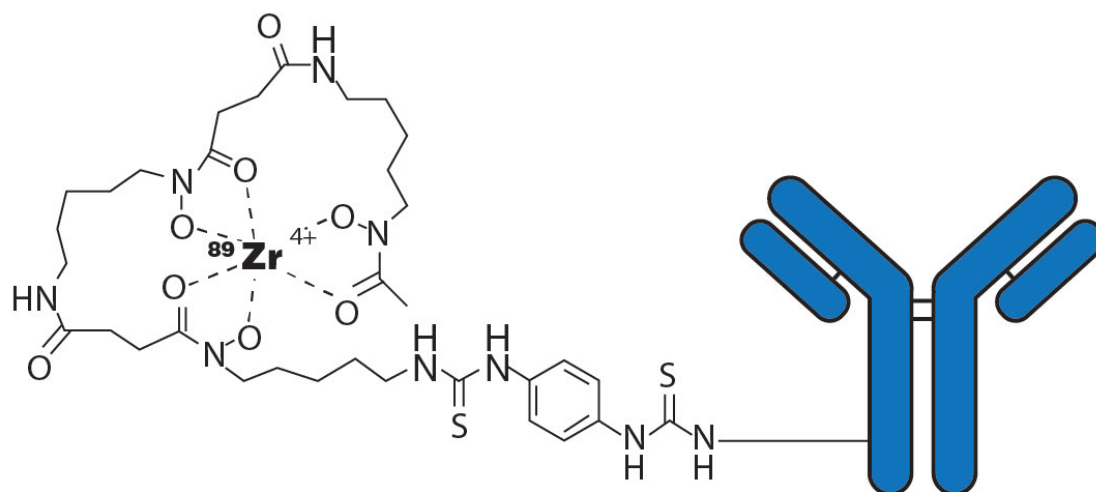


FIG. 21.1. Molecular structure of ^{89}Zr -trastuzumab.

21.2.2. Mechanism of retention

Trastuzumab is a humanized monoclonal antibody that targets HER2, which is overexpressed in some malignant and premalignant lesions and can therefore be used in PET imaging of these diseases [11, 80, 160, 161].

21.2.3. Pharmacology and toxicology

No data are available directly for ^{89}Zr -trastuzumab; however, the cold antibody (Herceptin) dose used in chemotherapy for cancer is in the range of 4–8 mg/kg. The total amount of antibody used in a single ^{89}Zr -PET scan is 5 mg, which is far below even the clinical levels.

21.3. METHODOLOGY

21.3.1. Activity, administration, dosimetry

The participating centre reported administering an activity of 182.8 MBq of ^{89}Zr -trastuzumab, while another group used 65 ± 18 MBq with a total mass of 5 mg of trastuzumab. Dosimetry estimates indicate that the organs receiving the highest absorbed doses are the liver, heart wall, kidney, lung and spleen, with mean values of 1.32, 1.12, 0.9, 0.81 and 0.8 mGy/MBq, respectively. The mean effective dose was 0.48 mSv/MBq [11, 80, 161–170].

21.3.2. Imaging protocol

Patient preparation does not require any special diet. Imaging is performed after the IV administration of 37 MBq and an uptake period of 4 days. Acquisition of the PET component starts from the pelvis, with 5 min/bed position. For the CT imaging protocol, see general comment in Section 1.3.

21.4. CLINICAL ASPECTS

21.4.1. Indications

This imaging technique was developed at the University Medical Centre in Groningen, the Netherlands [165]. Currently, this scan is not routinely performed in clinical practice, except in cases of a clinical dilemma, when the HER2 receptor status cannot be assessed by other means [166, 169]. The clinical value of this technique is currently being further investigated in the IMPACT Metastatic Breast Cancer Trial (NCT01957332). Meanwhile, several studies have been published using this technique, for example to predict patient outcome of trastuzumab emtansine treatment [11, 164, 167, 170].

21.4.2. Cases

21.4.2.1. Case No. 21.1

Clinical indication for PET–CT: Metastatic breast cancer, assessment of HER2 receptor status

Clinical history

A 47 year old woman with left breast cancer, pT2N1M0 (ER+, PR+, HER2–), diagnosed 9 years earlier, had undergone breast conserving surgery and axillary LND, followed by chemotherapy and loco-regional RT, and had subsequently started on adjuvant therapy. The patient presented with dyspnoea and CT demonstrated lung metastases and pleuritic carcinomatosis (ER+ ductal carcinoma in pleural fluid).

PET–CT findings

MIP and fused sagittal slice of thorax.

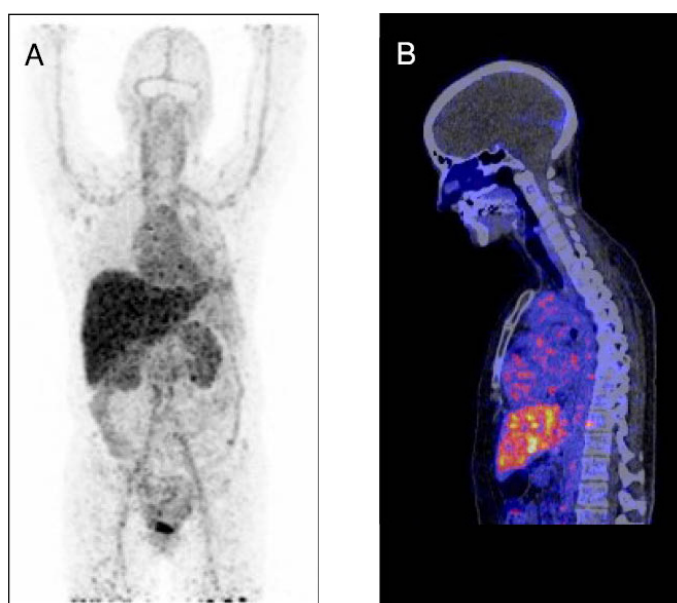
There is no ^{89}Zr -trastuzumab uptake in the known metastatic lesions. Physiologic ^{89}Zr -trastuzumab uptake is demonstrated in the large vessels, heart, liver, intestines and kidneys.

Follow-up: No anti-HER2 treatment was added to the subsequently started palliative anti-hormonal treatment.

Teaching points

No change in treatment plan was performed considering the PET–CT findings. Note the normal distribution of ^{89}Zr -trastuzumab PET–CT.

Keywords: Breast cancer, therapy planning, ^{89}Zr -trastuzumab biodistribution



Clinical indication for PET–CT: Metastatic breast cancer, assessment of HER2 receptor status and extent of disease within the chest

Clinical history

A 65 year old woman with left breast cancer, pT1N0M0 (ER–, PR–), diagnosed 8 years earlier, post-mastectomy and sentinel LN procedure. Five years after surgery, she presented with a left supraclavicular LN metastasis and was treated with RT with curative intent. There was not sufficient puncture material to determine the receptor status. Two years later, she presented with metastatic disease involving the sternum and multiple mediastinal and right axillary LNs. A sternal biopsy now showed ER+, PR+ and HER2+ disease. She was started on an aromatase inhibitor (first line), which, 7 months later, was switched to tamoxifen (second line) because of progression of the sternal lesion. Five months later, she presented with hoarseness. CT of the chest showed elevation of the left diaphragm, but no other potential cause for her complaints.

PET–CT findings

(A): MIP; (B): fused transaxial slices of neck and chest; (C): fused sagittal slice of chest.

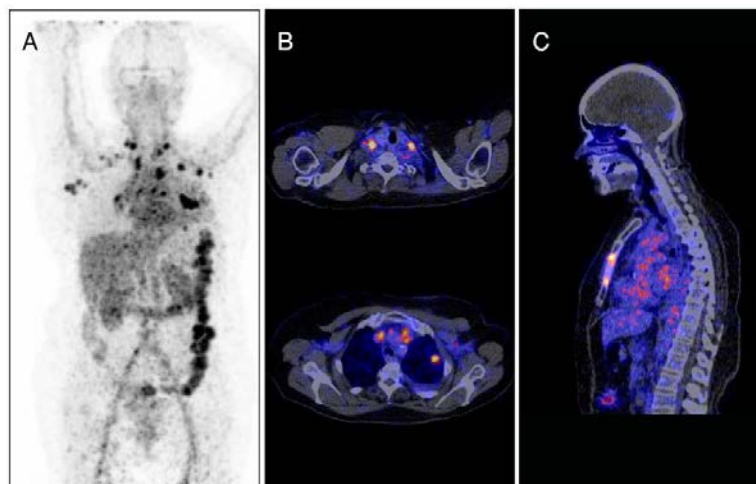
There are multiple ^{89}Zr -trastuzumab positive lesions in supraclavicular, mediastinal and axillary LNs, and in metastases in lungs, chest wall and sternal bone.

Follow-up: Anti-HER2 treatment was added to previously started palliative anti-hormonal treatment.

Teaching points

^{89}Zr -trastuzumab PET–CT may help in therapy stratification. In the present case, the treatment plan was changed (i.e. anti-HER2 treatment was added to the anti-hormonal treatment).

Keywords: Breast cancer, assessment of HER2 status, therapy planning, ^{89}Zr -trastuzumab



Clinical indication for PET–CT: Metastatic breast cancer, assessment of HER2 status

Clinical history

A 56 year old woman with left breast cancer, pT2N0M0 (ER+, PR+, HER2–), diagnosed 10 years earlier, post-mastectomy and axillary LND, followed by chemotherapy and 5 years of anti-hormonal treatment. Three years later, she presented with liver and bone metastases. Systemic treatment was instituted. As a result of her inclusion in a clinical trial, the pathology of the primary tumour was revised and the HER2 status was defined as positive.

PET–CT findings

(A): MIP; (B): fused sagittal slice; (C): PET, fused and CT transaxial slices of liver.

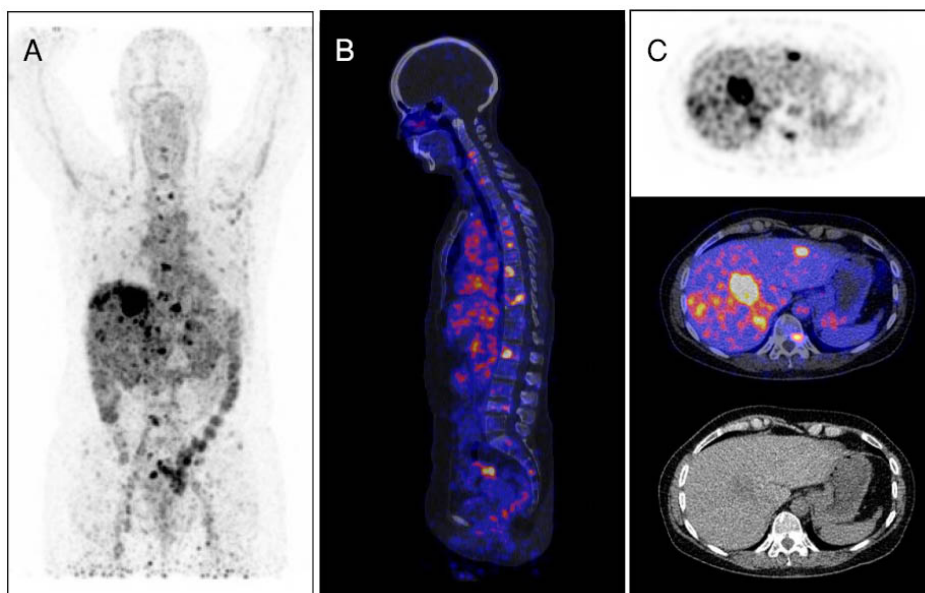
There is ⁸⁹Zr-trastuzumab uptake in known liver and bone metastases.

Follow-up: Anti-HER2 treatment (trastuzumab) was added to the subsequently started palliative anti-hormonal treatment.

Teaching points

⁸⁹Zr-trastuzumab PET–CT may play a role in therapy stratification. In this patient, the treatment plan was changed and anti-HER2 treatment was started.

Keywords: Breast cancer, HER2 status, therapy planning, ⁸⁹Zr-trastuzumab



22. YTTRIUM MICROSPHERES AFTER SELECTIVE INTERNAL RADIATION THERAPY (⁹⁰Y)

22.1. GENERAL CHARACTERISTICS

Name: ⁹⁰Y-microspheres

Synonyms: ⁹⁰Y glass microspheres, ⁹⁰Y resin microspheres

Radioisotope

⁹⁰Y is a β^- emitting radioisotope (half-life 64.1 hours), however coincidence imaging with ⁹⁰Y is possible owing to a minor decay branch to the first excited state of ⁹⁰Zr followed by internal pair production at the branching ratio of $31.86 \pm 0.47 \times 10^{-6}$. Recently, time of flight PET–CT scanners with high quality crystals have begun providing superior timing resolution that allows imaging of this phenomenon.

Radiosynthesis

The production of ⁹⁰Y-containing microspheres is performed mainly by two vendors, however some Member States also have their own local production routes. One formulation is composed of a proprietary biocompatible microsphere, coated with a partially cross-linked cation exchange polystyrene resin. ⁹⁰Y is incorporated into the resin matrix. Another method involves mixing natural Y with ultrapure aluminum oxide and silicone dioxide followed by melting in a furnace at 1500°C and cooling. In the next step the Y-containing glass is crushed and passed through a flame sprayer to produce spheridized glass particles followed by filtration through sieves to select those with a diameter of 20 to 30 microns. In the last step, the spheres are irradiated in a research reactor to yield ⁹⁰Y microspheres [171–173].

22.2. PHARMACOKINETICS

22.2.1. Physiological biodistribution and metabolism

⁹⁰Y microspheres accumulate permanently in the target vascular bed in hepatic tissue and are not metabolized.

22.2.2. Mechanism of retention

As mentioned above, following intraarterial administration, ⁹⁰Y microspheres accumulate permanently in the target vascular bed. ⁹⁰Y radioembolization brachytherapy is a therapeutic option for inoperable HCC [171–173].

22.2.3. Pharmacology and toxicology

There are no known pharmacological effects while the agent remains undistributed in the target organ acting as a reservoir for ⁹⁰Y radioisotope to irradiate the surrounding liver. Clinical toxicity after treatment, caused by radiation, was confined to grade 1–2 events, predominantly post-embolization symptoms. There was no grade 3–4 clinical toxicity, although laboratory toxicity grade 3–4 was observed in 38% of patients [171–173].

22.3. METHODOLOGY

22.3.1. Activity, administration, dosimetry

For resin based ^{90}Y microspheres, the activities for each region affected by the malignancy are: 1.14 GBq to the right lobe and 0.76 GBq to the left lobe. For glass ^{90}Y microspheres, a dose of 100 to 140 Gy is typically delivered to the liver compartment, with lower doses administered in patients with underlying liver disease of different aetiology [174–176].

22.3.2. Imaging protocol

Patient preparation does not require any special diet. Imaging is performed on the same day or the day after intra-arterial microsphere injection. Acquisition of the PET component includes the lower chest and upper abdomen (liver only), with 15–25 min/bed position. The CT component is acquired using a low dose protocol.

22.4. CLINICAL ASPECTS

22.4.1. Indications

^{90}Y microsphere imaging can be performed for assessment of microsphere distribution, to confirm absence of extrahepatic spread, as well as for post-treatment dosimetry.

22.4.2. Cases

22.4.2.1. Case No. 22.1

Clinical indication for PET–CT: Multifocal HCC, after selective internal radiation therapy (SIRT) with ^{90}Y -microspheres

Clinical history

A 65 year old man was assessed for newly diagnosed diabetes mellitus. Elevated liver enzymes were found during the workup, caused by liver cirrhosis, a consequence of a hepatitis B virus infection several years earlier. Multiple HCC deposits were found in both lobes of the cirrhotic liver, which could not be treated with surgery, chemo-embolization or radiofrequency ablation. The patient was treated with ^{90}Y glass microspheres, in doses of 3900 MBq to segments VI and VII, and 5300 MBq to segments IVA, V and VIII.

PET–CT protocol

Imaging of the liver was performed following an uptake period of 24 hours, for 2 bed positions, with an acquisition time of 15 min/bed position.

PET–CT findings

(A, B): whole body ^{99m}Tc -macroaggregate images; (C, D): SPECT coronal images; (E, F): coronal view of fused PET and diagnostic arterial phase CT; (G–J): PET coronal views displayed with different grey intensities.

Pre-therapy images were performed after intra-arterial injection of 150 MBq ^{99m}Tc -macroaggregates. Post-therapy images were acquired after intra-arterial injection of ^{90}Y microspheres.

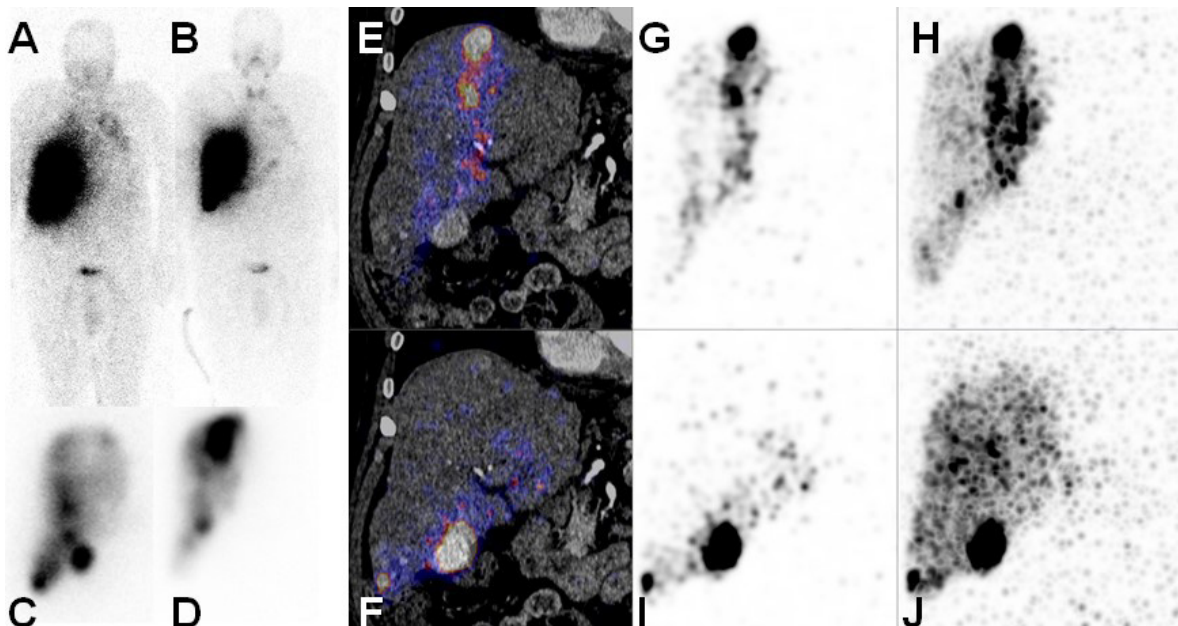
Whole body ^{99m}Tc -macroaggregate images show no significant shunting towards the lungs or bowels (A and B). SPECT coronal images show intense accumulation at the sites of HCC lesions in liver segments VI and VII (C), and IVA, V and VIII (D). Coronal view of fused PET and diagnostic arterial phase CT (E and F), and PET coronal views displayed with different grey intensities (G–J) show intense ^{90}Y microsphere accumulation at the sites of arterial contrast enhancement (i.e. in the HCC lesions).

Follow-up: Three months after treatment all HCC deposits decreased in size and showed less contrast enhancement. No new lesions were observed.

Teaching points

The post-therapy PET–CT study was important to assess whether the administered activity was correctly delivered to sites of disease.

Keywords: HCC, post-therapy study, ^{90}Y -microspheres



Clinical indication for PET–CT: HCC, evaluation following ^{90}Y -microsphere administration

Clinical history

A 62 year old man with HCC (55 mm, segment VIII) seen on contrast enhanced CT, angiography and MRI (A).

PET–CT findings

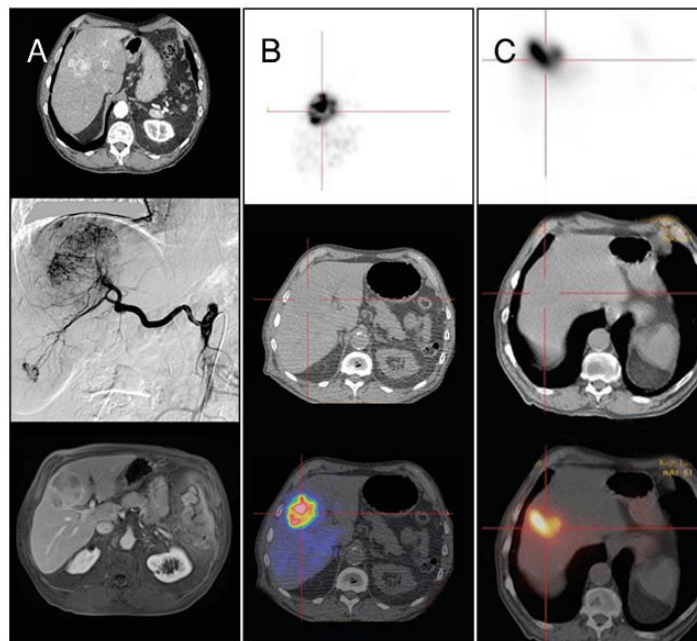
(A): contrast enhanced CT, angiography and MRI; (B): PET, CT and fused PET–CT with ^{90}Y microspheres; (C): SPECT, CT and fused SPECT–CT images with $^{99\text{m}}\text{Tc}$ -macroaggregates.

Pre-therapy images (C) were acquired after intra-arterial injection of 150 MBq $^{99\text{m}}\text{Tc}$ -macroaggregates. Post-therapy images (B) were acquired after intra-arterial injection of ^{90}Y microspheres. There is accumulation of the radiolabelled spheres in the lesion (B), in a very similar fashion to the pre-therapeutic $^{99\text{m}}\text{Tc}$ -macroaggregate SPECT–CT (C).

Teaching point

PET–CT verifies the distribution of microspheres and allows for precise dosimetry.

Keywords: HCC, ^{90}Y -SIRT



Clinical indication for PET–CT: Colon cancer metastatic to liver, evaluation following ^{90}Y -microsphere administration

Clinical history

A 69 year old man with metastatic colon cancer, previously treated with three lines of chemotherapy.

PET–CT findings

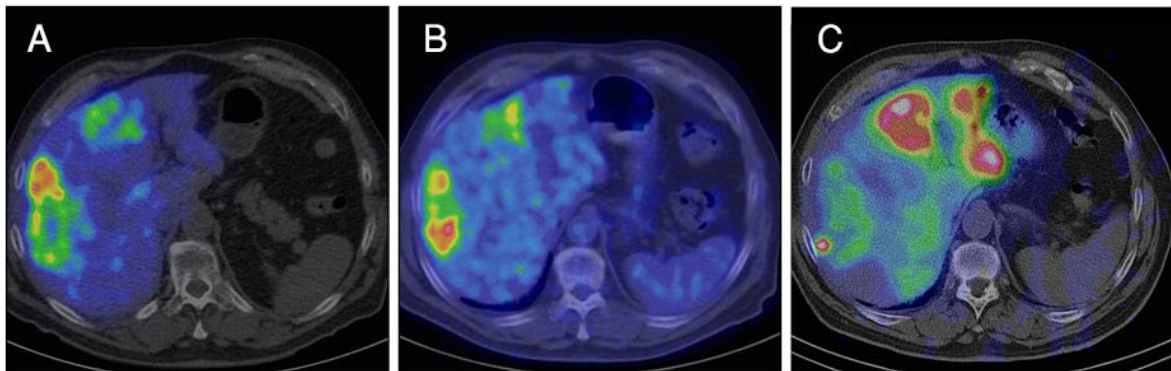
(A): PET–CT with ^{90}Y microspheres, transaxial fused view; (B): ^{18}F -FDG PET–CT, transaxial fused view; (C): SPECT–CT with $^{99\text{m}}\text{Tc}$ -macroaggregates, transaxial fused view.

There are multiple foci of ^{90}Y -microsphere uptake (A) corresponding to the active lesions seen on the ^{18}F -FDG study (B). In this case, the $^{99\text{m}}\text{Tc}$ -macroaggregate SPECT–CT was not predictive of microsphere distribution (C).

Teaching point

^{90}Y -PET–CT verifies the distribution of microspheres and allows for post-hoc dosimetry.

Keywords: Liver metastases, colorectal cancer, ^{90}Y -SIRT



ABBREVIATIONS

ADT	androgen deprivation therapy
AR	androgen receptor
BCR	biochemical recurrence
CNS	central nervous system
CT	computed tomography
DOPA	dihydroxy-phenylalanine
dt	doubling time
E_{\max}	maximum β energy
ER	oestrogen receptor
FDG	fluorodeoxyglucose
FDHT	fluoro-dihydro-testosterone
GLP-1	glucagon like peptide-1
HCC	hepatocellular carcinoma
HER2	human epidermal growth factor receptor 2
HPLC	high performance liquid chromatography
HPT	hyperparathyroidism
HTP	hydroxytryptophan
IV	intravenous
LN	lymph node
LND	lymph node dissection
miBG	metaiodobenzylguanidine
MIP	maximum intensity projection
MRI	magnetic resonance imaging
MTC	medullary thyroid cancer
NET	neuroendocrine tumour
NSCLC	non-small cell lung carcinoma
PET	positron emission tomography
PR	progesterone receptor
PSA	prostate specific antigen
PSMA	prostate specific membrane antigen
PTA	parathyroid adenoma
PTH	parathyroid hormone
RT	radiation therapy
SPECT	single photon emission computed tomography
SSTR	somatostatin receptor
SUV_{\max}	maximum standardized uptake value
TTR	testosterone rebound
US	ultrasound
VEGF-A	vascular endothelial growth factor A

REFERENCES

- [1] SELTZER, M.A., et al., Radiation dose estimates in humans for ^{11}C -acetate whole-body PET, *J. Nucl. Med.* **45** 7 (2004) 1233–1236.
- [2] KARANIKAS, G., BEHESHTI, M., ^{11}C -acetate PET/CT imaging: Physiologic uptake, variants, and pitfalls, *PET Clin.* **9** 3 (2014) 339–344.
- [3] SANDBLOM, G., SÖRENSEN, J., LUNDIND, N., HÄGGMAND, M., MALMSTRÖMDE, P.-U., Positron emission tomography with ^{11}C -acetate for tumor detection and localization in patients with prostate-specific antigen relapse after radical prostatectomy, *Urol.* **67** 5 (2006) 996–1000.
- [4] HAIN, S., MAISEY, M.N., Positron emission tomography for urological tumours, *BJU Int.* **92** 2 (2003) 159–164.
- [5] HO, C.L., YU, S.C.H., YEUNG, D.W.C., ^{11}C -acetate PET imaging in hepatocellular carcinoma and other liver masses, *J. Nucl. Med.* **44** 2 (2003) 213–221.
- [6] PARK, J.-W., et al., A prospective evaluation of ^{18}F -FDG and ^{11}C -acetate PET/CT for detection of primary and metastatic hepatocellular carcinoma, *J. Nucl. Med.* **49** 12 (2008) 1912.
- [7] LIU, R.-S., et al., PET imaging of brain astrocytoma with ^{11}C -acetate, *Eur. J. Nucl. Med. Mol. Imaging* **33** 4 (2006) 420–427.
- [8] GAYKEMA, S., et al., ^{89}Zr -bevacizumab PET imaging in primary breast cancer, *J. Nucl. Med.* **54** 7 (2013) 1014–1018.
- [9] JALILIAN, A.R., OSSO, J.A., Production, applications and status of zirconium-89 immunoPET agents, *J. Radioanal. Nucl. Chem.* **314** 1 (2017) 7–21.
- [10] BAHCE, I., et al., Pilot study of ^{89}Zr -bevacizumab positron emission tomography in patients with advanced non-small cell lung cancer, *EJNMMI Res.* **4** 1 (2014) 35.
- [11] GAYKEMA, S.B., et al., ^{89}Zr -trastuzumab and ^{89}Zr -bevacizumab PET to evaluate the effect of the HSP90 inhibitor NVP-AUY922 in metastatic breast cancer patients, *Clin. Cancer Res.* **20** 15 (2014) 3945–3954.
- [12] JANSEN, M.H., et al., Molecular drug imaging: ^{89}Zr -bevacizumab PET in children with diffuse intrinsic pontine glioma, *J. Nucl. Med.* **58** 5 (2017) 711–716.
- [13] OOSTING, S.F., et al., ^{89}Zr -bevacizumab PET visualizes heterogeneous tracer accumulation in tumour lesions of renal cancer patients and differential effects of anti-angiogenic treatment, *J. Nucl. Med.* **56** (2015).
- [14] OOSTING, S.F., et al., ^{89}Zr -Bevacizumab PET visualizes disease manifestations in patients with von Hippel-Lindau disease, *J. Nucl. Med.* **57** 8 (2016) 1244–1250.
- [15] VAN ASSELT, S.J., et al., Everolimus reduces ^{89}Zr -bevacizumab tumour uptake in patients with neuroendocrine tumours, *J. Nucl. Med.* **55** 7 (2014) 1087–1092.
- [16] VAN ES, S.C., et al., ^{89}Zr -bevacizumab PET: Potential early indicator of everolimus efficacy in patients with metastatic renal cell carcinoma, *J. Nucl. Med.* **58** 6 (2017) 905–910.
- [17] UMBEHR, M.H., MÜNTENER, M., HANY, T., SULSER, T., BACHMANN, L.M., The role of ^{11}C -choline and ^{18}F -fluorocholine positron emission tomography (PET) and PET/CT in prostate cancer: systematic review and meta-analysis, *Eur. Urol.* **64** 1 (2013) 106–117.
- [18] FANTI, S., et al., PET/CT with ^{11}C -choline for evaluation of prostate cancer patients with biochemical recurrence: Meta-analysis and critical review of available data, *Eur. J. Nucl. Med. Molec. Imaging* **43** 1 (2016) 55–69.
- [19] VON EYBEN, F.E., et al., Acquisition with ^{11}C -choline and ^{18}F -fluorocholine PET/CT for patients with biochemical recurrence of prostate cancer: a systematic review and meta-analysis, *Ann. Nucl. Med.* **30** 6 (2016) 385–392.
- [20] CECI, F., et al., Evaluation of prostate cancer with ^{11}C -choline PET/CT for treatment planning, response assessment, and prognosis, *J. Nucl. Med.* **57** Suppl. 3 (2016) 49s–54s.
- [21] CASTELLUCCI, P., CECI, F., FANTI, S., Imaging of prostate cancer using ^{11}C -choline PET/computed tomography, *Urol. Clinics* **45** 3 (2018) 481–487.
- [22] GRAZIANI, T., et al., ^{11}C -Choline PET/CT for restaging prostate cancer. Results from 4,426 scans in a single-centre patient series, *Eur. J. Nucl. Med. Mol. Imaging* **43** 11 (2016) 1971–1979.
- [23] CECI, F., et al., Impact of ^{11}C -choline PET/CT on clinical decision making in recurrent prostate cancer: Results from a retrospective two-centre trial, *Eur. J. Nucl. Med. Mol. Imaging* **41** 12 (2014) 2222–2231.
- [24] EVANGELISTA, L., GUTTILLA, A., ZATTONI, F., MUZZIO, P.C., ZATTONI, F., Utility of choline positron emission tomography/computed tomography for lymph node involvement identification in intermediate-to high-risk prostate cancer: A systematic literature review and meta-analysis, *Eur. Urol.* **63** 6 (2013) 1040–1048.
- [25] HEIDENREICH, A., et al., EAU guidelines on prostate cancer: Part II — Treatment of advanced, relapsing, and castration-resistant prostate cancer, *Eur. Urol.* **65** 2 (2014) 467–479.

- [26] DEGRADO, T.R., et al., Synthesis and evaluation of ^{18}F -labeled choline as an oncologic tracer for positron emission tomography: Initial findings in prostate cancer, *Cancer Res.* **61** 1 (2001) 110–117.
- [27] DEGRADO, T.R., REIMAN, R.E., PRICE, D.T., WANG, S., COLEMAN, R.E., Pharmacokinetics and radiation dosimetry of ^{18}F -fluorocholine, *J. Nucl. Med.* **43** 1 (2002) 92–96.
- [28] KRYZA, D., TADINO, V., FILANNINO, M.A., VILLERET, G., LEMOUCHEUX, L., Fully automated [^{18}F] fluorocholine synthesis in the TracerLab MX FDG Coincidence synthesizer, *Nucl. Med. Biol.* **35** 2 (2008) 255–260.
- [29] HOCEVAR, M., et al., Focused parathyroidectomy without intraoperative parathormone testing is safe after pre-operative localization with ^{18}F -fluorocholine PET/CT, *Eur. J. Surg. Oncol.* **43** 1 (2017) 133–137.
- [30] HUBER, G., et al., Benefit of ^{18}F -fluorocholine PET imaging in parathyroid surgery, *Eur. Radiol.* **28** 6 (2018) 2700–2707.
- [31] KLUIJFHOUT, W.P., et al., Fluorine-18 fluorocholine PET-CT localizes hyperparathyroidism in patients with inconclusive conventional imaging: A multicenter study from the Netherlands, *Nucl. Med. Comm.* **37** 12 (2016) 1246–1252.
- [32] LALIRE, P., LY, S., DEGUELTE, S., PATEY, M., MORLAND, D., Incremental value of ^{18}F -fluorocholine PET/CT in the localization of double parathyroid adenomas, *Clin. Nucl. Med.* **42** 3 (2017) 218–220.
- [33] QUAK, E., et al., F18-choline PET/CT guided surgery in primary hyperparathyroidism when ultrasound and MIBI SPECT/CT are negative or inconclusive: The APACH1 study, *Eur. J. Nucl. Med. Mol. Imaging* **45** 4 (2018) 658–666.
- [34] VELLANI, C., et al., Early and delayed ^{18}F -FCH PET/CT imaging in parathyroid adenomas, *Clin. Nucl. Med.* **42** 2 (2017) 143–144.
- [35] LARSON, S.M., et al., Tumour localization of $^{16}\beta$ - ^{18}F -fluoro-5 α -dihydrotestosterone versus ^{18}F -FDG in patients with progressive, metastatic prostate cancer, *J. Nucl. Med.* **45** 3 (2004) 366–373.
- [36] LAZARI, M., et al., Fully-automated synthesis of $^{16}\beta$ - ^{18}F -fluoro-5 α -dihydrotestosterone (FDHT) on the ELIXYS radiosynthesizer, *Appl. Rad. Isot.* **103** (2015) 9–14.
- [37] ZANZONICO, P.B., et al., PET-based radiation dosimetry in man of ^{18}F -fluorodihydrotestosterone, a new radiotracer for imaging prostate cancer, *J. Nucl. Med.* **45** 11 (2004) 1966–1971.
- [38] DEHDASHTI, F., et al., Positron tomographic assessment of androgen receptors in prostatic carcinoma, *Eur. J. Nucl. Med. Mol. Imaging* **32** 3 (2005) 344–350.
- [39] FOX, J.J., et al., Developing imaging strategies for castration resistant prostate cancer, *Acta Oncol.* **50** Suppl. 1 (2011) 39–48.
- [40] GLAUDEMANS, A.W., et al., Detection of intra-abdominal testicles with $^{16}\beta$ -[^{18}F]-fluoro-5 α -dihydrotestosterone positron emission tomography/computed tomography in a pubertal boy, *J. Pediatr.* **166** 3 (2015) 771–774.
- [41] TALBOT, J., et al., Current applications of PET imaging of sex hormone receptors with a fluorinated analogue of estradiol or of testosterone, *Q. J. Nucl. Med. Molec. Imaging* **59** 1 (2015) 4–17.
- [42] VENEMA, C.M., et al., Androgen and oestrogen receptor imaging in metastatic breast cancer patients as a surrogate for tissue biopsies, *J. Nucl. Med.* **58** 12 (2017) 1906–1912.
- [43] CHONDROGIANNIS, S., et al., Normal biodistribution pattern and physiologic variants of ^{18}F -DOPA PET imaging, *Nucl. Med. Commun.* **34** 12 (2013) 1141.
- [44] SOUSSAN, M., et al., Added value of early ^{18}F -FDOPA PET/CT acquisition time in medullary thyroid cancer, *Nucl. Med. Commun.* **33** 7 (2012) 775–779.
- [45] AMODRU, V., et al., Quantitative ^{18}F -DOPA PET/CT in pheochromocytoma: The relationship between tumour secretion and its biochemical phenotype, *Eur. J. Nucl. Med. Mol. Imaging* **45** 2 (2018) 278–282.
- [46] PICCARDO, A., et al., Comparison of ^{18}F -dopa PET/CT and ^{123}I -MIBG scintigraphy in stage 3 and 4 neuroblastoma: A pilot study, *Eur. J. Nucl. Med. Mol. Imaging* **39** 1 (2012) 57–71.
- [47] ADDEO, P., et al., The added diagnostic value of ^{18}F -fluorodihydroxyphenylalanine PET/CT in the preoperative work-up of small bowel neuroendocrine tumours, *J. Gastrointest. Surg.* **22** 4 (2018) 722–730.
- [48] LIAO, G.J., , CLARK, A.S., SCHUBERT, E.K., MANKOFF, D.A., ^{18}F -fluoroestradiol PET: Current status and potential future clinical applications, *J. Nucl. Med.* **57** 8 (2016) 1269–1275.
- [49] VENEMA, C.M., et al., Recommendations and technical aspects of $^{16}\alpha$ -[^{18}F] fluoro-17 β -estradiol PET to image the oestrogen receptor in vivo: The Groningen experience, *Clin. Nucl. Med.* **41** 11 (2016) 844–851.
- [50] VAN KRUCHTEN, M., et al., PET imaging of oestrogen receptors in patients with breast cancer, *Lancet Oncol.* **14** 11 (2013) e465–e475.
- [51] VAN KRUCHTEN, M., et al., PET imaging of oestrogen receptors as a diagnostic tool for breast cancer patients presenting with a clinical dilemma, *J. Nucl. Med.* **53** 2 (2012) 182.
- [52] VAN KRUCHTEN, M., et al., Positron emission tomography imaging of oestrogen receptor-expression in

- endometrial stromal sarcoma supports oestrogen receptor-targeted therapy: Case report and review of the literature, *Eur. J. Cancer* **49** 18 (2013) 3850–3855.
- [53] PETERSON, L.M., et al., Factors influencing the uptake of ^{18}F -fluoroestradiol in patients with oestrogen receptor positive breast cancer, *Nucl. Med. Biol.* **38** 7 (2011) 969–978.
- [54] LINDEN, H.M., et al., Fluoroestradiol positron emission tomography reveals differences in pharmacodynamics of aromatase inhibitors, tamoxifen, and fulvestrant in patients with metastatic breast cancer, *Clin. Cancer Res.* **17** 14 (2011) 4799–4805.
- [55] ABE, K., et al., O-(2- ^{18}F fluoroethyl)-L-tyrosine (^{18}F -FET) uptake in mouse thymoma cells, and its biodistribution in mice and human volunteers, *Acta Radiol.* **47** 10 (2006) 1042–1048.
- [56] GALLDIKS, N., et al., The use of dynamic O-(2- ^{18}F -fluoroethyl)-l-tyrosine PET in the diagnosis of patients with progressive and recurrent glioma, *Neuro Oncol.* **17** 9 (2015) 1293–1300.
- [57] ALBERT, N.L., et al., Response assessment in neuro-oncology working group and European association for neuro-oncology recommendations for the clinical use of PET imaging in gliomas, *Neuro Oncol.* **18** 9 (2016) 1199–1208.
- [58] UNTERRAINER, M., et al., Serial ^{18}F -FET PET imaging of primarily ^{18}F -FET-negative glioma: Does it make sense? *J. Nucl. Med.* **57** 8 (2016) 1177–1182.
- [59] KUNZ, M., et al., Hot spots in dynamic ^{18}F -FET-PET delineate malignant tumor parts within suspected WHO grade II gliomas, *Neuro Oncol.* **13** 3 (2011) 307–316.
- [60] POULSEN, S.H., et al., The prognostic value of FET PET at radiotherapy planning in newly diagnosed glioblastoma, *Eur. J. Nucl. Med. Mol. Imaging* **44** 3 (2017) 373–381.
- [61] GRIERSON, J.R., SHIELDS, A.F., Radiosynthesis of 3'-deoxy-3'- ^{18}F fluorothymidine: [^{18}F] FLT for imaging of cellular proliferation in vivo, *Nucl. Med. Biol.* **27** 2 (2000) 143–156.
- [62] OH, S.J., et al., Fully automated synthesis system of 3'-deoxy-3'- ^{18}F fluorothymidine, *Nucl. Med. Biol.* **31** 6 (2004) 803–809.
- [63] SHANKAR, L.K., The clinical evaluation of novel imaging methods for cancer management, *Nature Rev. Clin. Oncol.* **9** 12 (2012) 738.
- [64] TURCOTTE, E., et al., Toxicology evaluation of radiotracer doses of 3'-deoxy-3'- ^{18}F fluorothymidine (^{18}F -FLT) for human PET imaging: Laboratory analysis of serial blood samples and comparison to previously investigated therapeutic FLT doses, *BMC Nucl. Med.* **7** 1 (2007) 3.
- [65] VESSELLE, H., et al., ^{18}F -Fluorothymidine radiation dosimetry in human PET imaging studies, *J. Nucl. Med.* **44** 9 (2003) 1482–1488.
- [66] KENNY, L., et al., Imaging early changes in proliferation at 1 week post chemotherapy: A pilot study in breast cancer patients with 3'-deoxy-3'- ^{18}F fluorothymidine positron emission tomography, *Eur. J. Nucl. Med. Mol. Imaging* **34** 9 (2007) 1339–1347.
- [67] MENDA, Y., et al., Kinetic analysis of 3'-deoxy-3'- ^{18}F -fluorothymidine (^{18}F -FLT) in head and neck cancer patients before and early after initiation of chemoradiation therapy, *J. Nucl. Med.* **50** 7 (2009) 1028.
- [68] ZANDER, T., et al., Early prediction of nonprogression in advanced non-small-cell lung cancer treated with erlotinib by using [^{18}F]fluorodeoxyglucose and [^{18}F]fluorothymidine positron emission tomography, *J. Clin. Oncol.* **29** 13 (2011) 1701–1708.
- [69] CONTRACTOR, K.B., et al., [^{18}F]-3'-Deoxy-3'-fluorothymidine positron emission tomography and breast cancer response to docetaxel, *Clin. Cancer Res.* **17** 24 (2011) 7664–7672.
- [70] HERRMANN, K., et al., Predictive value of initial ^{18}F -FLT uptake in patients with aggressive non-Hodgkin lymphoma receiving R-CHOP treatment, *J. Nucl. Med.* **52** 5 (2011) 690.
- [71] AGOOL, A., et al., Radionuclide imaging of bone marrow disorders, *Eur. J. Nucl. Med. Mol. Imaging* **38** 1 (2011) 166–178.
- [72] OTT, K., et al., Molecular imaging of proliferation and glucose utilization: Utility for monitoring response and prognosis after neoadjuvant therapy in locally advanced gastric cancer, *Ann. Surg. Oncol.* **18** 12 (2011) 3316–3323.
- [73] LEUNG, K., Anti-1-amino-3- ^{18}F fluorocyclobutane-1-carboxylic acid, *Molec. Imaging Contrast Agent Database* (2010).
- [74] BROWN, P.C., Pharmacology/toxicology NDA review and evaluation, Center for Drug Evaluation and Research (2015), www.accessdata.fda.gov/drugsatfda_docs/nda/2016/208054Orig1s000PharmR.pdf
- [75] SCHUSTER, D.M., et al., Anti-1-amino-3- ^{18}F -fluorocyclobutane-1-carboxylic acid: Physiologic uptake patterns, incidental findings, and variants that may simulate disease, *J. Nucl. Med.* **55** 12 (2014) 1986–1992.

- [76] SÖRENSEN, J., OWENIUS, R., LAX, M., JOHANSSON, S., Regional distribution and kinetics of [¹⁸F] fluciclovine (anti-[¹⁸F] FACBC), a tracer of amino acid transport, in subjects with primary prostate cancer, *Eur. J. Nucl. Med. Mol. Imaging* **40** 3 (2013) 394–402.
- [77] KONDO, A., et al., Phase IIa clinical study of [¹⁸F] fluciclovine: Efficacy and safety of a new PET tracer for brain tumours, *Ann. Nucl. Med.* **30** 9 (2016) 608–618.
- [78] SAVIR-BARUCH, B., ZANONI, L., SCHUSTER, D.M., Imaging of prostate cancer using fluciclovine, *Urol. Clinics North Am.* **45** 3 (2018) 489–502.
- [79] ULANER, G.A., et al., Initial results of a prospective clinical trial of 18F-fluciclovine PET/CT in newly diagnosed invasive ductal and invasive lobular breast cancers, *J. Nucl. Med.* **57** 9 (2016) 1350–1356.
- [80] NATIONAL CENTER FOR BIOTECHNOLOGY INFORMATION, Molecular Imaging and Contrast Agent Database (MICAD), NCBI, Bethesda, MD (2013).
- [81] NATIONAL INSTITUTES OF HEALTH, Investigator's Brochure for [¹⁸F]Fluoromisonidazole, 1H-1-(3-[¹⁸F]-fluoro-2-hydroxy-propyl)-2-nitro-imidazole, [¹⁸F]FMISO: An Investigational Positron Emission Tomography (PET) Radiopharmaceutical for Injection and Intended for Use as an In Vivo Diagnostic for Imaging Hypoxia in Tumours, 5th edn, NIH, Bethesda, MD (2013).
- [82] CHENG, J., et al., ¹⁸F-fluoromisonidazole PET/CT: A potential tool for predicting primary endocrine therapy resistance in breast cancer, *J. Nucl. Med.* **54** 3 (2013) 333–340.
- [83] GAGEL, B., et al., [¹⁸F] fluoromisonidazole and [¹⁸F] fluorodeoxyglucose positron emission tomography in response evaluation after chemo-/radiotherapy of non-small-cell lung cancer: A feasibility study, *BMC Cancer* **6** 1 (2006) 51.
- [84] HIRATA, K., et al., ¹⁸F-Fluoromisonidazole positron emission tomography may differentiate glioblastoma multiforme from less malignant gliomas, *Eur. J. Nucl. Med. Mol. Imaging* **39** 5 (2012) 760–770.
- [85] LIN, Z., et al., The influence of changes in tumour hypoxia on dose-painting treatment plans based on ¹⁸F-FMISO positron emission tomography, *Int. J. Rad. Oncol. Biol. Phys.* **70** 4 (2008) 1219–1228.
- [86] LOPCI, E., et al., PET radiopharmaceuticals for imaging of tumour hypoxia: A review of the evidence, *Am. J. Nucl. Med. Mol. Imaging* **4** 4 (2014) 365.
- [87] NEHMEH, S.A., et al., Reproducibility of intratumor distribution of ¹⁸F-fluoromisonidazole in head and neck cancer, *Int. J. Rad. Oncol. Biol. Phys.* **70** 1 (2008) 235–242.
- [88] OKAMOTO, S., et al., High reproducibility of tumour hypoxia evaluated by ¹⁸F-fluoromisonidazole PET for head and neck cancer, *J. Nucl. Med.* **54** 2 (2013) 201–207.
- [89] RAJENDRAN, J.G., et al., Tumour hypoxia imaging with [F-18] fluoromisonidazole positron emission tomography in head and neck cancer, *Clin. Cancer Res.* **12** 18 (2006) 5435–5441.
- [90] RASEY, J.S., et al., Quantifying regional hypoxia in human tumours with positron emission tomography of [¹⁸F] fluoromisonidazole: A pretherapy study of 37 patients, *Int. J. Rad. Oncol. Biol. Phys.* **36** 2 (1996) 417–428.
- [91] REISCHL, G., et al., Imaging of tumour hypoxia with [¹²⁴I] IAZA in comparison with [¹⁸F] FMISO and [¹⁸F] FAZA: First small animal PET results, *J. Pharm. Sci.* **10** 2 (2007) 203–211.
- [92] RISCHIN, D., et al., Prognostic significance of [F-18]-misonidazole positron emission tomography-detected tumour hypoxia in patients with advanced head and neck cancer randomly assigned to chemoradiation with or without tirapazamine: A substudy of Trans-Tasman Radiation Oncology Group Study 98.02, *J. Clin. Oncol.* **24** 13 (2006) 2098–2104.
- [93] SPENCE, A.M., et al., Regional hypoxia in glioblastoma multiforme quantified with [¹⁸F] fluoromisonidazole positron emission tomography before radiotherapy: Correlation with time to progression and survival, *Clin. Cancer Res.* **14** 9 (2008) 2623–2630.
- [94] ESCHMANN, M., et al., Prognostic impact of hypoxia imaging with ¹⁸F-misonidazole PET in non-small cell lung cancer and head and neck cancer before radiotherapy, *J. Nucl. Med.* **46** (2005) 253–260.
- [95] TACHIBANA, I., et al., A prospective clinical trial of tumour hypoxia imaging with ¹⁸F-fluoromisonidazole positron emission tomography and computed tomography (F-MISO PET/CT) before and during radiation therapy, *J. Rad. Res.* **54** 6 (2013) 1078–1084.
- [96] WACK, L.J., et al., Comparison of [18F]-FMISO, [18F]-FAZA and [18F]-HX4 for PET imaging of hypoxia: A simulation study, *Acta Oncol.* **54** 9 (2015) 1370–1377.
- [97] ZIPS, D., et al., Exploratory prospective trial of hypoxia-specific PET imaging during radiochemotherapy in patients with locally advanced head-and-neck cancer, *Radiother. Oncol.* **105** 1 (2012) 21–28.
- [98] BOLLINENI, V.R., et al., PET imaging of tumour hypoxia using ¹⁸F-fluoroazomycin arabinoside in stage III-IV non-small cell lung cancer patients, *J. Nucl. Med.* **54** 8 (2013) 1175–1180.
- [99] BOLLINENI, V.R., et al., Dynamics of tumour hypoxia assessed by ¹⁸F-FAZA PET/CT in head and neck and lung

- cancer patients during chemoradiation: Possible implications for radiotherapy treatment planning strategies, *Radiother. Oncol.* **113** 2 (2014) 198–203.
- [100] DE BRUIN, L.B., et al., Assessment of hypoxic subvolumes in laryngeal cancer with ¹⁸F-fluoroazomycin-araboside (¹⁸F-FAZA)-PET/CT scanning and immunohistochemistry, *Radiother. Oncol.* **117** 1 (2015) 106–112.
- [101] VELIKYAN, I., ROSENSTROM, U., ERIKSSON, O., Fully automated GMP production of [⁶⁸Ga] Ga-DO3A-VS-Cys⁴⁰-exendin-4 for clinical use, *Am. J. Nucl. Med. Mol. Imaging* **7** 3 (2017) 111.
- [102] SELVARAJU, R.K., et al., Dosimetry of [⁶⁸Ga]Ga-DO3A-VS-Cys⁴⁰-exendin-4 in rodents, pigs, non-human primates and human: Repeated scanning in human is possible, *Am. J. Nucl. Med. Mol. Imaging* **5** 3 (2015) 259–269.
- [103] MONAZZAM, A., et al., Increased expression of GLP-1R in proliferating islets of Men1 mice is detectable by [⁶⁸Ga] Ga-DO3A-VS-Cys⁴⁰-exendin-4/PET, *Sci. Rep.* **8** 1 (2018) 748.
- [104] LUO, Y., et al., Glucagon-like peptide-1 receptor PET/CT with ⁶⁸Ga-NOTA-exendin-4 for detecting localized insulinoma: A prospective cohort study, *J. Nucl. Med.* **57** 5 (2016) 715–720.
- [105] GLUCAGON.COM, EXENDIN-4: Human data (2008), www.glucagon.com/exenatidehumandata.html
- [106] NEELS, O.C., et al., Development of a reliable remote-controlled synthesis of β-[¹¹C]-5-hydroxy-L-tryptophan on a Zymark robotic system, *J. Labelled Compd. Radiopharm.* **49** 10 (2006) 889–895.
- [107] ORLEFORS, H., et al., Whole-body ¹¹C-5-hydroxytryptophan positron emission tomography as a universal imaging technique for neuroendocrine tumours: Comparison with somatostatin receptor scintigraphy and computed tomography, *J. Clin. Endocr. Metab.* **90** 6 (2005) 3392–3400.
- [108] KOOPMANS, K.P., et al., Improved staging of patients with carcinoid and islet cell tumours with ¹⁸F-dihydroxyphenyl-alanine and ¹¹C-5-hydroxy-tryptophan positron emission tomography, *J. Clin. Oncol.* **26** 9 (2008) 1489–1495.
- [109] PAPOTTI, M., et al., *Neuroendocrine Tumours: A Multidisciplinary Approach*, Karger Medical Scientific Publishers, Rotterdam (2015).
- [110] VISSER, A.K., et al., [¹¹C]-5-HTP and microPET are not suitable for pharmacodynamic studies in the rodent brain, *J. Cereb. Blood Flow Metab.* **34** 1 (2014) 118–125.
- [111] DAVIS, J., YANO, Y., CAHOON, J., BUDINGER, T.F., Preparation of ¹¹C-methyl iodide and L-[S-methyl-¹¹C] methionine by an automated continuous flow process, *Int. J. Appl. Rad. Isot.* **33** 5 (1982) 363–369.
- [112] DELOAR, H.M., et al., Estimation of internal absorbed dose of L-[methyl-¹¹C] methionine using whole-body positron emission tomography, *Eur. J. Nucl. Med. Mol. Imaging* **25** 6 (1998) 629–633.
- [113] HARRIS, S.M., et al., Evaluation of the biodistribution of [¹¹C] methionine in children and young adults, *J. Nucl. Med.* **54** 11 (2013) 1902.
- [114] MITTERHAUSER, M., et al., New aspects on the preparation of [¹¹C] methionine: A simple and fast online approach without preparative HPLC, *Appl. Rad. Isot.* **62** 3 (2005) 441–445.
- [115] BEGGS, A.D., HAIN, S.F., Localization of parathyroid adenomas using ¹¹C-methionine positron emission tomography, *Nucl. Med. Comm.* **26** 2 (2005) 133–136.
- [116] GLAUDEMANS, A.W., et al., Value of ¹¹C-methionine PET in imaging brain tumours and metastases, *Eur. J. Nucl. Med. Mol. Imaging* **40** 4 (2013) 615–635.
- [117] ITO, K., Pitfalls of ¹¹C-methionine PET/CT in a series of patients with tumors and tumoral lesions, *J. Nucl. Med.* **57** Suppl. 2 (2016) 1233–1233.
- [118] ITO, K., MATSUDA, H., KUBOTA, K., Imaging spectrum and pitfalls of ¹¹C-methionine positron emission tomography in a series of patients with intracranial lesions, *Korean J. Radiol.* **17** 3 (2016) 424–434.
- [119] NAKAJIMA, R., KIMURA, K., ABE, K., SAKAI, S., ¹¹C-methionine PET/CT findings in benign brain disease, *Jpn. J. Radiol.* **35** 6 (2017) 279–288.
- [120] NOLTES, M.E., et al., Localization of parathyroid adenomas using ¹¹C-methionine pet after prior inconclusive imaging, *Langenbeck's Arch. Surg.* **402** 7 (2017) 1109–1117.
- [121] PALANICHAMY, K., CHAKRAVARTI, A., Diagnostic and prognostic significance of methionine uptake and methionine positron emission tomography imaging in gliomas, *Frontiers Oncol.* **7** (2017) 257.
- [122] PARVEZ, K., PARVEZ, A., ZADEH, G., The diagnosis and treatment of pseudoprogression, radiation necrosis and brain tumour recurrence, *Int. J. Mol. Sci.* **15** 7 (2014) 11832–11846.
- [123] SASAKI, M., et al., Differential diagnosis of thymic tumours using a combination of ¹¹C-methionine PET and FDG PET, *J. Nucl. Med.* **40** 10 (1999) 1595.
- [124] SMIRNIOTOPOULOS, J.G., MURPHY, F.M., RUSHING, E.J., REES, J.H., SCHROEDER, J.W., Patterns of contrast enhancement in the brain and meninges, *Radiographics* **27** 2 (2007) 525–551.
- [125] TEZELMAN, S., et al., Double parathyroid adenomas: Clinical and biochemical characteristics before and after parathyroidectomy, *Ann. Surg.* **218** 3 (1993) 300.

- [126] VERMA, N., COWPERTHWAIT, M.C., BURNETT, M.G., MARKEY, M.K., Differentiating tumour recurrence from treatment necrosis: A review of neuro-oncologic imaging strategies, *Neuro Oncol.* **15** 5 (2013) 515–534.
- [127] BEHESHTI, M., et al., ^{18}F -NaF PET/CT: EANM procedure guidelines for bone imaging, *Eur. J. Nucl. Med. Mol. Imaging* **42** 11 (2015) 1767–1777.
- [128] LÖFGREN, J., et al., A prospective study comparing $^{99\text{m}}\text{Tc}$ -hydroxyethylene-diphosphonate planar bone scintigraphy and whole-body SPECT/CT with ^{18}F -fluoride PET/CT and ^{18}F -fluoride PET/MRI for diagnosing bone metastases, *J. Nucl. Med.* **58** 11 (2017) 1778–1785.
- [129] OH, J.-R., AHN, B.-C., False-positive uptake on radioiodine whole-body scintigraphy: Physiologic and pathologic variants unrelated to thyroid cancer, *Am. J. Nucl. Med. Mol. Imaging* **2** 3 (2012) 362.
- [130] PHAN, H.T., et al., The diagnostic value of ^{124}I -PET in patients with differentiated thyroid cancer, *Eur. J. Nucl. Med. Mol. Imaging* **35** 5 (2008) 958–965.
- [131] FREUDENBERG, L., et al., Value of ^{124}I -PET/CT in staging of patients with differentiated thyroid cancer, *Eur. Radiol.* **14** 11 (2004) 2092–2098.
- [132] KIST, J.W., et al., ^{124}I PET/CT to predict the outcome of blind ^{131}I treatment in patients with biochemical recurrence of differentiated thyroid cancer: Results of a multicenter diagnostic cohort study (THYROPET), *J. Nucl. Med.* **57** 5 (2016) 701–707.
- [133] KUKER, R., SZTEJNBERG, M., GULEC, S., I-124 imaging and dosimetry, *Mol. Imaging Radionucl. Therapy* **26** Suppl. 1 (2017) 66.
- [134] PETTINATO, C., et al., Usefulness of ^{124}I PET/CT imaging to predict absorbed doses in patients affected by metastatic thyroid cancer and treated with ^{131}I , *Q. J. Nucl. Med. Mol. Imaging* **56** 6 (2012) 509–514.
- [135] BINSE, I., ROSENBAUM-KRUMME, S.J., BOCKISCH, A., Imaging of differentiated thyroid carcinoma: ^{124}I -PET/MRI may not be superior to ^{124}I -PET/CT, *Eur. J. Nucl. Med. Mol. Imaging* **43** 6 (2016) 1185–1186.
- [136] DE PONT, C., HALDERS, S., BUCERIUS, J., MOTTAGHY, F.M., ^{124}I PET/CT in the pretherapeutic staging of differentiated thyroid carcinoma: Comparison with posttherapy ^{131}I SPECT/CT, *Eur. J. Nucl. Med. Mol. Imaging* **40** 5 (2013) 693–700.
- [137] JENTZEN, W., et al., Optimized ^{124}I PET dosimetry protocol for radioiodine therapy of differentiated thyroid cancer, *J. Nucl. Med.* **49** 6 (2008) 1017–1023.
- [138] JENTZEN, W., et al., Assessment of lesion response in the initial radioiodine treatment of differentiated thyroid cancer using ^{124}I PET imaging, *J. Nucl. Med.* **55** 11 (2014) 1759–1765.
- [139] JENTZEN, W., et al., ^{124}I PET assessment of response of bone metastases to initial radioiodine treatment of differentiated thyroid cancer, *J. Nucl. Med.* **57** 10 (2016) 1499–1504.
- [140] KHORJEKAR, G.R., et al., Do negative ^{124}I pretherapy positron emission tomography scans in patients with elevated serum thyroglobulin levels predict negative ^{131}I posttherapy scans? *Thyroid* **24** 9 (2014) 1394–1399.
- [141] PETTINATO, C., et al., Pretherapeutic dosimetry in patients affected by metastatic thyroid cancer using ^{124}I PET/CT sequential scans for ^{131}I treatment planning, *Clin. Nucl. Med.* **39** 8 (2014) e367–e374.
- [142] PLYKU, D., et al., Recombinant human thyroid-stimulating hormone versus thyroid hormone withdrawal in ^{124}I PET/CT-based dosimetry for ^{131}I therapy of metastatic differentiated thyroid cancer, *J. Nucl. Med.* **58** 7 (2017) 1146–1154.
- [143] RUHLMANN, M., et al., High level of agreement between pretherapeutic ^{124}I PET and intratherapeutic ^{131}I imaging in detecting iodine-positive thyroid cancer metastases, *J. Nucl. Med.* **57** 9 (2016) 1339–1342.
- [144] WIERTS, R., et al., Dose-response relationship in differentiated thyroid cancer patients undergoing radioiodine treatment assessed by means of ^{124}I PET/CT, *J. Nucl. Med.* **57** 7 (2016) 1027–1032.
- [145] CARDINALE, J., et al., Procedures for the GMP-compliant production and quality control of [^{18}F]PSMA-1007: A next generation radiofluorinated tracer for the detection of prostate cancer, *Pharm. (Basel)* **10** (2017) 77.
- [146] AFSHAR-OROMIEH, A., et al., Radiation dosimetry of ^{68}Ga -PSMA-11 (HBED-CC) and preliminary evaluation of optimal imaging timing, *Eur. J. Nucl. Med. Mol. Imaging* **43** 9 (2016) 1611–1620.
- [147] DEMIRCI, E., et al., Normal distribution pattern and physiological variants of ^{68}Ga -PSMA-11 PET/CT imaging, *Nucl. Med. Commun.* **37** 11 (2016) 1169–1179.
- [148] FENDLER, W.P., et al., ^{68}Ga -PSMA PET/CT: Joint EANM and SNMMI procedure guideline for prostate cancer imaging — Version 1.0, *Eur. J. Nucl. Med. Mol. Imaging* **44** 6 (2017) 1014–1024.
- [149] SCHNEIDER, B., et al., Preparation and chemical analysis of clinical-grade ^{68}Ga -PSMA-HBED-CC, an emerging tracer for imaging of prostate cancers, *J. Nucl. Med.* **57** Suppl. 2 (2016) 1117.
- [150] CALAIS, J., et al., Impact of ^{68}Ga -PSMA-11 PET/CT on the management of prostate cancer patients with biochemical recurrence, *J. Nucl. Med.* **59** 3 (2018) 434–441.

- [151] KRATOCHWIL, C., et al., Targeted alpha-therapy of metastatic castration-resistant prostate cancer with ^{225}Ac -PSMA-617: Dosimetry estimate and empiric dose finding, *J. Nucl. Med.* **58** 10 (2017) 1624–1631.
- [152] MAURER, T., et al., Diagnostic efficacy of ^{68}Ga -PSMA positron emission tomography compared to conventional imaging for lymph node staging of 130 consecutive patients with intermediate to high risk prostate cancer, *J. Urol.* **195** 5 (2016) 1436–1443.
- [153] MOTTET, N., et al., EAU guidelines on prostate cancer: Part II — Treatment of advanced, relapsing, and castration-resistant prostate cancer, *Eur. Urol.* **59** 4 (2011) 572–583.
- [154] RAHBAR, K., et al., German multicenter study investigating ^{177}Lu -PSMA-617 radioligand therapy in advanced prostate cancer patients, *J. Nucl. Med.* **58** 1 (2017) 85–90.
- [155] ZAMBOGLOU, C., et al., MRI versus ^{68}Ga -PSMA PET/CT for gross tumour volume delineation in radiation treatment planning of primary prostate cancer, *Eur. J. Nucl. Med. Mol. Imaging* **43** 5 (2016) 889–897.
- [156] AMBROSINI, V., FANI, M., FANTI, S., FORRER, F., MAECKE, H.R., Radiopeptide imaging and therapy in Europe, *J. Nucl. Med.* **52** S2 (2011) 42S–55S.
- [157] HOFMANN, M., et al., Biokinetics and imaging with the somatostatin receptor PET radioligand ^{68}Ga -DOTATOC: Preliminary data, *Eur. J. Nucl. Med.* **28** 12 (2001) 1751–1757.
- [158] JANSSEN, I., WOLF, K.I., CHUI, C.H., MILLO, C.M., PACAK, K., Relevant discordance between ^{68}Ga -DOTATATE and ^{68}Ga -DOTANOC in SDHB-related metastatic paraganglioma: Is affinity to somatostatin receptor 2 the key? *Clin. Nucl. Med.* **42** 3 (2017) 211–213.
- [159] VIRGOLINI, I., et al., Procedure guidelines for PE/CT tumour imaging with ^{68}Ga -DOTA-conjugated peptides: ^{68}Ga -DOTA-TOC, ^{68}Ga -DOTA-NOC, ^{68}Ga -DOTA-TATE, *Eur. J. Nucl. Med. Mol. Imaging* **37** 10 (2010) 2004–2010.
- [160] DRUGS.COM, Herceptin (2020), www.drugs.com/pro/herceptin.html
- [161] BOEKHOUT, A.H., BEIJNEN, J.H., SCHELLENS, J.H.M., Trastuzumab, *Oncologist* **16** 6 (2011) 800–810.
- [162] DIJKERS, E.C., et al., Development and characterization of clinical-grade ^{89}Zr -trastuzumab for HER2/neu immunoPET imaging, *J. Nucl. Med.* **50** 6 (2009) 974–981.
- [163] LAFOREST, R., et al., [^{89}Zr]Trastuzumab: Evaluation of radiation dosimetry, safety, and optimal imaging parameters in women with HER2-positive breast cancer, *Mol. Imaging Biol.* **18** 6 (2016) 952–959.
- [164] O'DONOGHUE, J.A., et al., Pharmacokinetics, biodistribution, and radiation dosimetry for ^{89}Zr -trastuzumab in patients with esophagogastric cancer, *J. Nucl. Med.* **59** 1 (2018) 161–166.
- [165] DIJKERS, E., et al., Biodistribution of ^{89}Zr -trastuzumab and PET imaging of HER2-positive lesions in patients with metastatic breast cancer, *Clin. Pharmacol. Ther.* **87** 5 (2010) 586–592.
- [166] GAYKEMA, S.B., et al., Zirconium-89-trastuzumab positron emission tomography as a tool to solve a clinical dilemma in a patient with breast cancer, *J. Clin. Oncol.* **30** 6 (2012) e74–75.
- [167] GEBHART, G., et al., Molecular imaging as a tool to investigate heterogeneity of advanced HER2-positive breast cancer and to predict patient outcome under trastuzumab emtansine (T-DM1): The ZEPHIR trial, *Ann. Oncol.* **27** 4 (2015) 619–624.
- [168] SCHRÖDER, C., et al., Abstract P5-03-06: Clinical value of ^{89}Zr -trastuzumab PET in HER2-positive breast cancer patients with a clinical dilemma, *Cancer Res.* **77** 4 (2017).
- [169] ULANER, G.A., HYMAN, D.M., LYASHCHENKO, S.K., LEWIS, J.S., CARRASQUILLO, J.A., ^{89}Zr -trastuzumab PET/CT for detection of human epidermal growth factor receptor 2-positive metastases in patients with human epidermal growth factor receptor 2-negative primary breast cancer, *Clin. Nucl. Med.* **42** 12 (2017) 912–917.
- [170] ULANER, G.A., et al., Detection of HER2-positive metastases in patients with HER2-negative primary breast cancer using ^{89}Zr -trastuzumab PET/CT, *J. Nucl. Med.* **57** 10 (2016) 1523.
- [171] KAO, Y.-H., et al., Post-radioembolization yttrium-90 PET/CT: Part 1 — Diagnostic reporting, *EJNMMI Res.* **3** 1 (2013) 56.
- [172] SMITS, M.L., et al., Correction: Clinical and laboratory toxicity after intra-arterial radioembolization with ^{90}Y -microspheres for unresectable liver metastases, *PLoS One* **8** 10 (2013).
- [173] WESTCOTT, M.A., COLDWELL, D.M., LIU, D.M., ZIKRIA, J.F., The development, commercialization, and clinical context of yttrium-90 radiolabeled resin and glass microspheres, *Adv. Rad. Oncol.* **1** 4 (2016) 351–364.
- [174] GIAMMARILE, F., et al., EANM procedure guideline for the treatment of liver cancer and liver metastases with intra-arterial radioactive compounds, *Eur. J. Nucl. Med. Mol. Imaging* **38** 7 (2011) 1393.
- [175] GNESIN, S., et al., Partition model-based $^{99\text{m}}\text{Tc}$ -MAA SPECT/CT predictive dosimetry compared with ^{90}Y TOF PET/CT posttreatment dosimetry in radioembolization of hepatocellular carcinoma: A quantitative agreement comparison, *J. Nucl. Med.* **57** 11 (2016) 1672–1678.

- [176] WILLOWSON, K.P., TAPNER, M., QUEST Investigator Team, BAILEY, D.L., A multicentre comparison of quantitative ^{90}Y PET/CT for dosimetric purposes after radioembolization with resin microspheres, *Eur. J. Nucl. Med. Mol. Imaging* **42** 8 (2015) 1202–1222.

LIST OF CONTRIBUTORS TO DRAFTING AND REVIEW

Castellucci, P.	Policlinico S. Orsola Malpighi, Italy
Dierckx, R.	University Medical Center Groningen, Netherlands
El-Haj, N.	International Atomic Energy Agency
Farsad, M.	Central Hospital Bozen, Italy
Giammarile, F.	International Atomic Energy Agency
Hustinx, R.	Service de Médecine Nucléaire et d'Imagerie Oncologique, Belgium
Jalilian, A.	International Atomic Energy Agency
Núñez Miller, R.	International Atomic Energy Agency
Paez, D.	International Atomic Energy Agency
Rossi, S.	CUDIM, Uruguay

Consultants Meetings

Vienna, Austria: 21–24 March 2017, 29 January–2 February 2018



ORDERING LOCALLY

IAEA priced publications may be purchased from the sources listed below or from major local booksellers.

Orders for unpriced publications should be made directly to the IAEA. The contact details are given at the end of this list.

NORTH AMERICA

Bernan / Rowman & Littlefield

15250 NBN Way, Blue Ridge Summit, PA 17214, USA

Telephone: +1 800 462 6420 • Fax: +1 800 338 4550

Email: orders@rowman.com • Web site: www.rowman.com/bernan

REST OF WORLD

Please contact your preferred local supplier, or our lead distributor:

Eurospan Group

Gray's Inn House

127 Clerkenwell Road

London EC1R 5DB

United Kingdom

Trade orders and enquiries:

Telephone: +44 (0)176 760 4972 • Fax: +44 (0)176 760 1640

Email: eurospan@turpin-distribution.com

Individual orders:

www.eurospanbookstore.com/iaea

For further information:

Telephone: +44 (0)207 240 0856 • Fax: +44 (0)207 379 0609

Email: info@eurospangroup.com • Web site: www.eurospangroup.com

Orders for both priced and unpriced publications may be addressed directly to:

Marketing and Sales Unit

International Atomic Energy Agency

Vienna International Centre, PO Box 100, 1400 Vienna, Austria

Telephone: +43 1 2600 22529 or 22530 • Fax: +43 1 26007 22529

Email: sales.publications@iaea.org • Web site: www.iaea.org/publications



THE ROLE OF PET/CT IN RADIATION TREATMENT PLANNING FOR CANCER PATIENT TREATMENT

IAEA-TECDOC-1603
ISBN 978-92-0-110408-3

Price: €15.00

A GUIDE TO CLINICAL PET IN ONCOLOGY: IMPROVING CLINICAL MANAGEMENT OF CANCER PATIENTS

IAEA-TECDOC-1605
ISBN 978-92-0-110608-7

Price: €15.00

APPROPRIATE USE OF FDG-PET FOR THE MANAGEMENT OF CANCER PATIENTS
IAEA Human Health Series No. 9

STI/PUB/1438 (94 pp.; 2010)
ISBN 978-92-0-101610-2

Price: €39.00

PLANNING A CLINICAL PET CENTRE

IAEA Human Health Series No. 11

STI/PUB/1457 (146 pp.; 2010)
ISBN 978-92-0-104610-9

Price: €42.00

STANDARD OPERATING PROCEDURES FOR PET/CT: A PRACTICAL APPROACH FOR USE IN ADULT ONCOLOGY

IAEA Human Health Series No. 26

STI/PUB/1616 (116 pp.; 2013)
ISBN 978-92-0-143710-5

Price: €35.00

PET/CT ATLAS ON QUALITY CONTROL AND IMAGE ARTEFACTS

IAEA Human Health Series No. 27

STI/PUB/1642 (89 pp.; 2014)
ISBN 978-92-0-101014-8

Price: €60.00

CLINICAL PET/CT ATLAS: A CASEBOOK OF IMAGING IN ONCOLOGY

IAEA Human Health Series No. 32

STI/PUB/1680 (201 pp.; 2015)
ISBN 978-92-0-101115-2

Price: €70.00

Despite the proven benefits of fluorodeoxyglucose (FDG) as a positron emission tomography (PET) radiopharmaceutical in oncology, FDG has limitations in the assessment of several relevant tumours, such as prostate cancer. Therefore, there has been a pressing need for the development and clinical application of new PET radiopharmaceuticals that can enable imaging of these tumours more precisely. Accordingly, several non-FDG PET radiopharmaceuticals have been introduced into the clinical arena in the last few years, in some countries more rapidly than in others. Indeed, it is expected that this trend will continue to spread internationally, since the use of positron emission tomography-computed tomography (PET-CT) with different radiopharmaceuticals, catering to the type of tumour and biological process that needs to be assessed, enables greater precision in medicine.

The objective of this publication is to provide a case-based presentation of the normal biodistribution, variants and pitfalls, and different imaging patterns for the main indications for each of the new non-FDG PET radiopharmaceuticals. This should facilitate the interpretation and recognition of common variants and pitfalls, to ensure that clinical study reports are accurate and helpful.

IAEA HUMAN HEALTH SERIES